UNIVERSITY OF NATAL

ESTIMATING SOLAR RADIATION FOR WATER-USE AND YIELD SIMULATIONS UNDER PRESENT AND PROJECTED FUTURE CLIMATE USING CROPSYST

by

MICHAEL GHEBREKRISTOS ABRAHA

B. Sc. (University of Asmara)

submitted in partial fulfillment of the requirement for the degree of

MASTER OF SCIENCE IN AGRICULTURE

in Agrometeorology, SPACRU, School of Applied Environmental Sciences

Faculty of Science and Agriculture

University of Natal

Pietermaritzburg

South Africa

June 2003

DECLARATION

I declare that the results contained in this thesis are from my original work except where acknowledged.

Signed 

Michael G Abraha

Date 12/08/03

Signed 

Prof. M J Savage

(Supervisor)

ACKNOWLEDGEMENTS

I wish to express my heartfelt gratitude to my supervisor, Prof. M J Savage, for the inspiration, encouragement and guidance, and especially for making himself available for advice at all times, towards the completion of this work.

I owe also a debt of gratitude to: Ms. J Moodley and Mr. P N Dovey (Agrometeorology) of the School of Applied Environmental Sciences, University of Natal, for their patience and endless technical assistances; Mr. V Dorasamy and Mr. E Abib (Soil Science) of the School of Applied Environmental Sciences, University of Natal, for laboratory set up of physical and chemical soil analysis; Ms. S Bezuidenhout (Crop Protection Section) of the Department of Agriculture and Environmental Affairs, Cedara who made her field trial and soil water content data available for this work.

Special thanks are also due to: Mr. S B Dovey of the Institute for Commercial Forestry Research (ICFR), for loan of soil core sampler; and Council for Scientific and Industrial Research (CSIR) for loan of LAI-2000 plant canopy analyzer.

Weather data source for: Cedara (1970 to 2002) and Ukulinga (1959 to 1966), from Agricultural Research Council, Institute of Soil, Climate and Water, Pretoria, South Africa; Cedara (2002 to 2003) from Mr. N van Rij (Crop Protection Section) of the Department of Agriculture and Environmental Affairs, Cedara; Durban (1980 to 1988), from South African Weather Bureau Service; and Seven Oaks (1998 to 2001), from Council for Scientific and Industrial Research (CSIR) is gratefully acknowledged.

Data sets for model calibration and validation for: maize from Mr. K Lawrance, ARC-Grain Crops Institute, (Cedara sub-centre); and oats, ryegrass and rye from the Department of Plant Production and Soil Science, University of Pretoria is also gratefully acknowledged.

I would also like to express my sincere appreciation to colleagues M F Gebregiorgis, T A Ghebreab, M G Mengistu and T W Abezghi for their invaluable discussions, comments and fieldwork assistance.

The Water Research Commission and the National Research Foundation are gratefully acknowledged for previously funding the equipment used in this research. The World Bank in Agreement with the Human Resources Development of the University of Asmara, Eritrea for funding the research are gratefully acknowledged.

TABLE OF CONTENTS

Page

DECLARATION i

ACKNOWLEDGEMENTS ii

TABLE OF CONTENTS iii

LIST OF TABLES viii

LIST OF FIGURES x

LIST OF APPENDICES xiii

ABSTRACT xiv

1 INTRODUCTION 1

2 MODELS: A BRIEF DESCRIPTION 4

2.1 INTRODUCTION 4

2.2 SYSTEMS, MODELS AND SIMULATION 5

2.3 MODEL TYPES 5

2.4 CROP SIMULATION MODELS 7

2.5 DATA REQUIREMENTS FOR MODEL OPERATION 9

2.6 CALIBRATION AND VALIDATION OF CROP SIMULATION MODELS 10

2.6.1 Model calibration 11

2.6.2 Model validation 12

2.7 SENSITIVITY AND UNCERTAINTY ANALYSIS 14

2.7.1 Sensitivity analysis 14

2.7.2 Uncertainty analysis 15

2.8 EVALUATION OF MODEL PERFORMANCE 16

2.9 CONCLUSIONS 18

3 CROP SIMULATION APPLICATIONS: LITERATURE REVIEW 19

3.1 INTRODUCTION 19

3.2 OVERVIEW OF IRRIGATION SCHEDULING METHODS 19

TABLE OF CONTENTS (continued)

Page

3.2.1 Irrigation timing criteria for soil water balance techniques 21
3.3 SOIL WATER BALANCE COMPONENTS VISITED 22
3.4 APPLICATION OF CROP GROWTH MODELS 24
3.4.1 Crop management 25
3.4.2 Climatic application 33
3.4.3 Policy analysis tool 37
3.4.4 Research applications 38
3.5 CONCLUSIONS 39

4 CropSyst MODEL DESCRIPTION 40

4.1 INTRODUCTION 40
4.2 SOIL WATER BALANCE 42
4.2.1 Precipitation and irrigation 42
4.2.2 Shallow water table 43
4.2.3 Interception 43
4.2.4 Runoff 43
4.2.5 Infiltration and soil water movement 44
4.2.6 Reference evaporation 45
4.2.7 Partitioning potential crop evapotranspiration 47
4.2.7.1 Potential transpiration 47
4.2.7.2 Potential residue evaporation 47
4.2.7.3 Potential soil evaporation 48
4.2.7.4 Actual residue evaporation 48
4.2.7.5 Actual soil evaporation 48
4.2.7.6 Actual crop transpiration 48
4.3 MODELLING CROP DEVELOPMENT AND GROWTH 51
4.3.1 Water dependent growth 52
4.3.2 Radiation and temperature dependent growth 52
4.3.3 Nitrogen dependent growth 54
4.4 SOIL-PLANT NITROGEN BUDGET 54
4.5 MODEL INPUT DATA FILES 55

TABLE OF CONTENTS (continued)

Page

5 SITE, PLANT, SOIL AND INSTRUMENT DESCRIPTION 57

5.1 SITE DESCRIPTION 57
5.2 CROPS 58
5.2.1 Oats 58
5.2.2 Italian rye grass 59
5.2.3 Rye 59
5.2.4 Maize 59
5.3 INSTRUMENTS 60
5.3.1 Diviner 2000 and Profile Probe 60
5.3.2 Watermark and Tensiometers 60
5.3.3 LAI 2000 plant canopy analyzer (PCA) 63
5.3.4 Automatic weather station 66
5.4 SOIL 67
5.4.1 Particle-size analysis 68
5.4.2 Water retention and bulk density 69

6 SOLAR RADIANT DENSITY ESTIMATION FOR CROP SIMULATIONS 75

6.1 INTRODUCTION 75
6.2 ESTIMATION OF SOLAR RADIANT DENSITY 76
6.2.1 Solar radiant density estimation from sunshine duration 77
6.2.2 Solar radiant density estimation from common meteorological observations 78
6.3 MATERIALS AND METHODS 81
6.3.1 Data 81
6.3.2 Formulae 82
6.3.2.1 Bristow and Campbell (B-C) model 82
6.3.2.2 Donatelli and Campbell (D-C) model 83
6.3.2.3 Modified B-C model 84
6.3.2.4 Donatelli and Bellocchi (D-B) model 84
6.3.2.5 Hargreaves model 84
6.3.2.6 Ramkrishnan and Ritchie (R-R) model 85
6.3.2.7 Clemence model 85
6.3.2.8 HKS model 86
6.3.2.9 Mahmood and Hubbard (M-H) model 86
6.3.3 Coefficients 87

TABLE OF CONTENTS (continued)

Page

6.3.4 Statistical evaluation 88
6.3.5 Crop simulations 92
6.4 RESULTS AND DISCUSSION 93
6.4.1 Conventional statistics 94
6.4.2 Statistical evaluation using an expert system 103
6.3.3 Application to crop simulations 104
6.5 CONCLUSIONS AND RECOMMENDATIONS 108

7 CropSyst MODEL CALIBRATION AND VALIDATION 109

7.1 INTRODUCTION 109
7.2 MATERIALS AND METHODS 110
7.2.1 Calibration and validation data 110
7.2.2 The model 111
7.2.3 Application of CropSyst in irrigation scheduling 112
7.3 CALIBRATION 113
7.4 RESULTS AND DISCUSSION 113
7.4.1 Fallow land 113
7.4.2 Oats, Italian ryegrass and rye 118
7.4.3 Maize 124
7.5 CONCLUSIONS AND RECOMMENDATIONS 127

8 CREATING SCENARIOS USING GENERATED WEATHER DATA 129

8.1 INTRODUCTION 129
8.2 WEATHER DATA GENERATION USING THE ClimGen MODEL 130
8.3 CLIMATIC SCENARIOS 132
8.4 MATERIALS AND METHODS 134
8.5 RESULTS AND DISCUSSION 138
8.5.1 Generated weather data 138
8.5.2 Yield simulations using observed and generated weather data 140
8.5.3 Yield simulations under different climatic scenarios 144
8.6 CONCLUSIONS AND RECOMMENDATIONS 149

TABLE OF CONTENTS (continued)

Page

9 CONCLUSIONS AND RECOMMENDATIONS 151

References 156

Appendix A 166
Appendix B 167
Appendix C 168
Appendix D 172
Appendix E 175

LIST OF TABLES

Table Page

5.1 Monthly statistics of weather variables as calculated from 1970 to 2002 for Cedara, KwaZulu-Natal, South Africa 57

5.2. Measured (using LIA-2000 PCA) and corrected values of leaf area index of oats, Italian ryegrass and rye at various times during the 2002/03 growing season at Cedara, KwaZulu-Natal, South Africa 66

5.3 List of weather variables and sensors used for the observation of the weather variables during the 2002-2003 growing season at Cedara, KwaZulu-Natal, South Africa 67

6.1 Details of various models used for estimation of solar radiant density 80

6.2 Location of meteorological stations and length of data records used for estimation of solar radiant density 82

6.3 Membership classes of indices according to expert judgment following Bellocchi *et al.* (2002) 89

6.4 Assignment of expert weight to the module accuracy based on membership class of the indices *RRMSE*, *EF* and P(*t*) following Bellocchi *et al.* (2002) 89

6.5 Assignment of expert weight to the module pattern based on membership class of the indices PI_{doy} and PI_{Tn} following Bellocchi *et al.* (2002) 91

6.6 Summary of decision rules describing the effect of the three modules on the value of the indicator (I_{rad}) following Bellocchi *et al.* (2002) 91

6.7 Calibrated model coefficients for Cedara, Durban, Seven Oaks and Ukulinga in KwaZulu-Natal, South Africa 94

6.8. Statistical results of measured (sunshine derived) solar radiant density values against model-predicted values for Cedara, Durban, Seven Oaks and Ukulinga 97

6.9 Statistical indices for the Durban location using B-C model coefficients of observed and sunshine derived solar radiant density for both observed and sunshine derived data sources 98

6.10 Performance of solar radiant density models according to the indicator, I_{rad}, calculated using an expert perception for Cedara, Seven Oaks and Ukulinga in KwaZulu-Natal, South Africa (the numbers in brackets indicate rank of the model for the specific location) 103

6.11 Statistical comparison 20 years of simulated maize grain yield (tons ha^{-1}) using CropSyst with different dataset of solar radiant density for Cedara, KwaZulu-Natal, South Africa 105

6.12 Ranking of the models according to statistical indices calculated from application in crop simulation for Cedara, KwaZulu-Natal, South Africa (1 indicates best ranking and 9 worst ranking according to the respective statistical index) 107

LIST OF TABLES (continued)

Table Page

7.1 Statistical results of calibration and validation (other than the data used for calibration) of the CropSyst model soil water balance against field-measured soil water content (m3 m-3) for a fallow land (from 29 April to 22 November 2002) at Cedara, KwaZulu-Natal, South Africa 115

7.2 Statistical results of validation of the CropSyst model soil water balance against field-measured soil water content (m3 m-3) under oats, Italian ryegrass and rye at Cedara, KwaZulu-Natal, South Africa 118

7.3 Observed precipitation and irrigation, and simulated irrigation amounts for oats, Italian ryegrass and rye for part of the 2002 growing season at Cedara, KwaZulu-Natal, South Africa 121

7.4 Comparison of observed and model-predicted results on growth stages and grain yield of maize at Cedara, KwaZulu-Natal, South Africa 124

7.5 Statistical results of calibration of the CropSyst model soil water balance against field-measured soil water under maize at Cedara, KwaZulu-Natal, South Africa 125

8.1. General statistical comparison of observed (1971 to 2000) and generated weather data series for Cedara, KwaZulu-Natal, South Africa 136

8.2 Comparison of observed (1971-2000) and generated weather data for Cedara, KwaZulu-Natal, South Africa (the numbers in the rows labeled "Rejected" indicate the number of months that gave significant results at the 5% level of significance, a large number of significant result indicate poor performance of the model) 139

8.3. Maize grain yield (tons ha-1) as simulated by the CropSyst model using observed and generated weather data series of 30 years using different planting dates for Cedara, KwaZulu-Natal, South Africa 141

8.4 Simulated maize grain yields for baseline (generated weather data) and hypothesized climatic scenarios for Cedara, KwaZulu-Natal, South Africa 145

LIST OF FIGURES

Figure Page

3.1 Simulation of soybean yield response to (a) planting date at Gainesville, Florida and (b) row spacing for two maturity groups at Florida and Iowa, using historical weather data (after Boote *et al.*, 1996) 26

3.2 (a) Simulation of soybean yield response to three irrigation strategies, (b) simulation of soybean irrigation water requirements for three irrigation management strategies, (c) simulation of maize irrigation water requirements, average over 16, 21, 23 and 23 years, using historical weather data for Gainesville, Florida and (d) simulated cumulative probabilities of maize yields for two nitrogen levels (200 and 300 kg ha^{-1}) in irrigated and rainfed soils for maize planted in April 1 (after Jones and Ritchie, 1990) 28

3.3 Simulated millet yield distributions derived at various forecast dates using historical decadal rainfall totals up to the day of forecast and probabilistic weather thereafter, for the 1986 and 1990 seasons in Dori, Burkina Faso (after Thornton and Wilkens, 1998) 31

3.4 Observed and model-predicted (1982-1985) maize production for the U.S. Cornbelt (after Hodges *et al.*, 1987) 31

3.5 Simulated soybean yield response to decrease or increase in temperature for two maturity groups in Gainesville (Florida) and Ames (Iowa) using historical weather data. The arrows indicate mean seasonal air temperature over soybean growth cycle at both Ames and Gainesville (after Boote *et al.*, 1996) 34

3.6 Cumulative distribution plot for grain yields of (a) maize and (b) soybean, simulated using historical weather data at Urbana, IL. The number of years exceeding specific yields are plotted against yield (after Sinclair and Rawlins, 1993) 35

4.1 Graphical representation of the effect of air temperature on biomass accumulation 53

5.1 Mean monthly values of (a) solar radiant density; (b) maximum, minimum and average air temperatures; and (c) mean precipitation and pan evaporation as calculated from 1970 to 2002 for Cedara, KwaZulu-Natal, South Africa (Source data- ARC-ISCW) 58

5.2 The relationship between South African (SA) and USDA particle-size classification system 68

5.3 Soil water retentivity curves for several soil layers down the soil profile (WM – soil water potential measured using Watermark sensor only, WMT – Watermark and tensiometer, Lab – laboratory measured using pressure apparatus, and Hupper and Hlower – retentivity curves constructed using the Hutson LEACHM (ISCI-Crop Science, 2001; Acutis and Donatelli, 2003) model at Cedara, KwaZulu-Natal, South Africa 73

LIST OF FIGURES (continued)

Figure Page

5.4 Drainage curve following flooding of the measurement plot at Cedara, KwaZulu-Natal, South Africa 74

6.1 Measured solar radiant density against solar radiant density derived from sunshine hours for Durban, KwaZulu-Natal, South Africa (n = 4017) 93

6.2 Graphical comparison of the performance of the B-C (left) and Modified B-C (right) models for Cedara (a) and (b), Seven Oaks (c) and (d) and Ukulinga (e) and (f), KwaZulu-Natal, South Africa 95

6.3 Graphical presentation of the B-C model estimates for Durban using coefficients developed from (a) observed solar radiant density values as applied to observed values, (b) sunshine hours derived solar radiant density values to observed values, (c) sunshine hours derived solar radiant density values to sunshine hours derived solar radiant density values and (d) observed solar radiant density values to sunshine hours derived solar radiant density values (e) solar radiant density values generated using observed coefficients against sunshine hours derived coefficients 99

6.4 Graphical presentation of the performance of the B-C (a) and D-C (b) models for Ukulinga, KwaZulu-Natal, South Africa 101

6.5 Cumulative probability of maize grain yield distributions as simulated by CropSyst model using 20-years of observed and model-estimated solar radiant density at Cedara, KwaZulu-Natal, South Africa 106

7.1 Model-predicted (lines and symbols) and observed- using Diviner 2000 (symbols) volumetric soil water content distribution on days 9, 57 and 146 days after starting date of simulation (2002), representing relatively dry, medium and wet range soil surfaces, in a fallow land at Cedara, KwaZulu-Natal, South Africa 117

7.2 LAI (a) calibration (Kromdraai open cast mine, Mpumalanga province) and (b) validation (Cedara, KwaZulu-Natal, South Africa) for rye 119

7.3 Predicted (using Priestley-Taylor) and calculated (using Penman-Monteith) ET_c (mm) for rye during the 2002 growing season at Cedara, KwaZulu-Natal, South Africa 120

7.4 Observed precipitation and irrigation, simulated irrigation (with 0.4 and 0.6 maximum allowable depletion) and soil water depletion for (a) oats, (b) Italian ryegrass, and (c) rye for part of the 2002 growing season at Cedara, KwaZulu-Natal, South Africa. Planting date was on April 12, 2002 122

7.5 Graphical comparison of model-simulated and field-observed phenological stages of maize over a period of four years at Cedara, KwaZulu-Natal, South Africa 125

7.6 Simulated (lines) and observed- using Diviner 2000 (points) volumetric soil water content distribution against days after planting (DAP) for the different depths under maize crop in the 2003 growing season at Cedara, KwaZulu-Natal, South Africa. Planting date was on November 21, 2002 126

LIST OF FIGURES (continued)

Figure Page

8.1 (a) Cumulative and (b) frequency distribution functions of grass reference evaporation (ET_o) as calculated by ClimGen using the observed (1971-2000) and generated weather data series for Cedara, KwaZulu-Natal, South Africa 140

8.2 Maize grain yield comparisons over 30-year period as simulated by CropSyst using observed (1971-2000) and generated weather data series (a) simple line graph and (b) cumulative probability functions, for Cedara, KwaZulu-Natal, South Africa 140

8.3 Grain yield of maize as simulated by CropSyst model for planting days of the year 294 (October 21), 309 (November 5) and 323 (November 19) using (a) observed (1971-2000) and (b) generated weather data for Cedara, KwaZulu-Natal, South Africa 142

8.4 Grain yield of maize as simulated by the CropSyst model using (a) observed (1971-2000) and (b) generated weather data series for planting days of the year 294 (October 21), 309 (November 5) and 323 (November 19) and precipitation received during the growing period at Cedara, KwaZulu-Natal, South Africa 143

8.5 Cumulative probability distribution of maize grain yields under (a) baseline period (b) elevated [CO_2] – Scenario A (c) elevated [CO_2], 2 ^{o}C increment to the mean daily air temperature along with 10 (20%) increment to daily precipitation – Scenario B and C (d) elevated [CO_2], 4 ^{o}C increment to the mean daily air temperature along with 10 (20%) increment to daily precipitation for early, locally practiced and late planting dates, and (e) early (f) locally practiced, and (g) late planting dates for all scenarios 146

LIST OF APPENDICES

Page

Appendix A: Physical and chemical soil characteristics on a layer by layer basis from an upper and lower slope during the 2002/2003 growing seasons at the experimental site, Cedara, KwaZulu-Natal, South Africa (soil texture analysis is based on United States Department of Agriculture classification system)---------- 166

Appendix B: Particle-size analysis (South Africa) for the experimental sites under National Cultivar Trials: maize, during the 1997/98 to 2001/02 growing seasons at Cedara, KwaZulu-Natal, South Africa (soil texture analysis is based on the South African classification system) ---------- 167

Appendix C: CR23X datalogger program for soil water potential sensors (tensiometers and Watermark sensors)---------- 168

Appendix D: CR10X datalogger Program for PR1 profile probe sensor and rainguage to measure soil water content and rainfall/irrigation ---------- 172

Appendix E: Crop parameters for oats, rye grass, rye and maize ---------- 175

ABSTRACT

ESTIMATION OF SOLAR RADIANT DENSITY FOR WATER-USE AND YIELD SIMULATION UNDER PRESENT AND PROJECTED FUTURE CLIMATE USING CROPSYST

by

Michael G. Abraha

Supervisor: Prof. Michael J. Savage

Agricultural scientists are faced with the challenge of producing enough food for the increasing world population. Hence the need to develop tools for managing soil and plant systems to increase food production in order to meet the world food demand in the future. Crop simulation models have become promising tools in predicting yield and related components from a set of weather, soil, plant and management data inputs. This study describes the estimation of solar radiant density, a crucial input in crop simulation models; calibration and validation of a soil-plant growth simulator, CropSyst, for management purposes; and generation of weather data for assessment of crop production under possible climate changes in the future.

Daily solar radiant density, an input required by most crop simulation models, is infrequently observed in many stations. This may prevent application of crop simulation models for specific locations. Long-term data records of daily minimum and maximum air temperatures, precipitation, sunshine hours and/or solar radiant density were obtained for Cedara, Durban, Seven Oaks and Ukulinga in KwaZulu-Natal, South Africa. Solar radiant density was estimated from sunshine hours using the Ångstrom equation and ten other models that involved daily minimum and maximum air temperatures and/or precipitation along with

extraterrestrial radiant density. Coefficients for the Ångström equation and one of the other ten models were specifically developed for South African conditions; the remaining models required fitting coefficients using the available data for all locations. The models were evaluated using (i) conventional statistics that involved, root mean square error (*RMSE*) along with its systematic and unsystematic components, slope, intercept, index of agreement (*d*), and coefficient of determination (R^2); and (ii) a fuzzy expert system that involved a single modular indicator (I_{rad}) aggregated from the modules of accuracy (aggregation of the indices relative *RMSE*, model efficiency and *t*-student probability), correlation (Pearson's correlation coefficient) and pattern (aggregation of pattern index *vs* day of year and pattern index *vs* minimum air temperature). For each index, two functions describing membership to the fuzzy subsets Favourable (F) and Unfavourable (U) were defined. The expert system calculates the modules according to both the degree of membership and a set of decision rules. Solar radiant density estimated from sunshine hours for the Durban station resulted in R^2, *RMSE* (MJ m^{-2}) and *d* index of 0.90, 2.32 and 0.97 respectively. In the absence of observed solar radiant density data, estimations from sunshine hours were used for derivation of coefficients as well as evaluation of the models. For Durban, the performance of the models was generally poor. For Cedara, Seven Oakes and Ukulinga two of the models resulted in a high *d* index and smallest systematic *RMSE*. The solar radiant density estimated from each model was also used as an input to simulate maize grain yields using the soil-plant growth simulator, CropSyst. The models were ranked according to their ability to simulate grain yields that match those obtained from using the observed solar radiant density. The rankings according to crop simulation, conventional statistics and expert system were compared.

The CropSyst model was also evaluated for its ability to simulate crop water-use of fallow and cropped (oats, Italian ryegrass, rye and maize) plots at Cedara, KwaZulu-Natal, South Africa. Soil characteristics, initial soil water conditions, irrigation and weather data were inputted to CropSyst. Crop input parameters for oats, Italian ryegrass and rye were used, with little modifications, as determined from field experiments conducted at Kromdraai open cast mine, Mpumalanga province, South Africa. Crop input parameters for maize were either determined from field experiments or taken from CropSyst crop input parameters documentation and adjusted within a narrow specification range of values as dictated by CropSyst. The findings indicated that CropSyst was generally able to simulate reasonably well

the water-use of fallow and cropped (oats, Italian ryegrass, rye and maize) plots; leaf area index and crop evapotranspiration of rye; and grain yield and developmental stages of maize. The validated CropSyst model was also used to simulate timing and amount of irrigation water, and investigate incipient water stress in oats, Italian ryegrass and rye.

The CropSyst model was used to investigate potential effects of future climate changes on the productivity of maize grain yields at Cedara, KwaZulu-Natal, South Africa. The effect of planting date (local planting date, a fortnight earlier and a fortnight later) was also included in the study. A 30-year baseline weather data input series were generated by a stochastic weather generator, ClimGen, using 30 years of observed weather data (1971 to 2000). The generated weather data series was compared with the observed for its distributions of daily rainfall and wet and dry series, monthly total rainfall and its variances, daily and monthly mean and variance of precipitation, minimum and maximum air temperature, and solar radiant density. Four months of the year failed to reproduce distributions of wet and dry series, daily precipitation, and monthly variances of precipitation of the observed weather data series. In addition, Penman-Monteith reference evaporation (ET_o) was calculated using the observed and generated data series. Cumulative probability function of ET_o calculated using the generated weather data series followed the observed distribution well. Moreover, maize grain yields were simulated using the generated and observed weather data series with local, a fortnight earlier and a fortnight later planting dates. The mean simulated grain yields for the respective planting dates were not statistically different from each other; the grain yields simulated using the generated weather data had significantly smaller variance than the grain yields simulated using the observed weather data series. When the generated weather data series was used an input, the early planting date as compared to the locally practiced and late planting dates resulted in significantly greater simulated grain yields. The grain yields simulated using the observed weather data for the early and local planting dates were not statistically different from each other.

The baseline period was modified by synthesized climate projections to create future climatic scenarios. The climate changes considered corresponded to doubling of $[CO_2]$ from 350 to 700 $\mu l\ l^{-1}$ without air temperature and water regime changes, and doubling of $[CO_2]$ accompanied by increases in mean air temperature and precipitation changes of 2 ^{o}C and 10%, 2 ^{o}C and 20%, 4 ^{o}C and 10%, and 4 ^{o}C and 20% respectively. Solar radiant density was also

estimated from daily air temperature range for all scenarios that involved change in mean air temperature. In addition, input crop parameters of radiation-use and biomass transpiration efficiencies were modified for maize, in CropSyst, to accommodate changes in elevated levels of [CO_2]. Equivalent doubling of [CO_2], without air temperature or water regime changes, resulted in increased simulated grain yields as compared to the baseline period. Adding 2 ^{o}C to the mean daily temperature and 10% to the daily precipitation of a [CO_2] elevated atmosphere reduced the grain yield but still kept it above the level of the baseline period grain yield. Adding 4 ^{o}C to the mean daily temperature and 10% to the daily precipitation further decreased the yield. Increasing the daily precipitation by 20% instead of 10% did not change the simulated grain yield as compared to the 10% increments. Early planting date, for all scenarios, also resulted in higher yields, but the relative increment in grain yield was higher for the late planting dates with scenarios that involved increment in mean air temperature. In general, this study confirmed that doubling of [CO_2] increases yield but the accompanied increase in mean air temperature reduces yield.

1 INTRODUCTION

The world's population is projected to increase from its present 6.3 billion to 8.9 billion by the year 2050 (United Nations, 2003). Africa's population growth rate is the highest in the world with its present 2.5% increase per year (United Nations, 2003) and during the last quarter century it almost doubled but per capita food production declined by 14% (World Bank, 2001). Water is the most limiting resource in food production. A study that is undertaken by the World Bank on water supply and demand from 1995 to 2025 has shown that, at national level, all African countries will suffer from physical or economic water scarcity (Seckler and Amarasinghe, 2000). More water will be diverted from agricultural uses towards industrial, commercial and domestic uses (United Nations, 1997a), hence agriculture, in all African nations, will face acute shortage of water supplies. This urges agricultural scientists to search for more innovative ways of increasing crop production with less water to meet the food demand of the increasing population of Africa.

One option of increasing crop production could be by proper management of the limited water resource, which, unfortunately is characterized by large variations from one growing season to another. There are many methods that have been developed to supply water to crops at the right time and in the right amount with varying level of complexity and accuracy. These methods involve the soil, crop, atmosphere or a combination thereof and accordingly require a profound understanding of the system they employ.

The impact of water on crop productivity could not be analyzed independent of weather, soil, crop and management practices. Assessment of crop productivity would require integration of all these variables into a comprehensive cropping system. This would be laborious, time consuming and expensive to be undertaken solely by the cumbersome conventional procedures of field experimentation (Pala *et al.*, 1996).

In the past two decades, crop simulation models that employ inputs from weather, soil, crop and management practices in order to provide predictions of growth and development of crops (Jones and Ritchie, 1990), soil water status and nutrient dynamics of the soil (Pala *et al.*, 1996) have become available. However, crop simulation models need to be validated for the specific location, soil and crop of interest before they could be of any value to a region. A

validated crop simulation model can be used to assess the risks and consequences of alternative management practices (planting density, irrigation, fertilizer levels, crop varieties, soil types, etc), provided long-term historical weather data are available, by employing input data of varying management practices (Uehara and Tsuji, 1998).

The minimum weather dataset that are required by most crop simulation models include daily precipitation, minimum and maximum air temperatures and solar radiant density. Sometimes full weather dataset necessary for assessing management practices may not often be readily available. For example, solar radiant density is infrequently observed in meteorological stations and could be complemented using data from nearby sites or estimated from other more readily available meteorological observations. At other times, the length of data available may be insufficient for assessing risks imposed by long-term weather variability. Models (weather generators) that generate weather data from historical observed weather data for as many years as required, with similar statistics to the historical observed weather data, have addressed this problem (Richardson and Wright, 1984). The generated weather data can be used in a similar fashion to the historic weather data in assessing risks involved with adopting certain management strategies.

Crop simulation models could also be linked, combined or integrated with geographic information systems (GIS) to visualize and analyze interactions in soil variability, environment and management practices (Hartkamp *et al.*, 1999). Crop simulation models have been used in yield forecasting using observed and generated weather data (e.g., Hodges *et al.*, 1987; Thornton *et al.*, 1997; Thornton and Wilkens, 1998). They have also been used to investigate the effect of climate change on crop productivity and the environment by modifying the observed or generated weather data by plausible projected changes in means and variances of the future climate (e.g., Sinclair and Rawlins 1993; Boote *et al.*, 1996; Donatelli *et al.*, 2000; Tubiello *et al.*, 2000; Williams *et al.*, 2001).

The CropSyst (Version 3.02.26) (Stöckle and Nelson, 2000; Stöckle *et al.*, 2003) model is a crop simulation model developed to study the effect of cropping systems management and weather on crop productivity and the environment. This study is undertaken with the intention of testing the CropSyst model in its ability to simulate yield and water-use of certain crops at Cedara, KwaZulu-Natal, South Africa.

The main objectives of this study include:

i) to evaluate the ability of the CropSyst (Version 3.02.26) model to simulate development and growth of maize and water-use of fallow and cropped (oats, Italian ryegrass, rye and maize) lands;

ii) to estimate solar radiant density from sunshine hours; daily air temperature ranges and/or precipitation for use as input in the CropSyst model, and

iii) to assess the effect of climate change (increase in $[CO_2]$, mean air temperature and precipitation) on grain yield of maize productivity.

2 MODELS: A BRIEF DESCRIPTION

2.1 INTRODUCTION

Cropping systems involve physical, chemical and biological processes, with incessant interaction and exchange of matter and energy in the soil around the root zone of the plant, the plant and the atmosphere. The attention of agricultural and environmental scientists have focused on explaining the complex processes that happen within the crops as affected by the soil and the atmosphere, and their management in an optimal sustainable manner with little or no adverse consequences on the system. During the last 20 years, computer simulation models have assisted their efforts so that biological systems can be manipulated with far better ease than with the traditional procedures of experimentation. These computer simulation models have proved useful in giving insight into understanding the operation of the complex system, prediction of crop yields, both temporally and spatially, and addressing the problem of environmental issues (Hillel 1977; Savage 2001).

But the use of crop growth models for specific purposes requires verification of the model (Whisler *et al.*, 1986). Verified models do not usually yield to biologists' expectations (de Wit, 1982) and perhaps this is why de Wit (1982) and Passioura (1973) stated that simulation models are more of an art than science. Moreover, these two scientists have shed their word of caution in using simulation models: de Wit (1982) argued that the terms model and system should not be used interchangeably in biology as in engineering since crop simulation models are not simplified representations of the conceptual ideas of biologists. He warned "fools rush in where wise men fear to tread and this rushing in simulation in biology is done by agronomists, perhaps because they are fools, but maybe they deal with systems in which technical aspects overrule more and more the biological aspects." Passioura's (1973) warning goes on that biological systems cannot be successfully simulated as physical systems because the processes involved in biological systems are poorly understood as compared to physical systems.

2.2 SYSTEMS, MODELS AND SIMULATION

A system can be defined as part of the universe, composed of interdependent and interacting, living and non-living components, distinguished from its surrounding environment by physical or conceptual boundaries. Individual parts of a system are often studied in isolation in order to understand the system's mechanism. This may, however, lead to disregard of other important aspects, such as interactions and feedbacks, and thus to oversimplification of the conceptions on how the complex system operates. Models offer a good chance of developing a more comprehensive conception of the complex system as a whole by attempting to assemble and integrate the individual component parts of a system. Data and theories concerning a system can be logically organized into a model for the purpose of simulating the natural behaviour of a system (Hillel, 1977).

If the time dimension is introduced to simulation models, then dynamic simulation models come into existence (de Wit, 1982). These models work under the assumption that the state of the system can be quantified at any moment, and that changes in the state of the system can be described by mathematical equations (de Wit, 1982). These models are characterized by certain variables (de Wit, 1982) like:

(i) state variables that characterize the state of the system;

(ii) driving variables that characterize the effect of the environment on the system; and

(iii) rate variables that characterize the rate of change of the state variables at a certain instant as a result of specific processes.

Simulation models without the time dimension bear to static simulation models, which often constitute part of dynamic simulation models (de Wit, 1982).

2.3 MODEL TYPES

In all our modelling attempts we try to make a system simpler than it really is by considering only the factors pertinent to the problem at hand and ignoring other factors in the context that they are irrelevant (Hillel, 1977) or well-managed to affect the response of our system (Jones and Ritchie, 1990). Thus, a model can be defined as a simplified representation of a real system (Hillel, 1977; de Wit, 1982). Various types of models are recognized based on their purpose and the data they employ as well as an intuitive understanding of the system (Savage, 2001). Following are descriptions of several types of models that are mostly encountered in

agricultural systems. The below-mentioned types of models are not exhaustive and not necessarily mutually exclusive. A model may encompass several of these in conjunction.

Empirical or regression models are based on observed quantitative relationships among variables without any insight into the functional or causal operations that may exist between the variables (Hillel, 1977; Whisler *et al.*, 1986). In an agronomic context, empirical models are often used to predict crop yields from a set of soil, climate and management data (Savage, 2001). The predictions do always have a component of error since the variables can seldom be kept constant from year to year and their use in other geographical areas, with a different climate, management and cropping system is not usually justified (Savage, 2001). While such models may be used for interpolation, they should not be used for temporal or spatial extrapolation (Savage, 2001). Empirical or regression models become more prevalent, with decreasing resolution, as our understanding of causality decreases (Whisler *et al.*, 1986).

Deterministic or mathematical models are developed to overcome the limitations imposed in regression models by mimicking, as much as is feasible within calculation time, the actual processes that are known to occur in the soil, plant and atmosphere (Savage, 2001). These models attempt to explicitly represent causality between variables (Whisler *et al.*, 1986) and their observed behaviour based on the physical laws controlling flow of mass and energy that can be described in a mathematical fashion (Hillel 1977; Savage 1993; Savage 2001). Hence they are more exact. These models presume that a system or process operates such that the occurrence of a given set of events leads to a uniquely-definable outcome (Addiscott and Wagenet, 1985). They become feasible as our understanding of causality increases with increasing resolution (Whisler *et al.*, 1986). Deterministic models can be either mechanistic or functional models (Hillel 1977; Savage 2001). The distinctions between mechanistic and functional models as described by Addiscott and Wagenet (1985) are:

(i) mechanistic models are usually based on rate parameters and incorporate the most fundamental mechanisms of each process in the model, as is presently understood (e.g. soil water flow being represented by Darcy's law); and

(ii) functional models are usually based on capacity parameters at fixed time intervals and use the same process as mechanistic models but do not claim to adhere to the fundamental mechanisms. Such models require less input data and expertise for their use (e.g., the soil water model could be based on soil water storage parameter

and involve layers to depict the vertical distribution and availability of water to plants).

Stochastic models are based upon the probability of occurrence of some event or exogenous variable (Whisler *et al.*, 1986) and presuppose that outcomes are uncertain arising from probability calculations to determine the likelihood of future events given certain criteria, as opposed to certain outcomes in deterministic models (Addiscott and Wagenet, 1985; Savage, 2001). Stochastic models account for the inherent variability within a system by giving statistical credibility to the input conditions and model predictions (Addiscott and Wagenet, 1985). Weather variables are often treated in a stochastic manner or probability of occurrence and as such may be combined with a mechanistic crop model (Whisler *et al.*, 1986).

Parameter models are hydrological models which deal with the development and analysis of hydrological and physical characteristics of a large area to generate hydrological data sequence that are not usually measured (Savage, 2001).

2.4 CROP SIMULATION MODELS

Crop modelling defined by Sinclair and Seligman (1996) as the dynamic simulation of crop growth by numerical integration of constituent processes with the aid of computers, is a technology used to construct a relatively transparent surrogate for a real crop, one that can be analyzed and manipulated with far greater ease than the complex and cumbersome original. During the last two decades, with increased understanding of the soil-plant-atmosphere system and development of high-speed computers, crop growth models have been successfully used to provide predictions of growth and yield of crops (Jones and Ritchie, 1990). Many crop models or their parts have been found to be invaluable in assisting researchers to understand and quantify certain processes involved in the soil-plant-atmosphere system (Whisler *et al.*, 1986). In addition, crop simulation models have been widely used in interpreting experimental results in quest of management strategies that maximize specific objectives (Whisler *et al.*, 1986). However, Whisler *et al.* (1986) have underlined that this should not mean that models can be complete substitutes for field experiments, rather they should be validated with field experiments to increase their accuracies and lower the over-all costs of field experiments. A proven model can simulate scenarios, provided long-term historical weather data are available,

by employing input data of varying management strategies for as many years as weather data are available (Uehara and Tsuji, 1998). The simulation results could, subsequently, help to evaluate or assess the risks and consequences of alternative practices involved in the simulation (Uehara and Tsuji, 1998). If such experiments were to be conducted in the field they may be very expensive, considering the personnel and time constraint involved (Whisler *et al.*, 1986). Crop growth models can also be used as agronomic grower tools for a specific soil, crop and management combinations to answer "what if..." questions and compare profitability of options (Whisler *et al.*, 1986). It is, however, advisable that all modelling efforts be accompanied by appropriate statistical analysis (Savage 1993; Savage, 2001) to leave room for the incomplete knowledge and inevitable 'assumptions' we make in modelling a system.

Crop simulation models have been extensively used to study the effect of certain management options on crop production. For example, Jones and Ritchie (1990) used the model CERES-Maize to investigate options of irrigation and nitrogen fertilization strategy by simulating grain yield of maize at Gainesville, Florida. MacRobert and Savage (1995, 1998) used the CERES-wheat model to investigate deficit irrigation options in Zimbabwe. A simple soil water balance model was also used in real time on farm irrigation scheduling in the western United States (Hill, 1991). Boote *et al.* (1996) used the CROPGRO model to evaluate the effect of planting date, row spacing and cultivar on yield of soybean at Gainesville, Florida. Zhou *et al.* (2003) have used a sugar cane model to investigate Zimbabwean variety differences in sugar cane growth and development. Crop simulation models have also been applied in forecasting future yields on a regional basis, e.g., Thornton *et al.* (1997) and Thornton and Wilkens (1998) used the CERES-Millet to predict the yield of millet for Dori in Burkina Faso. Crop simulation models have also been applied to investigate the effect of climate change on crop production, e.g., Tubiello *et al.* (2000) used the CropSyst model to study the effect of a doubled [CO_2] on crop production at two locations in Italy.

For better results, it is imperative that the component parts of a model be of the same level of organization so that the model will be balanced (Whisler *et al.*, 1986; Ritchie, 1991). To circumvent a lack of balance in crop simulation models, Whisler *et al.* (1986) and Ritchie (1991) recommended that a multidisciplinary team approach be adopted in model building. Moreover, crop simulation models should be modular in structure to facilitate the

comprehension of organization and logic of the program, and save the costs associated with modification and improvement of models to suit particular applications (Ritchie, 1991).

2.5 DATA REQUIREMENTS FOR MODEL OPERATION

All crop models require information, depending on the level of complexity at which they operate, on management of the crop, weather during the growing season, soil conditions at the start of simulation and crop cultivar traits, etc. The International Benchmark Sites for Agrotechnology Transfer (IBSNAT) has defined a minimum amount of data (minimum dataset), for each of the above set of variables, necessary for model operation (Hunt and Boote, 1998).

The management data may consist of latitude of the site, elevation, planting date, row spacing, plant population, dates, amounts and methods of irrigation, residue management, amount and timing of fertilizer applications, chemical applications and other similar information (Whisler *et al.*, 1986; Hunt and Boote, 1998).

Weather input frequency could be hourly, daily or weekly depending on the complexity level of the model (Hunt and Boote, 1998). Availability of data and ease of manipulation, however, make daily time step weather data to be most appropriate for crop simulation models (Hunt and Boote, 1998). The required weather data include daily records of solar radiant density above the crop canopy, maximum and minimum air temperature above the crop and precipitation (Whisler *et al.*, 1986; Ritchie, 1991; Hunt and Boote, 1998). Some models also welcome data on water vapour pressure and wind speed whenever available (e.g., CropSyst). All the required weather data for a particular site during a particular period may not be available. In such instances, data from a nearby site can be used to replace most of the variables except precipitation (Hunt and Boote, 1998). Most models also include other models in their software package for calculating surrogate data. The weather data generating model of Stöckle and Nelson (1999) and Stöckle *et al.*, (2001) in CropSyst and daily rainfall generating model of Geng *et al.* (1986) in Villalobos and Fereres (1989) have been successfully used as a means of substituting the actual weather data.

There is a tremendous variation in the amount of soil data required for different crop simulation models. Whisler *et al.* (1986) and Hunt and Boote (1998) have identified:

(i) models that treat the below-ground soil as an entity and as such require information about the rooting depth of the soil and its water holding capacity only; and

(ii) models that divide the soil into layers and require information for each soil layer on thickness of the layers, textural class, water release curve characteristics (especially drained upper limit and lower limit), bulk density, organic carbon, pH, initial condition at the start of the season and some other information. Input information for the soil in general using local system and/or USDA-SCS classification is also required (Ritchie, 1991; Hunt and Boote, 1998).

Crop cultivar information required for model operation varies greatly among models. Some models do not require crop cultivar as input, e.g., where one overriding environmental factor determines productivity. Other models may need recalibration for genotypes differing from the one used during the model construction (Hunt and Boote, 1998).

2.6 CALIBRATION AND VALIDATION OF CROP SIMULATION MODELS

A model should be scientifically valid, its assumptions must conform to basic scientific principles, and realistic, it must incorporate the major processes and phenomena which govern the systems behaviour (Hillel, 1977). A model can be scientifically and logically valid within itself and yet fail to be realistic, simply because of the continual impact of factors disregarded in the analysis which may obscure the phenomena of direct interest (Hillel, 1977; Savage 1993). A valid simulation model should be able to predict the actual system now and in the future with sufficient accuracy (Hillel, 1977; Savage 1993; Savage, 2001). This requires sufficient evidence, of considerable time and effort, and judging the evidence objectively (Hillel, 1977; Savage 1993; Savage, 2001).

"Model building is an enjoyable if arduous task whereas model testing can be heartbreaking; perhaps this is why many models are published without being tested" (Whisler *et al.*, 1986). Validation of a model is important but invariably difficult (Hillel, 1977; Ritchie, 1991; Savage 1993; Savage, 2001) because of the myriad of factors involved in a system.

2.6.1 Model calibration

Data used for developing crop simulations are usually gathered from controlled environments (Whisler *et al.*, 1986) simply because the environmental variables can be varied easily as opposed to those in the field situation. When crop simulation models developed in this way are used for the purpose of predictions in the field, it is usual to find some discrepancies between measured data and simulated outputs (Whisler *et al.*, 1986). It is crucial, therefore, to understand how a model represents the biological, physical and chemical processes in a system of interest to correctly interpret these discrepancies and subsequently adjust them so that simulation outputs would agree with measured data (Whisler *et al.*, 1986). This process is called calibration. Calibration is meant to account for the empiricism which is often at the base of the relations used in models (Donatelli and Stöckle, 1999).

Model calibration requires datasets with all the information required as inputs to run the model (e.g., crop management, aerial and soil environments, and genotype characteristics) together with some data on plant performance and soil initial conditions (CAMASE, 1995). CAMASE (1995) defined calibration criterium as a function of parameter values and the calibration data that provide a measure of the compatibility of the parameter values with the data. The definition included four standards:

(i) point calibration which results in a single optimal parameter vector often compatible with the available calibration data, but usually non-robust;

(ii) set calibration that yields a set of parameter vectors compatible with the calibration data;

(iii) distribution calibration that results in a probability distribution of parameter vectors compatible with the calibration data; and

(iv) robust calibration that leads to results that are rather insensitive to minor changes in the calibration data.

Model parameters for parameter estimating procedures, during calibration, should be chosen based on ranking as to their contribution to output uncertainty (Donatelli and Stöckle, 1999). Donatelli and Stöckle (1999) suggested that parameters (of the CropSyst model) be adjusted in the sequence:

(i) crop phenology (thermal time at emergence, flowering and physiological maturity);

(ii) crop morphology (maximum root depth and PAR extinction coefficient); and

(iii) crop physiological parameters (specific leaf area, stem/leaf partitioning coefficient, leaf area duration, optimum temperature for growth and the duration of the effect).

Most useful plant performances for calibration as suggested by Hunt and Boote (1998) include:

(i) the time of occurrence of the major stages of plant development;

(ii) the dry weights of the major organs at various times throughout the growing season;

(iii) the final yield and its components;

(iv) the number of branches, leaves, fruits and other organs; and

(v) the main stem and branch heights. For water and nutrient stress they suggested a record of the distribution of roots, water and inorganic nitrogen in the soil profile during the course of the growing season.

If a model is not embedded in a parameter-estimating procedure, independent subsystems are identified and calibrated, taking care that once a subsystem is calibrated, that subsystem is not modified in following calibration steps, followed by calibration of single parameters from each independent subsystem (CAMASE, 1995).

A model has to be recalibrated if it were to be used for purposes of simulating soils and cultivars other than for which it was calibrated (Whisler *et al.*, 1986). While calibration is a necessary part of a model development, it can easily be abused (Whisler *et al.*, 1986). Model parameters should be adjusted for a good reason (Savage, 1993) and great caution should be exercised during the adjustment not to bypass the range known for those parameters (Donatelli and Stöckle, 1999). Otherwise, the process-based model will be degraded and calibration may become merely a work of art, which yields good predictions of statistical regression (Donatelli and Stöckle, 1999), but provides no assessment of prediction uncertainty (CAMASE, 1995).

2.6.2 Model validation

Ideally, there should be exact agreement between simulated outputs and field-measured data for a location of interest (Savage, 1993; Savage, 2001). Unfortunately, this is hardly ever the case. The reason for this could simply be the inherent inadequacy of a model to represent natural systems (Hillel, 1977) and/or errors incurred during experimentation and observation (Whisler *et al.*, 1986).

Validation is a process whereby the model outputs are compared with the experimental observations other than those used to build and calibrate the model, followed by identification and correction of errors in the model until it is suitable for the intended purpose (Whisler *et al.*, 1986). Model predictions and measured data will never lie on the 1:1 line; trends over time are one of the most useful tools to evaluate model performance (Donatelli and Stöckle, 1999).

The dataset for validation should be of high quality (garbage in, garbage out) (Donatelli and Stöckle, 1999), not previously used for model development or calibration (Hillel, 1977; Whisler *et al.*, 1986; Savage, 1993; CAMASE, 1995; Savage, 2001) and representative for the situations in which the model is to be used (CAMASE, 1995).

The purpose for which the model is being validated should be comparable and compatible with the objectives for which the model was developed (CAMASE, 1995). Should any model be proven valid for practical use, the specific purpose and range of acceptable error size with due respect to the specific purpose for which it is valid should be clearly stated (CAMASE, 1995). In validating a model, it is crucial that the processes or natural resources limiting the behaviour of the model be recognized or else using the model in conditions where non-simulated processes dominate may cause erroneous estimates for most of the simulated processes (Donatelli and Stöckle, 1999). To stress the point of objectivity (Hillel 1977; Savage, 2001), validation should be repeatable by other scientists, independent of the modellers (CAMASE, 1995).

Validation should be performed for most useful plant performances for which the model is calibrated. These may include timing of major phonological events, dry matter at certain growth stages, final yield, evapotranspiration, soil water and nitrogen levels, etc (Hunt and Boote, 1998).

Crop models are a collection of hypotheses, and hypotheses cannot be proven absolutely correct; hence crop models cannot be completely validated. However, validation of a model for a range of situations and conditions, starting with the simpler components and advancing towards the more complex, provides ample opportunity to identify area of weakness of the model (Whisler *et al.*, 1986; Savage 1993; Savage, 2001).

There are three ways in which the validation problem can be approached (Cohen and Cynert, 1961) as cited by Hillel (1977):

(i) use of statistical methods to test whether the actual and model-generated timing of events agree;

(ii) regression analysis of model-generated versus actual data and check whether the intercept and slope are significantly different from zero and one respectively; and

(iii) perform a factor analysis on the set of generated time paths and a second factor analysis on the set of observed time paths and see if the two factor loadings are significantly different from each other.

2.7 SENSITIVITY AND UNCERTAINTY ANALYSIS

Simulation output is solely dependent on the structural organization of a model (Ritchie, 1991) and perfection of input data (Donatelli and Stöckle, 1999). The input data can be split into two groups (Kleijnen, 1994), namely user-controlled inputs and inputs that are relatively uncontrollable. The keen modeller may want to know, assuming that the model is perfect, what happens to the output if these controllable inputs are changed, i.e. how sensitive will the output be to changes in certain inputs? Do the data contain flaws, maybe due to natural variability (e.g. weather, soil or genetic variation) or experimental and observational error? If so what is the uncertainty they pose to the simulation output? These questions need to be addressed by sensitivity and uncertainty analysis in conjunction with regression analysis measures (Kleijnen, 1994).

2.7.1 Sensitivity analysis

Sensitivity analysis is the systematic investigation of the behaviour of a model through changes in the model inputs and the analysis of its effect in the model outputs (Savage, 1993; CAMASE, 1995). Responses generated from sensitivity analysis are generally crucial to check whether the model agrees or not with theoretical expectations (Savage, 1993; CAMASE, 1995). Identification of specific inputs to which the output is sensitive signals that attention should be given to those inputs during data collection (Savage, 1993; Kleijnen, 1994). If this input happens to be a controllable one, then optimization techniques can be adopted through management (Kleijnen, 1994).

Sensitivity analysis can be performed by (CAMASE, 1995):

(i) one-at-a-time sensitivity analysis in which one model input is made to vary at a time over some range, keeping all other inputs at their nominal value, in order to observe the output response;

(ii) factorial sensitivity analysis in which several inputs are made to vary simultaneously in order to include interactions between inputs;

(iii) fractional sensitivity analysis considers only a fraction of the input combinations large enough to permit the estimation of interactions between the inputs; and

(iv) local (differential) sensitivity analysis in which responses are analyzed to very small variations around some setting of the input, e.g. nominal values.

Accurate or reliable data should be collected on the important environmental input variables that occur in the real world. If successful, then validation techniques may proceed. Otherwise, uncertainty analysis should be performed (Kleijnen, 1994).

2.7.2 Uncertainty analysis

Uncertainty analysis is the study of output uncertainty as a function of a careful inventory of the different sources of uncertainty present in the model. Uncertainty, ignoring flaws of the model, is a measure of the uncertainty in a model output due to the uncertainties in all the component model inputs. In deterministic crop growth modelling, for example, input data flaws from crop, soil, weather and management may cause uncertainties in the simulated outputs (CAMASE, 1995).

Crop parameter inputs could be erroneous due to random errors related to size and number of observations and systematic errors related to bias in the experiment, measurement, observation and calibration procedures. In addition, crop input parameters may exhibit spatial and temporal variability. Soil and weather inputs required by crop models also show spatial and temporal variation and may have considerable measurement errors (Aggarwal, 1995).

In uncertainty analysis, the model inputs are sampled from certain distributions to quantify the consequences of the uncertainties in the model inputs, for the model outputs. The model is run with the sampled input values to yield an estimated distribution of output of response values characterized by location and dispersion. This distribution may be combined with regression analysis to show inputs that contribute most to output uncertainty (Kleijnen, 1994).

Large uncertainty contributions of individual inputs or groups of inputs to model output indicate that it is worthwhile to know more about these (groups of) inputs, whereas it is less productive to gain new information about other inputs. By the same argument, uncertainty analysis provides support in the selection of calibration parameters (CAMASE, 1995).

2.8 EVALUATION OF MODEL PERFORMANCE

Models have been traditionally evaluated by using Pearson's Product-Moment Correlation Coefficient (r) and sometimes the coefficient of determination (r^2) for comparison of the observed (O) and predicted (P) values. Both r and r^2 as a measure of model performance have been critically criticized as inadequate (Willmott, 1981; 1982) and alternative sets of indices have been proposed (Willmott, 1981) for comparison of O and P values.

Willmott (1981) recommended that the following groups of descriptions be computed and reported for comparison of O and P values:

(i) observed and predicted means ($\overline{O}$ and $\overline{P}$, respectively) and their standard deviations (s_o and s_p, respectively);

(ii) slope (b) and intercept (a) of a least-squares regression between the predicted (dependent variable) and observed (independent variable);

(iii) total root mean square error ($RMSE$) and its systematic (biased or non-random) and unsystematic (unbiased or random) components ($RMSE_s$ and $RMSE_u$, respectively); and

(iv) index of agreement (d).

It has also been mentioned that these summary statistics be accompanied by simple graphics to clarify the relative model's prediction ability.

In evaluating model performance against actual measured data, we strive for a slope (b) of unity and intercept (a) of zero, so that our model will predict events in time and space perfectly (Willmott, 1981; Savage, 1993; Savage, 2001). No model is expected to exactly fit the observed data (Willmott, 1981; Savage, 1993; Donatelli and Stöckle, 1999; Savage, 2001), hence it is not common to find values of unity and zero for b and a respectively (Willmott, 1981). Systematic over- or under-predictions (Willmott, 1981) produce characteristic variations in a and b. These parameters should therefore be computed and reported in order that they may be interpreted and used in partitioning the major sources of error (Willmott,

1981). For a "good" model $RMSE_s$ should approach zero while the $RMSE_u$ should approach $RMSE$ (Willmott, 1981). $RMSE_s$ and $RMSE_u$ following Willmott (1981) are computed as follows:

$$RMSE_s = \left[n^{-1} \sum_{i=1}^{n} \left(\hat{P}_i - O_i \right)^2 \right]^{0.5} \quad 2.1$$

$$RMSE_u = \left[n^{-1} \sum_{i=1}^{n} \left(P_i - \hat{P}_i \right)^2 \right]^{0.5} \quad 2.2$$

$$RMSE = \left[RMSE_s + RMSE_u \right]^{0.5} \quad 2.3$$

where n is the number of observations, and $\hat{P}_i$ is derived from $\hat{P}_i = a + bO_i$.

Willmott (1981) suggested an index of agreement (d) which reflects the degree to which the observed variate is accurately estimated by the simulated variate. The index of agreement (d) following Willmottt (1981) is expressed by:

$$d = 1 - \frac{\sum_{i=1}^{n} \left(P_i - O_i \right)^2}{\sum \left[\left| P_i' \right| + \left| O_i' \right| \right]^2}, \qquad 0 \le d \le 1 \quad 2.4$$

where $P_i' = P_i - \bar{O}$ and $O_i' = O_i - \bar{O}$.

This index of agreement (d) is a measure of the degree to which a model's predictions are error free or the degree to which the observed deviations about $\bar{O}$ correspond, both in magnitude and sign, to the predicted deviations about $\bar{O}$. At the same time, d is a standardized measure developed in order that (i) it may easily be interpreted and (ii) cross-comparisons of its magnitudes for a variety of models, regardless of units, can readily be made. It varies between 0.0 for complete disagreement, and 1.0 for complete agreement between the observed and predicted observations. Relationships described by d often tend to complement the information contained in $RMSE$, $RMSE_s$ and $RMSE_u$ (Willmott, 1981).

Finally Willmott (1981; 1982) suggested that the interpretation of these measures be descriptive, based on sound scientific grounds rather than on the measures' of statistical significance.

2.9 CONCLUSIONS

Understanding complex cropping systems can be simplified using models. Dynamic crop simulation models can be useful as research tools, teaching aids, and agronomic grower tools. Whenever these crop simulation models are used for specific situation they have to be calibrated and validated using input dataset of soil, weather, management and crop cultivar information. The output from these simulation models is largely dependent on the input dataset. Input data that contribute most to the output should be identified through sensitivity analysis and great caution exercised in the data collection of such inputs. Uncertainty analysis is a necessary requirement if the reliability of the input data is questionable. Crop simulation models should be evaluated using indices of total mean square error (*RMSE*) and its systematic ($RMSE_s$) and unsystematic ($RMSE_u$) components, and the index of agreement (*d*).

3 CROP SIMULATION APPLICATIONS: LITERATURE REVIEW

3.1 INTRODUCTION

The need for measuring the amount of water supplied to crops has grown as the scarcity on the one hand and the excess of water on the other hand has become a limitation to crop production. There has been a lot of searching and re-searching in this field with a prime concern of nourishing crops with water at the right time and in the right amount. The attempts range from those involving simple observations on the plant or soil to measurements involving sophisticated instruments either directly on the plant, soil, atmosphere or a combination thereof. The incipient stress that is experienced in the crop is a result of interaction of the crop, soil and atmosphere; hence irrigation management would yield more to specified objectives if these three components could be measured precisely and accurately. Nowadays computer models that use information from the crop, soil and atmosphere, at various levels of integrity and complexity, are available to assist agriculturalists on deciding when and how much water to supply to crops. It has also been recognized that it is not only the water but also other management practices as well that have negative impacts on crop production. In addition, environmental issues entering the scene have made the system too complex to manage, hence the need for a better management tool. Coupling of the soil water balance with crop groth models have been found to be promising tools in satisfying several of the objectives in an optimal manner. These crop growth models could be used at farm and/or regional levels, and research sites. They could assist the users in planning ahead by exploring the past, performing management decisions, yield forecasting, studying the effect of global climate change on crop productivity and identifying research needs and priorities in relation to various objectives.

3.2 OVERVIEW OF IRRIGATION SCHEDULING METHODS

The primary objective of irrigation scheduling methods is to apply water to maintain crop evapotranspiration when precipitation is insufficient and water stored in the soil has been depleted to a level which decreases crop productivity significantly (Phene *et al.*, 1989). Any method of irrigation scheduling should be capable of alerting the irrigator at the right time to apply the right amount of water without adversely affecting yield and quality of the

harvestable product. Most of the methods that have been employed and investigated so far use the soil, plant, atmosphere system or a combination thereof as a means of scheduling irrigation. Some of these methods, standing alone, may not tell when or how much water to irrigate - hence the need to be complemented by other irrigation scheduling methods.

Phene *et al.* (1989) have broadly classified approaches of irrigation scheduling as: (i) plant indicators; (ii) soil indicators and (iii) soil water balance techniques. In addition to these, surface energy balance methods that allow for the measurement or calculation of the total evaporation at the surface are available (M J Savage, SPACRU, University of Natal, pers. comm. 2002).

Techniques available for assessing plant water stress for scheduling irrigation using the plant indicators approach include appearance and growth indicators of water stress (Haise and Hagan, 1967), leaf temperature and reflectance measurement (Jackson, 1977), plant water measurements (Savage and Cass, 1984) and stomatal apertures (Haise and Hagan, 1967). Most of these techniques require highly trained expertise and/or sophisticated instrumentation. The major problem with such techniques lies in that the decision of when-to-irrigate may be reached after the plant has undergone certain water stress that may adversely affect the plant and cause significant reduction in yield (Singh *et al.*, 1995). Most of these techniques, even at best, may indicate time of irrigation but give no information on the amount of water to be irrigated (Hillel, 1990).

Soil indicators for irrigation scheduling involve observation and measurement of soil water content, soil water potential or both. These techniques may include detection of soil water content by appearance and feel (Merriam, 1960, as cited by Singh *et al.*, 1995), gravimetry (Reynolds, 1970), neutron probe (Long and French, 1967; Gear *et al.*, 1977), TDR (time-domain reflectometry) (Top and Davis, 1985), FDR (frequency domain reflectometry) (Lukangu *et al.*, 1999), Enviroscan/Diviner 2000 (Sentek Environmental Technologies, 2000), tensiometry (Cassell and Klute, 1986), Watermark sensors (Armstrong *et al.*, 1987), electrical resistance blocks (Carlson and Salem, 1987) and heat dissipation units (Phene *et al.*, 1971). These techniques also require experts or experienced personnel and/or certain instruments. The 'when' and 'how much' water to irrigate may be answered if lower and upper threshold values of soil water content or potential are determined. The lower point would serve as a signal to commence irrigation and the upper point, a time to stop irrigation thereby giving

information on the amount of water to be applied for irrigation. This may be simplified if a relation between volumetric soil water content and soil matric potential is established. The former indicates the amount of water to be applied and the latter indicates the ease of availability of water to plants, hence timing of irrigation.

The amount of soil water available to the plant is not a function of the soil alone, but also the plant and the atmosphere, and may yield better when considered from the soil, plant and atmosphere perspective. Soil water balance techniques of irrigation scheduling are based on such principle. Use of the soil water balance technique to manage irrigation involves estimating the amount of water stored in the crop root zone from the component parts: precipitation, irrigation, interception, runoff, soil evaporation and transpiration, upward movement of water and deep percolation. This allows the irrigator to maintain a balance of the plant available water in the soil profile of the root zone. Though many variations in formulation of the soil water balance techniques exist, depending on the level of complexity, a general equation that encompasses all the components can mathematically be represented as:

$$\frac{dW}{dt} = Pr + Ir + Wt - In - Ro - Pe - Es - Tr \qquad 3.1$$

where $\frac{dW}{dt}$ is the change in soil water content over time in the crop root zone due to addition of water through precipitation (Pr), irrigation (Ir) and supply of water from shallow water table (Wt) and loss of intercepted water through evaporation from the plant canopy foliage (In), surface runoff (Ro), percolation below the root zone (Pe), evaporation from the soil and residue (Es) and transpiration by the plant (Tr).

Most crop growth simulations use the last technique as part of their model for monitoring the soil water balance in the root zone. Hence due emphasis will be given to this technique of irrigation scheduling as part of crop growth model in following sub-sections.

3.2.1 Irrigation timing criteria for soil water balance techniques

The decision of when to apply irrigation water is generally affected by several factors: aim of the irrigation (maximizing crop yield, maximizing net returns, environmental considerations, etc), availability and quality of water, climate (humid, semi-arid, arid, etc), crop

content and soil depth of adjacent soil layers (e.g., Ritchie, 1998). Several soil water balance models may by-pass this component. Some models also by-pass interception, others incorporate it by considering some assumptions. For example, Stroosnijder (1982) and Campbell and Diaz (1988) assumed that interception by the canopy is the same as the fractional interception of radiation and storage capacity of the canopy. Runoff is usually calculated using curve number techniques developed by the USDA-Soil Conservation Service. It can also be computed from locally developed correlation between amount of storm water and runoff (Stroosnijder, 1982). In most irrigated lands, runoff is not considered in soil water balance equations because it is assumed not to occur from irrigated fields. Drainage beyond the root zone is usually computed as a function of water content at field saturation and drained upper limit (e.g., Ritchie, 1998). Soil and plant evaporation are the most important components of the soil water balance models, and their estimation deserves more attention.

Many methods of estimating reference evaporation have been developed. These methods use air temperature, energy balance, evaporation devices or a combination thereof for estimation of reference evaporation (Hatfield and Fuchs, 1990; Jensen *et al.*, 1990) and thereby potential crop evapotranspiration. Although the soil water balance can accommodate any of the above methods, the energy balance or combination methods are more commonly used in crop growth models. The potential crop evapotranspiration needs to be partitioned into potential transpiration and potential soil evaporation from the soil surface, basically using Ritchie's (1972) approach. This approach uses leaf area index (LAI) as a main criterion for the partition. The difficulty of measuring LAI for this partitioning has been recognized and thus certain procedures have been introduced into the crop simulation models for its simulation (Ritchie, 1998). Net radiant density is a required variable in the energy balance or combination method of reference evaporation estimation. This variable is usually estimated from solar radiant density data that is required as an input in most crop simulation models. If solar radiant density is not observed at the respective sites, it can be estimated from air temperature (e.g., Ramkrishnan and Ritchie, 2000) and rainfall data (e.g., Campbell and Diaz, 1988).

Ritchie (1972) calculated the rate of soil evaporation based on two stages: the constant rate and falling rate stage. In the constant rate stage, the soil is sufficiently wet to allow transport of water from the topsoil layer to the adjacent atmosphere at a potential evaporation rate. During this stage of drying, the supply of energy reaching the soil surface is assumed to be

content and soil depth of adjacent soil layers (e.g., Ritchie, 1998). Several soil water balance models may by-pass this component. Some models also by-pass interception, others incorporate it by considering some assumptions. For example, Stroosnijder (1982) and Campbell and Diaz (1988) assumed that interception by the canopy is the same as the fractional interception of radiation and storage capacity of the canopy. Runoff is usually calculated using curve number techniques developed by the USDA-Soil Conservation Service. It can also be computed from locally developed correlation between amount of storm water and runoff (Stroosnijder, 1982). In most irrigated lands, runoff is not considered in soil water balance equations because it is assumed not to occur from irrigated fields. Drainage beyond the root zone is usually computed as a function of water content at field saturation and drained upper limit (e.g., Ritchie, 1998). Soil and plant evaporation are the most important components of the soil water balance models, and their estimation deserves more attention.

Many methods of estimating reference evaporation have been developed. These methods use air temperature, energy balance, evaporation devices or a combination thereof for estimation of reference evaporation (Hatfield and Fuchs, 1990; Jensen *et al.*, 1990) and thereby potential crop evapotranspiration. Although the soil water balance can accommodate any of the above methods, the energy balance or combination methods are more commonly used in crop growth models. The potential crop evapotranspiration needs to be partitioned into potential transpiration and potential soil evaporation from the soil surface, basically using Ritchie's (1972) approach. This approach uses leaf area index (LAI) as a main criterion for the partition. The difficulty of measuring LAI for this partitioning has been recognized and thus certain procedures have been introduced into the crop simulation models for its simulation (Ritchie, 1998). Net radiant density is a required variable in the energy balance or combination method of reference evaporation estimation. This variable is usually estimated from solar radiant density data that is required as an input in most crop simulation models. If solar radiant density is not observed at the respective sites, it can be estimated from air temperature (e.g., Ramkrishnan and Ritchie, 2000) and rainfall data (e.g., Campbell and Diaz, 1988).

Ritchie (1972) calculated the rate of soil evaporation based on two stages: the constant rate and falling rate stage. In the constant rate stage, the soil is sufficiently wet to allow transport of water from the topsoil layer to the adjacent atmosphere at a potential evaporation rate. During this stage of drying, the supply of energy reaching the soil surface is assumed to be

limiting the actual soil evaporation. As the soil becomes drier, actual soil evaporation becomes more dependent on the soil properties and less on the available energy and the falling rate stage starts to take effect. At this stage of drying, actual soil evaporation is dependent on the soil hydraulic properties and the time spent in this stage. Other models (e.g., van Keulen 1975; Campbell and Diaz 1988) compute actual soil evaporation at this stage as a function of potential soil evaporation and the remaining evaporable water in the soil.

In most soil water balance models crop water uptake and actual crop water transpiration are considered to be equal, assuming crop water storage is negligible (e.g., Stöckle and Nelson, 2000). When water is freely available transpiration proceeds at a potential rate. When water is limiting, actual transpiration from each soil layer is simulated as a function of the difference in water potential between the soil and plant xylem within that layer (e.g., Campbell and Diaz, 1988; Campbell and Stöckle, 1993; Stöckle and Nelson, 2000).

It is not only the water that moves into the soil but also the plant roots grow and extend to where there is water, hence correct simulation of root growth is necessary for correct simulation of water uptake by plant root under water limiting conditions (Campbell and Diaz, 1988). CropSyst uses a logistic function modified from a sinusoidal function of Borg and Grimes (1986) to simulate root growth as a function of time. DSSAT models simulate root growth based on soil properties and the amount of assimilate partitioned to the roots (Ritchie, 1985). Ritchie (1985) has pointed out his concern on the shortcomings of the-to-date available algorithms and equations for estimation of the dynamics of root growth in the soil. He suggested that more quantitative root growth information be developed rather than the presently employed equations with crude general assumptions that are difficult to verify experimentally.

3.4 APPLICATION OF CROP GROWTH MODELS

It is clear that the crop plays an important role in the soil water balance model, hence correct simulation of growth and development of crops is necessary (Campbell and Stöckle, 1993). When the soil water balance is coupled with a crop model, a strong tool whose benefit goes well beyond irrigation scheduling is conceived. Crop simulation models can be very beneficial in providing researchers, consultants, farmers, policy makers and other users with information

concerning suitability of particular strategies (Thornton and Wilkens, 1998) to specified objectives under variable weather conditions.

3.4.1 Crop management

In crop production environment the future is variable and hardly predictable. Hence all practices involved are associated with a certain level of risk to the agricultural community. Weather, pests, diseases, cost of production (Thornton and Wilkens, 1988), crop varieties and management practices (Uehara and Tsuji, 1998) are among the variables that may cause variability in yield. Crop simulation models cannot be used to predict yield in the future, but they can be used to simulate probabilistic yield options that would probably happen under various conditions (Uehara and Tsuji, 1998). Soil, crop and management practices, location and long-term historical weather are the required inputs for such applications (Whisler *et al.*, 1986; Ritchie, 1991; Hunt and Boote, 1998). The user is required to clearly define his/her objective. Running the simulation with specific objectives would enable the user to identify the constraints involved and thereby diagnose management practices in order to minimize the associated risk and maximize the objectives (Uehara and Tsuji, 1998). The objectives could be risk avoidance and food security in case of subsistence farming, maximizing the net returns as in intensive agricultural systems and a combination of food security and environmental issues at the governmental level (van Keulen and Penning de Vries, 1993).

In crop growth models, risk is analyzed from the simulation outcomes of yield (or any output the model is capable of producing) probability distribution containing the mean, variance and other descriptive statistics. Weather and management risks associated with growing a crop and thus the risks associated with the adoption of new crop variety or management strategies can be assessed. The variables often employed for analyzing risk include planting date, row spacing, planting density, irrigation and fertilizer management levels, crop varieties, soil conditions, etc under a variety of weather conditions (Uehara and Tsuji, 1998).

Hoogenboom (2000) has defined three methods of running crop simulations for management applications: (i) strategic application; (ii) tactical application; and (iii) yield forecasting application. A strategic application involves running crop simulation models prior to the planting of the crop to assess alternative management strategies through a probabilistic

distribution of outcomes for single or multi-year growing season(s). In the multi-year strategic management the output or leftover from one growing season, in terms of soil water and nutrients, is used as an input into the next growing season (Hoogenboom, 2000). The CropSyst model (Stöckle and Nelson, 2000; Stöckle *et al.*, 2003) is constructed under such premises. The pattern over time from such simulations may indicate the stability or instability in the production systems, hence the associated risks. The strategic application can also be used at a farm or regional level (spatial scale) by linking crop simulation models with geographic information systems (GIS) (Hoogenboom, 2000). Historical or statistically generated weather data are usually used for their simulation (e.g., Thornton and Wilkens, 1998).

Boote *et al.* (1996) used the CROPGRO model to evaluate soybean response to planting date in Gainesville, Florida, both under rainfed and irrigated conditions (Fig. 3.1(a)). Based on model simulation, the highest yield were found for days of year which correspond to the recommended planting dates in that region. The lower yield outside these planting dates could be, in general, due to decreased plant height and lower leaf area index for both early and late planting dates. This was attributed to shorter life cycle duration and lower solar irradiance for the later planting date; and longer day length and higher temperature (less optimum conditions) for the early planting date during seed filling. Low rainfall could also be a cause of early season water deficit for the rainfed condition. Ritchie (1985) has also used CERES-Wheat to predict yield in response to early and late planting dates in Altus, Oklahoma in relation to the soil water balance. The late planting date was preferable owing to the use of less stored soil water during the early stage and saving more for the grain filling stage.

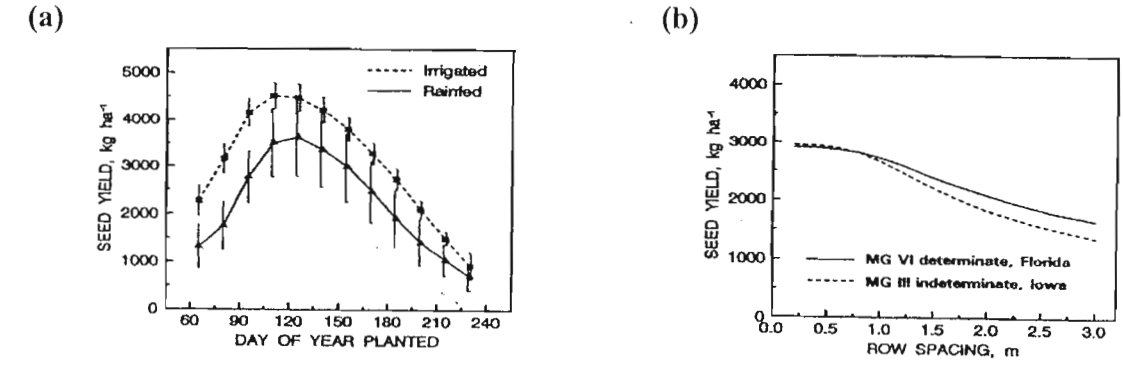

Fig. 3.1 Simulation of soybean yield response to (a) planting date at Gainesville, Florida and (b) row spacing for two maturity groups at Florida and Iowa, using historical weather data (after Boote *et al.*, 1996)

Boote *et al.* (1996) also used the CROPGRO model to predict yield in response to row spacing for indeterminate and determinate cultivars of soybean in Florida and Iowa respectively (Fig. 3.1(b)). Yield simulations from row spacing of 0.2 m and 1.0 m with a constant plant population were compared. The response was in general greater for the 0.2 m row spacing and the increase in yield was higher for Iowa than for Florida. This result confirmed to what is generally accepted in that region; response to row spacing is greater in the Midwestern USA (Iowa) than in the Southern USA (Florida). They attributed this, among other factors, to the slower early canopy development in the cooler Midwest.

Ritchie (1985) has simulated yield from short and long maturing genotypes of wheat using the CERES-Wheat model for Altus, Oklahoma to decide on a better variety for the site, based on the soil water balance. The shorter maturing variety was superior and the credit was given to the reduced risk of depleting the soil water before maturity. Boote *et al.* (1996) have also used the CROPGRO model for selection of soybean cultivars based on simulated yield response in three sites of the Midwestern USA. The model simulation results were consistent with what is generally practiced at those sites.

Jones and Ritchie (1990) have investigated certain options of irrigation strategy using the SOYGRO model by simulating grain yield of soybean in Gainesville, Florida. Three irrigation control depths, four different irrigation threshold levels of available water and one rainfed treatment were used for the simulation. This resulted in thirteen combinations, including the rainfed treatment. From the simulations, a combination with high yield and minimum water use was chosen (Fig. 3.2 (a) and (b)). Irrigation and nitrogen fertilization management in maize for the same site using the CERES-Maize model was also investigated. Maize yield was simulated for irrigated and rainfed conditions using four planting dates and four levels of nitrogen fertilization, all in all 32 combinations (Fig. 3.2 (c) and (d)), to attain the best combination. In such instances, the difference in response to yield between certain combination treatments becomes small and it is imperative that the user incorporates some economic aspects into the simulation.

The agreement between the selection of management practices using the simulated results and locally accepted practices showed that the crop growth models employed for the specific set of conditions were well calibrated and validated. The simulation results from the strategic application also revealed that crop simulation models could be used to maximize certain objectives (e.g., high yield with minimum water) from a combination of management practices

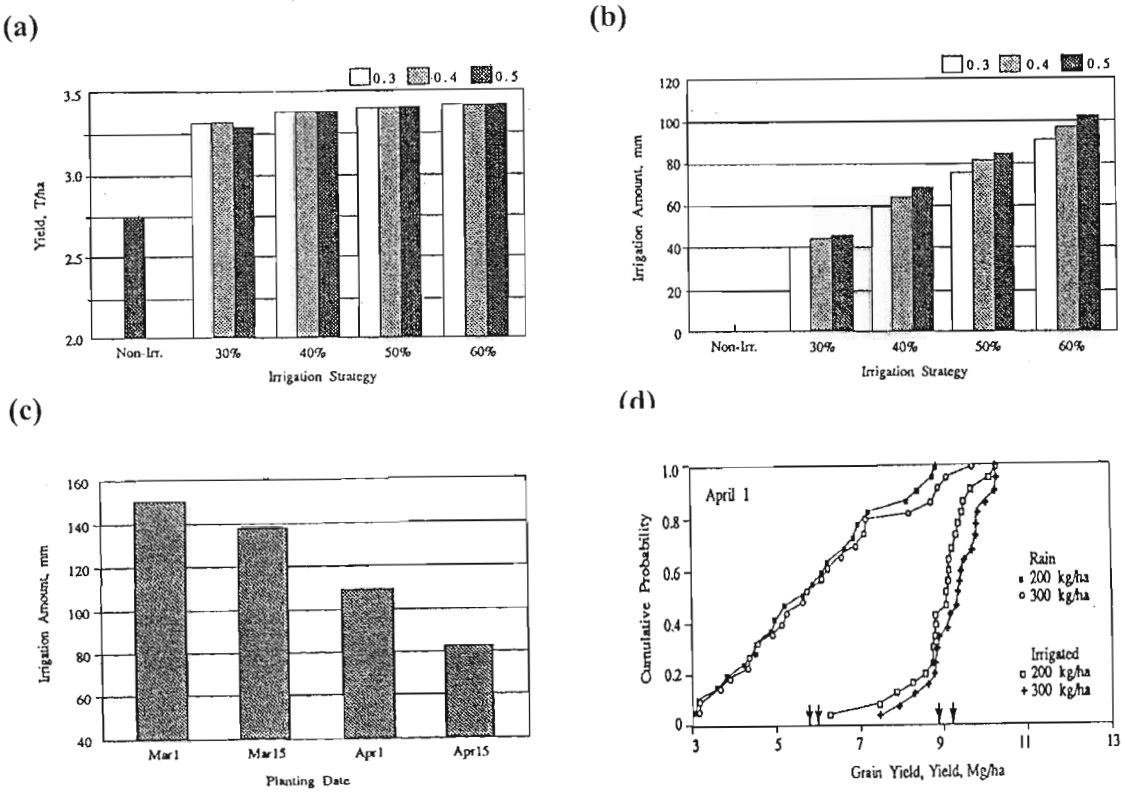

Fig. 3.2 (a) Simulation of soybean yield response to three irrigation strategies, (b) simulation of soybean irrigation water requirements for three irrigation management strategies, (c) simulation of maize irrigation water requirements, average over 16, 21, 23 and 23 years, using historical weather data for Gainesville, Florida, and (d) simulated cumulative probabilities of maize yields for two nitrogen levels (200 and 300 kg ha^{-1}) in irrigated and rainfed soils for maize planted in April 1 (after Jones and Ritchie, 1990)

depending on probabilistic yield simulation outcomes.

Tactical management application refers to running crop simulation models prior to or during the growing season in response to the current soil and weather conditions. Historical or generated weather data are used for the unknown future weather conditions to be replaced from weather forecasts, as they become available, and later from observations. The succession of historical or generated weather data by weather forecasts and further by observations during the growing season reduces the prediction error. Certain management combinations could be used for the simulation and the probability outcomes could be used for assessing the risks involved in selection of management options (Hoogenboom, 2000).

In arid and semi-arid regions, where the onset and intensity of the first rain plays a decisive role in crop production, tactical decisions of planting date, crop variety (short or long season cutlivars), planting density, and timing, amount and type of fertilizer using crop simulation models could be indispensable in avoiding risks (van Keulen and Penning de Vries, 1993).

In the western United States, on farm tactical decisions of irrigation scheduling were made using a simple 'soil water balance model'. Weather related information was supplied through a local newspaper and the farmers were required to specify soil and crop inputs. The soil water can then be tracked on the basis of rainfall, irrigation, soil physical parameters and weather variables. The soil water was also updated from field measurements using a neutron moisture probe. Irrigation scheduling for the following week was also estimated by introducing weather prediction into the system (Hill, 1991).

When only one objective is considered, comparison of production may provide a simple understanding of decisions between alternative strategies to minimize risks (Ritchie, 1985) but as the objectives increase in number and diversity, incorporation of economic factors into decision making seems inevitable. An optimization procedure can also be integrated into crop growth models to allow the computer to automatically search for management strategy that maximizes specific objectives for the user (Alocilja and Ritchie, 1990).

MacRobert and Savage (1998) developed a wheat irrigation optimization program, WIRROPT7, to predict irrigation strategy for wheat in Zimbabwe that aimed at attaining maximum net returns. The program used ZIMWHEAT crop model, a modified version of CERES-Wheat for Zimbabwe. It was used for decisions regarding the use of deficit irrigation within the constraints of land and water availability. It requires inputs of soil, crop management, weather, irrigation constraints and economic criteria. The model outputs include within season irrigation application dates, phenology and yield. The outputs were then interpreted into monetary values for determination of the best irrigation strategy that brings maximum net returns.

Thornton and MacRobert (1994) have used gross margins as a criterion for scheduling application of nitrogen fertilizer of maize using a linkage of CERES-Maize crop model and an optimization program in Gainesville, Florida. Traditionally predetermined schedule and schedules based on weather data (for single years and average across all years) were used. The gross margins from the simulation result of the three scheduling treatments were compared. The yearly-optimized schedule had highest gross margin followed by the across-all-years optimized schedule. From this it was concluded that in the absence of real weather data, nitrogen fertilization should be scheduled on the basis of simulation from long-term weather data. The authors were, from a management point of view, skeptical about unrealistically small amounts of nitrogen applications resulting from the optimization processes.

A cotton simulation model, GOSSYM (Whisler *et al.*, 1986), has been coupled with an expert system (COMAX) to develop an on-farm tactical decision for irrigation and fertilizer recommendation. The EPIPRE (Rabbinge and Bastiaans, 1989) model for wheat pest management in the Netherlands has also been successfully used for on-farm pest management decisions. The GOSSYM-COMAX and EPIPRE models were effective in teaching the model users on how they can incorporate their experience and field observations into on-farm applications (Sinclair and Seligman, 1996; Hoogenboom, 2000).

Crop simulation models for application of forecasting use the same simulation principles as tactical applications except that the final interest is yield or any other outcome that the model is capable of predicting rather than management decisions (Hoogenboom, 2000). Yield forecasting, usually regionally, can provide information necessary for marketing at growers level and estimation of the effects of production on future prices at national level (Hodges *et al.*, 1987) and on food security (Thornton and Wilkens, 1998).

Thornton *et al.* (1997) and Thornton and Wilkens (1998) have used CERES-Millet to illustrate millet yield forecasts for Dori in northern Burkina Faso for the 1986 and 1990 growing seasons (Fig. 3.3). The pre-season yield was predicted on the basis of probabilistically generated weather data so that it was the same for both growing seasons at the start of the simulation, thereafter yield prediction continued on a decadal basis. Remotely sensed estimates of rainfall in real time, embedded in a geographical information system, replaced the historical rainfall data. The standard error of prediction, which was large at the beginning of the season, became smaller with progressive replacement of generated weather data. The fourth forecast, from total of eleven during the growing season, indicated that the yield would be below and above average for the 1986 and 1990 growing seasons respectively.

Hodges *et al.* (1987) used CERES-Maize in the US Cornbelt for regional yield forecasting. Historical weather data from the Cornbelt, matching weather forecasts for the coming 30 days, based on Monthly Outlook from the National Weather Service were used. These were replaced by observed weather data in the model to the date of forecast, aiming to narrow the prediction error. Yield was forecasted on a bi-weekly basis. The final model-predicted yields for the years of 1983, 1984 and 1985 were 97, 98 and 101% (Fig. 3.4) of the national official

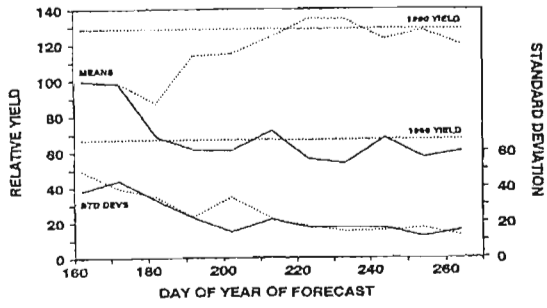

Fig. 3.3 Simulated millet yield distributions derived at various forecast dates using historical decadal rainfall totals up to the day of forecast and probabilistic weather thereafter, for the 1986 and 1990 seasons in Dori, Burkina Faso (after Thornton and Wilkens, 1998)

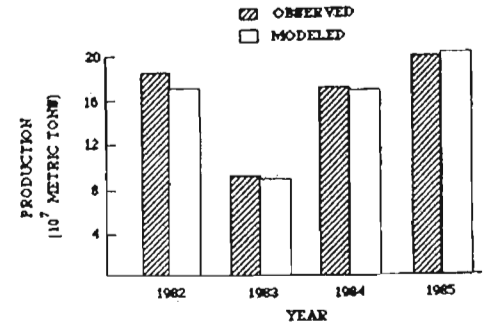

Fig. 3.4 Observed and model-predicted (1982-1985) maize production for the U.S. Cornbelt (after Hodges *et al.*, 1987)

reports (1982 was used for calibration). Production forecast for the last year was made during the growing season.

Conventional simulation exercises have been conducted using point data across spatially variable environment representing multiple fields or regions (Engel *et al.*, 1997). Management practices recommended on the basis of such inputs may not be sufficient enough to represent the entire field and resulting simulations may probably contain errors in the prediction. Physical and chemical soil properties and their variability within fields in time and space are the largest constraints. In an attempt to overcome such problems recent developments include linking, combining or integrating crop simulation models with GIS to visualize and analyze interactions in soil variability, environment and management practices both at farm and regional levels (Hartkamp *et al.*, 1999). This could significantly improve the understanding and interpretation of simulation results provided a computer system that can organize data, define land-use practices across a spatial scale, simulate responses to alternative agricultural practices and, analyze and present simulated results is available (Engel *et al.*, 1997). A region or field can be divided into many smaller homogenous units (usually in terms of soil and weather) so that individual field inputs can be optimized for a specified objective maximization (Boote *et al.*, 1996; NRC, 1997; Hartkamp *et al.*, 1999). This is termed precision farming, alias prescription farming, site-specific farming or variable-rate application. This is made feasible by the availability of field combine monitors and global positioning sensors (GPS) that can produce crop response maps for entire fields (Boote *et al.*, 1996; Hartkamp *et al.*, 1999).

Lal *et al.* (1993) have used a regional agricultural decision support system, known as Agricultural and Environmental Geographic Information System (AEGIS) that links a geographic mapping tool ARC/INFO with DSSAT models to investigate crop management strategies for three areas in Puerto Rico. The study area was divided into eleven internally homogenous units based on soil properties and productivity levels. The DSSAT-BEANGRO Vl.01, dry bean model, was used to illustrate the simulation of yield and irrigation requirements for the areas under study using historical weather data.

Management practices for the simulation included twelve planting dates, two cultivars (long and short season) and two irrigation conditions (rainfed and irrigated). The most important feature of AEGIS (Lal *et al.*, 1993) and other similar programs is their ability to produce thematic maps that assist in understanding and interpreting the results. These maps are the result of the interaction of soil types, environmental variables and management scenarios. The simulated yield maps clearly revealed the yield variation within the study sites due to soil and weather variability. The variation in yield was attributed to the differences in water holding capacity among soils and the variable climate at sites within the study area. The long season variety outperformed the short season variety in the humid areas and also in the semi-arid areas when yield in the long run was considered. Hence the long season variety was recommended for all study sites. The highest yielding planting dates matched with what is practiced at the two of the areas but for the third one, these dates varied considerably for rainfed and irrigated conditions. Irrigation also impaired the effect of planting date, and reduced the yield difference among the sites, though the irrigation requirements varied, increasing from humid to arid environments (Lal *et al.*, 1993).

Engel *et al.* (1997) have developed software called AEGIS/WIN (Agricultural and Environmental Geographic Information System for Windows) by linking the geographic mapping tool Arc View 2 with DSSAT for analysis and evaluation of spatially varying land characteristics, land-use management and agricultural production. The software was used for a simulation experiment by selecting CROPGRO-Peanut from the DSSAT shells for the Southwest Experimental Station at Plains, GA. The study area was divided into 125 internally homogenous polygons with similar soil type and land-use. Two management scenarios were used for the simulation, rainfed and irrigated.

The output maps from AEGIS/WIN that were reported clearly depicted the spatial distribution of yield as influenced by soil type and management practices. Based on the

simulation, the irrigation simulation yields were higher with less variability than rainfed yields, signifying reduced risk for farmers under irrigated conditions. In addition, the amount of irrigation water under non-stress conditions for soils within each plot was investigated with the high yielding plots requiring the highest irrigation water amount. In the same manner, the plots were ranked according to their susceptibility to nitrogen leaching under rainfed and irrigated conditions. All soil types under irrigated conditions showed similar leaching potential.

A question that has to be asked in such management practices is: how effective would this method be in attaining specific goals as compared to other management options? Or how much increase in net return could be achieved by adopting such management strategy over other strategies? Whether such management options, outside research areas, would be viable or not remains to be seen in the future.

3.4.2 Climatic applications

Despite improved crop varieties and irrigation systems, the influence of weather and climate remains a key factor in determining agricultural production (Rosenzweig, 1995). In the last two decades, there has been an increasing consensus among atmospheric scientists on the popular prediction of global warming in the coming decades arising from increased atmospheric greenhouse gas concentrations (Houghton *et al.*, 1992). This effect has been quantified (though the projections are still controversial) to create climatic change scenarios on what the future is likely to be. Worldwide observations from the period of 1951 to 1990 have also confirmed that the daily minimum air temperature of the global landmass has increased by about three times than that of the daily maximum air temperature, thus decreasing the daily air temperature range (Karl *et al.*, 2002). Smith and Hulme (1998) have reviewed means of projecting future climatic variables and stated that global circulation models (GCMs), at present, are the only tools that estimate changes in climate due to increased greenhouse gas concentrations for a large number of climatic variables in a physically based consistent manner. Yet GCMs are not good enough to fully and immaculately represent future changes in climatic variables, thus for better results, they have to be complemented with synthetic climatic scenarios (Smith and Hulme, 1998).

Crop simulation models can be used to accommodate changes in future climatic variables to investigate their impacts on crop production and explore 'what if...' scenarios in seeking

adaptation and mitigation strategies (Curry *et al.*, 1990). Similarly crop simulation models can be employed to address the issue of climatic variability such as El Niño and La Niña (Phillips *et al.*, 2002).

Hoogenboom (2000) has outlined three ways on which projected climatic changes can be applied to serve as inputs to crop simulation models:

(i) historical weather variables of 30 or more years, modified by a synthetic consistent figure representing fixed climatic changes (e.g., Boote *et al.*, 1996);

(ii) historical weather data modified by projected changes of future weather variables resulting from GCMs (e.g., Curry *et al.*, 1990); and

(iii) use of generated weather data whose basis is historical weather data, and modified in the same way as (i) or (ii) (e.g., Donatelli *et al.*, 2000).

Boote *et al.* (1996) have illustrated the response of two soybean cultivars at Ames, Iowa and Gainesville, Florida using the CROPGRO model under rainfed agriculture to changes in air temperature (Fig. 3.5). The mean seasonal air temperature during the growing season for Ames and Gainesville was 21.9 and 27.0 °C respectively for the simulation period. The model predicted a mean seasonal air temperature range of 23 to 24 °C for optimal growth. Decreasing the mean air temperature during the growing season by 2 to 4 °C decreased and increased yield at Ames and Gainesville respectively, while increasing mean air temperature by 2 to 4 °C increased and decreased yield at Ames and Gainesville respectively. From these simulations it was concluded that an increase in the mean air temperature by 2 to 4 °C due to greenhouse effect would reduce soybean yield in the southwestern USA but yields in half of the Midwestern USA may be only moderately affected.

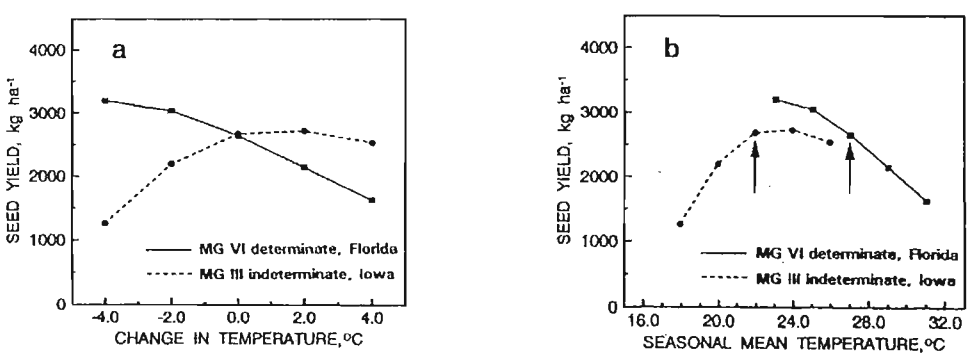

Fig. 3.5 Simulated soybean yield response to decrease or increase in air temperature for two maturity groups in Gainesville (Florida) and Ames (Iowa) using six years of historical weather data. The arrows indicate mean seasonal air temperature over soybean growth cycle at both Ames and Gainesville (after Boote *et al.*, 1996)

Sinclair and Rawlins (1993) have predicted possible inter-seasonal variations in crop yields as effected by global environmental change, maintaining the current weather variability as is, for maize and soybean in Midwest USA at three sites. GCMs and a mechanistic crop growth model were employed for projection of future weather and simulation of yield respectively. A baseline historical weather data with fixed planting date followed by progressive and cumulative increment of increased level of $[CO_2]$ = 600 $\mu l\ l^{-1}$, 3 °C increase to daily maximum and minimum air temperatures, a fortnight earlier planting date and 15% addition to the precipitation amount of each rainy day was used for the simulation. Thus each crop consisted of five combination treatments at each site. The evaluation was based on comparison of season-to-season yield variation and mean yield from each scenario against the baseline. For maize no significant season-to-season variability across years was found for all treatment combinations (Fig 3.6 (a)). Increased $[CO_2]$ caused an increase in yield but the increment was offset when a 3 °C increase in air temperature was introduced into the simulation. This was attributed to shortened growing season due to increased air temperature. Bringing the planting date a fortnight earlier did not help the crop escape the warm temperature, still keeping the yield similar to that of the baseline. The 15% increase in precipitation, however, increased mean maize yield by a level of 10% from the baseline mean yield. In the case of soybean, the scenario was different involving increased season-to-season variability of yield as well as mean yield for all treatment combinations as compared to the baseline (Fig 3.6 (b)). Soybean yield responded positively to increased level of $[CO_2]$, only to be reduced by the introduction of the 3 °C increase of air temperature but still above the baseline. This reduction was

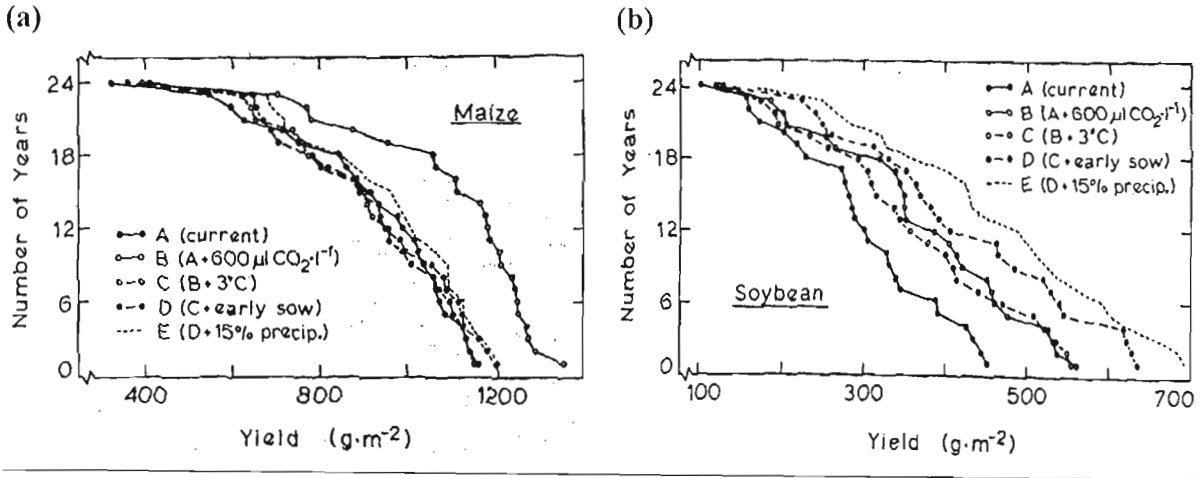

Fig. 3.6 Cumulative distribution plot for grain yields of (a) maize and (b) soybean, simulated using historical weather data at Urbana, IL. The number of years exceeding specific yield are plotted against yield (after Sinclair and Rawlins, 1993)

compensated for when the planting date was brought a fortnight earlier. The increase in precipitation resulted not only in the highest yield predictions but also the highest season-to-season variability in yield. Based on the findings it was concluded that management practices have to be carefully tailored to changing scenarios to reduce risk to the grower.

Williams *et al.* (2001) investigated the impact of possible global climatic changes on farm level yields, soil erosion and economic returns of maize in the Midwestern USA. The Hadley Centre Unified Model (HADCM2), DSSAT crop models, Water Erosion Prediction Project (WEPP) and a simple spreadsheet were used for climate projection, growth simulation, soil erosion simulation and computation of net returns respectively. The research was conducted under present and future climatic scenarios (2050-2059) and management practices consisting of no-till maize, no-till maize-winter rye, maize-beans rotation and also a baseline chisel ploughed and planted with maize on May 1. The HADCM2 model predicted a 3.5 ^{o}C increase in average daily air temperature assuming a doubling of [CO_2] and an increase in mean precipitation of 25 mm per month. The evaluation was based on a comparison of the net returns between both climatic scenarios and within a single climatic scenario for each management practice against the baseline. The simulations from the projected scenarios resulted in reduced yield and net return, and increased runoff and soil erosion. Both baselines showed the highest net returns within the respective climatic scenario. The simulation also revealed that the no-till continuous maize was only 2% less in net returns while the simulated soil erosion was much lower as compared to the baseline. Simulations from the maize-winter rye treatment also resulted in very low simulated soil erosion but a 24% loss of net return as compared to the baseline. Based on these simulation results it was concluded that adoption of cropping systems that are less prone to erosion while maintaining the present yield under changed climate are necessary.

Donatelli *et al.* (2000) have evaluated the impacts of scenarios of climate change on sugar beet production in Italy at two sites. The Hadley GCM and a cropping system CropSyst (Stöckle and Nelson, 2000) were used for estimating changes in future climate and simulating sugar beet yields respectively. Weather data was generated based on historical weather data and modified by GCM outputs to serve as input to the CropSyst model. The GCM output resulted in a consistent increase in air temperature at both sites throughout the simulation period (2040-2090) and increased rainfall during the winter season for all projected years followed by increased and decreased rainfall in the summer for the early and late projection

years respectively. Management strategies of different levels of irrigation and planting dates were incorporated in quest of maximum yield under the created scenarios. The simulation from the modified climate resulted in reduced sugar beet yield but adjusting the planting dates of the simulation eliminated the reduction in yield. The crop owes this increased yield under adjusted planting date to increased photosynthetic activity due to elevated [CO_2] levels and soil water recharge during winter months as compared to the current situations. From the simulation results it was concluded that the threat that climate change poses to sugar beet production in Italy could be minimized by adoption of certain management techniques.

El Niño or La Niña, a recurring weather scenario, has affected global agricultural productivity negatively. It is now possible to predict this El Niño or La Niña event by as much as one year before its occurrence (Phillips *et al.*, 2002). This provides an opportunity for deciding on management options early enough to avoid the likelihood of drought (Phillips *et al.*, 2002).

Phillips *et al.* (2002) investigated the effect of changing planting dates during El Niño or La Niña on maize yield in Zimbabwe at four sites. El Niño or La Niña years were identified from 39 years of observed historical weather data. The former was identified by decreased precipitation and shortened rainy season as compared to normal and La Niña years. Simulation exercises were performed using identified El Niño years with normal, a fortnight earlier and a fortnight later than normal planting dates. The El Niño years gave lower yields but with the planting date adjusted to a fortnight earlier than normal, the yield was improved. This was attributed, in case of the El Niño years, to shift of the pollination period before the onset of the dry spell. Under La Niña years, early planting helped the plants to utilize and store nitrogen fertilizers on their leaves which otherwise would have been leached away under normal planting date before plant growth is strong enough to take it up.

3.4.3 Policy analysis tool

Environmental considerations, at present, are sensitive issues that warrant attention for sustainable agriculture. Policy makers are faced with the challenge of ensuring the practice of agriculture without abuse of the environment in response to increasing population growth, though much abuse has already been done (Savage, 2001). Fertilizer management, soil erosion and climatic effects are among the factors that need to be considered (Boote *et al.*, 1996).

Crop simulation models can assist policy makers in deciding the best management decision to reduce fertilizer and pesticide leaching, and soil erosion. Large area yield forecasting as illustrated by Thornton and Wilkens (1998) can provide information for early warning systems and thereby mitigation strategies. Moreover, response of yield to probable climatic change can be simulated to aid policy makers in their final decision (Boote *et al.*, 1996).

3.4.4 Research applications

Crop simulation models require a thorough understanding of the complex interactions that occur in the soil and atmosphere in relation to the plant. This calls for teamwork between soil scientists, agrometeorologists and plant scientists (Savage, 2001) and also economists to evaluate the profitability of adoption of certain practices (Boote *et al.*, 1996) in relation to specified objective(s). Individual scientists from each discipline usually adopt a reductionist approach to examine and develop certain processes or sub-models that are further systematically analyzed in an interdisciplinary manner resulting in an integrated and balanced model (Boote *et al.*, 1996). This enables the participants to predict the future behaviour of the cropping system under varying environmental and future conditions in a reasonable manner (Savage, 1993; Boote *et al.*, 1996). By doing so the participants gain an insight into the working nature of the system beyond their respective disciplines (Savage, 1993; Boote *et al.*, 1996). Once such models have been constructed they can be employed to interpret experimental results within a matter of minutes, in the quest of management strategies that maximize specific objectives, which may consume a life career of an agronomist if traditional procedures were to be followed (Whisler *et al.*, 1986).

Crop simulation models can also be used to quantify the gap between actual and potential yield, and hence diagnose yield gaps. Actual crop yield is a result of the genetic potential of the crop and its interaction with weather conditions, physical and chemical properties of the soil, insects, weeds, pests and management practices (Jones and Ritchie, 1990). Climatic or non-climatic factors could be the cause for the gap between the actual and potential yield (Boote *et al.*, 1996). Muchow *et al.* (1990) used a crop growth model to evaluate maize yields across tropical, subtropical and temperate climates in the USA and Australia, and concluded that much of the variation in maize yield was associated with variation in air temperature and solar irradiance. The maize yield increased with increase in solar irradiance but decreased with increase in air temperature. At present there is little that can be done to alter the air

temperature and solar irradiance at a large scale in order to narrow the yield gap. So efforts to diagnose yield gaps are concentrated on the actual and climatic potential. In climatic potential the factors that determine yield are the genetic characteristics of the crop and environmental factors assuming other factors are well managed to affect yield. Crop simulation models can assist in identifying management practices that limit climatic potential yield, hence mitigation actions can be proposed accordingly.

The problem with most crop simulation models is that it is impossible to consider all the factors that reduce yield. For example, most crop models do not consider all the essential nutrients, damage by insects, disease and weeds. At present most crop simulation models are site-specific in application and yield reduction due to soil and weather variability can be masked. Only when the limitations in crop models are obviated would the diagnosis of yield gaps be fully addressed.

3.5 CONCLUSIONS

Soil water balance models can be used to schedule irrigation amount and timing efficiently. These models coupled with crop models could perform a variety of tasks in the uncertain world. Crop simulation models have been applied extensively and successfully in crop management. They can be used for planning ahead in the future by combining resources from historical weather data, soil, crop and management practices. They could also be used for undertaking on-farm tactical decisions using historical as well as forecasted weather data both locally and regionally. Forecasting yields within the scope of management using crop simulation models could assist in early warning systems ensuring food security and information on production and price relations on a regional or national basis. In addition, these crop simulation models can be used to explore the fate of agricultural crop production with probable climate change scenarios. Crop simulation models are also used to investigate negative impacts of crop production on the environment under varying management practices. These make crop simulation models efficient tools in policy analysis, minimizing abuse of the environment by crop production. Moreover, crop simulation models have been of tremendous help for the researcher in interpreting experimental results and identification of research needs. Despite all the effort researchers are shedding on this field there still seems to be a gap in addressing issues like soil variability, disease, pests and weeds in crop production using crop simulation models.

4 CropSyst MODEL DESCRIPTION

4.1 INTRODUCTION

CropSyst is a user-friendly, conceptually simple but sound multi-year multi-crop daily time step crop growth simulation model. The model has been developed to serve as an analytic tool to study the effect of cropping systems management on productivity and the environment. The model simulates the soil water budget, soil-plant nitrogen budget, crop canopy and root growth, dry matter production, yield, residue production and decomposition, and soil erosion. Management options include: cultivar selection, crop rotation (including fallow years), irrigation, nitrogen fertilization, tillage operations, and residue management. The model code is written in C++ and can be run on WINDOWS or UNIX-based platforms (Stöckle and Nelson, 2000; Stöckle *et al.*, 2003).

The CropSyst model, like most crop models, integrates the soil, crop, weather and management factors in its component sub-models. The essential components of the model include water budget, soil-plant nitrogen budget, crop growth, soil erosion and residue accumulation and decomposition. These sub-models are integrated to provide predictions of crop development and growth, water and nitrogen balance, salinity, daily residue fate, soil erosion by water and pesticide fate (Stöckle and Nelson, 2000; Stöckle *et al.*, 2003).

CropSyst has been used to model the growth of field crops like maize, wheat, barley, soybean, and sorghum in the Western US, Southern France, Northern and Southern Italy, Northern Syria, Northern Spain and Western Australia with reasonably good results (Stöckle, 1996). Stöckle and Campbell (1985) and Stöckle *et al.* (1994) applied CropSyst to predict grain yield and above-ground biomass of maize in response to a variety of water stress conditions using field experiments conducted at Davis, California during 1974 and 1975 and at Fort Collins, Colorado during 1974. An index of agreement, *d*, 0.950 and 0.954 between the predicted and observed maize grain yield and biomass were reported (Stöckle *et al.*, 1994). Stöckle *et al.* (1994) also applied the CropSyst model to predict the response of irrigated wheat under varying irrigation levels only, and irrigation and nitrogen levels together at Logan, Utah for an experiment conducted during 1983. They reported *d* values of 0.979 and 0.961 in response to water only, and 0.975 and 0.996 to water and nitrogen together for grain

yields and above-ground biomass respectively. CropSyst's predictions of evapotranspiration for irrigated maize at Davis, California (1974 and 1975) and soil water for rainfed spring wheat at Davenport, Washington State (1983) matched well with field measurements conducted using lysimeter and neutron probe respectively (Campbell and Stöckle, 1993; Stöckle *et al.*, 1994). CropSyst, on its application to test the impact of crop production on the environment, followed the trend of observed nitrogen and chloride distribution well (Stöckle *et al.*, 1994). But at the deeper levels the observations were by far larger than the simulated nitrogen and chloride concentrations, signifying additional testing of solute transport in CropSyst (Stöckle *et al.*, 1994). CropSyst's novel feature also lies in its ability to predict crop water use, leaf area index, above-ground biomass, nitrogen dynamics and yield for a number of growing seasons or years without reinitialization. CropSyst predictions of crop water use and yield agreed well with observed records of gravimetric soil water content and yield for twelve crop-seasons during the growing seasons of 1985 to 1991 including crop rotation of sorghum, sunflower and wheat, and management practices of tillage, fertilization and water at Foggia, Italy (Stöckle *et al.*, 1994; Donatelli *et al.*, 1996). Reasonably good predictions of grain yield for maize and barley, and good predictions for soybean were also reported from CropSyst simulations of twelve crop-seasons during the 1985 to 1991 growing seasons at Modena, Italy (Donatelli *et al.*, 1996). Pala *et al.* (1996) validated the CropSyst model for its ability to simulate green leaf area index, above-ground biomass, evapotranspiration and crop nitrogen for two wheat cultivars during a period of three growing seasons (1989/90 to 1991/92) under different water and nitrogen levels at Tel Hadya, Syria. The simulations resulted in an overall d index that ranged from 0.90 to 0.98 and *RMSE* (root mean square error) about 10% with the exception of two observations that resulted in 25 and 32%. The CropSyst model has also been applied to account for varying soil and irrigation water salinity conditions at Davis, California (maize), Fort Collins, Colorado (maize) and Zaragoza, Spain (barley) (Ferrer and Stöckle, 1996). The CropSyst model also includes a weather generator model, ClimGen (Stöckle and Nelson, 1999; Stöckle *et al.*, 2001), to overcome the inadequacy of observed weather data. The CropSyst model is also linked to a geographic information system (GIS) for application of spatially structured data such as soil characteristics, land-use, precipitation, planting dates and other similar data over a region of interest (Stöckle, 1996).

The CropSyst model has also been applied to study the effect of possible climate change on crop production at certain locations in Italy (Donatelli *et al.*, 2000; Tubiello *et al.*, 2000).

Some of the sub-models of CropSyst will be described in the following sections with more emphasis on the water budget and crop growth sub-models.

4.2 SOIL WATER BALANCE

Water plays a key role in determining crop development and growth. CropSyst computes the amount of water used for crop development and growth by modelling the components of the soil water balance. The water balance components considered by CropSyst include: irrigation, precipitation, shallow water table (using finite difference), rainfall intercepted by the crop foliage and surface residue, surface runoff and residue evaporation, infiltration through soil layers, transpiration, deep percolation and water stored in the soil profile (Stöckle and Nelson, 2000; Stöckle *et al.*, 2003):

$$\frac{dW}{dt} = Pr + Ir + Wt - In - Ro - Pe - Es - Tr \qquad 4.1$$

where $\frac{dW}{dt}$ is the change in soil water content over time, Pr is the precipitation, Ir is the irrigation amount, Wt is the supply of water from a shallow water table, In is the amount of water intercepted by canopy foliage and surface residue, Ro is the surface runoff, Pe is the percolation below the root zone, Es is evaporation from the soil and residue, and Tr is the transpiration from the plant.

4.2.1 Precipitation and irrigation

Precipitation and irrigation are the only components that can be easily determined from measurements whereas the other components of the soil water balance need to be modelled. Precipitation amounts can be obtained from actual (generated) daily weather data. Irrigation amounts and timing can be either user-selected or automatically assigned. The current version of CropSyst does not consider runoff or canopy/residue interception of applied irrigation water. All irrigation amounts scheduled or calculated, therefore, are infiltrated into the soil (Stöckle and Nelson, 2000).

4.2.2 Shallow water table

The supply of water from the water table is obtained by setting a saturated bottom boundary to the soil profile at a user-specified depth. This is available, in CropSyst, only for finite difference water transport solution (Donatelli and Stöckle, 1999).

4.2.3 Interception

When precipitation occurs, a fraction of the precipitation that falls on the crop is intercepted by the crop foliage and crop residue, and becomes liable to evaporation without entering the soil or plant (Campbell and Diaz, 1988). The amount of precipitation intercepted by the crop is modelled following Campbell and Diaz (1988), assuming that the fractional interception of precipitation by the canopy is the same as the fractional interception of radiation (FI_c). The actual amount of precipitation that is intercepted, In, is then computed by multiplying the FI and storage capacity of canopy for water, assumed to be 1 mm for full canopy cover.

$$In = 0.001 \cdot FI_c \qquad 4.2^*$$

Interception by surface residue is computed as a function of the amount of surface residue matter, the amount of water currently stored in the residue matter and the maximum water holding capacity of the residue (assumed to be 4 kg of water kg^{-1} of residue) on the ground. When precipitation occurs, and after canopy interception is deducted, the residue layer is filled to its saturated water content (4 kg water kg^{-1} residue) and the remainder of the water then moves into the soil, layer by layer. Residue evaporation proceeds at a potential residue evaporation rate, unless limited by residue water content (Stöckle *et al.*, 1994).

4.2.4 Runoff

CropSyst provides three options (Stöckle and Nelson, 2000) for determining runoff:

(i) no runoff simulation in which CropSyst infiltrates all non-intercepted precipitation and irrigation;

*Hereafter, all equations that follow are taken from the CropSyst User's Manual (Stöckle and Nelson, 2000) unless indicated otherwise

(ii) runoff simulated by employing the USDA-SCS curve number method as a function of current soil water content in the upper one meter (weighted by depth, field slope, and curve number); and

(iii) numerical solution which is available only with the finite difference infiltration model. The last method requires the soil surface storage parameter to be specified in the corresponding soil file.

In the USDA-SCS curve number method, the curve number is automatically selected from other inputs such as soil texture, hydrologic condition, hydrologic group, land-use and selected management practices (Donatelli and Stöckle, 1999). Runoff is then deducted from the water available to enter the soil prior to infiltration. Using USDA-SCS curve number method, daily runoff (*Ro*, m), after the precipitation event is computed:

$$Ro = \begin{cases} \dfrac{(R-0.2S)^2}{R+0.8S} \; if \; R > 0.2S \\ 0.0 \; if \; R \leq 0.2S \end{cases} \qquad 4.3$$

where R (m) is the daily rainfall and S (m) is the surface retention factor.

The remaining water, after interception and runoff are subtracted from precipitation, is assumed to infiltrate into the soil.

4.2.5 Infiltration and soil water movement

The water which is neither intercepted by the crop foliage and surface residues, and which did not end up as runoff, becomes available for infiltration into the soil. CropSyst provides two options for simulating infiltration: (i) the capacity (cascading) method which simulates infiltration and water storage by dividing the soil into layers of 0.10 m (or less) thicker. Any water in a layer exceeding field capacity moves to the next layer and water penetrating past the root zone is lost as drainage. This method assumes that there is no upward flow of water in the soil profile, so the source of evaporated water is precipitation and/or irrigation entering the topsoil layer (Donatelli and Stöckle, 1999; Stöckle and Nelson, 2000); and (ii) finite difference method which uses a numerical solution of Richard's equation for water flux in the soil. This method allows up or downward movement of water. Water moving up out of the first soil

layer may contribute to water ponded on the surface, that can also contribute to infiltration in the following days and/or runoff, depending on surface storage (Stöckle and Nelson, 2000).

4.2.6 Reference evaporation

The reference evaporation models employed in CropSyst are two-step approaches, where the grass reference evaporation from a reference crop, defined as a short (0.12 m high) clipped grass, completely covering the ground, and with plentiful water supply and not short of nutrients, is multiplied by a crop coefficient to obtain the potential crop evapotranspiration (Allen *et al.*, 1998). CropSyst provides three options for the computation of the daily reference evaporation (ET_o, m):

(i) Priestley-Taylor method (following Priestley and Taylor, 1972) which requires only maximum and minimum air temperature and solar radiant density; and

(ii) Penman-Monteith method (following Monteith, 1965) which, in addition, requires maximum and minimum relative humidity or dew point temperature and wind speed; and

(iii) a simpler implementation of the Priestley-Taylor model which only requires air temperature (Stöckle and Nelson, 2000; Stöckle *et al.*, 2003).

The Priestley-Taylor method computes the daily ET_o:

$$ET_o = \frac{\alpha \cdot \Delta \cdot (R_{net} - G)}{(\Delta + \gamma) \cdot \rho_w \cdot \lambda} \qquad 4.4$$

where ET_o (m) is the reference evaporation, α (unitless) is the Priestley-Taylor constant location parameter, Δ (kPa $°C^{-1}$) is the slope of the saturation water vapour pressure function of air temperature, R_{net} (MJ m^{-2}) is daily net radiant density, G (MJ m^{-2}) is the daily soil heat density assumed to be 10% of net radiant density, ρ_w is the density of water (kg m^{-3}), γ (kPa $°C^{-1}$) is the psychrometric constant and λ (MJ kg^{-1}) is the specific latent heat of vapourization.

The Priestley-Taylor constant (α) is a proportionality factor that compensates for the elimination of the aerodynamic component of the Penman-Monteith model. Priestley and Taylor (1972) experimentally derived an average value of 1.26 for α in short grass and humid conditions for calculating ET_o. The constant should be increased for arid and semi-arid

climates. The model adjusts this during execution depending on the value of the water vapour pressure deficit for each simulation day (Stöckle and Nelson, 2000).

The Penman-Monteith model computes the daily ET_o:

$$ET_o = \frac{\Delta \cdot (R_{net} - G) + \left(\frac{DF \cdot (e_s(T_{avg}) - e) \cdot C_{va}}{r_a} \right)}{\left[\Delta + \gamma \cdot \left(1 + \frac{r_c}{r_a} \right) \right] \cdot \rho_w \cdot \lambda} \qquad 4.5$$

where DF (0 to 1) is the fraction of the day that is in daylight, C_{va} (MJ m^{-3} $°C^{-1}$) is the volumetric heat capacity of air taken as 1.2×10^{-3}, ($e_s(T_{avg})$ - e) (kPa) is the water vapour pressure deficit, r_a and r_c (day m^{-1}) are the aerodynamic and canopy resistances to water vapour transfer of the reference crop. For a short clipped grass (0.12 m high) and standardized height (2 m) of wind speed, air temperature and relative humidity sensors (following Allen *et al.*, 1998):

$r_a = 208/u_2$ and

$r_c = 0.000787034$ (this may be adjusted in the case of CO_2 simulation),

where u_2 (m s^{-1}) is the wind speed at 2 m.

The ET_o value computed either from the Priestley-Taylor or Penman-Monteith adjusted to potential crop evapotranspiration (ET_{pot}) of the current crop (or fallow) is given by:

$$ET_{pot} = ET_o \cdot K_c \qquad 4.6$$

where ET_{pot} (m) is the daily potential crop evapotranspiration, ET_o (m) is the Priestley-Taylor or Penman-Monteith reference evaporation and K_c (0 to 1.2) is the ET crop coefficient.

The potential crop evapotranspiration is then partitioned into crop transpiration, soil evaporation and residue evaporation.

4.2.7 Partitioning potential crop evapotranspiration

The daily potential crop evapotranspiration (ET_{pot}) determined by any of the three ET models requires partitioning into potential transpiration (Tr_{pot}), potential soil evaporation (Es_{pot}), and potential residue evaporation (Er_{pot}) for water management and crop development and growth simulation purposes.

4.2.7.1 Potential transpiration

CropSyst computes daily potential crop transpiration (Tr_{pot}) as a function of fractional interception of radiation by the canopy, FI_c, and daily potential crop evapotranspiration, ET_{pot}, following Stöckle and Campbell (1985):

$$Tr_{pot} = FI_c \cdot ET_{pot} \tag{4.7}$$

where FI_c is the fraction of incident radiation intercepted by the crop green leaf area.

4.2.7.2 Potential residue evaporation

Potential residue evaporation (Er_{pot}) is a function of residue mass and canopy cover:

$$Er_{pot} = FC_r \cdot \left(1 - FI_c\right) \cdot ET_{pot} \tag{4.8}$$

where FC_r is the fraction incident radiation intercepted by the residue, estimated from the mass of residue following Gregory (1982):

$$FC_r = 1 - e^{-A_m \cdot M} \tag{4.9}$$

where A_m ($m^2\ kg^{-1}$) is the area covered by one average straw per mass of one average straw crop parameter and M ($kg\ m^{-2}$) the total residue mass per unit area.

4.2.7.3 Potential soil evaporation

CropSyst computes potential soil evaporation (Es_{pot}) as follows:

$$Es_{pot} = (1 - FC_r) \cdot (1 - FI_c) \cdot ET_{pot} \qquad 4.10$$

4.2.7.4 Actual residue evaporation

Actual residue evaporation is assumed to be proportional to the ratio of residue water content to residue water holding capacity (4 kg water (kg residue)$^{-1}$) when residue water content is lower than its water holding capacity; otherwise it is assumed to be at its potential rate (Stöckle and Nelson, 2000).

4.2.7.5 Actual soil evaporation

Actual soil evaporation is simulated by postulating two stages of drying. During the first stage, the evaporation proceeds at the potential rate until the water content in the top evaporative soil layer reaches the permanent wilting point (*PWP*). For second stage drying (it is slightly different for the finite difference model), following Campbell and Diaz (1988):

$$Es_{act} = Es_{pot} \cdot \left[\frac{\theta - \theta_d}{\theta_{ll} - \theta_d} \right]^2 \qquad 4.11$$

where Es_{act} (m) is the daily actual soil evaporation, Es_{pot} (m) is the daily potential soil evaporation, θ (m^3 m^{-3}) is the water content of the top soil layer, θ_{ll} (m^3 m^{-3}) is the lower limit water content of the topsoil layer, and θ_d (m^3 m^{-3}) is the air-dry water content soil of the topsoil layer, estimated as one third of permanent wilting point.

4.2.7.6 Actual crop transpiration

CropSyst computes daily crop transpiration starting from emergence through active growth until physiological maturity. Outside of this period of growth, transpiration is assumed to be zero (Stöckle and Nelson, 2000).

In CropSyst, crop water uptake and actual crop transpiration are considered equal, assuming crop water storage is negligible. For the calculation of crop water uptake, the soil

profile is divided into layers, and the water uptake of each layer is calculated from the water potential difference between the soil and the plant xylem, multiplied by plant conductance (mainly determined by root conductance). The soil conductance is assumed to be large compared to root conductance so that water uptake is not limited by water movement towards the roots (Stöckle *et al.*, 1994; Stöckle and Nelson, 2000).

CropSyst computes the daily water uptake from each soil layer:

$$WU_l = \frac{K \cdot C_l}{1.5}\left(\psi_{sl} - \psi_{xl}\right) \qquad 4.12$$

where WU_l (kg m^{-2}) is the daily water uptake from each soil layer, K is a unit conversion constant (86400 s day^{-1}), C_l (kg s m^{-4}) is the layer root conductance for layer l, ψ_{sl} and ψ_{xl} (J kg^{-1} or m^2 s^{-2}) are, respectively, the soil and plant xylem water potential of layer l and the value 1.5 is a factor that converts total root conductance to total plant hydraulic conductance.

The soil water potential for each soil layer is calculated following Campbell (1985):

$$\psi_{sl} = -a\theta_l^{-b} \qquad 4.13$$

where θ_l (m^3 m^{-3}) is the water content of the l^{th} soil layer, a and b are parameters whose values vary with soil texture. The values of these parameters can be estimated from water contents at upper limit (θ_{ul}) and lower limit (θ_{ll}) with approximated soil water potentials of -30 J kg^{-1} and -1500 J kg^{-1} respectively for some crop species.

$$a = -30 \cdot \theta_f^{\,b} \qquad 4.14$$

$$b = \frac{\ln\left[-1500/-30\right]}{\ln\left[\theta_{ul}/\theta_{ll}\right]} \qquad 4.15$$

CropSyst computes plant xylem water potential (ψ_{xl}):

$$\psi_{xl} = \overline{\psi_{sl}} - \frac{1.5 \cdot Tr_{pot}}{C_{Tc} \cdot K} \qquad 4.16$$

where $\overline{\psi_{sl}}$ is the average of the soil layer water potentials whose value depends on the soil water potential and the fraction of total root length in each soil layer (f_l) and C_{Tc} is the current total root conductance.

If ψ_{xl} from the above equation is less than the xylem water potential just before the beginning of stomatal closure ($\psi_{x,sc}$) due to water deficit, but larger than (less negative) wilting plant water potential ($\psi_{xl,wilt}$), then ψ_{xl} is recalculated:

$$\psi_{xl} = \overline{\psi_{sl}} - \frac{1.5 \cdot Tr_{pot} \frac{\psi_{xl} - \psi_{xl,wilt}}{\psi_{x,sc} - \psi_{xl,wilt}}}{C_{Tc} \cdot K} \qquad 4.17$$

Because ψ_{xl} is on both sides of the above equation, its value is calculated by solving for ψ_{xl}:

$$\psi_{xl} = \overline{\psi_{sl}} \cdot \frac{C_{Tc} \cdot K \cdot \left(\psi_{x,sc} - \psi_{xl,wilt}\right) + 1.5 \cdot Tr_{pot} \cdot \psi_{xl,wilt}}{C_{Tc} \cdot K \cdot \left(\psi_{x,sc} - \psi_{xl,wilt}\right) + 1.5 \cdot Tr_{pot}} \qquad 4.18$$

If ψ_{xl} from the above equation is less than $\psi_{xl,wilt}$ then CropSyst sets ψ_{xl} equal to $\psi_{xl,wilt}$.

The layer root conductance (C_l) is determined from the current total root conductance (C_{Tc}) and the fraction of root length in each layer (f_l):

$$C_l = f_l \cdot C_{Tc} \qquad 4.19$$

The current total root conductance is computed as:

$$C_{Tc} = C_T FI_c \qquad 4.20$$

where the C_T (maximum root conductance) value can be estimated if a maximum uptake rate is assumed for a fully developed green crop, unstressed, fully watered, with unrestricted root penetration, and under an environment providing large atmospheric evaporative demand. Under these set of conditions, any evaporative demand larger than the maximum uptake rate will only induce stomatal closure (Stöckle and Nelson, 2000):

$$C_T = \frac{1.5 \cdot WU_{\max}}{(\psi_{ul} - \psi_{l,sc}) \cdot K} \qquad 4.21$$

where $WU_{\max}$ (kg m^{-2}) is the maximum crop water uptake rate, ψ_{ul} (J kg^{-1}) the soil water potential at the upper limit and $\psi_{x,sc}$ (J kg^{-1}) is the leaf potential just before the beginning of stomatal closure due to water deficit.

CropSyst, then, computes the total daily water uptake WU_t as the sum of water uptake from individual soil layers.

$$WU_t = \sum_{l=1}^{n} WU_l \qquad 4.22$$

4.3 MODELLING CROP DEVELOPMENT AND GROWTH

CropSyst simulates crop development and growth using a generic crop simulator. Crop development is simulated based on thermal time required to complete certain phenological stages. Changes in accumulated thermal time due to water stress, photoperiod and vernalization requirements are accounted for in the model whenever pertinent (Stöckle and Nelson, 2000; Stöckle *et al.*, 2003).

Daily crop growth is expressed as biomass increase per unit ground area. Above-ground crop growth is represented in terms of above-ground biomass accumulation. CropSyst models this growth as: water, radiation, nitrogen and temperature limited crop growth (Stöckle and Nelson, 2000; Stöckle *et al.*, 2003).

4.3.1 Water dependent growth

CropSyst computes the daily water-limited biomass accumulation following Tanner and Sinclair (1983), based on the observed relationship between plant transpiration and biomass accumulation (Stöckle *et al.*, 1994; Stöckle and Nelson, 2000; Stöckle *et al.*, 2003):

$$G_T = \frac{K_{BT} \cdot Tr_{act}}{\Delta e} \qquad 4.23$$

where G_T (kg m^{-2}) is the daily transpiration-dependent biomass production, K_{BT} (kg kPa kg^{-1}) is the above-ground biomass-transpiration ratio, Tr_{act} (kg m^{-2}) is the daily actual transpiration and Δe (kPa) the mean daily water vapour pressure deficit of the air.

4.3.2 Radiation and temperature dependent growth

The Tanner-Sinclair relationship has the advantage of capturing the effect of site atmospheric humidity on transpiration-use efficiency. However, this relationship becomes unstable at low Δe values; for sure, when Δe approaches zero this equation would predict infinite growth. To obviate this problem CropSyst incorporates a second equation for estimating biomass production, following Monteith (1981), based on crop-intercepted PAR (Stöckle and Donatelli, 1996; Stöckle *et al.*, 2003):

$$G_R = e \cdot I_{PAR} \qquad 4.24$$

where G_R (kg m^{-2}) is the daily intercepted PAR-dependent biomass production, e (kg MJ^{-1}) is the radiation-use efficiency factor, and I_{PAR} (MJ m^{-2}) is the daily amount of crop-intercepted photosynthetically active radiation.

Although the parameter e includes the effect of temperature regime prevailing during its experimental determination, air temperature limitations during early growth are not normally accounted for, as a single value is determined for the vegetative period or, more usually, for the entire growing season. It was recognized that this might result in over-prediction of biomass production during early growth, particularly in the case of winter crops. CropSyst includes a temperature limitation factor (T_{lim}) to correct the value of e during early growth

which is assumed to increase linearly from zero to one as air temperature fluctuates from the base temperature for development to an optimum temperature for an early growth (Stöckle *et al.*, 1994; Stöckle and Donatelli, 1996; Stöckle *et al.*, 2003). This is depicted graphically in Fig. 4.1.

$$T_{lim} = \begin{cases} 1.0 \ if \ T_{avg} > T_{opt} \\ 0.0 \ if \ T_{avg} < T_{base} \\ \dfrac{\left(T_{avg} - T_{base}\right)}{\left(T_{opt} - T_{base}\right)} otherwise \end{cases} \qquad 4.25$$

where T_{avg} (°C) is the daily average air temperature, T_{base} (°C) is the thermal time base temperature and T_{opt} (^{o}C) is the optimal air temperature for growth.

Temperature limitation is applied if the current thermal time is less than a user-selected threshold. If it is larger than the threshold, it is assumed that the temperature effect, which is empirically derived using observations during the linear phase of biomass accumulation when temperatures are warmer, is accounted for in the radiation-use efficiency factor, *e* (Stöckle and Donatelli, 1996).

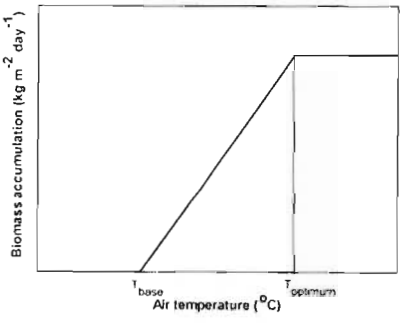

Fig. 4.1 Graphical representation of the effect of air temperature on biomass accumulation

4.3.3 Nitrogen dependent growth

The values of G_T and G_R, the transpiration-dependent and crop-intercepted PAR-dependent biomass production respectively, are compared and the minimum is used as "potential growth" to determine the nitrogen-dependent biomass production (only if nitrogen simulation is enabled). The nitrogen-dependent growth is a function of potential growth after radiation and water limitations have been applied, the critical and minimum crop nitrogen concentration and the crop nitrogen concentration expected after a new growth, as modified by Stöckle *et al.* (1994), Stöckle and Nelson (2000) and Stöckle *et al.* (2003) from Godwin and Jones (1991):

$$G_N = G_{Npot} \cdot \left(1 - \frac{N_{crit} - N_c}{N_{crit} - N_{min}}\right) \qquad 4.26$$

where G_{Npot} (kg m^{-2}) is the daily potential growth after radiation and water limitations have been applied, N_{crit} (kg kg^{-1}) is plant critical nitrogen concentration below which plant biomass growth is reduced, N_{min} (kg kg^{-1}) is the minimum plant nitrogen concentration at which biomass growth stops, and N_c (kg kg^{-1}) is the current plant nitrogen concentration.

4.4 SOIL-PLANT NITROGEN BUDGET

The nitrogen budget in CropSyst includes N transformations, ammonium sorption, symbiotic N fixation, crop N demand and crop N uptake. Nitrogen transformations of net mineralization, nitrification and denitrification are simulated. The water and nitrogen budgets interact to produce a simulation of N transport within the soil. Chemical budgets (pesticides, salinity), including pesticide decay and absorption also interact with the water balance. All balances within the model are checked at each time step and errors are reported in case of departures from set threshold values (Stöckle and Donatelli, 1996; Stöckle and Nelson, 2000; Stöckle *et al.*, 2003).

4.5 MODEL INPUT DATA FILES

In order to run the CropSyst model, five data files are required: these include location, soil, crop, management and simulation control files. Stöckle and Donatelli (1996); Stöckle and Nelson (2000); and Stöckle *et al.* (2003) have summarized the information required for each data file as follows:

The Location file includes information such as latitude, weather file code name and directories, rainfall intensity parameters, freezing climate parameters (for locations where soil might freeze), selection of ET models and associated parameters and generalized information on wind for locations where daily wind data are not available.

The Soil file includes surface soil cation exchange capacity and pH, parameters for the curve number approach (runoff calculation), surface soil texture, and layer thickness, upper and lower limits, bulk density, and bypass coefficient for each and every soil layer. The latter is an empirical parameter to add dispersion to solute transport, particularly when using the cascading approach for soil water redistribution.

The Management file includes automatic and scheduled management events. Automatic events (irrigation and nitrogen fertilization) are generally specified to provide optimum management for maximum growth, although irrigation can also be set for deficit irrigation. Management events can be scheduled using actual date, relative date (relative to year of planting), or using synchronization with phenological events (e.g., number of days after flowering). Scheduled events include irrigation (application date, amount, chemical or salinity content), nitrogen fertilization (application date, amount, source- organic and inorganic-, and application mode- broadcast, incorporated, injected), tillage operations (primary and secondary tillage operations, which are basically related to residue fate), and residue management (grazing, burning, chopping, etc.).

The Crop file allows users to select parameters to represent different crops and crop cultivars using a common set of parameters. This file includes: phenology (thermal time requirements to reach specific developmental stages, modulated by photoperiod and vernalization requirements if pertinent); morphology (maximum LAI, root depth, specific leaf area and other parameters defining canopy and root characteristics); growth (transpiration-biomass coefficient, radiation-use efficiency, stress response parameters, etc.), residue (decomposition and shading parameters for crop residues), nitrogen parameters (defining crop

N demand and root uptake); harvest index (unstressed harvest index and stress sensitivity parameters), salinity tolerance and CO_2 elevation response.

The Simulation Control file combines the different types of input files as desired to produce specific simulation runs. It specifies the start and ending day of the simulation and the crop rotation to be simulated, and sets the values of all parameters requiring initialization. Also inputs to this file allow users to switch on/off the simulation of soil erosion, soil salinity, nitrogen and [CO_2] effects on crop growth, and to select soil water redistribution and runoff models.

Input data files from soil, crop, weather and management factors are integrated in the CropSyst model according to the equations and logic that have been described in Sections 4.2, 4.3, 4.4 and 4.5 to simulate desired process(es). The desired simulated processes could be crop development and growth, soil water balance, soil nitrogen balance, salinity, daily residue fate, soil erosion, and/or pesticide fate. This is made possible by allowing users to select or define certain parameters of their preferences in the five input data files.

The next chapter will focus on description of the site, crops, soil and instruments used during the experimentation. It also discusses the methods used for data collection in the study. The data obtained during the experimentation will serve either as data input for crop simulation exercises or as means of validation against simulated outputs.

5 SITE, CROP, SOIL AND INSTRUMENT DESCRIPTION

5.1 SITE DESCRIPTION

The study was conducted at Cedara Department of Agriculture and Environmental Affairs, located Northwest of Pietermaritzburg in the KwaZulu-Natal Midlands at 29°32´S, 30 °15´E and altitude of 1076 m. According to the Bioclimatic groups of the Natal region, Cedara lies in the Mist Belt zone. Meteorological data from 1970 to 2002 for Cedara was obtained from the Agricultural Research Council, Institute of Soil, Climate and Water, Pretoria, South Africa. Mean monthly averages and standard deviations of the available weather variables are presented in Table 5.1 and Fig. 5.1. Solar radiant density was calculated from sunshine duration using Ångström's (1924) equation with coefficients developed by Reid (1986) specifically for South African conditions. Mean annual rainfall and class A pan evaporation were 844 and 1495 mm respectively indicating that the annual rainfall does not meet the evaporative demand in the area. Fig. 5.1 (c) signifies that supplementary irrigation is required in summer whereas full irrigation is required in winter to meet the evaporative demand of crops.

Table 5.1 Monthly statistics of weather variables as calculated from 1970 to 2002 for Cedara, KwaZulu-Natal, South Africa

Variable	Maximum monthly average		Minimum monthly average		Maximum mean monthly total		Minimum mean monthly total	
	Month	Value	Month	Value	Month	Value	Month	Value
I_s	February	20.50 ± 1.33	June	12.41 ± 0.51	-	-	-	-
T_x	February	25.30 ± 1.27	June	19.19 ± 0.96	-	-	-	-
T_n	February	15.32 ± 0.78	June	3.35 ± 0.83	-	-	-	-
T_{avg}	February	20.31 ± 0.92	June	11.32 ± 0.68	-	-	-	-
Pr	-	-	-	-	January	139.97 ± 59.71	June	13.00 ± 15.08
E_p	-	-	-	-	January	153.34 ± 18.77	June	82.46 ± 10.83

I_s solar radiant density (MJ m^{-2})
T_x, T_n, and T_{avg} maximum, minimum and average air temperatures respectively (°C)
Pr precipitation (mm)
E_p pan evaporation (mm)

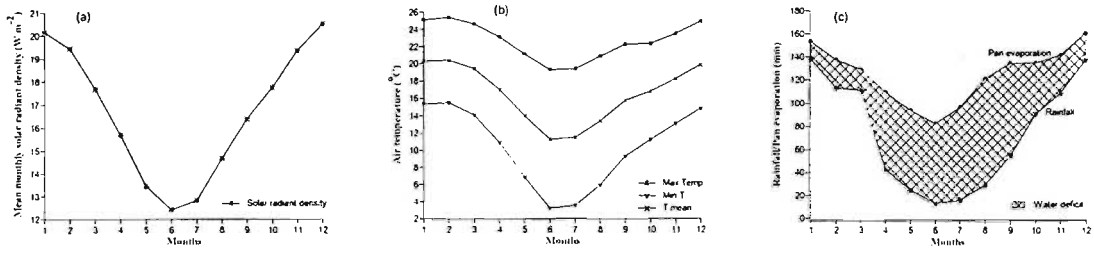

Fig. 5.1 Mean monthly values of (a) solar radiant density; (b) maximum, minimum and average air temperatures; and (c) mean precipitation and pan evaporation as calculated from 1970 to 2002 for Cedara, KwaZulu-Natal, South Africa (Source data- ARC-ISCW)

The experimental field was oriented in the East-West direction with a slope of 6.0 % in the North-South direction. It consisted of 48 plots distributed randomly, each 18 m by 6 m, sown with oats, Italian ryegrass, and rye or left bare in which weeds were controlled by hand or herbicide.

5.2 CROPS

The study area was planted with oats, Italian ryegrass and rye, or left bare (weeds controlled by hand or herbicide) during winter and with maize during summer. The winter plants were sown during the second week of April, and the maize in late November.

5.2.1 Oats

Oats (*Avena sativa* L. cv. Drakensberg) is a cool-season annual grass and grows best in cool, moist climate. It is produced for its hay and seed. It also serves as an excellent cover crop. It is susceptible to air temperatures of 7 ^{o}C or less during germination and seedling stage and hot, dry weather during reproduction. It has a fibrous root system which may extend from 0.85 to 1.95 m. Its above-ground height ranges from 0.60 to 1.50 m. It can grow in a variety of soils with pH as low as 4.5 (UC SAREP, 2002c).

In the study site, oats was sown with a planting density of 90 kg ha^{-1} and a distance of 0.15 m between rows. Oats showed succulent growth type with wider blade than Italian ryegrass and rye. It was also susceptible to lodging by wind and rain.

5.2.2 Italian ryegrass

Italian ryegrass (*Lolium multiflorum* L. cv. Midmar) is a cold tolerant winter-annual grass. It is used for grazing, hay, cover crop and green manure. It has a vigorous seedling establishment that provides a rapid ground cover. It has a fibrous and extensive root system that may extend to a depth of 1.80 m. Its above-ground height may range from 0.90 to 1.20 m. It can grow in a variety of soils with pH range of 6 to 7 (UC SAREP, 2002a).

Italian ryegrass was sown with a planting density of 30 kg ha^{-1} and a distance of 0.15 m between rows. Italian ryegrass, like oats, showed succulent growth type but with narrower blades. It grew as a bunch of grasses rendering a good cover to the ground.

5.2.3 Rye

Rye (*Secale cereale* L. cv. MacBlue) is a cool-season annual grass. Its seeds may germinate at temperatures as low as -3 to -5 °C. It is cultivated mainly for its grain, hay, pasture, green manure and cover crop. It has extensive fibrous roots that may attain a depth ranging from 0.90 to 2.30 m. Its above-ground height may range from 0.90 to 1.80 m. It can grow in a variety of soils (in fact is a volunteer weed) with a range of pH 4.5 to 8, but grows best in well-drained loam and clay soils with pH range 5 to 7 (UC SAREP, 2002b).

Rye was sown with a planting density of 123 kg ha^{-1} and a distance of 0.15 m between rows. It showed an erect, slender growth with narrow leaf blades.

5.2.4 Maize

Maize (*Zea mays* L. cv. PAN 6568) is a warm-season crop grown for its grain, silage and industrial uses. It grows best in areas where the mid-season air temperature ranges between 21 and 27 °C in a season length of 120 to 180 days. Yield of maize declines as mean summer temperatures deviate from 25 °C. Its maximum root depth may extend from 1.50 to 2.00 m. Its above-ground height may range from as low as 0.60 to 6.00 m. It can grow in a variety of soils with a range of pH from 5 to 8 (Miracle, 1966).

Maize was sown with a plant density of 44000 seeds per hectare and a distance of 0.75 m between rows.

5.3 INSTRUMENTS

5.3.1 Diviner 2000 and Profile Probe

Water plays a key role in determining crop development and growth. The CropSyst (Stöckle and Nelson, 2000; Stöckle *et al.*, 2003) model accounts for changes in crop developmental rate due to water stress. It also computes above-ground biomass accumulation at times of high water vapour pressure deficit (Δe) using a relationship between plant transpiration and biomass accumulation. The CropSyst model computes the amount of water used for crop development and growth by modelling the components of the soil water balance. The water balance components considered by CropSyst model include: irrigation, precipitation, shallow water table (finite difference), rainfall intercepted by the crop foliage and surface residue, surface runoff and residue evaporation, infiltration through soil layers, transpiration, deep percolation and water storage in the soil profile (Stöckle and Nelson, 2000; Stöckle *et al.*, 2003). Therefore, measuring soil water content in the field provides a good opportunity to compare measured values with the model-simulated soil water output.

Field soil water content observations were made using the Diviner 2000 (Sentek Environmental Technologies, Stepney, Australia). Diviner 2000 is a portable device that measures soil water content at different depths of the root zone within the soil profile. It consists of a portable probe and a data display unit. The probe consists of a metal rod with a probe cap and a sensor at the bottom. Soil water observations down to the depth of the probe are made through a wall of a PVC access tube into which the probe is inserted. To take a reading, the sensor is simply swiped in and out of the access tube, measuring at regular intervals of 100 mm down the depth of the probe (Sentek Environmental Technologies, 2000).

Diviner 2000 has the advantages of fast measurement time, on-site inspection of readings, allowing repetitive readings at fixed points along the profile, large sampling volume (~ 1.96 litres), no radiation hazard and accuracy to within 1% of the actual soil water measurements. The sensor requires full contact between the soil and access tube as air present inbetween may distort the response of the sensor. Soil water readings may also be affected by distortion of the soil structure that may be caused during access tube installation. Though the manufacturers provide calibration for a range of soils, for accurate measurements the sensor needs to be calibrated for the specific soil at the experimental site (Sentek Environmental Technologies, 2000).

The PR1 Profile Probe (Delta-T Devices, Cambridge, UK) was used for continuous measurement of soil water content at different depths along the soil profile for determination of drained upper limit. It was also used for construction of retentivity curves along with simultaneous measurements of soil water potential. The Profile Probe consists of a sealed composite rod, approximately 25 mm in diameter, with electronic sensors (in the form of pairs of stainless steel rings) arranged at fixed intervals along its length. When taking readings, the probe is inserted into an access tube and the output from each sensor at the fixed intervals along the probe could be obtained either manually by using a hand-held meter or automatically by connecting the probe to a datalogger (Delta-T Devices, 2001).

The Profile Probe has similar advantages and drawbacks as the Diviner 2000. The difference lies in that the Profile Probe can be connected to a datalogger for unattended continuous observations at different depths along the soil profile. This is not possible with Diviner 2000 because it contains only a single sensor whereas the Profile Probe contains multi-sensors. The diameter of the access tube is also smaller in the Profile Probe (~28 mm) than in the Diviner 2000 (~50 mm). The measurement of influence of the Profile Probe is 120° (representative reading requires three measurements) while 360° in the case of Diviner 2000.

Diviner 2000 and Profile Probe use changes in electrical capacitance to measure soil water content. They generate high frequency electromagnetic waves (in excess of 100 MHz) around the sensor(s), extending through the access tube into the soil. Part of the electromagnetic wave is reflected back depending on the dielectric constant of the soil, of which water, by far, is the highest contributor. So the sensor(s) correlate the frequency of the reflected wave from each depth to the volumetric soil water content (Sentek Environmental Technologies, 2000; Delta-T Devices, 2001).

5.3.2 Watermarks and Tensiometers

Watermark (Irrometer, Riverside CA, USA) is a sensor that measures soil water potential by relating the sensor's electrical resistance to the soil surrounding the sensor. Watermark consists of two concentric electrodes embedded in a reference matrix material. The matrix material has a consistency similar to fine sand and is held in place by a synthetic membrane (Thompson and Armstrong, 1987) for protection against deterioration. An internal gypsum tablet buffers against the salinity levels found in irrigated soils (Campbell Scientific, 1996).

The Watermark sensor can measure soil water potential in the range of -10 to -200 kPa, does not need regular servicing and is relatively inexpensive (Thompson and Armstrong, 1987). But it is insensitive to soil water potential above (less negative) -10 kPa and the measurement is also temperature dependent.

Soil water potential is calculated from the sensor's resistance and soil temperature. A linear relationship may be assumed between the soil water potential and the sensor's resistance and temperature in the range of 0 to -200 kPa (Campbell Scientific, 1996). But for more accurate results, Thompson and Armstrong (1987), have developed a non-linear equation between soil water potential, sensor resistance and soil temperature:

$$\psi_{sw} = \frac{R_s}{0.01306 \cdot [1.062 \cdot (34.21 - T_s + 0.0106 T_s^2) - R_s]} \qquad 5.1$$

where ψ_{sw} is the soil water potential (kPa), R_s is the measured resistance and T_s is the soil temperature.

The soil water potential above (less negative) -10 kPa was measured using automatic tensiometers. An automatic tensiometer consists of a porous ceramic cup, a connecting tube (usually filled with deaerated water) and an electrical pressure transducer (Thornton-Dobb and Lorentz, 2001).

Water moves in and out of the tensiometer's ceramic cup in response to pressure differences between the ceramic cup and surrounding soil. The pressure of water inside the ceramic cup comes into equilibrium with the pressure of the surrounding soil water. The pressure of the surrounding soil water is then inferred from the output of the electrical pressure transducer. The tensiometers work better in the wet range than in the dry range. They require regular attention and servicing especially in the dry range at high suction in which air bubbles may be trapped in the connecting tube. At such instances the soil water potential may continue to change but tensiometers fail to register it (Cassell and Klute, 1986).

5.3.3 LAI-2000 plant canopy analyzer (PCA)

The CropSyst model grows the crop based on inputs from soil, plant and daily weather data. By doing so it generates the leaf area index (LAI), leaf area per unit ground area, of the crop with time. The generated LAI is used for calculating radiation and precipitation interception that are further used in modelling potential soil evaporation and transpiration, and biomass accumulation (Stöckle and Nelson, 2000; Stöckle *et al.*, 2003). If the generated LAI happens to be incorrect then it is likely that all the output variables dependent on it will contain certain errors. So this makes the LAI a very important variable in crop modelling and provides a good opportunity for comparison with measured LAI.

Direct measurements of LAI are destructive, time consuming and labour intensive requiring sampling, cutting and measuring of individual leaves. Indirect measurements, on the other hand, are non-destructive, provide fast measurement time and sample a large area. Indirect measurements of LAI involve measurement of radiation above and below the plant canopy and combine this with radiation transfer theories for estimation of LAI and other canopy attributes (Norman and Campbell, 1989).

Indirect measurements were used for estimating LAI using LAI-2000 plant canopy analyzer (PCA) (LI-COR, Lincoln, Nebraska, USA). The LAI-2000 PCA consists of a control unit LAI-2070, optical sensor LAI-2050 and view caps for the LAI-2050. The LAI-2070 control unit contains the necessary electronics to record the sensor's data and compute final outputs. The LAI-2050 hosts a fish-eye lens with a hemispheric field of view and five concentric rings of photodiode detectors. The fish-eye lens is used to focus the hemispherical image onto the concentric ring detectors. Each detector ring views a different portion of the sky. The view caps are used to mask the sensor's azimuthal field of view from the operator, sun or certain parts of the canopy (LI-COR Inc., 1990).

The plant canopy analyzer uses a gap fraction method to deduce information about amount and characteristics of foliage by the probability that a ray of light from a given zenith angle will pass uninterrupted through a plant canopy (Hicks and Lascano, 1995). The LAI-2000 PCA measurements are based upon four assumptions (LI-COR Inc., 1990) of the canopy being measured:

(i) the foliage is black, thus it neither transmits nor reflects radiation,

(ii) the foliage elements are small compared to the area of view of each detector ring,

(iii) the foliage is randomly distributed, and

(iv) the foliage is randomly azimuthally oriented.

No canopy conforms to all these assumptions. The first assumption could be true if diffuse or uniformly overcast sky prevails. The LAI-2050 also contains an optical filter that rejects radiation of wavelengths longer than 490 nm where plant canopies reflect or transmit most of the radiation. The second assumption is true as long as the distance from the optical sensor to the nearest foliage is greater than four times the leaf width. Low-height crops, like grasses, may violate this assumption. Foliage is not randomly distributed but shows systematic clumping. The fourth assumption is violated by species that exhibit some degree of heliotropism (LI-COR Inc., 1990).

The LAI-2000 PCA measurement includes not only leaves but also stems, branches and reproductive organs as well and it cannot distinguish between live and dead leaves and hence the difficulty in separating photosynthetically active leaves (Welles and Norman, 1991).

The basic technique of LAI-2000 PCA combines measurements from beneath and above the canopy with the sensor leveled and viewing skywards. The ratio (below to above) for a given view angle can be expressed by the probability of diffuse non-interceptance $T(\theta)$ (LI-COR Inc., 1990):

$$T(\theta) = \frac{diffuse\ intensity\ below\ the\ canopy\ at\ view\ angle\ \theta}{diffuse\ intensity\ above\ the\ canopy\ at\ view\ angle\ \theta} \qquad 5.2^{*}$$

$T(\theta)$ depends on foliage orientation, foliage density and path length through the canopy. According to Beer-Lambert Law:

$$T(\theta) = exp\left[-G(\theta)\cdot\mu\cdot S(\theta)\right] \qquad 5.3$$

where $G(\theta)$ is the fraction of foliage projected towards angle θ, μ is the foliage density (m^2 foliage m^{-3} canopy) and $S(\theta)$ is the path length through the canopy.

Foliage density is computed following Miller (1967):

* Hereafter, all the equations that are in Section 5.3.3 are taken from the LAI-2000 PCA (LI-COR Inc., 1990) manual unless indicated otherwise

$$\mu = -2 \int_0^{\pi/2} \frac{\ln\ (T(\theta))}{S(\theta)} \cdot \sin\theta \cdot d\theta \qquad 5.4$$

In a full cover, homogenous canopy, foliage density is related to LAI by canopy height z, and path length S is related to canopy height by the zenith angle θ:

$$LAI = \mu \cdot z \qquad 5.5$$

$$S(\theta) = \frac{z}{\cos\theta} \qquad 5.6$$

Substituting these relationships in Eq. 5.4 yields an expression for LAI:

$$LAI = -2 \int_0^{\pi/2} \ln\ (T(\theta)) \cdot \cos\theta \cdot \sin\theta \cdot d\theta \qquad 5.7$$

The LAI-2000 implements this equation by numerical integration using the five measured angles. The detector geometry fixes the value of $\sin\theta\, d\theta$ allowing computation of a constant weighing factor $w(\theta_i)$ for each ring. The numerical integration then becomes:

$$LAI = -2 \sum_{i=1}^{5} \ln\ (T(\theta_i)) \cdot \cos\theta_i \cdot w(\theta_i) \qquad 5.8$$

where i refers to each of the detector rings with view angle centered at θ_i.

LAI was measured in the fields of oats, Italian ryegrass and rye using LAI-2000 PCA (Table 5.2). Jovanovic and Annandale (1998) found LAI of oats and rye measured with LAI-2000 PCA to be over-estimated as compared to directly measured LAI. Therefore, the PCA-measured LAI for oats and rye was corrected according to their findings (Table 5.2). They have also found that the LAI of Italian ryegrass as measured by PCA to be heavily under-estimated as compared to directly measured LAI. In the field at Cedara, however, the PCA-observed values of Italian ryegrass were as equally over-estimated as LAI of oats and rye

Table 5.2 Measured (using LAI-2000 PCA) and corrected values of leaf area index of oats, Italian ryegrass and rye as at various times during the 2002/03 growing season at Cedara, KwaZulu-Natal, South Africa

Date	Oats	Oats (corrected)	Italian ryegrass	Rye	Rye (corrected)
27/06/02	3.17 (0.24)†	2.18	2.82 (0.25)	2.19 (0.12)	1.04
12/07/02	3.09 (0.21)	2.13	2.58 (0.15)	2.39 (0.18)	1.13
26/07/02	4.20 (0.19)	2.87	2.85 (0.21)	2.83 (0.22)	1.32
08/08/02	5.31 (0.22)	3.61	3.66 (0.17)	3.66 (0.15)	1.70
19/08/02	6.70 (0.23)	4.55	4.12 (0.16)	4.70 (0.16)	2.17

† numbers in brackets represent standard errors

and were not corrected.

The orientation of the rows was in the East-West direction with 18 m by 6 m plot size. The spacing between rows was 0.15 m with different planting densities that rendered the canopies to be homogenous. The measurement protocol involved one above-canopy reading followed by four below-canopy readings, at four positions within a plot, in a diagonal transect across the rows with a 270° field of view oriented along the row direction.

Measurement of LAI using LAI-2000 PCA is usually made during diffuse or uniformly overcast sky conditions so that the reflectance and transmittance from the plant parts would be at its lowest. Hicks and Lascano (1995) evaluated the influence of solar direction on LAI-2000 PCA measurements in direct sunlight by shading the sensors and the sample area. Best agreement between LAI-2000 PCA and destructively measured LAI values was found when PCA observations were made either during uniformly overcast conditions or around solar noon using the shading method. Following Hicks and Lascano (1995), all observations of LAI were made around solar noon by shading both the sensor and sampling area with a cream patio umbrella (2.56 m in diameter) that was manually held to block the direct rays from the sun. The measurements were conducted every two to three weeks until the time of harvest. Stakes were put on the four positions in each plot where LAI measurements were made so that the changes in LAI could be tracked over time.

5.3.4 Automatic weather station

Microclimatic data for the length of the growing season was obtained from an automatic weather station (AWS) approximately 100 m away from the experimental site. The AWS consisted of a battery-operated datalogger connected to various sensors (Table 5.3). It was also

Table 5.3 List of weather variables and sensors used for the observation of the weather variables during the 2002-2003 growing season at Cedara, KwaZulu-Natal, South Africa

Variable	Unit	Sensor	Model	Measurement height (m)
Solar irradiance	MJ m^{-2}	Pyranometer	LI-COR pyranometer	2.75
Air temperature	°C	T and RH† probe	CS500 Vaisala	1.5
Relative humidity	%	T and RH probe	CS500 Vaisala	1.5
Wind speed	m s^{-1}	Three cup anemometer	Schiltknecht 57227	2.5
Wind direction	°	Wind vane	Schiltknecht 57227	2.5
Precipitation	mm	Tipping bucket	Pronamic 9603	3.0
Net irradiance	MJ m^{-2}	Net radiometer	REBS, Q*7.1	1.0
Soil heat flux	MJ m^{-2}	Soil heat flux plates	Middleton Instruments, CN3	-0.08
Soil temperature	°C	Type E thermocouple	-	-0.02 and -0.06

†T and RH = temperature and relative humidity

equipped with a solar panel, facing in a northern direction, and a radio antenna for telecommunication purposes.

5.4 SOIL

Realistic simulation and interpretation of crop models require precise specifications of certain soil physical and chemical aspects. Soil is a heterogeneous complex system, made up of three phases: the solid phase, which constitutes the soil matrix, liquid phase consisting the soil water and the gaseous phase making up the soil atmosphere (Hillel, 1982). These three phases are in continuous interaction with each other and the environment to characterize the soil system (Hillel, 1982) and accordingly state the well being of plants. Therefore it becomes imperative that the soil is analyzed for its chemical and physical behaviour, since the continuous interactions render the soil to have different chemical and physical attributes that affect crop productivity.

Chemical and physical soil characteristics that are required as inputs by the CropSyst model include, among others, aspects such as CEC, pH, steepness and slope length, particle-size distribution, bulk density, water retention and hydraulic conductivity (Stöckle and Nelson, 2000; Stöckle *et al.*, 2003).

5.4.1 Particle-size analysis

Particle-size analysis is a means of measuring the size distribution of individual particles in the soil sample and separating them into distinct particle-size groups. The relative proportions of particle-size groups may determine mineral composition of the soil and accordingly the behaviour of the soil interactions with fluid and solutes (Hillel, 1982).

The CropSyst model requires particle-size analysis of soil profile on a layer-by-layer basis down to the bottom of the root zone for calculation of water content (at drained upper limit and lower limit) and hydraulic conductivity. It uses a particle-size classification system according to the United States Department of Agriculture (USDA). The relationship between USDA and South African system of classification (MacVicar, 1977) is depicted in Fig. 5.2.

The analysis involved determination of particle-size distribution according to the USDA system of classification for soil layers comprising the ranges of 0 to 100 mm, 100 to 200 mm, 200 to 300 mm, 300 to 400 mm, 400 to 600 mm, 600 to 800 mm, and 800 to 1000 mm, for soil samples taken from upper and lower slopes in the field. The result of the analysis is presented in Appendix A.

The measurement primarily involved dispersing a sample of soil in aqueous suspension and determining the settling velocity of the agitated soil particles. Soil samples were dried at ambient temperature and gently ground to pass through a 2-mm sieve. A 20-g soil sample was dispersed chemically and mechanically by adding 10 ml of calgon solution and using ultrasound respectively. The dispersed sample was washed through a 0.053-mm sieve into

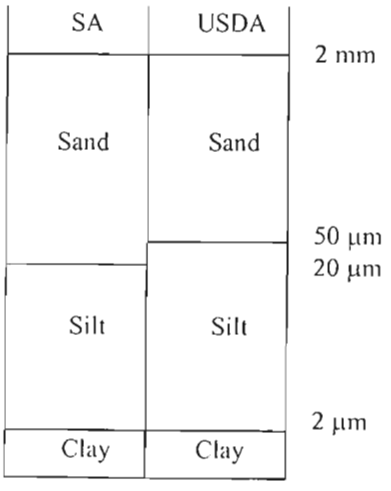

Fig. 5.2 The relationship between South African (SA) and USDA particle-size classification system

measuring cylinder and filled up to one litre with distilled water. The leftover was oven dried at 105°C overnight for determining the sand fraction. The soil water was left to equilibrate with ambient temperature and then was brought into suspension by firm up and down strokes. After an appropriate settling time, 20-ml samples were taken for silt (coarse and fine) and clay content determinations at 100 and 75 mm below the surface respectively and placed in an oven at 105°C overnight. The oven-dried sand fraction was put in a nest of sieves arranged in the order of sieve apertures 0.500, 0.250 and 0.106 mm for further refinement (Johnston, 2000).

5.4.2 Water retention and bulk density

Crop growth models require accurate modelling of the soil water balance. Usually information about soil water storage, plant-available water (PAW), evaporation and transpiration, and irrigation is deduced from soil water content for specified soil layers at saturation, drained upper limit and lower limit (Stöckle and Nelson, 2000). So it seems imperative that a soil water content and soil water potential at the above points for all soil layers down to the bottom of the root zone be determined.

The amount of water that is contained in a unit mass or volume of soil and the energy status of water (usually matric potential) in the soil are important factors affecting availability of water to plants. The relationship between the two is graphically represented by the soil water retentivity curve. The soil water retentivity curve is affected by texture, structure and degree of compaction. This makes the graph a useful tool in establishing the readily plant-available water and aeration status of a soil profile (Schulze *et al.*, 1985).

Soil water retentivity curve may be determined by simultaneous measurement of soil water potential and soil water content in the field, by application of successive increment of pressure to soil cores and measuring their water content after equilibrium has been attained in the laboratory or from simple mathematical models that estimate retentivity curves based on easily measurable soil properties such as particle-size and bulk density (e.g., Hutson, 1986).

Traditionally the drained upper and lower limits have been determined by mounting soil samples on pressure chambers and measuring soil water contents at potentials of -33 kPa or -10 kPa and -1500 kPa respectively (Ritchie, 1981). These static water limits inferred from laboratory measurements may often differ from field-measured values (Ritchie, 1981). Ratliff *et al.* (1983) found that laboratory estimates obtained using -33 kPa measurements over-

estimated the upper limit for silt loams, silty clays, and clays; under-estimated the lower limit for sands, loamy sands, sandy loams, and sandy clay loams; and nearly equal for loams and silty clay loams. It was pointed out that the under-estimation for sands and loamy sands could be due to lack of using -10 kPa as an estimate of drained upper limit in the laboratory. The application of -1500 kPa pressure in laboratory conditions also over-estimated the lower limit for loams, silty clays, and clays; under-estimated for loams sands, silt loams, and sandy clay loams; and nearly equal for sands, sandy loams, silty clay loams and clay loams.

Ritchie (1981) suggested that for accurate soil water balance calculations, the upper and lower limits of water availability should be determined in the field. Field measurements of these limits require measurement of soil water status with time in each layer of the soil profile down to the root tip. The drained upper limit is taken as the highest field-measured water content of a soil after it had been thoroughly wetted and allowed to drain until drainage became practically negligible; and the lower limit as the lowest field-measured water content of a soil after plants had stopped extracting water and were at or near premature death or became dormant as a result of water stress (Ratliff *et al.*, 1983).

Usually it is difficult to measure the lower limit in the field because of the difference in root growth dynamics between and within crops and also lack of the occurrence of conditions that promote the lower limit (Ritchie, 1981). Savage *et al.* (1996) have conducted *in-situ* soil water potential measurements using soil psychrometers to determine the lower limit of soil water potential from cotton in a rain-sheltered lysimeter with fine silty clay loam soils and from sorghum in a glass house pots with fine sandy loam soils. From this study, it was concluded that the commonly used -1500 kPa lower limit of soil water potential can be used for soil water balance calculations requiring absolute accuracy.

All the above problems add up to make laboratory and field measurements of determining the available water limits to be expensive, laborious and time consuming. This prompted several workers to develop mathematical models that attempt to relate these limits to easily measurable soil properties, although such efforts have been met with only partial success owing to the complex and variable nature of the soil (Hutson, 1986).

In this study retentivity curves from field measurement, laboratory measurement and model estimates (ISCI–Crop Science, 2001; Acutis and Donatelli, 2003) were constructed to serve as model inputs. The instruments that were used for in field measurement of soil water

potential measure in the range of 0 to -200 kPa, hence a hyperbolic equation developed by Gardener *et al.* (1970) is used to derive the soil water content at lower (more negative) values of soil water potential:

$$\ln\theta = \frac{-1}{b}\cdot\psi_{sw} + \frac{\ln a}{b} \qquad 5.9$$

where θ and ψ_{sw} are the soil water content and potential respectively at a certain depth in the soil profile, a and b are coefficients determined by regression analysis.

Field measurement of soil water retentivity curve was accomplished by simultaneous measurement of soil water potential and soil water content at three depths at a time in a bare plot. Six tensiometers and six Watermark sensors connected to a CR23X (Appendix C) and a PR1 (Profile Probe) connected to a CR10X (Appendix D) were used for measurement of soil water potential and soil water content. A vertical hole of 25 mm in diameter was augured for all the sensors. Well-soaked tensiometers and Watermark sensors, and an access tube (for the Profile Probe) were snug fit into the 25-mm diameter vertical holes using slurry made from the soil augured out. During the first period of measurement two tensiometers and two Watermark sensors were placed at depths of 100 mm, 300 mm and 600 mm and during the second period of measurement, at depths of 200 mm and 400 mm. The access tube for the Profile Probe was inserted to a depth of 1000 mm and the probe takes readings at depths of 100 mm, 200 mm, 300 mm, 400 mm, 600 mm and 1000 mm. Both dataloggers were programmed to take readings every three hours starting from midnight.

For laboratory measurement of the soil water retentivity curve, undisturbed soil core samples were taken at intervals of 100 mm from the above 600 mm and at intervals of 200 mm from 600 to 1000 mm soil depth at three adjacent positions using soil core sampler. The soil samples were trimmed flush with each end of the sleeve, a nylon cloth was secured on the lower end of the core with a rubber bund. These samples were let to stand in a trough full of water to a level of 3 mm from the top of the core for saturation. After saturation, the samples were weighed and transferred to a tension table with the suction set to 1 kPa. The samples were weighed every 48 hours and the tension increased by 1 or 2 kPa until 10 kPa was reached. The cores were then placed in a saturated disc of filter paper on a 100-kPa ceramic

plate and transferred to a pressure pot. A pressure of 50 and 100 kPa was progressively applied until equilibrium was attained. Each core was weighed before it was subjected to a progressive suction. The soil cores, without the nylon clothes, were then allowed to dry at 105 °C for four days for determination of bulk density (Johnston, 2000).

For determination of water retention at 1500 kPa, disturbed, air-dried soil samples were made to pass through a 2-mm sieve. Retaining rings placed on top of filter paper were filled with soil samples and compacted slightly with rubber bung. Water was placed in a ceramic setup of a high-pressure chamber so that the soil wetted up slowly by capillary movement. The soil was allowed to soak for about 30 minutes and afterwards a 1500-kPa pressure applied. After equilibrium had been attained, the soil was oven dried for determination of water content (Johnston, 2000).

The retentivity curves as determined from field, laboratory and a Hutson LEACHM model (ISCI–Crop Science, 2001; Acutis and Donatelli, 2003) are presented in Fig. 5.3. The laboratory-measured and model-estimated retentivity curves over-estimated the *in-situ* measurements at some depths and under-estimated it at other depths. The retentivity curves of the laboratory-measured and model-estimated were more or less better correlated, with the laboratory-measured retentivity curve having higher soil water content values in all depths at all given soil water potential values. At 100 mm depth, the field-measured retentivity curve had much lower soil water content at all soil water potentials as compared to the laboratory-measured and model-estimated retentivity curves. This very low water content of *in-situ* retentivity curve could be due to evaporative loss of soil water from the soil surface and upper soil layer (Ratliff *et al.*, 1983) arising from not well covering the surface plot with a plastic. At depths of 200 and 300 mm, the trend from the three retentivity curves were similar, with the *in-situ* retentivity curve having higher soil water content at all soil water potentials as compared to laboratory-measured and model-estimated soil water. At depths of 400 and 600 mm, the *in-situ* retentivity curves had had lower soil water content as compared to the laboratory-measured and model-estimated values. The soil water content at 600 mm did not change much while the soil water potential was changing continuously. At 1000 mm depth, there were no *in-situ* measurement of retentivity curves, and the laboratory-measured retentivity curve had higher values of soil water content than model-estimated values. Field measurement of soil water content at 1000 mm showed no change with time (Fig. 5.4).

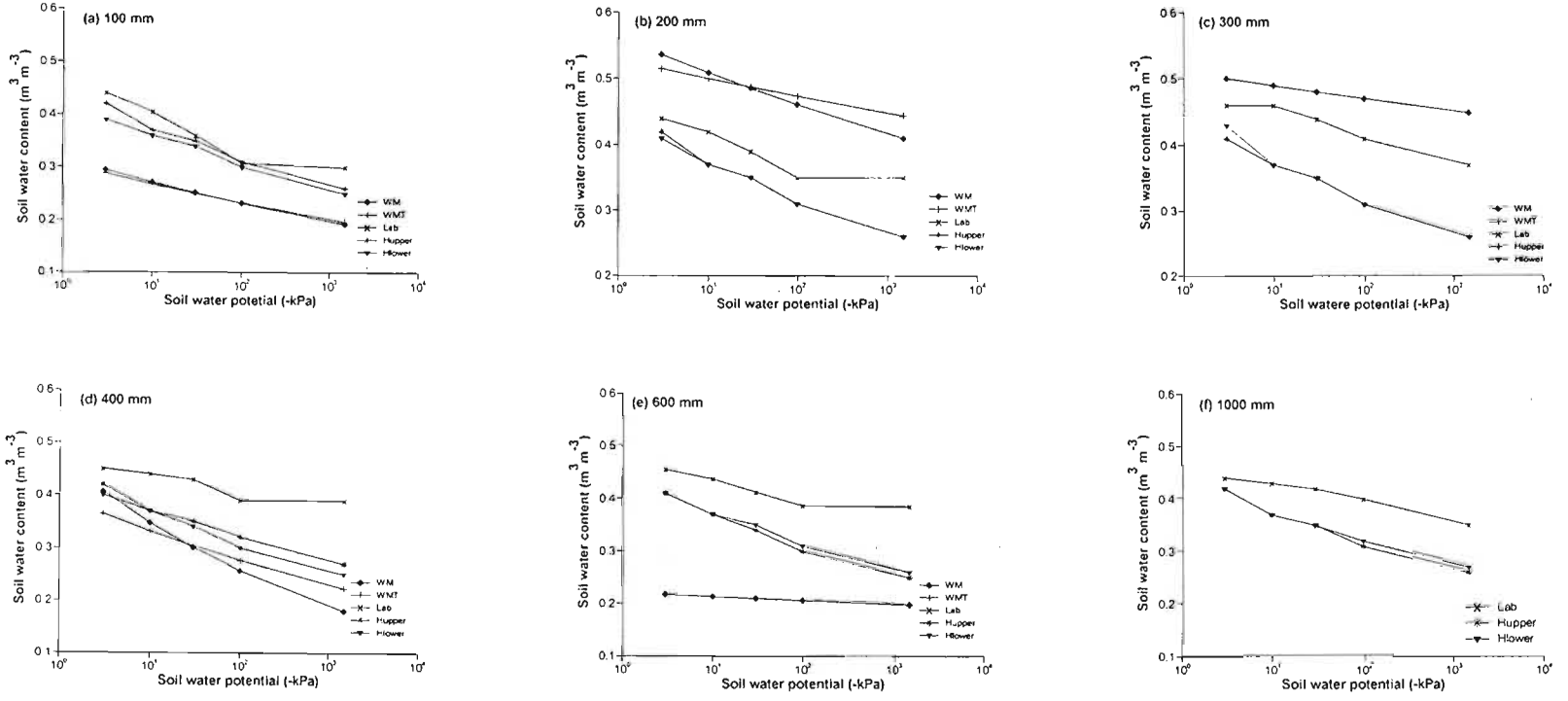

Fig. 5.3 Soil water retentivity curves for several soil layers down the soil profile (WM – soil water potential measured using Watermark sensor only, WMT – Watermark and tensiometer, Lab – laboratory-measured using pressure apparatus, and Hupper and Hlower – retentivity curves constructed using the Hutson LEACHM (ISCI–Crop Science, 2001; Acutis and Donatelli, 2003) model at Cedara, KwaZulu-Natal, South Africa

Retentivity curves constructed from soil water potential measurement using Watermark sensors only and Watermark sensors and tensiometers did give similar results but with a higher R^2 in case of the latter. Of particular interest is that, the laboratory-measured retentivity curve at lower soil water potential at all depths showed a very minute decrease in soil water content. This could be attributed due to lack of attaining equilibrium between the applied pressure from the pressure chamber and the samples (Campbell, 1988). These results coincide with laboratory-measured retentivity curves performed at Cedara (Schmidt and Schulze, 1989). The PAW computed from such retentivity curve maybe low. The hyperbolic equation that was used for estimating *in-situ* retentivity curve construction may do so accurately at higher soil water potentials (high soil water content) as signified from measurements of soil water versus time (Fig. 5.4) in determination of the upper limit, but is much less accurate when the soil is dry (Campbell, 1988). These two uncertainties make *in-situ* field measurement of the lower limit of soil water content indispensable.

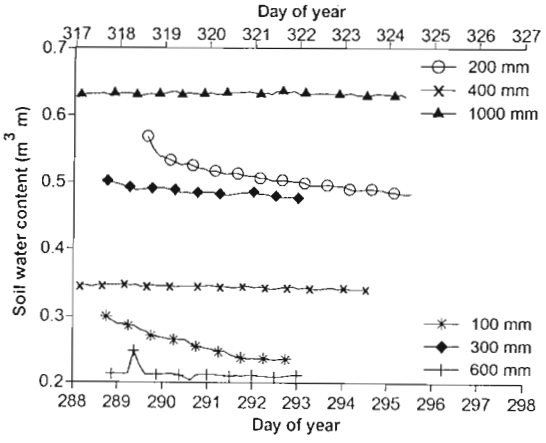

Fig. 5.4 Drainage curve following flooding of the measurement plot at Cedara, KwaZulu-Natal, South Africa

6 SOLAR RADIANT DENSITY ESTIMATION FOR CROP SIMULATIONS

6.1 INTRODUCTION

In the past two decades, with increased understanding of the soil-plant-atmosphere system and development of high-speed computers, crop simulation models have been successfully used to provide predictions of growth and yield of crops (Jones and Ritchie, 1990). Most crop simulation models, however, require a minimum dataset of daily records of solar radiant density, maximum and minimum air temperatures and precipitation (Whisler *et al.*, 1986; Ritchie, 1991; Hunt and Boote, 1998). Measurement of solar radiant density has required instrumentation that, until the last decade, was too expensive or unreliable to be used at most meteorological stations (Hook and McClendon, 1992). As a consequence, solar radiant density data, a crucial input to crop simulation models for computation of evapotranspiration and plant biomass growth (Ramkrishnan and Ritchie, 2000), is not as readily available as measurements of air temperature and precipitation. The lack of such data record prevents application of crop simulation models for the purpose of calibration, validation and examination of 'what if...' scenarios (Hook and McClendon, 1992) at sites where records on past crop experiments and other weather variables are available. This has triggered researchers to develop a number of methods for estimating solar radiant density (e.g., Swift, 1976; Cengiz *et al.*, 1981; Bristow and Campbell, 1984; Hargreaves *et al.*, 1985; Clemence, 1992; Hunt *et al.*, 1998). These methods vary in data input requirement and complexity of the equations employed.

Weather generators (Richardson and Wright, 1984; Stöckle and Nelson, 1999; Stöckle *et al.*, 2001) can be used to generate weather data based on historical meteorological data. Although such data may be used for creating possible scenarios, they cannot be used for calibration and validation of crop simulation models (Hook and McClendon, 1992).

In South Africa, as in most parts of the world, direct measurements of solar radiant density are rare (Clemence, 1992) but sunshine duration observed in meteorological stations have been successfully used for computation of solar radiant density (Schulze, 1976; Reid, 1986).

In this study historical weather data from four meteorological stations in KwaZulu-Natal is considered. Three out of the four stations included sunshine duration as part of the weather

data records, one station included both sunshine and solar radiant density data and one site included solar radiant density measurements only. The records of solar radiant density and sunshine duration from these weather stations have years with no measured and/or frequent missing records throughout the dataset. Sometimes, also, the records seem to lie out of the range that would normally be expected. With this notion in mind, the objective of this study is to examine various models and evaluate their performance for the purpose of supplying solar radiant density data to a plant growth simulator, CropSyst (Stöckle and Nelson, 2000; Stöckle *et al.*, 2003).

6.2 ESTIMATION OF SOLAR RADIANT DENSITY

Solar radiant density can be estimated using sunshine hours, daily maximum and minimum air temperature differences, precipitable water content, cloudiness, relative humidity and/or atmospheric transmissivity along with extraterrestrial radiant density (Bristow and Campbell, 1984). Most models compute daily solar radiant density as a fraction of extraterrestrial radiation, which is readily calculable from geometry of the earth. Extraterrestrial daily radiant density (I_{ex}, MJ m^{-2}) is estimated following Gates (1980):

$$I_{ex} = \frac{I_{sc}}{\pi} \cdot \left(\frac{\bar{d}}{d}\right) \cdot (\sin\phi \cdot \sin\delta + \cos\phi \cdot \cos\delta \cdot \cos h) \qquad 6.1$$

where I_{sc} (117.5 MJ m^{-2}) is the solar constant, $\left(\frac{\bar{d}}{d}\right)$ represents the ratio of mean to actual earth-sun distance, ϕ (radians) is the latitude of the location (north positive and south negative), δ (radians) is the solar declination and h (radians) is the half daylength.

The ratio of mean to actual earth-sun distance, solar declination and half daylength are computed following RadEst tool (beta v3.00) (ISCI-Crop Science, 2002).

$$\left(\frac{\bar{d}}{d}\right) = 1 + 0.0334 \cdot \cos(0.01721 \cdot doy - 0.0552) \qquad 6.2$$

$$\delta = arcsin\left[0.39875 \cdot sin(4.869 + 0.0172 \cdot doy + 0.03345 \cdot sin(6.224 + 0.0172 \cdot doy))\right] \qquad 6.3$$

$$h = arccos\ (-tan\ \phi \cdot tan\ \delta) \qquad 6.4$$

where *doy* is the day of year.

Since extraterrestrial radiant density is readily calculable, there remains to estimate the daily total atmospheric transmissivity so that solar radiant density could be computed as a fraction of extraterrestrial radiant density.

6.2.1 Solar radiant density estimation from sunshine duration

In weather stations where sunshine duration is recorded, solar radiant density can be estimated using an equation first proposed by Ångström (1924). Ångström's equation was based on a linear relationship between sunshine duration and solar radiant density. The original equation has undergone certain revisions of which Doorenbos and Pruitt (1977) recommend a generalized form for the Penman equation:

$$I_s = I_{ex}(a + b\frac{n}{N}) \qquad 6.5$$

where I_s (MJ m^{-2}) is the total daily solar radiant density received at a site, I_{ex} (MJ m^{-2}) is the extraterrestrial daily solar radiant density; a and b are constants that depend on location, season and state of atmosphere; n (hours) is the actual sunshine duration recorded; and N (hours) is the maximum possible sunshine hours (daylength).

Several researchers have indicated that the values of a and b do vary considerably both seasonally and spatially (Glover and McCulloch, 1958; Rietveld 1978; Reid, 1986). Whenever possible, the values of a and b should be computed on a local basis although this might require quality solar radiant density data. For South African conditions, Reid (1986), based on eleven locations, found that both coefficients are definitely not constant either spatially or over the full spectrum of sunshine hours. Although the relationship between both coefficients and n/N appeared to be poor (Reid, 1986), it was linear in the case of a and hyperbolic in the case of b (Rietveld, 1978; Reid 1986). For better estimation of solar radiant density, Reid (1986) suggested that sufficient data be available for over smaller intervals of n/N for the location of interest separately. Reid (1986) found that both coefficients based on conditions of mean monthly values of n/N could be summarized as follows:

$$I_s = I_{ex}(0.22 + 0.65\frac{n}{N}) \quad for\frac{n}{N} < 0.5 \quad (a)$$
$$I_s = I_{ex}(0.29 + 0.47\frac{n}{N}) \quad for\frac{n}{N} > 0.5 \quad (b) \qquad 6.6$$
$$I_s = I_{ex}(0.26 + 0.56\frac{n}{N}) \quad for\,all\frac{n}{N} \qquad (c)$$

for the eleven locations in South Africa.

In this study the first two equations are adopted but instead of mean monthly *n/N* as used by Reid (1986), daily *n/N* is used for determination of *a* and *b* coefficients. However, it is noted that Reid (1986) did not give coefficients for *n/N* equal to 0.5. The sharp change in coefficients, for the transition between *n/N* less and greater than 0.5, may also result in large differences of outputs for two close *n/N* values around the transition.

In the absence of measured sunshine duration, solar radiant density has to be computed from other more commonly observed meteorological variables.

6.2.2 Solar radiant density estimation from common meteorological observations

The daily solar radiant density that is received at the earth's surface strongly affects the thermal conditions at the surface. Hence minimum and maximum air temperature differences (ΔT) can be used as an index of cloudiness and solar radiant density load (Bristow and Campbell, 1984). Clear-sky conditions result in high air temperature during the day and lower air temperature during the night due to greater solar radiant density load during the day and reduced long wave emissivity from the atmosphere during the night (Donatelli and Campbell, 1998). Overcast conditions result in reduced air temperature during the day and higher air temperature during the night because of increased interception of solar radiant density during the day and greater emissivity from clouds at night (Donatelli and Campbell, 1998).

Solar radiant density is greatly reduced during rainy days (Bristow and Campbell, 1984) and some approaches account for this by introducing precipitation into their models (e.g., Bristow and Campbell, 1984; Hunt *et al.*, 1998). Atmospheric water vapour pressure is also sometimes used as an index of transmissivity along with diurnal air temperature range (e.g., Thornton and Running, 1999) but this may detract from the simplicity of the data input since there are many stations which do not observe relative humidity (or water vapour pressure).

Bristow and Campbell (1984) were able to account for 70 to 90% of the variation in total incoming solar radiant density from three datasets by formulating a model based on the above principle. The Bristow and Campbell (1984) model (B-C, Table 6.1) computes daily incoming solar radiant density by estimating the daily transmissivity coefficient and multiplying it by extraterrestrial radiant density. The theoretical concept of energy exchange on the surface boundary layer upon which the B-C model was founded, its reasonable accuracy, and simple data requirements made it attractive and an ideal tool for estimation of solar radiant density (Goodin *et al.*, 1999). As a result, this model has attracted the attention of many researchers and it has been subjected to modification several times to suit specific conditions (e.g., Donatelli and Marletto, 1994; Donatelli and Campbell, 1998; Goodin *et al.*, 1999; Thornton and Running, 1999; Donatelli and Bellocchi, 2001). Basically all the modifications tend to change the transmissivity, t_i, part of the equation. Donatelli and Marletto (1994) pointed out that the B-C model-simulated solar radiant density showed a shift in time of predicted versus observed values and under-estimation of predicted values during the summer for their dataset. Consequently they modified the B-C model by introducing average air temperature and a minimum air temperature function but their model was regarded as over-parameterized by Donatelli and Campbell (1998), causing lack of robustness in model parameters and lack of model stability. Donatelli and Campbell (1998) presented a model (D-C, Table 6.1) by further modification of the B-C model based on the Donatelli and Marletto (1994) findings. They also formulated a model that estimates solar radiant density when there was no observed solar radiant density data for deriving the coefficients. To differentiate the former from the latter a D-CWORAD notation will be used to indicate the latter throughout the following sections.

Goodin *et al.* (1999) modified the B-C model by introducing daily extraterrestrial radiant density, I_{ex}, as an extra term in the equation for estimating t_i. The I_{ex} term is meant to act as a scaling factor, allowing ΔT to accommodate a greater range of solar radiant density values.

The B-C model was also modified by Thornton and Running (1999) by introducing a water vapour pressure term to the t_i equation of the B-C model in an attempt to derive parameters that give accurate results at locations with different climates without refitting model parameters on a case-by-case basis.

Table 6.1 Details of various models used for estimation of solar radiant density

Authors	Model abbreviation	Model requirements	Comments
Bristow KL, Campbell GS (1984)	B-C	I_{ex}, T_x, T_n, P and I_s*	Exponential function
Clemence BSE (1992)	Clemence	I_{ex}, T_x, T_n, and I_s	Polynomial fucntion
Donatelli M, Bellocchi G (2001)	D-B	I_{ex}, T_x, T_n, P and I_s	Exponential and trigonometric function
Donatelli M, Campbell GS (1998)	D-C	I_{ex}, T_x, T_n, P and I_s	Exponential function
Donatelli M, Campbell GS (1998)	D-CWORAD	I_{ex}, T_x, and T_n	Exponential function
Goodin DG, Hutchinson JMS, Vanderlip RL, Knapp MC (1999)	Modified B-C	I_{ex}, T_x, T_n, and I_s	Exponential function
Hargreaves GL, Hargreaves GH, Riley JP (1985)	Hargreaves	I_{ex}, T_x, T_n, and I_s	Polynomial function
Hunt LA, Kuchar L, Swanton CJ (1998)	HKS	I_{ex}, T_x, T_n, P and I_s	Polynomial function
Mahmood R, Hubbard KG (2002)	M-H	I_c, T_x, T_n, and I_s	Exponential and Trigonometric function
Ramkrishnan BP, Ritchie JT (2000)	R-R	I_{ex}, T_x, T_n, and I_s	Polynomial function

*I_{ex}, extraterrestrial radiant density (MJ m^{-2})
I_c, clear sky solar radiant density (MJ m^{-2})
T_x, daily maximum air temperature (°C)
T_n, daily minimum air temperature (°C)
I_s, solar radiant density (MJ m^{-2})

Moreover the B-C model was modified by Donatelli and Bellocchi (2001) to account for the effect of seasonal variation of the clear sky transmissivity and the ΔT by introducing a trigonometric function.

Hunt *et al.* (1998) developed a model in a similar fashion to the above but with a simple linear relationship between daily incoming solar radiant density and diurnal air temperature range, maximum air temperature and precipitation. Hargreaves *et al.* (1985) also developed a model based on a simple linear relationship between diurnal air temperature range and daily transmissivity coefficient, but without refinements for precipitation. Clemence (1992) also used diurnal air temperature range and maximum air temperature to develop a region specific model for South Africa. Ramkrishnan and Ritchie (2000) used diurnal air temperature range and minimum air temperature to estimate solar radiant density. Mahmood and Hubbard (2002) estimated daily incoming solar radiant density from clear sky solar radiant density and diurnal air temperature range.

6.3 MATERIALS AND METHODS

6.3.1 Data

Meteorological data was obtained from Agricultural Research Council, Institute of Soil, Climate and Water, Pretoria, South Africa, for Cedara and Ukulinga stations; Council for Scientific and Industrial Research (CSIR) for Seven Oaks; and South African Weather Bureau Service for the Durban station. These stations hold long-term daily records of precipitation and minimum and maximum air temperatures. All but the Seven Oaks station included records of sunshine duration. Minimum and maximum relative humidity, wind speed and Class A pan evaporation were also observed at Cedara and Ukulinga stations but not in a continuous manner. In addition to these observations, the Durban and Seven Oaks stations included solar radiant density records. Further information of the meteorological stations and weather data records is given in Table 6.2.

The observed sunshine duration from the three sites were converted to daily solar radiant density values (MJ m^{-2}) using Eq. 6.6 (*a*) and (*b*). Estimated values were compared with observed daily solar radiant density values for the Durban meteorological station using regression analysis (n = 4017). For the Cedara and Ukulinga stations, since they did not have

Table 6.2 Location of meteorological stations and length of data records used for estimation of solar radiant density

Location	Latitude (S)	Longitude (E)	Elevation (m)	Data record[a]
Cedara	-29°32′	30°17′	1076	1970-1997
Ukulinga	-29°40′	30°24′	775	1959-1966
Durban	-29°58′	30°57′	8	1977-1987
Seven Oaks	-29°11′	30°40′	1100	1998-2001

[a] These records may include either sunshine records, observed solar radiant density or both.

observed solar radiant density, the solar radiant density estimated from sunshine duration was considered as an observation and used for calibration and evaluation of all models or equations that estimate solar radiant density.

6.3.2 Formulae

Several formulae/models that estimate solar radiant density from extraterrestrial radiant density, diurnal air temperature range, and/or precipitation were obtained from the literature and applied to the four stations under study. Basically all the models either implicitly or explicitly employ the tenet that has been described in Section 6.2.2. Following is the detail of the models that were used in estimating daily solar radiant density.

6.3.2.1 Bristow and Campbell (B-C) model

Bristow and Campbell (1984) developed an exponential relationship between atmospheric transmittance and the diurnal air temperature range. Daily solar radiant density at a horizontal plane on the earth's surface is computed by multiplying extraterrestrial radiant density by the estimated daily total atmospheric transmittance (beta v3.00) (ISCI-Crop Science, 2002).

The B-C model is part of a suite of models contained within the RadEst tool (beta v3.00) (ISCI-Crop Science, 2002; Donatelli *et al.*, 2003):

$$I_s = t_i \cdot I_{ex} \qquad 6.7$$

$$t_i = b_0 \left[1 - exp\left(\frac{-b_1 \Delta T^{b_2}}{DT_m} \right) \right] \qquad 6.8$$

where I_s (MJ m^{-2}) is the estimated daily total solar radiant density, t_i is the daily total atmospheric transmittance, I_{ex} (MJ m^{-2}) is the extraterrestrial daily radiant density, b_0 is clear day transmissivity, b_1 and b_2 are empirical coefficients that display the physics involved in the relationship DT_m is the monthly air temperature range and ΔT (°C) is the diurnal air temperature range given as:

$$\Delta T_{(i)} = T_{x(i)} - \left(\frac{T_{n(i)} + T_{n(i+1)}}{2} \right), \quad \text{if } \Delta T_{(i)} \leq 2 \text{ then } \Delta T_{(i)} = 2 \qquad 6.9$$

where T_x and T_n are the daily maximum and minimum air temperatures respectively, and (i) and ($i+1$) represent the current day and the day after.

The mean of the two consecutive minimum air temperatures is so used to reduce the effect of large scale warm (which may imply a greater irradiance load) and cold (a lower irradiance load) air masses in temperate regions where advection is common, otherwise minimum and maximum air temperature difference may suffice for the tropics. The model also adjusts measured ΔT on rainy days to account for reduced radiation by setting $\Delta T(i)$ equal to 0.75 times the measured $\Delta T(i)$ (Bristow and Campbell, 1984).

6.3.2.2 Donatelli and Campbell (D-C) model

Donatelli and Campbell (1998) modified the t_i term of the B-C model to account for seasonality:

$$t_i = b_0 \left[1 - exp\left(-b_1 \cdot 0.017 \cdot exp\left(exp\left(-0.053 \cdot T_{avg} \right) \right) \cdot \Delta T_i^2 \cdot exp\left(\frac{T_n}{T_{nc}} \right) \right) \right] \qquad 6.10$$

where T_{nc} is an empirical coefficient and T_{avg} is the daily average air temperature (other variables assume their original definitions).

A modified version of the D-C model, D-CWORAD was also used to estimate solar radiant density of temperate areas by setting the b_0 term equal to 0.75 and deriving the coefficients T_{nc} and b_1 without the need for having observed solar radiant density:

$$T_{nc} = 3.286 \cdot exp\left(1.81 \cdot \frac{DT_j}{DT_y}\right), \quad \text{if } T_{nc} > 31 \text{ then } T_{nc} = 31 \qquad 6.11$$

$$b_1 = -0.0134 \cdot DT_j + 0.0063 \cdot T_{nc} + 0.26 \qquad 6.12$$

where DT_j and DT_y are average long term monthly air temperature ranges of the hottest month and of the whole year without the hottest month respectively.

6.3.2.3 Modified B-C model

Goodin *et al.* (1999) have modified the t_i part of the B-C model by introducing an extra I_{ex} term in the equation:

$$t_i = b_0\left[1 - exp\left(-b_1 \frac{\Delta T^{b_2}}{I_{ex}}\right)\right] \qquad 6.13$$

6.3.2.4 Donatelli and Bellocchi (D-B) model

The D-B model also modified the t_i part of the B-C model to account for the effect of seasonal variation of the clear sky transmissivity and ΔT by introducing a trigonometric function (Donatelli and Bellocchi, 2001):

$$t_i = b_0\left[1 + c_1 \cdot sin\left(\frac{i \cdot \pi}{180} \cdot c_2\right)\right] \cdot \left[1 - exp\left(\frac{-b_1 \cdot \Delta T_i^2}{DT_{week}}\right)\right] \qquad 6.14$$

where c_1 and c_2 are empirical parameters accounting for seasonal effects, and DT_{week} is the weekly air temperature range.

6.3.2.5 Hargreaves model

Hargreaves *et al.* (1985) estimated solar radiant density, I_s from the equation:

$$I_s = b_0 + b_1\sqrt{DT} \cdot I_{ex} \qquad 6.15$$

where $DT = T_x - T_n$ (compare with Eq. 6.9) 6.16

6.3.2.6 Ramkrishnan and Ritchie (R-R) model

Following Ramkrishnan and Ritchie (2000) solar radiant density was estimated:

$$I_s = CDR \cdot FCD \tag{6.17}$$

where CDR is clear day daily total solar radiant density (MJ m^{-2}) and FCD is the fraction of clear day:

$$CDR = I_{ex} \cdot b_0^{OAM} \tag{6.18}$$

where OAM is optical air mass (a function of atmospheric pressure at sea level and the observation site, and zenith angle of the sun) and b_0 is clear day transmissivity given by:

$$b_0 = 0.87 - 0.003 \cdot T_n \tag{6.19}$$

$$\text{and, } FCD = 1.05 - \frac{0.9}{1 + \left(\frac{DT}{T_o}\right)^3} \tag{6.20}$$

where T_o is inflection point temperature (°C) computed using quality solar radiant density data and DT.

6.3.2.7 Clemence model

The Clemence model was specifically developed for South African conditions. Solar radiant density was estimated following Clemence (1992):

$$I_s = b_0 + b_1 \cdot I_{ex} \cdot DT + b_2 \cdot T_x - b_3 \cdot T_x \cdot DT \tag{6.21}$$

The coefficients were the result of a combined regression analysis using twelve stations in South Africa.

6.3.2.8 HKS model

The HKS model estimates solar radiant density based on diurnal air temperature range and precipitation (Hunt *et al.*, 1998):

$$I_s = b_0 + b_1 \cdot I_{ex} \cdot DT^{0.5} + b_2 T_x + b_3 \cdot P + b_4 \cdot P^2 \qquad 6.22$$

where P (mm) is daily total precipitation.

6.3.2.9 Mahmood and Hubbard (M-H) model

The M-H model estimates daily incoming solar radiant density based on clear sky solar radiant density and diurnal air temperature range. Clear sky solar radiant density was estimated following Cengiz *et al.* (1981):

$$I_c = 0.04188\left\{A + B\left(\frac{2\pi(doy + 10.5)}{365} - \left(\frac{\pi}{2}\right)\right)\right\} \qquad 6.23$$

where I_c (MJ m^{-2}) is clear day solar radiant density, A and B are constants estimated following Cengiz *et al.* (1981):

$$\begin{aligned} A &= \left\{\sin\phi \cdot (46.355 \cdot LD - 574.3885) + \left(816.41 \cos\phi \sin\left(\frac{\pi \cdot LD}{24}\right)\right)\right\} \cdot (0.29\cos\phi + 0.52) \\ B &= \left\{\sin\phi \cdot (574.3885 - 1.509 \cdot LD) - 26.59 \cos\phi \sin\left(\frac{\pi \cdot LD}{24}\right)\right\} \cdot (0.29\cos\phi + 0.52) \end{aligned} \qquad 6.24$$

where LD is the maximum daylength in a year (hours).

The clear day solar radiant density, I_c, is further corrected using an empirical atmospheric transmissivity function that was derived from a comparison of estimated clear-sky solar radiant density and measured values at the earth's surface (Mahmood and Hubbard, 2002):

$$t_i = 0.8 + 0.12 \cdot c^{1.5} \quad \text{where } c = \left| \frac{182 - doy}{183} \right| \qquad 6.25$$

The coefficients for effective transmissivity correction functions were developed through a number of trials for three sites in the Northern Great Plains, USA (Mahmood and Hubbard, 2002).

The corrected clear-sky solar radiant density was computed following Mahmood and Hubbard (2002):

$$I_{cc} = t_i \cdot I_c \qquad 6.26$$

where I_{cc} (MJ m^{-2}) is the corrected clear-sky solar radiant density.

Finally the total daily solar radiant density is computed as a function of corrected clear-sky solar radiant density and daily air temperature range:

$$I_s = b_0 \cdot DT^{b_1} \cdot I_{cc}^{\ b_2} \qquad 6.27$$

6.3.3 Coefficients

Coefficients for each location and formula were derived. For models contained within the RadEst tool (beta v3.00) (ISCI-Crop Science, 2002; Donatelli *et al.*, 2003) (B-C, D-C and D-B models) iterative optimization utilities were provided for determination of the coefficients. This required at least two years data of precipitation, maximum and minimum air temperatures and solar radiant density. For the Modified B-C model a two-step process was involved in deriving the coefficients. In the first step b_0 was empirically determined as the best value of the upper bound of transmissivity values by the scatter plots of t_i against $\Delta T/I_{ex}$ (SPE, 1996). The other parameters were then derived using a nonlinear least-squares technique (SPE, 1996). Derivation of coefficients for the Hargreaves model involved simple linear regression and for the HKS and M-H models involved multiple linear regression with log transformations whenever necessary (Genstat, 2002). For the Clemence (1992) model, developed for South African conditions, there was no need to alter the coefficients. Lastly, derivation of coefficients for the R-R model was calculated straight forward from the formula.

6.3.4 Statistical evaluation

Model response was evaluated by: (i) conventional statistics and (ii) using an expert system following Bellocchi *et al.* (2002).

In the conventional statistics, measures of residuals ($RMSE_s$, $RMSE_u$ and $RMSE$) (see Section 2.8), agreement (slope and intercept, and Willmott index of agreement (d)) (see Section 2.8) and correlation determination (R^2) were used to evaluate the performance of the solar radiant density models.

The expert system makes use of decision rules to combine several statistics into one aggregate measure that enables a comprehensive assessment of the model's performance in a consistent and reproducible manner (Bellocchi *et al.*, 2002). The system defines three indicator modules (Bellocchi *et al.*, 2002):

(i) accuracy that accounts for input variables from measures of residuals including relative root mean square error ($RRMSE$), model efficiency (EF) and two-tailed paired t test;

(ii) correlation which depends on the correlation coefficient (r) between estimated and measured values; and

(iii) pattern that considers the pattern of the residuals against independent variables in the model: pattern indices against day of year (PI_{doy}) and pattern indices against daily minimum air temperature (PI_{Tn}).

The three indicator modules, in turn, are aggregated into a single modular indicator using decision rules that enable the models to be ranked accordingly. Aggregation of indices into modules, and modules into a single indicator could be accomplished by the software application IRENE (ISCI, 2001; Fila *et al.*, 2003).

The decision rules are merely based on the expert judgment of the authors from working on a multi-year weather data over a wide range of localities. Three membership classes (subsets) are defined for all the indices: favourable (F), unfavourable (U) and partial (fuzzy) membership (Table 6.3). Membership functions that are S shaped in transition interval were used because they provide smoother variations of the input values than functions that are linear in the transition interval. These membership classes, along with decision rules, are used to calculate a dimensionless module whose value ranges between 0 (best model performance) and 1 (worst model performance). Several of these modules (three in this case) are then

Table 6.3 Membership classes of indices according to expert judgment following Bellocchi *et al.* (2002)

Module	Index	Membership		
		F	U	Partial
Accuracy	*RRMSE*	≤ 20.00	≥ 40.00	20.00 – 40.00
	EF	≥ 0.90	≤ 0.40	0.40 - 0.90
	P(t)	≥ 0.10	≤ 0.05	0.10 – 0.05
Correlation	*r*	≥ 0.90	≤0.70	0.70 – 0.90
Pattern	PI_{dov}	≤ 1.00	≥ 2.50	1.00 – 2.50
	PI_{Tm}	≤ 1.00	≥ 2.50	1.00 – 2.50

aggregated, once again based on expert decision rules, into a single modular indicator that can be used to evaluate and rank the models of interest (Bellocchi *et al.*, 2002).

The index *RRMSE* may, theoretically, hold values between zero and positive infinity, and the smaller the value the better the performance of the model. The index *EF* may vary from negative infinity to one, with positive values close to one indicating a better model performance and negative values indicating that the average measured value is a better predictor than the model used. P(*t*) is used for the two-tailed paired *t* test with value of one being the best value and zero the worst value. The module accuracy is then computed from the input indices according to eight decision rules (Table 6.4). In setting up the decision rules the relative importance of each index is taken into consideration and weights were allocated accordingly. More weight is given, in decreasing order to the indices *RRMSE*, *EF* and P(*t*) (Table 6.4) (Bellocchi *et al.*, 2002).

Table 6.4 Assignment of expert weight to the module accuracy based on membership class of the indices *RRMSE*, *EF* and P(*t*) following Bellocchi *et al.* (2002)

Membership class			Expert weight
RRMSE	*EF*	P(*t*)	
F	F	F	0.00
F	F	U	0.20
F	U	F	0.40
F	U	U	0.60
U	F	F	0.40
U	F	U	0.60
U	U	F	0.80
U	U	U	1.00

$$RRMSE = 100 \cdot \frac{RMSE}{\overline{M}} \tag{6.28}$$

$$EF = 1 - \frac{\sum_{i=1}^{n}(E_i - M_i)^2}{\sum_{i=1}^{n}(M_i - \overline{M})^2} \tag{6.29}$$

$$t = \frac{\overline{D}}{s_D} \tag{6.30}$$

where E_i and M_i are the i^{th} estimated and measured values respectively, n is the number of pairs of E_i and M_i observations, $\overline{M}$ is the average measured value, $\overline{D}$ is the average of the differences between E_i and M_i, and s_D is the standard error of the differences between E_i and M_i. The computed t is compared against the critical t with 2 × (n - 1) degrees of freedom.

The module correlation depends on single basic index, correlation coefficient (r). The correlation coefficient (r) may vary from -1 (full negative correlation) to 1 (full positive correlation). In solar radiation models, the closer r is to 1 the better is the performance of the model. The membership classes attributed to r are F for $r \geq 0.9$ and U for $r \leq 0.7$. The computation of the module correlation follows, since there is only one index in the module, two decision rules: if r is F then 0, if r is U then 1 (Bellocchi *et al.*, 2002):

$$r = \frac{\sum_{i=1}^{n}\left(E_i - \overline{E}\right)\cdot\left(M_i - \overline{M}\right)}{\left[\sum_{i=1}^{n}\left(E_i - \overline{E}\right)^2 \cdot \sum_{i=1}^{n}\left(M_i - \overline{M}\right)^2\right]^{0.5}} \tag{6.31}$$

where $\overline{E}$ is the average of the estimates.

The module pattern considers two independent variables: day of year and minimum air temperature. Equal weights are assigned to both variables in computing the module pattern (Table 6.5). The pattern of residuals against independent variables indicates variables that are not accounted for by the model (Donatelli *et al.*, 2000; Bellocchi *et al.*, 2002). Following Donatelli *et al.* (2000) and Bellocchi *et al.* (2002) *PI* is computed as:

Table 6.5 Assignment of expert weight to the module pattern based on membership class of the indices PI_{doy} and PI_{Tn} following Bellocchi *et al.* (2002)

Membership class		Expert weight
PI_{doy}	PI_{Tn}	
F	F	0.00
F	U	0.50
U	F	0.50
U	U	1.00

$$PI = \max_{l,m=1,\ldots,4;l\neq m}\left|\frac{1}{q_l}\cdot\sum_{i_l=1}^{q_l}R_{i_l}-\frac{1}{q_m}\cdot\sum_{i_m=1}^{q_m}R_{i_m}\right| \qquad 6.32$$

where R is the model residual, l and m indicate two groups being compared, q_l and q_m represent the number of residuals in the groups, i_l and i_m identify each value of residuals in the groups. The PI values have the same units as the variable under study (in this case, MJ m^{-2}).

The above three modules are also in turn aggregated, in the same manner as for the indices, according to eight decision rules, into a single indicator, I_{rad}. In setting up the decision rules the relative importance of each module is taken into consideration and weights were allocated accordingly. More weight is given, in decreasing order to the modules accuracy, pattern and correlation (Table 6.6) (Bellocchi *et al.*, 2002).

Table 6.6 Summary of decision rules describing the effect of the three modules on the value of the indicator (I_{rad}) following Bellocchi *et al.* (2002)

Membership class			Expert weight
Accuracy	Correlation	Pattern	
F	F	F	0.00
F	F	U	0.30
F	U	F	0.15
F	U	U	0.45
U	F	F	0.55
U	F	U	0.85
U	U	F	0.70
U	U	U	1.00

6.3.5 Crop simulations

The solar radiant density estimated either from sunshine hours (considered as observed) or using a model, along with minimum and maximum air temperatures and precipitation was used to simulate grain yields of maize (*Zea mays* L. cv. PAN 6568) at Cedara. The only variable that kept changing with each simulation was the solar radiant density as estimated from the different solar radiation models. A soil plant growth simulator, CropSyst (Stöckle and Nelson, 2000; Stöckle *et al.*, 2003) was used for the simulation purposes. A Hutton, Doveton (Appendix B) type soil (MacVicar, 1977) and a PAN 6568 maize cultivar with plant row spacing of 0.75 m and plant population density of 44000 per hectare were assumed. Crop parameters for maize PAN 6568 were set according to calibration and validation exercises (Appendix E), using experimental data obtained from the National Cultivar Trials: maize (Maree and Bruwer, 1998; Du Plessis and Bruwer, 1999, 2000, 2001, 2002). Planting date was set to 5th November (day of year 309) (as practiced by local farmers). After harvest, 40% of the fraction of the maize stalk was assumed to be left on the field to be incorporated later into the soil by tillage practices. The simulation was run for 20 continuous years in rotation along with fallow conditions. A finite difference technique was used for redistribution of water in the soil. The soil water was initialized to near the upper limit following a substantial amount of precipitation at the day of the start of simulation. The simulations were set to start on the same day for all datasets. Nitrogen simulation was disabled assuming that nitrogen was not a limiting factor for yield. The effect of estimated solar radiant density on simulated grain yield was analyzed using absolute difference between total accumulated yields, mean and R^2 during the 20-year simulation period, standard deviation and *RMSE* for individual estimates per year and maximum error between the simulated yields. A t-test was also conducted to test significance of the equality of mean simulated grain yield for the 20-year simulation period between grain yields simulated using the observed solar radiant density and estimated from all of the models. The calculated statistical measures were used in ranking the performance of the solar radiant density models on their ability to produce yield simulations that match with yield simulations from using the observed solar radiant density.

6.4 RESULTS AND DISCUSSION

Data of both sunshine and solar radiant density were available for only one station, Durban, from 1977 to 1987. Solar radiant density estimates were made using regression coefficients of *a* and *b* developed by Reid (1986) for South African conditions based on daily values of *n/N*. The equations seem to slightly over-estimate the lower values of solar radiant density and under-estimate the higher values of solar radiant density (Fig. 6.1).

For three stations, Cedara, Ukulinga and Durban, solar radiant density estimated in the same manner from sunshine hours served as observed solar radiant density to evaluate and rank the performance of the solar radiant density models. In addition, observed solar radiant density from Durban and Seven Oaks was used.

Ten solar radiant density models were used (Table 6.1), of which three were contained within the RadEst suite of models (beta v3.00) (ISCI-Crop Science, 2002; Donatelli *et al.*, 2003) and the rest obtained from the literature and incorporated into a spreadsheet. These models were calibrated for the specific locations under study. The fitted coefficients of each location for each model resulting from the calibration are presented in Table 6.7.

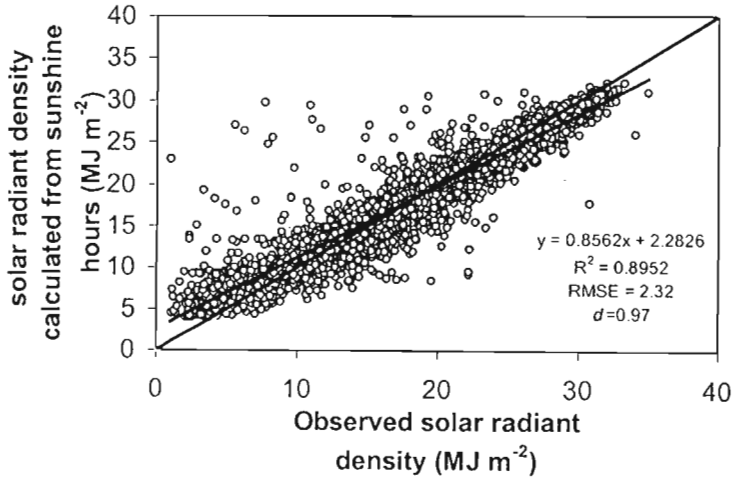

Fig. 6.1 Measured solar radiant density against solar radiant density derived from sunshine hours for Durban, KwaZulu-Natal, South Africa (n = 4017)

Table 6.7 Calibrated model coefficients for Cedara, Durban, Seven Oaks and Ukulinga in KwaZulu-Natal, South Africa

Model	Coefficients	Location*				
		Measured		Estimated from sunshine hours		
		Durban	Seven Oaks	Durban	Cedara	Ukulinga
B-C	b_0	0.730	0.760	0.730	0.740	0.720
	b_1	0.207	0.130	0.209	0.132	0.140
	b_2	2.000	2.000	2.000	2.000	2.000
D-C	b_0	0.730	0.760	0.730	0.740	0.720
	b_1	0.451	0.420	0.477	0.419	0.420
	T_{nc}	17.900	106.100	19.300	104.800	60.300
D-CWORAD	b_0	0.750	0.750	0.750	0.750	0.750
	b_1	0.208	0.233	0.208	0.219	0.229
	T_{nc}	13.057	16.573	13.057	13.951	15.695
D-B	b_0	0.730	0.760	0.730	0.740	0.720
	b_1	0.198	0.140	0.213	0.142	0.150
	c_1	0.029	-0.080	-0.040	-0.081	-0.080
	c_2	0.008	0.010	0.008	0.008	0.010
Modified B-C	b_0	0.685	0.715	0.725	0.700	0.670
	b_1	5.300	-1.250	5.900	3.290	4.800
	b_2	1.129	1.595	1.085	1.150	1.060
Hargreaves	b_0	-3.34	0.472	-0.904	0.440	1.680
	b_1	0.234	0.160	0.210	0.151	0.143
R-R	T_o	5.580	9.050	5.580	9.660	8.350
Clemence	b_0	0.692	0.692	0.692	0.692	0.692
	b_1	0.052	0.052	0.052	0.052	0.052
	b_2	0.443	0.443	0.443	0.443	0.443
	b_3	0.030	0.030	0.030	0.030	0.030
HKS	b_0	-7.650	-1.790	-6.300	-0.620	1.535
	b_1	0.203	0.132	0.174	0.140	0.139
	b_2	0.294	0.241	0.352	0.114	0.039
	b_3	-0.191	1.293	-0.170	0.150	-0.230
	b_4	0.001	0.056	0.001	0.002	0.003
M-H	b_0	0.273	0.451	0.497	0.577	0.687
	b_1	0.674	0.863	0.616	0.574	0.590
	b_2	0.937	0.533	0.787	0.671	0.611

* - coefficients are developed either from measured or estimated (from sunshine hours) solar radiant density

6.4.1 Conventional statistics

For the Durban station, all of the models over-estimated lower and under-estimated higher values of solar radiant density. The Modified B-C, HKS, Hargreaves, M-H and Clemence models over-estimated lower and under-estimated higher values of solar radiant density throughout all stations. Performance of the B-C model was generally good for Cedara, Seven Oaks and Ukulinga. The D-CWORAD model slightly over-estimated solar radiant density values for Cedara and Ukulinga with slight under-estimation of higher values at Seven Oaks. A graphical comparison of B-C and the Modified B-C models is given in Fig. 6.2. Of note is that the Modified B-C model decreased the slope value and increased the intercept as

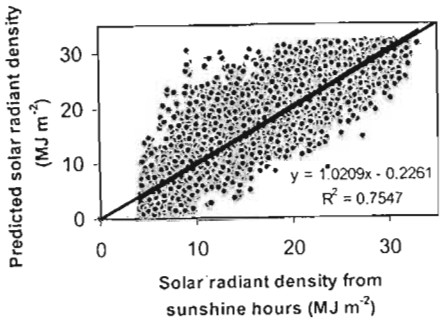

(a) Cedara B-C

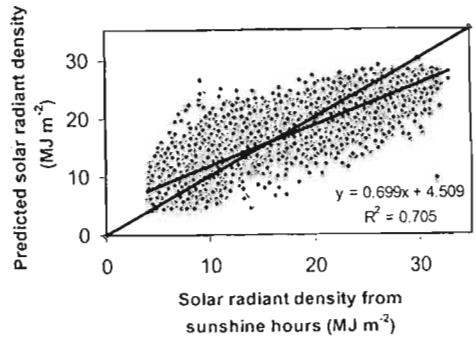

(b) Cedara Modified B-C

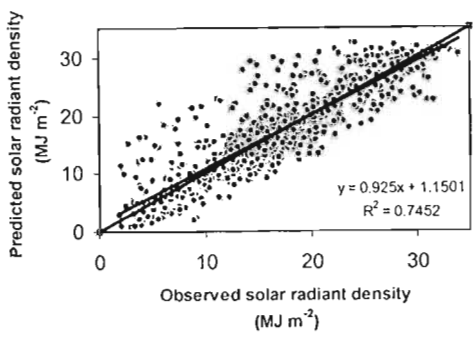

(c) Seven Oaks B-C

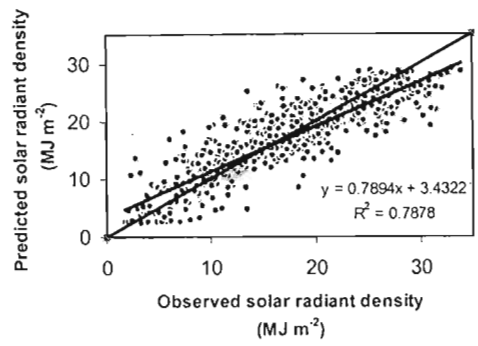

(d) Seven Oaks Modified B-C

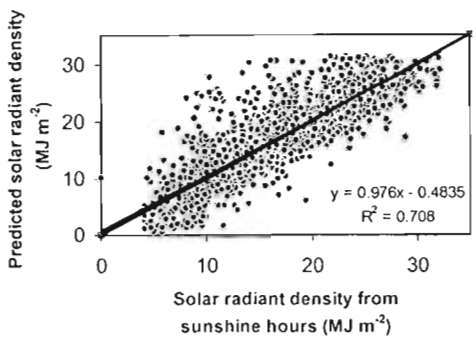

(e) Ukulinga B-C

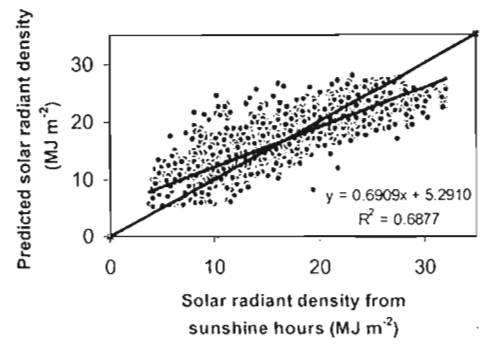

(f) Ukulinga Modified B-C

Fig. 6.2 Graphical comparison of the performance of the B-C (left) and Modified B-C (right) models for Cedara (a) and (b), Seven Oaks (c) and (d) and Ukulinga (e) and (f), KwaZulu-Natal, South Africa

compared to the B-C model for the regression analyses shown in Fig. 6.2. The D-C and D-B models performed well for Cedara but over-estimated the lower and under-estimated the higher values of solar radiant density at Seven Oaks and Ukulinga. The magnitude of over- and under-estimation of the D-C and D-B models was smaller than the other models. The performance of the R-R model was generally good for Cedara and Ukulinga, and with a slight over-estimation of lower values of solar radiant density at Seven Oaks.

Further evaluation of the performance of the models was carried out by computing the correlation determination (R^2), total, systematic and unsystematic root mean square errors (*RMSE*) and index of agreement (*d*) (Table 6.8). The performance of all models was, in general, poor for the Durban station. Most of these models have not been tried under maritime climates and this may signify that other better models may need to be developed for such environments. Nevertheless, the data from Durban station showed that the performance of the solar radiant density models for measured and sunshine derived solar radiant density were similar. Coefficients developed from sunshine hours derived solar radiant density resulted in a slight improvement of slope (increase) and intercept (decrease), which was reflected in a slight improvement of the *RMSE*, as compared to coefficients developed from observed solar radiant density. This improvement could be due to the extraterrestrial radiation value that appears on both sides of the equations in case of the former. The range of R^2, *d* and *RMSE* for Durban using observed solar radiant density were 0.51 to 0.60, 0.78 to 0.85 and 4.51 to 5.25 MJ m^{-2}; and using values derived from sunshine hours 0.54 to 0.60, 0.82 to 0.86 and 4.16 to 4.88 MJ m^{-2} respectively. The coefficients developed using measured solar radiant density were used for solar radiant density derived from sunshine hours and *vise versa*. The statistical outputs seem to be affected by the data inputs used rather than by the coefficients. Thus, similar statistical outputs were obtained for the observed or sunshine derived solar radiant density by using either of the coefficients (Table 6.9, Fig. 6.3).

The Clemence (1992) model, which was developed specifically for South African conditions, showed highly variable statistical outputs, usually with high *RMSE* for all locations. In fact, Clemence (1992) found this model to perform better for winter rainfall areas rather than summer rainfall areas. All locations included in this study are summer rainfall areas. So, discussions will concentrate on the results obtained using the remaining models under the locations of Cedara, Seven Oaks and Ukulinga.

Table 6.8 Statistical results of measured (sunshine derived) solar radiant density values against model-predicted values for Cedara, Durban, Seven Oaks and Ukulinga in KwaZulu-Natal, South Africa

Site	Statistic	Model[$]								
		B-C	D-C	D-B	Modified B-C	Hargreaves	R-R	HKS	D-CWORAD	M-H
Cedara[*] (n[†]= 6576)	slope	1.02	0.94	0.89	0.70	0.71	1.01	0.74	1.02	0.69
	intercept	-0.23	1.37	2.03	4.75	4.46	-1.13	4.25	0.53	4.48
	R^2	0.75	0.74	0.73	0.70	0.71	0.75	0.73	0.73	0.73
	d	0.93	0.93	0.92	0.91	0.91	0.91	0.87	0.91	0.91
	$RMSE_s$	0.31	0.55	0.78	1.87	1.84	1.07	1.61	0.99	1.98
	$RMSE$[‡]	3.54	3.43	3.43	3.34	3.29	3.68	3.24	3.92	3.25
Durban (n = 2192)	slope	0.64	0.61	0.65	0.42	0.59	0.65	0.59	0.58	0.53
	intercept	6.28	6.77	6.12	8.77	7.21	4.89	6.69	4.90	6.70
	R^2	0.55	0.56	0.55	0.60	0.56	0.58	0.57	0.51	0.54
	d	0.85	0.85	0.85	0.78	0.84	0.85	0.85	0.81	0.82
	$RMSE_s$	2.56	2.74	2.51	4.09	3.01	2.90	2.86	3.52	3.33
	$RMSE$	4.73	4.65	4.76	4.72	4.64	5.08	4.51	5.25	4.77
Durban[*] (n = 2192)	slope	0.72	0.67	0.65	0.47	0.55	0.72	0.59	0.65	0.53
	intercept	4.93	4.55	5.14	8.63	7.54	2.97	5.97	3.47	7.21
	R^2	0.56	0.57	0.55	0.60	0.54	0.58	0.58	0.54	0.54
	d	0.86	0.86	0.85	0.83	0.84	0.85	0.85	0.82	0.83
	$RMSE_s$	1.80	2.04	2.20	3.30	2.79	2.35	3.15	3.09	2.92
	$RMSE$	4.31	4.2	4.28	4.16	4.19	4.53	4.82	4.88	4.24
Seven Oaks (n = 730)	slope	0.92	0.87	0.83	0.79	0.60	0.94	0.67	0.91	0.69
	intercept	0.89	1.90	2.75	3.43	6.59	1.86	5.04	0.95	4.48
	R^2	0.74	0.74	0.74	0.79	0.65	0.75	0.75	0.73	0.72
	d	0.93	0.92	0.92	0.94	0.87	0.92	0.91	0.92	0.90
	$RMSE_s$	0.70	1.02	1.21	1.48	2.76	1.23	2.34	0.78	2.27
	$RMSE$	3.82	3.75	3.69	3.22	4.15	3.97	3.57	3.98	3.78
Ukulinga[*] (n = 1826)	slope	0.98	0.93	0.86	0.69	0.68	1.06	0.69	1.02	0.70
	intercept	0.48	1.36	2.70	5.29	5.34	-1.33	5.10	0.73	4.69
	R^2	0.71	0.71	0.68	0.69	0.67	0.71	0.67	0.69	0.68
	d	0.91	0.91	0.91	0.90	0.89	0.91	0.90	0.89	0.90
	$RMSE_s$	0.26	0.50	0.94	1.85	1.88	0.55	1.80	1.06	1.78
	$RMSE$	3.64	3.49	3.51	3.25	3.36	3.93	3.31	4.10	3.31

[$] Model abbreviations: B-C – Bristow KL, Campbell GS; D-C – Donatelli M, Campbell GS; D-B – Donatelli M, Bellocchi G; Modified B-C – Goodin DG, Hutchinson JMS, Vanderlip RL, Knapp MC; Hargreaves – Hargreaves GL, Hargreaves GH, Riley JP; R-R – Ramkrishnan BP, Ritchie JT; HKS – Hunt LA, Kuchar L, Swanton CJ; DC-WORAD – Donatelli M, Campbell GS; M-H – Mahmood R, Hubbard KG.

[*] Statistical analyses are computed using solar radiant density derived from sunshine hours against model-predicted

[†] n refers to the number of data points used for the analysis

[‡] $RMSE$ (MJ m^{-2}), $RMSE_s$ and $RMSE_u$ are yearly averages of all the years analyzed

Table 6.9 Statistical indices for the Durban location using B-C model coefficients of observed and sunshine derived solar radiant density for both observed and sunshine derived data sources

Coefficients	Data source	Slope	Intercept (MJ m^{-2})	R^2	d	$RMSE_s$ (MJ m^{-2})	$RMSE$ (MJ m^{-2})
Observed	Observed	0.638	6.283	0.550	0.851	2.560	4.725
Sunshine-derived	Observed	0.637	6.333	0.550	0.852	2.562	4.728
Sunshine-derived	Sunshine-Derived	0.715	4.933	0.563	0.863	1.795	4.308
Observed	Sunshine-derived	0.713	4.900	0.563	0.863	1.795	4.307

The HKS model (Table 6.1), which uses daily air temperature range and precipitation as input components to estimate solar radiant density, gave few incidences of unreasonably lower values (<0 MJ m^{-2}) and/or higher values (>100 MJ m^{-2}) of solar radiant density at high precipitation and low daily air temperature range records. The corresponding observed solar radiant density at such instances was usually below 10 MJ m^{-2}. Assuming these days were completely overcast, the value of estimated solar radiant density was corrected by multiplying the extraterrestrial radiation by a value of 0.25 (Gates, 1980).

The R^2 for Cedara, Seven Oaks and Ukulinga ranged from 0.70 to 0.75, 0.65 to 0.79 and 0.67 to 0.71 for number of observations 6575, 730 and 1826 respectively. Considering the number of observations involved, the coefficient of correlations resulting from the observed and model-predicted solar radiant density values were good indications of the models' performance and readiness for further statistical analysis. The range of the *RMSE* for Cedara, Seven Oaks and Ukulinga were 3.24 to 3.92, 3.22 to 3.98 and 3.25 to 4.10 MJ m^{-2} respectively. The Modified B-C, HKS and M-H models gave consistently smaller *RMSE* value in all three locations. Goodin *et al.* (1999) found that the Modified B-C model gave lower *RMSE* as compared to the B-C model for Manhattan, Kansas, USA. Hunt *et al.* (1998) also found similar results when they compared the HKS model against the B-C model for Ontario stations, in Canada. Mahmood and Hubbard (2002), however, found that the B-C model gave slightly lower values of *RMSE* when compared to M-H and the Modified B-C models in the Northern Great Plains, USA.

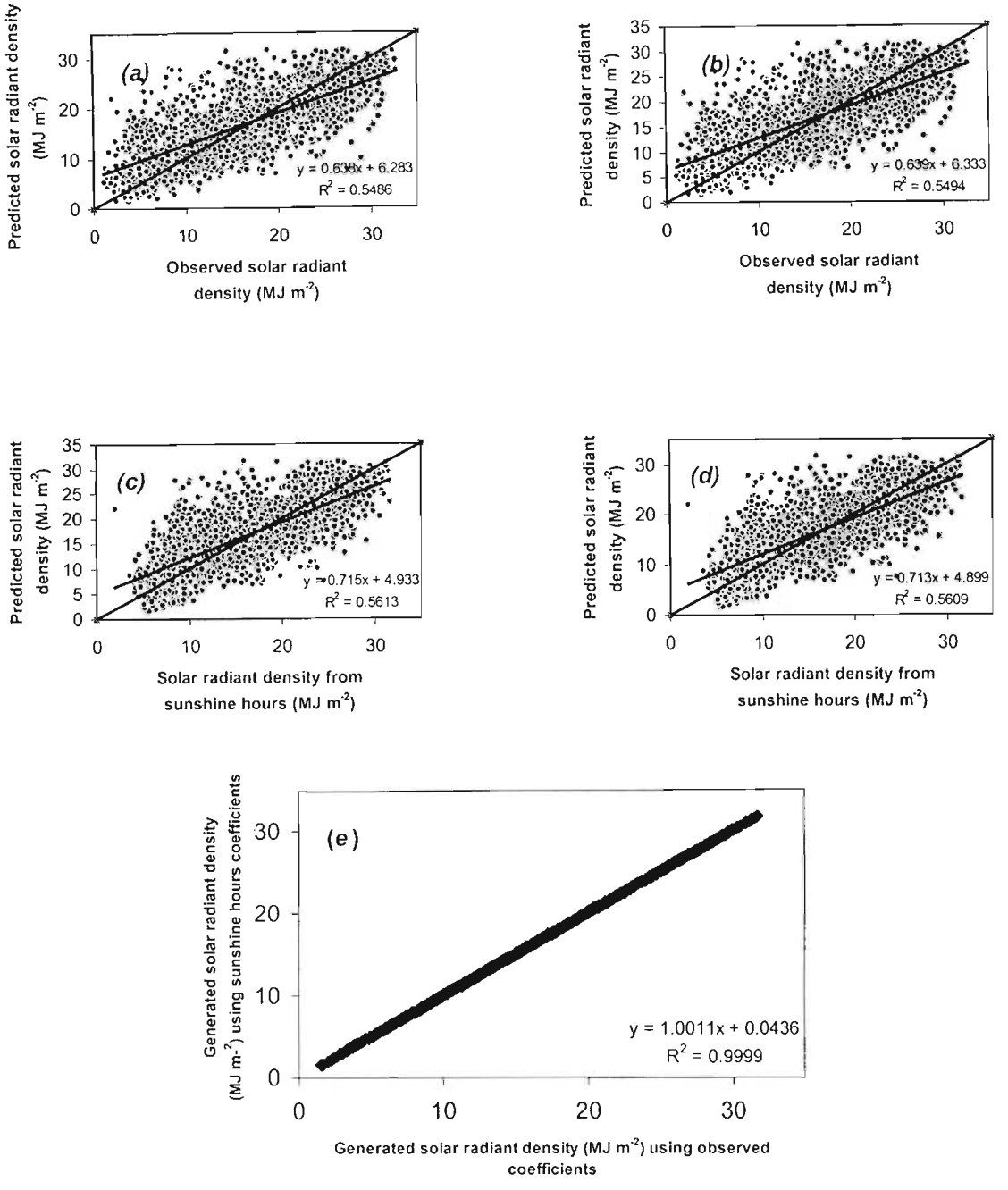

Fig. 6.3 Graphical presentation of the B-C model estimates for Durban using coefficients developed from (a) observed solar radiant density values as applied to observed values, (b) sunshine hours derived solar radiant density values to observed values, (c) sunshine hours derived solar radiant density values to sunshine hours derived solar irradiance values and (d) observed solar radiant density values to sunshine hours derived solar radiant density values and (e) solar radiant density values generated using observed coefficients against sunshine hours derived coefficients

For the three locations in this study, all of the models that are contained within the RadEst suite of models (beta v3.00) (ISCI-Crop Science, 2002; Donatelli *et al.*, 2003), D-CWORAD model and the R-R model resulted in slightly higher *RMSE* than the Modified B-C, HKS and M-H models with the D-CWORAD resulting in the largest (poor) *RMSE*.

Though the Modified B-C, HKS and M-H models seem to have the lowest *RMSE* as compared to the other models, it seems necessary to divide this error into its systematic ($RMSE_s$) and unsystematic ($RMSE_u$) components for evaluation of performance of the models (Willmott, 1981). For a perfect model the ratio of the $RMSE_s$ and $RMSE_u$ to the *RMSE* should be zero and one respectively. All the models encapsulated in the RadEst suite of models (beta v3.00) (ISCI-Crop Science, 2002; Donatelli *et al.*, 2003), the D-CWORAD and R-R models consistently resulted in the lowest, closer to zero, $RMSE_s$ to *RMSE* ratio.

The range of the Willmott's index of agreement, *d*, for Cedara, Seven Oaks and Ukulinga were 0.87 to 0.92, 0.87 to 0.94 and 0.86 to 0.91 respectively. All models but the HKS resulted in a *d* index greater than 0.90 for Cedara. For Seven Oaks, the Hargreaves model was the only model that resulted in a *d* index lower than 0.90. For Ukulinga the picture was slightly different with Hargreaves and D-CWORAD models resulting in a *d* index lower than 0.90. The models contained within the RadEst suite of models (B-C, D-C and D-B models) yielded the highest *d* index value in all locations except at Seven Oaks where they were outsmarted by the Modified B-C model. The RadEst suite of models, the Modified B-C, R-R and M-H models resulted in *d* index value of greater than 0.90 for all three locations.

According to these statistical indices the models contained in the RadEst suite of models (beta v3.00) (ISCI-Crop Science, 2002; Donatelli *et al.*, 2003) seem to be generally better tools for estimation of solar radiant density at Cedara. This is mainly due to the better fit of the slope and intercept along with a high *d* index and lower $RMSE_s$.

Although the Modified B-C, at Seven Oaks, resulted in the highest *d* index value and by far the lowest *RMSE*, it slightly over-estimated lower values and under-estimated higher values of solar radiant density (Fig. 6.2 (d)). Removing the bias from the Modified B-C model in order to remove the over- and under-estimation resulted in an increase of the *RMSE* and its systematic, and unsystematic components as well. The B-C model, with a *d* index value next to the Modified B-C model, had lower $RMSE_s$ and reasonably low *RMSE*, hence it could be regarded as a better model for this location.

The RadEst suite of models resulted in highest *d* index value for Ukulinga along with the R-R model but larger *RMSE* as compared to the Modified B-C, M-H, HKS and Hargreaves models. For this location the R-R and B-C models did not over- or under-estimate solar radiant density values. But their *RMSE* was larger than the other models. The D-C model showed a slight over-estimation and under-estimation of higher and lower values respectively (Fig. 6.4) but it yielded the highest *d* index, also a *RMSE* smaller than the B-C model. So, for this location it is recommended that either the B-C or D-C model be used.

The statistical indices that are calculated for all the models in the three locations had shown to be comparable to other works on the same models but different locations. Goodin *et al.* (1999) and Mahmood and Hubbard (2002) have reported over- and under-estimation of lower and higher values of solar radiant density respectively when they applied the B-C, Modified B-C and M-H models to the Northern Great Plains, USA. Goodin *et al.* (1999) reported a *RMSE* of 3.91 and 4.14 MJ m^{-2} for the Modified B-C and B-C models respectively for the Manhattan, Kansas. Mahmood and Hubbard (2002) applied the models M-H, B-C and Modified B-C for the same region and came up with a range of *RMSE* 3.9 to 4.93, 3.53 to 4.78 and 7.06 to 9.16 MJ m^{-2} respectively. They attributed the discrepancy in the result of *RMSE* in the two studies to the difference of the dataset they have used. Their report on the index of agreement, *d*, was in the range of 0.90 to 0.94, 0.91 to 0.94 and 0.56 to 0.68 for the M-H, B-C and Modified B-C respectively. For Cedara, Seven Oaks and Ukulinga the *RMSE* (MJ m^{-2}) of the above models was in the range of 3.26 to 3.78, 3.53 to 3.81 and 3.22 to 3.34, and *d* index value in the range of 0.90 to 0.91, 0.91 to 0.93 and 0.91 to 0.94. Although the statistical indices reported for the three sites under study is opposite to the Mahmood and Hubbard

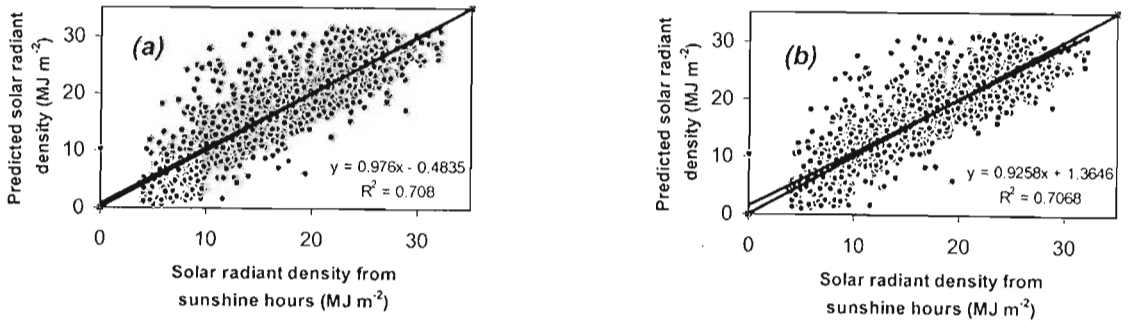

Fig. 6.4 Graphical presentation of the performance of the B-C (a) and D-C (b) models for Ukulinga, KwaZulu-Natal, South Africa

(2002) ranking of the models, the values reported here seem to be better than they reported.

Mahmood and Hubbard (2002) found that minimum and maximum air temperature reporting time from midnight to midnight to give better estimation of solar radiant density as compared to 08h00 to 16h00 reporting time for the above three models. The time interval from which the minimum and maximum air temperature reports are made could also have a significant influence in these models. In addition, in the context of using such data for crop simulation, the minimum and maximum air temperature readings reported from instantaneous measurements of short time interval, like 10 s, may have no significant physiological impact on the plants as compared to those averaged over longer time periods.

Donatelli and Campbell (1998) evaluated the performance of the D-C and D-CWORAD models based on *RMSE* for certain locations in Italy, France, The Netherlands and USA. They reported a range of *RMSE* from as low as 2.37 to 4.99 and 2.44 to 5.02 MJ m^{-2} for the D-C and D-CWORAD models respectively. In this study, for the D-C model the range of *RMSE* was from 3.43 to 3.75 and for the D-CWORAD 3.92 to 4.10 for the Cedara, Seven Oaks and Ukulinga locations. Considering that these two models are evaluated on a global basis, the *RMSE* for the three locations fell well within the range though a bit far to the right in the case of the D-CWORAD model.

Using the HKS and Hargreaves models, Hunt *et al.* (1998) reported a *RMSE* ranging from 3.4 to 4.1 and 4.2 to 4.7 MJ m^{-2} respectively. For the Cedara, Seven Oaks and Ukulinga locations these results ranged from 3.24 to 3.57 and 3.29 to 4.15 MJ m^{-2} for the HKS and the Hargreaves models respectively. This signifies that these models performed better for these locations but the abnormally extreme results for the HKS model and its correction should be kept in mind.

The range of *RMSE* achieved from the R-R model for the Cedara, Seven Oaks and Ukulinga locations ranged from 3.77 to 3.97 MJ m^{-2}. It can be said that this model's performance was rather poor as compared to a *RMSE* of 2.99 MJ m^{-2} reports made by Ramkrishnan and Ritchie (2000) for India. Ramkrishnan and Ritchie (2000) used solar radiant density computed from the R-R model in crop modelling and found good agreement in the model predictions of biomass and evapotranspiration when compared with model outputs using observed solar radiant density. Rivington *et al.* (2002) also used solar radiant density

estimates from the D-C model in CropSyst but found it inferior to solar radiant density estimates from sunshine duration and neighbouring stations for southern England locations.

6.4.2 Statistical evaluation using an expert system

Evaluation of the performance of the solar radiant density models using conventional statistics was made difficult because of the several statistics considered and the contrasting results they give. One model may be ranked first according to one statistic but may not be so according to another statistic. It seems more weight was given to, according to decreasing importance, slope and intercept, $RMSE_s$ and d. The weights were rather implicit and subjective, and there was no clear cut-off on what value of which statistical index was considered good or bad. To obviate such difficulties, Bellocchi *et al.* (2002) employed a fuzzy expert system. The system they employed assigns clear cut-offs on what value of which statistic to be considered good or bad and weights on the relative importance of the statistical indices based on decision rules. This enables the expert system to combine several of the statistics into one aggregate module, and several modules into a single indicator (Bellocchi *et al.*, 2002).

The number of years either with sunshine hours or solar radiant density data for Cedara, Seven Oaks and Ukulinga that were used for calculation of the indicator, I_{rad}, other than those used for derivation of coefficients, were 20, 2 and 5 years respectively. The models are ranked according to I_{rad} in Table 6.10 for the three locations. The ranking revealed that there was no model as such which outperformed all the other models in all locations consistently. The HKS model seems to do well with a score of second at Cedara, first at Seven Oaks and

Table 6.10 Performance of solar radiant density models according to the indicator, I_{rad}, calculated using an expert perception for Cedara, Seven Oaks and Ukulinga in KwaZulu-Natal, South Africa (the numbers in brackets indicate rank of the model for the specific location)

Location	Cedara (n = 20)	Seven Oaks (n = 2)	Ukulinga (n = 5)
B-C	0.302 [7]	0.273 [3]	0.421 [7]
D-B	0.143 [1]	0.302 [6]	0.314 [4]
D-C	0.180 [3]	0.275 [4]	0.331 [6]
D-CWORAD	0.593 [9]	0.438 [9]	0.702 [9]
Hagreaves	0.233 [5]	0.376 [8]	0.329 [5]
HKS	0.164 [2]	0.162 [1]	0.245 [3]
M-H	0.181 [4]	0.286 [5]	0.232 [2]
Modified B-C	0.236 [6]	0.168 [2]	0.123 [1]
R-R	0.388 [8]	0.359 [7]	0.553 [8]

third at Ukulinga. The Modified B-C was also ranked first at Ukulinga and second at Seven Oaks, but 6th at Cedara. The D-B model was ranked first at Cedara but was sixth and fourth at Seven Oaks and Ukulinga respectively. The models which did not perform well, however, produced a large I_{rad} value consistently in all locations and could be easily identified. The D-CWORAD model was ranked last in all locations with I_{rad} value ranging from 0.438 to 0.702. The R-R model was also ranked second to last at Cedara and Ukulinga and third to last at Seven Oaks.

The values of the modules achieved from the calculation indicate the strength of the model in dealing with residuals, correlations and patterns (Bellocchi *et al.*, 2002). The D-B model was ranked first at Cedara because the model was able to produce small *PI*'s (a relatively uniform distribution of residuals over the range of T_n and *doy*), otherwise it produced roughly similar residuals and correlations when compared with the other models. The Modified B-C was ranked first at Ukulinga and this is largely attributed to the small residuals and *PI's* it produced. Although the HKS model was ranked first at Seven Oaks, the number of years involved for calculating I_{rad} were only two and not large enough to draw a conclusive model ranking. The D-CWORAD and R-R stood at the last of the ranking in all locations. This was because they failed to produce residuals that are small and uniformly distributed over the range of T_n and *doy* but produced a reasonably good correlation.

6.4.3 Application to crop simulations

Statistical results of maize grain yield simulations during the 20-year period for Cedara are shown in Table 6.11. Total yield is the yield accumulated during the simulation period for each dataset. Difference is the absolute difference in simulated grain yield between the data series that use observed and model estimated solar radiant density (negative values indicate the direction of change). Max. error is the largest absolute difference in simulated grain yields between the above datasets (negative values indicate the direction of change). The other statistical values assume their usual meanings. Graphs depicting cumulative probability distributions of the simulated grain yields over the 20-year period of simulation from using model estimated and observed solar radiant density are also given in Fig. 6.5.

Table 6.11 Statistical comparison of 20 years of simulated maize grain yield (tons ha^{-1}) using CropSyst with different dataset of solar radiant density for Cedara, KwaZulu-Natal, South Africa

Statistics	"Observed"	B-C	D-B	D-C	D-CWORAD	Modified B-C	Hargreaves	HKS	M-H	R-R
Total yield	219.29	225.17	220.89	215.75	232.24	210.22	213.56	213.53	207.21	207.12
Difference		5.88	1.60	-(3.53)	12.96	-(9.07)	-(5.72)	-(5.76)	-(12.07)	-(12.17)
Max. error		-(0.95)	0.48	0.92	3.43	1.52	0.97	0.91	1.51	1.57
Mean	10.96	11.26	11.04	10.79	11.61	10.51	10.68	10.68	10.36	10.36
Std. Dev	1.59	1.84	1.61	1.65	2.62	1.17	1.48	1.50	1.21	1.42
RMSE		0.51	0.26	0.41	1.45	0.75	0.40	0.40	0.80	0.75
R^2		0.96	0.98	0.95	0.84	0.89	0.97	0.97	0.92	0.92
P value		0.592	0.876	0.733	0.351	0.310	0.559	0.561	0.184	0.210

In general, the 20-year grain yield simulations gave values of R^2 ranging from 0.84 to 0.98. Apart from yield simulated from using solar radiant density estimated from two models, namely D-CWORAD and Modified B-C, all other simulated yields using estimated solar radiant density from the other models resulted in R^2 value greater than 0.90. The solar radiant density estimated from the B-C, D-B, D-C, Hargreaves and HKS models resulted in absolute errors less than one ton ha^{-1}, the Modified B-C, M-H and R-R resulted in absolute errors that range from zero to two while the D-CWORAD produced an absolute error that ranged between zero and 3.43 tons ha^{-1}.

All the models are ranked according to their ability to simulate yield that matches the yield simulated from using the observed solar radiant density data according to each statistic in Table 6.12. The D-B model was superior to all models in producing simulated yields that match those from using the observed solar radiant density according to all the statistical measures employed. This is also reflected in the cumulative distribution graphs (Fig. 6.5) in which the simulated yield from using solar radiant density estimated from the D-B model followed the simulated yield from using the observed solar radiant density well. The D-CWORAD scored the worst in four out of the five statistical measures. The R-R model also scored second to last in three out of the five statistical measures. The M-H and Modified B-C were also among those whose performance was not good according to the statistical measures. The HKS model was ranked second according to three statistical measures. But since the weights that are given to these statistical measures are not known it is difficult to set the overall ranking, apart for the D-B and probably the D-CWORAD and R-R models. For the other models the ranking should be done according to particular interest of application, until

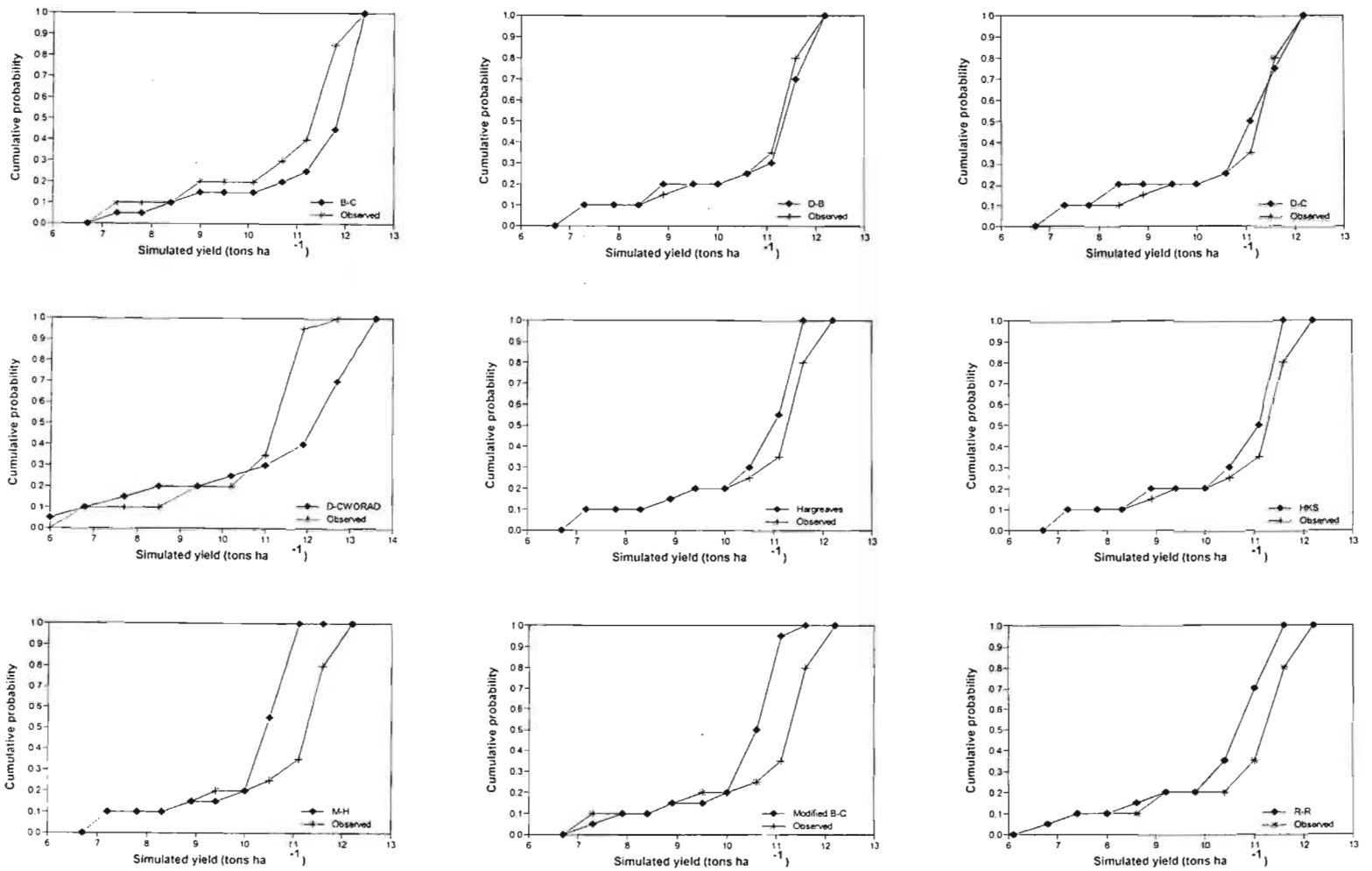

Fig. 6.5 Cumulative probability of maize grain yield distributions as simulated by CropSyst model using 20-years of observed and model-estimated solar radiant density at Cedara, KwaZulu-Natal, South Africa

Table 6.12 Ranking of the models according to statistical indices calculated from application in crop simulation for Cedara, KwaZulu-Natal, South Africa (1 indicates best ranking and 9 worst ranking according to the respective statistical index)

Model	Difference between totals	Absolute Max. error	P value (equality of mean)	*RMSE*	R^2
B-C	5	4	3	5	4
D-B	1	1	1	1	1
D-C	2	3	2	4	5
D-CWORAD	9	9	6	9	9
Modified B-C	6	7	7	6	8
Hargreaves	3	5	5	3	3
HKS	4	2	4	2	2
M-H	7	6	7	8	6
R-R	8	8	8	7	7

some kind of expert system involving these and/or some additional statistics becomes available. For example, if the interest is to minimize the difference between accumulated yields, then the D-C model should be chosen next to the D-B model. If the interest is minimizing the absolute error between the simulations, then the HKS model should be chosen next to the D-B model.

The ranking of the models according to their ability to reproduce the grain yield simulated from using observed solar radiant density agreed reasonably well with the rankings made using expert perception at Cedara. The D-B model is ranked first according to both the expert judgment and application in crop simulation models at Cedara. The HKS was ranked second according to the expert perception and it also scored three second and two fourth positions out of five in the yield simulation application. The D-C model was ranked third according to the expert judgment and it also scored two second and one third position in the yield simulation application. The D-CWORAD was ranked last by the expert judgment and it also scored four last positions out of five in the yield simulation application. The R-R model was ranked second to last by the expert judgment and it also scored three second to last and two third to last positions. The rankings according to expert judgment and grain yield simulations seem to be out of phase for the B-C and M-H models. The B-C model was ranked seventh according to the expert judgment but the statistical measures scored in the yield simulation for B-C model ranged from third to fifth. The M-H model was also ranked fourth according to the expert judgment but the scores of the statistical measures in the yield simulation ranged from sixth to

eighth. Assigning clear cut-offs for when a statistical index is considered to be good or bad and weights to the statistical measures like those done by Bellocchi *et al.* (2002) for the solar radiant density models could have solved the problem of ranking the solar radiation models according to their application in crop simulation models.

6.5 CONCLUSIONS AND RECOMMENDATIONS

In the absence of solar radiant density, estimates can be made from either sunshine hours or more readily available meteorological observations of air temperature and/or precipitation along with extraterrestrial radiant density. Whenever these models/equations are applied, for more accurate results, location specific coefficients must be calibrated using observed solar radiant density. Models that use their source of data from air temperature and/or precipitation were found to be inferior to equations that use sunshine hours for estimation of solar radiant density. And yet, these models were useful in addressing the lack of solar radiant density data for the purpose of running crop simulation exercises for past crop experiments in areas where solar radiant density is not observed. In the same manner, missing observations of solar radiant density in stations where it is observed (computed from sunshine hours) can be estimated. The B-C and D-C models were found to have the highest index of agreement, d, smallest $RMSE_s$ and reasonably lower *RMSE*. These criteria make the B-C and D-C models to be better tools for estimation of solar radiant density at Cedara, Seven Oaks and Ukulinga according to conventional statistics than the other models tested. According to expert judgment the D-B model for Cedara, HKS model for Seven Oaks and Modified B-C model for Ukulinga were found to be best estimators of solar radiant density. The ranking of the models according to their application in reproducing simulated grain yields at Cedara agreed well with expert judgment ranking and not with the conventional statistics. The number of years considered should be many for more accurate and sound statistical evaluation of the models.

7 CropSyst MODEL CALIBRATION AND VALIDATION

7.1 INTRODUCTION

In many regions of the world where crop production is practiced, future crop yield is variable and hardly predictable. Crop production in a region is determined to a large extent by water supply, which, unfortunately, is characterized by large variations among growing seasons. Scarcity, as well as excess, of water has a negative impact on crop production. The impact of water supply on crop production has initiated the need for measuring the amount of water supplied to crops. There are many methods, of varying sophistication, that have been developed to determine the timing and amount of water supply to a crop (Section 3.2).

However, the impact of applied water on productivity cannot be analyzed independent of weather, soil, field hydrology, crop characteristics and management practices. Computer simulation models (e.g., CERES, CropSyst, EPIC) which integrate these factors into a comprehensive cropping system to predict their effects on the soil water balance, nutrient dynamics, and development and growth of crops are available. Reliability of these computer simulation models lies solely in their predictive capability and to this end validation of a model becomes a necessary prerequisite using field experiment if the model is to be applied for purposes of management practices (Pala *et al.*, 1996).

CropSyst (Stöckle and Nelson, 2000; Stöckle *et al.*, 2003) is a multi-year, multi-crop, daily time step crop growth simulation model developed to study the effect of cropping systems management on crop productivity and the environment. This study is undertaken to evaluate the ability of CropSyst to simulate (i) crop water-use under fallow land and various crops (oats, Italian ryegrass, rye and maize) plots; (ii) leaf area index (LAI) of oats, Italian ryegrass and rye; and (iii) crop growth and development of maize at Cedara, KwaZulu-Natal, South Africa.

7.2 MATERIALS AND METHODS

7.2.1 Calibration and validation data

Crop and soil data for the purpose of calibration were obtained: (i) for oats (*Avena sativa* L. cv. Overberg), Italian ryegrass (*Lolium multiflorum* L. cv. Midmar) and rye (*Secale cereale* L. cv. SSR 1) (including weather data without solar radiant density) from Univ. of Pretoria, Department of Plant and Soil Science from experiments conducted at Kromdraai open cast mine (25°48′S, 29°05′E, altitude 1510 m), in the highveld region, close to Witbank (Mpumalanga province), South Africa, during the 1994 growing season, and (ii) for maize (*Zea mays* L. cv. PAN 6568) from cropping system experiments conducted at Cedara (29°32′S, 30°17′E, altitude 1076 m), Department of Agriculture and Environmental Affairs, KwaZulu-Natal, South Africa, during the growing seasons of 1997/98 to 2001/02 as part of National Cultivar Trial: maize (Maree and Bruwer, 1998; Du Plessis and Bruwer, 1999, 2000, 2001, 2002). Daily weather data (sunshine hours, precipitation and maximum and minimum air temperatures) for Cedara were obtained from the Agricultural Research Council, Institute of Soil, Climate and Water, Pretoria, South Africa. The sunshine hours were converted into solar radiant density as suggested by Reid (1986). Solar radiant density was also estimated using the D-C model (Donatelli and Bellochi, 2001) (see Chapter 6) for days with missing sunshine hours (e.g., part of the year 1998).

The crop, soil and weather data for validation were collected from a field trial established at Cedara during the 2002/03 growing seasons. Oats (*Avena sativa* L. cv. Drakensberg), Italian ryegrass (*Lolium multiflorum* L. cv. Midmar) and rye (*Secale cereale* L. cv. MacBlue) were planted on April 12, 2002 each in an 18 m by 6 m plot with three replications. (Note that the oats and rye varieties used for purposes of validation were different from those used for calibration). The distance between rows was 0.15 m for all three crops with planting density (kg ha^{-1}) of 90, 30 and 123 for oats, Italian ryegrass and rye respectively. Leaf area was measured on average on a bi-weekly basis starting two months after establishment for oats, Italian ryegrass and rye using the LAI-2000 plant canopy analyzer (PCA). All three crops were irrigated using an overhead sprinkler irrigation system. Maize was planted on November 21, 2002 in 18 m by 6 m plot with three replications with a distance of 0.75 m between rows and planting density of 44000 seeds per hectare. The soil at the experimental site was

classified as Hutton, Doveton type (MacVicar, 1977). The physical and chemical properties of the soil determined from laboratory analysis are presented in Appendix A. Soil water content was measured to a depth of 1000 mm at intervals of 100 mm during the field experimentation, every three days, with a Diviner 2000 (Sentek Environmental Technologies, Stepney, Australia). The observations were average measurements taken from two access tubes within each plot. Inputs such as soil texture, bulk density, pH, CEC and water content at -33 kPa and -1500 kPa that are required by the model for simulation were either observed in the field and/or analyzed in the laboratory. Weather data for the 2002/03 growing seasons was also collected from an automatic weather station located approximately 100 m from the experimental site. The fallow plots were hand-weeded throughout the observation period in order to keep them devoid of vegetation.

Initial soil water conditions for all depths in the simulation were provided where measurements were available, otherwise simulation was made to start two days following substantial rainfall in which the initial soil water contents of all layers were set to near the upper limit. The nitrogen and salinity sub-routines were not used hence there was no need to initialize them.

7.2.2 The model

CropSyst is a user-friendly, conceptually simple but sound multi-year, multi-crop daily time step crop growth simulation model. The model has been developed to serve as an analytic tool to study the effect of cropping systems management on productivity and the environment. The model simulates the soil water budget, soil-plant nitrogen budget, crop canopy and root growth, dry matter production, yield, residue production and decomposition, and erosion. Management options include: cultivar selection, crop rotation (including fallow years), irrigation, nitrogen fertilization, tillage operations, and residue management. The model code is written in C++ and can be run on WINDOWS or UNIX-based platforms (Stöckle and Nelson, 2000; Stöckle *et al.*, 2003).

CropSyst computes the amount of water used for crop development and growth by modelling the components of the soil water balance. The water balance components considered by CropSyst include: irrigation, precipitation, shallow water table (finite difference), rainfall intercepted by the crop foliage and surface residue, surface runoff and

residue evaporation, infiltration through soil layers, transpiration, deep percolation and water storage in the soil profile. Daily crop growth is expressed as biomass increase per unit ground area. Above-ground crop growth is represented in terms of above-ground biomass accumulation. CropSyst models this growth as: water, radiation, nitrogen and temperature limited crop growth (Stöckle and Nelson, 2000; Stöckle *et al.*, 2003).

In this simulation exercise, the water redistribution in the soil profile is calculated using a finite difference approach in which water moves up and down depending on the soil water potential of adjacent layers. The presence of surface residue and water table are ignored.

7.2.3 Application of CropSyst in irrigation scheduling

Automatic irrigation was simulated from 47 up to 170 days after planting with planned maximum allowable soil water depletion for fields of oats, Italian ryegrass and rye. This simulation time corresponded to the time when the plant roots had achieved more than half of their maximum rooting depth. The depth of depletion observation was set to 0.4 m for Italian ryegrass and rye, and 0.7 m for oats. The irrigation simulation applications refilled the soil layers of the root zone to 100% PAW depending on the depletion of the observation depth (0.4 m for Italian ryegrass and rye, and 0.7 m for oats) and the root growth into the soil layer when PAW was depleted to a fraction of 0.4 and 0.6. In CropSyst, the amount of irrigation water to be applied is calculated as (Stöckle and Nelson, 2000):

$$\sum_{l=1}^{nl}(\theta_{new}-\theta_l)\cdot RD_l, \quad \text{if } PAW_l < PAW_{refill} \tag{7.1}$$

where nl refers to the number of soil layers, θ_l ($m^3\ m^{-3}$) is the water content of layer l, RD_l (mm) is the root depth into layer l (if the root grows through the layer, RD_l is set to the thickness of the layer), PAW_l (0 to 1) is the current plant available water for layer l given as:

$$PAW_l = \frac{\theta_l - \theta_{ll}}{\theta_{ul} - \theta_{ll}} \tag{7.2}$$

PAW_{refill} (0 to 1) is the point of plant available water to refill to, θ_{new} (m^3 m^{-3}) is the water content when the soil is refilled to PAW_{refill} and is computed as:

$$\theta_{new} = PAW_{refill} \cdot (\theta_{ul} - \theta_{ll}) + \theta_{ll} \qquad 7.3$$

θ_{ul} and θ_{ll} (m^3 m^{-3}) are the water content at the upper and lower limits of layer l respectively.

Net irrigation multiplier was taken as one. This was mainly done for the sake of comparison. The current version of CropSyst (Version 3.02.26) does not consider runoff or canopy/residue interception of applied irrigation water (Stöckle and Nelson, 2000). During the simulation, all observed irrigation amounts applied to the experimental fields, therefore, were infiltrated into the soil. Maximum irrigation application during the day was limited to 20 mm.

7.3 CALIBRATION

It is usual to find some discrepancies between measured data and simulated outputs when a model is used for environments other than for which it is developed (Whisler *et al.*, 1986). It is, therefore, crucial to correctly interpret these discrepancies and subsequently adjust them so that simulation outputs would agree with measured data (Whisler *et al.*, 1986). Such adjustments were made by fine tuning the soil and crop input parameter values, that are either available in CropSyst or obtained from other sources, within a narrow range of fluctuation as dictated by the CropSyst User's Manual (Stöckle and Nelson, 2000) in relation to available field data on crop developmental stages, yield characteristics and patterns of water use. Other inputs, like weather, soil (when available) and management data input were used as they were observed in the field.

7.4 RESULTS AND DISCUSSION

7.4.1 Fallow land

The soil water balance was calibrated using soil water measurements observed with Diviner 2000 at a fallow land from 29 April 2002 (day of year 119) to 22 November 2002 (day of year 326) at Cedara, KwaZulu-Natal, South Africa. The field-observed soil water contents at -33 kPa and -1500 kPa were out of the range than that specified by the CropSyst User's Manual

(Stöckle and Nelson, 2000) and preliminary simulation using those values resulted in an over-estimation of soil water content as compared to the field-observed soil water content. This discrepancy can be explained to some extent by the soil water measuring instruments used at the field experimentation. The water content at -33 kPa and -1500 kPa for this purpose were obtained from observations using a Profile Probe (Delta-T Devices, Cambridge, UK) (because of its readiness to be automated) whereas the field water observations at the experimental plots were observed using Diviner 2000 (Sentek Environmental Technologies, Stepney, Australia). Both instruments were calibrated as per the manufacturer's instructions. The observations they bear seem to be similar in the middle range whereas at the high and low ranges the Profile Probe results in slightly higher and lower values than observed by the Diviner 2000 respectively. The CropSyst model also estimates water contents at -33 kPa and -1500 kPa from the soil texture inputted. This did not either result in a good simulation that agreed well with the observed data. The soil water content at -33 kPa and -1500 kPa were then calibrated as per the narrow specification range of values given in the CropSyst User's Manual so that the simulation outputs would agree with measured data (Stöckle and Nelson, 2000).

The finite difference infiltration technique adopted for the simulation made the calibration process of the soil water balance difficult because of the effect of calibration of one layer on the other layers. The calibration process by itself did not produce satisfactory statistical results, especially at lower depths (Table 7.1). This can be attributed to three reasons:

(i) the Diviner 2000 was quick to pick up changes in soil water at lower depths whereas the CropSyst model was slow which resulted in a time mismatch;

(ii) at such depths, the Diviner 2000 resulted in observations that have a slightly zigzag pattern whereas the model's simulation were almost in a straight line with very slight changes in water content; and

(iii) for a given amount of applied irrigation or precipitation, the model's response was greater than was actually observed in the field using Diviner 2000.

The depletion rate of the soil water seems to be similar in both the observed and simulated cases. This could be a cause of accumulation of incorrect soil water amount by the model as compared to the observed during frequent irrigation or precipitation. This may require reinitialization of the modelled soil water following irrigation or precipitation.

Table 7.1 Statistical results of calibration and validation (other than the data used for calibration) of the CropSyst model soil water balance against field-measured soil water content (m^3 m^{-3}) for a fallow land (from 29 April to 22 November 2002) at Cedara, KwaZulu-Natal, South Africa

	Depth (mm)	Slope	Intercept	R^2	$RMSE_s$	$RMSE_u$	$RMSE$	d
Calibration (n = 54)	100	1.446	-0.078	0.667	0.034	0.031	0.046	0.732
	200	1.285	-0.053	0.559	0.032	0.025	0.04	0.636
	300	1.268	-0.043	0.752	0.039	0.014	0.042	0.577
	400	1.014	-0.003	0.596	0.002	0.011	0.011	0.855
	500	0.786	0.086	0.323	0.012	0.012	0.017	0.574
	600	0.505	0.177	0.192	0.006	0.010	0.011	0.644
	700	0.380	0.215	0.124	0.007	0.009	0.011	0.616
	800	0.290	0.248	0.109	0.007	0.008	0.011	0.601
	900	0.251	0.265	0.108	0.008	0.008	0.011	0.588
	1000	0.220	0.274	0.177	0.014	0.007	0.016	0.596
Validation (n = 70)	100	1.748	-0.158	0.759	0.027	0.029	0.040	0.803
	200	1.660	-0.163	0.756	0.027	0.019	0.033	0.712
	300	1.846	-0.249	0.804	0.020	0.012	0.023	0.695
	400	0.915	0.036	0.525	0.010	0.011	0.014	0.739
	500	0.611	0.144	0.350	0.017	0.009	0.019	0.563
	600	0.354	0.225	0.210	0.010	0.007	0.013	0.590
	700	0.227	0.266	0.117	0.014	0.007	0.015	0.495
	800	0.106	0.306	0.026	0.014	0.006	0.015	0.407
	900	0.051	0.329	0.006	0.009	0.006	0.011	0.459
	1000	0.124	0.303	0.041	0.011	0.007	0.013	0.540

R^2 is coefficient of determination
$RMSE$, $RMSE_s$ and $RMSE_u$ (m^3 m^{-3}) are the total, systematic and unsystematic root mean square errors
d is Willmott's index of agreement

Soil water observations during days when there was irrigation or precipitation were excluded from the evaluation and statistical analysis of the model. This is because of observation and calculation time mismatch by Diviner 2000 and the model. The soil water observation may be made before irrigation is applied or precipitation occurs but the model calculates the soil water at the end of the day including water from irrigation or precipitation in which a large discrepancy may result between the observed and simulated soil water on these days.

The validation resulted, though not good by itself, in some statistics that are better than achieved from calibration (Table 7.1). The slope and intercept were better in the calibration regression equations but the R^2, $RMSE$ (root mean square error) and d index (Willmott's index of agreement) (Willmott, 1981) (see Section 2.8) were better in case of the validation dataset for the upper soil layers. The slope of the resulting validation dataset regression line was

generally far from one in all soil layers except for the 400-mm depth, with a value greater than one for the upper soil layers and less than one (approaching zero) for the deeper soil layers (Table 7.1). The intercept is also far from zero, again with the exception of the 400-mm depth, with negative values for the upper three layers and positive values for the lower layers (Table 7.1). The R^2 value was generally good for the three upper soil layers but keeps degrading itself towards zero with depth (Table 7.1). The *RMSE* was rather relatively higher (less agreement between observed and simulated) for the above three layers but their *d* index value was relatively higher (Table 7.1). The deeper soil layers had lower *RMSE* but the *d* index value was relatively low (less agreement between observed and simulated).

The agreement between the observed and simulated volumetric soil water was generally good for the relatively dry and medium range, but was not as good for relatively wet soil (Fig. 7.1 (a), (b) and (c)). The model's responses during wet days were greater than what is really observed in the field especially for the top layer. Fig. 7.1 shows the comparison of observed and model-simulated volumetric soil water content, for selected days on the basis of the wetness of the upper soil layers. Fig. 7.1 (a) represents the observed (symbols) and model-simulated (lines and symbols) for a relatively dry soil, nine days following the starting day of simulation. It can be seen from Fig. 7.1 (a) that the agreement between the observed and model-simulated volumetric soil water content is generally good. Fig. 7.1 (b) represents observed and model-simulated soil water with relatively medium wetness, 57 days after the starting day of the simulation. In the medium wetness range, again, the agreement between observed and model-simulated soil water was generally good. For the relatively wet range, a day is selected after precipitation occurred at the observation site (Fig. 7.1 (c)). It is clear from (Fig. 7.1 (c)) that the model over-estimated volumetric soil water content along the soil profile down to the observed depth, with more pronounced over-estimation at the topsoil layer. The volumetric soil water content of the selected days are depicted in one graph in Fig. 7.1 (d), and it can be seen that the soil water content at the upper soil layers varied from time to time. This could be attributed to the effect of variable surface temperature and solar radiant density that is experienced by the topsoil layers. Fig. 7.1 (d) also shows that the soil water at the deeper soil layers does not change much. This is probably because of the absence of plant roots that could extract water from deeper layers.

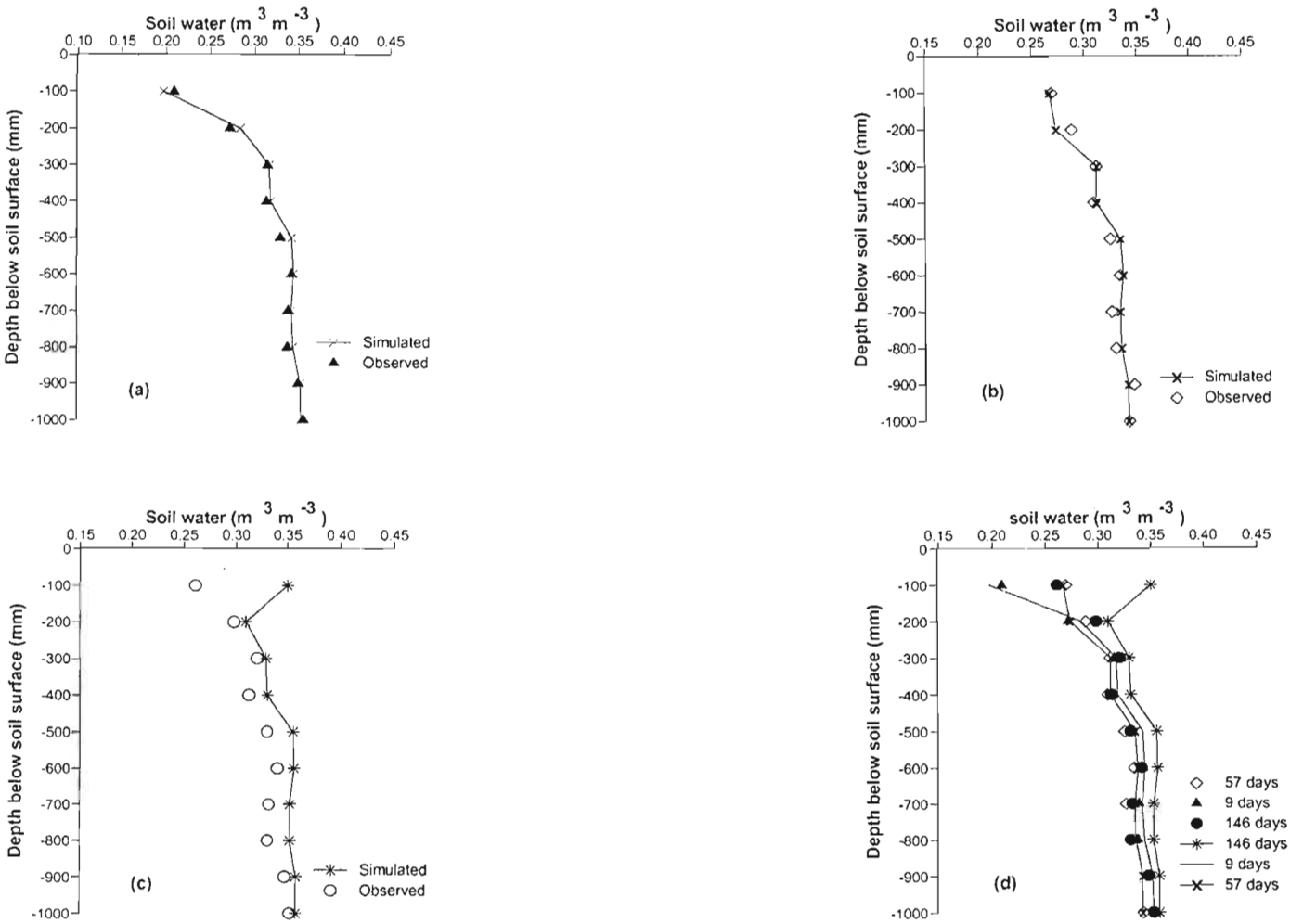

Fig. 7.1 Model-predicted (lines and symbols) and observed- using Diviner 2000 (symbols) volumetric soil water content distribution on days 9, 57 and 146 days after starting date of simulation (2002), representing relatively dry, medium and wet range soil surfaces, in a fallow land at Cedara, KwaZulu-Natal, South Africa

7.4.2 Oats, Italian ryegrass and rye

The calibration data for oats, Italian ryegrass and rye included, among others, soil water content (observed using neutron probe) and LAI (measured using LI-3000 area meter). Jovanovic *et al.* (1999) used these data, along with other data, for the development of crop parameters for the SWB (Soil Water Balance) model (Benadé *et al.*, 1996). The SWB and CropSyst models have the same parent model (pers. comm. Jovanovic, 2003), and hence the crop parameters developed for one of the models may be used in the other model. The crop parameters developed for the SWB model using the calibration dataset, however, required very minor adjustments when used as input to the CropSyst model. The adjusted crop parameters are presented in Appendix E.

The soil water content was validated for the depth of the root zone in each crop. The statistics between the observed and simulated for the depth of the root zone for oats, Italian ryegrass and rye is presented in Table 7.2. In general the agreement was reasonably good at all depths for all crops. At each depth, the statistical results achieved were better for these crops than for the fallow land except for the *RMSE*. The simulated soil water content under oats over-estimated the soil water at the first three upper depths. The *d* index was reasonably good

Table 7.2 Statistical results of validation of the CropSyst model soil water balance against field-measured soil water content (m^3 m^{-3}) under oats, Italian ryegrass and rye at Cedara, KwaZulu-Natal, South Africa

Crop	Depth (mm)	Slope	Intercept	R^2	$RMSE_s$	$RMSE_u$	$RMSE$	d
Oats (n = 56)	100	0.869	0.084	0.726	0.053	0.032	0.061	0.781
	200	0.853	0.083	0.649	0.043	0.030	0.052	0.757
	300	0.966	0.049	0.708	0.039	0.023	0.045	0.739
	400	0.629	0.110	0.619	0.013	0.016	0.020	0.867
	500	0.385	0.196	0.387	0.019	0.015	0.024	0.746
	600	0.219	0.248	0.161	0.029	0.015	0.032	0.608
	700	0.393	0.217	0.173	0.019	0.022	0.029	0.636
Italian ryegrass (n = 42)	100	1.124	0.045	0.871	0.070	0.025	0.074	0.744
	200	1.035	0.038	0.640	0.047	0.034	0.058	0.726
	300	0.884	0.049	0.536	0.019	0.026	0.032	0.779
	400	0.570	0.112	0.240	0.012	0.024	0.027	0.707
Rye (n = 48)	100	0.949	0.067	0.804	0.060	0.018	0.062	0.651
	200	0.727	0.068	0.721	0.010	0.012	0.016	0.896
	300	0.508	0.123	0.605	0.015	0.010	0.019	0.793
	400	0.636	0.083	0.772	0.012	0.007	0.013	0.859

R^2 is coefficient of determination
$RMSE$, $RMSE_s$ and $RMSE_u$ (m^3 m^{-3}) are the total, systematic and unsystematic root mean square errors
d is Willmott's index of agreement

for the lower depths but the slope and intercept deviated greatly from one and zero respectively. Starting from the fourth layer downwards, the trend of the simulated soil water followed the observed well until a very high amount of precipitation occurred, 100 days after planting. This resulted in higher observed soil water but the model was slow to reflect it and caused under-estimation of soil water for sometime during the simulation period. Runoff was disabled during this simulation, so the model was trying to infiltrate the maximum amount of water into the soil according to the infiltration rate and soil water content of the soil and leave the leftover water to infiltrate on the next day. This could be the reason for the under-estimation of soil water for sometime during the simulation following the high amount of precipitation.

The simulation of soil water under Italian ryegrass and rye was similar to that of oats. In the first 100-mm depth the model consistently over-estimated the soil water. In the last 400-mm, the trend was good until a very high amount of precipitation occurred, 100 days after planting, to which the model was slow to respond.

Jovanovic and Annandale (1998) found LAI of oats and rye, measured with LAI-2000 PCA, to be over-estimated as compared to directly measured LAI. Therefore, the PCA-measured LAI for oats and rye was corrected according to Jovanovic and Annandale (1998). They have also found that the LAI of Italian ryegrass measured with PCA was heavily under-estimated as compared to directly measured LAI. In the field at Cedara, however, the PCA-observed values of Italian ryegrass were as equally over-estimated as oats and rye. The calibration and validation of the adjusted LAI for rye is presented in Fig. 7.2. The model validation (Fig. 7.2 (b)) under-estimated higher and lower values and over-estimated middle

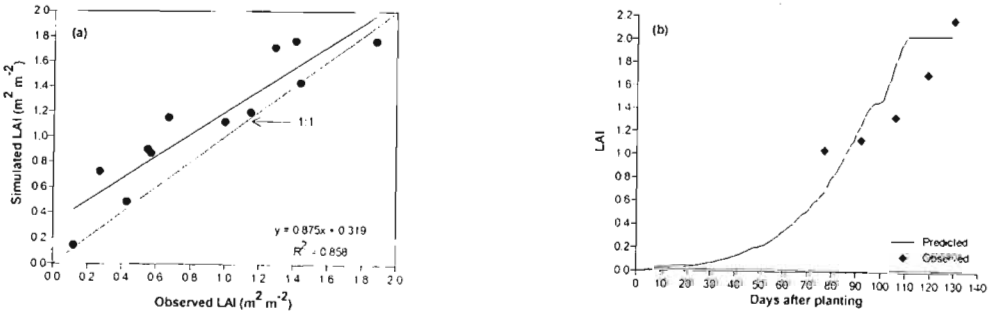

Fig. 7.2 LAI (a) calibration (Kromdraai open cast mine, Mpumalanga province) and (b) validation (Cedara, KwaZulu-Natal, South Africa) for rye

values of the corrected PCA-measured LAI of rye. It was not possible to present the calibration and validation of LAI for oats and Italian ryegrass because the management of these crops in the calibration dataset represented one cycle between two harvests whereas in the field trial these crops were let to physiological maturity without any harvest in-between. For precise and correct calibration of LAI, the PCA should be calibrated for the specific field conditions against direct measurements.

Crop evapotranspiration (ET_c) of rye was calculated as the product of crop coefficient (K_c) and reference evaporation (ET_o) (Allen *et al.*, 1998). The K_c coefficient is meant to incorporate the effect of the crop and soil characteristics into ET_o (Allen *et al.*, 1998). An average single K_c value of wheat (1.25) is calculated based on the length of period of the crop's growth stage (mid-season) and average values of minimum relative humidity (46.1%) and wind speed (6.4 m s^{-1}). This K_c value was adopted in computation of ET_c of rye. ET_o was computed using the FAO Penman-Monteith equation using a spreadsheet by Savage (2002) from observations of net irradiance, soil heat flux density, water vapour pressure deficit (Δe), wind speed and air temperature. The CropSyst model also computed crop evapotranspiration using the Priestley-Taylor equation with a constant α value (1.2 to 1.3) of 1.26 and aridity factor (0.0 to 0.1 kPa) of 0.03. The calculated and simulated ET_c for rye are presented graphically in Fig. 7.3. The agreement was good with the model slightly over-estimating lower and under-estimating higher values of ET_c.

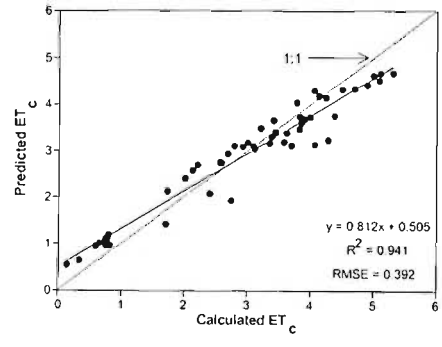

Fig. 7.3 Predicted (using Priestley-Taylor) and Calculated (using Penman-Monteith) ET_c (mm) for rye during the 2002 growing season at Cedara, KwaZulu-Natal, South Africa

The observed precipitation and irrigation, irrigations simulated with plant available water (PAW) and maximum allowable depletions of 0.4 and 0.6 (Table 7.3) along with their respective soil water depletion are presented in Fig. 7.4. The irrigation simulation applications refilled the soil layers of the root zone to 100% PAW depending on the depletion of the observation depth (0.4 m for Italian ryegrass and rye, and 0.7 m for oats) and root growth into the soil layer.

The plant available water of the observed irrigation applications for oats did not fall below the critical 0.4 maximum allowable depletion (50.1 mm) during the simulation period. It can be said that the observed irrigation schedule was timely with less than 100% PAW refill (Fig. 7.4 (a)). The amount of observed irrigation water application used to refill the soil water to less than 100% PAW seems to consider anticipation of recharge of soil water from precipitation that may occur later in the growing season. This may also mean frequent irrigation if precipitation did not occur later in the growing season. Frequent irrigation with less water would also encourage loss of more water due to evaporation from air, plant leaves and the soil surface. The 0.4 depletion level happened to schedule irrigation just a few days before a cumulative precipitation of 103 mm occurred in three days time. This resulted in plant available water greater than unity (runoff was disabled for the irrigation simulations because it is assumed that no runoff would occur from irrigation and the precipitation that might occur in winter is of light intensity). No irrigation was required according to the 0.6 maximum allowable depletion level. During the simulation period, the soil water was above the 0.6 maximum allowable depletion or 33.4 mm critical soil water level. The model simulations may over-estimate the amount of irrigation needed because of the slight under-estimation of soil water content simulation at the lower depths.

Table 7.3 Observed precipitation and irrigation, and simulated irrigation amounts for oats, Italian ryegrass and rye for part of the 2002 growing season at Cedara, KwaZulu-Natal, South Africa

Crop	Simulation period (2002)	Total precipitation (mm)	Irrigation (mm)		
			Maximum allowable depletion		
			Observed	0.4	0.6
Oats	29/05 to 30/09	260.2	61.0	34.0	0.0
Italian ryegrass	29/05 to 30/09	260.2	61.0	110.2	60.3
Rye	29/05 to 30/09	260.2	61.0	100.0	80.0

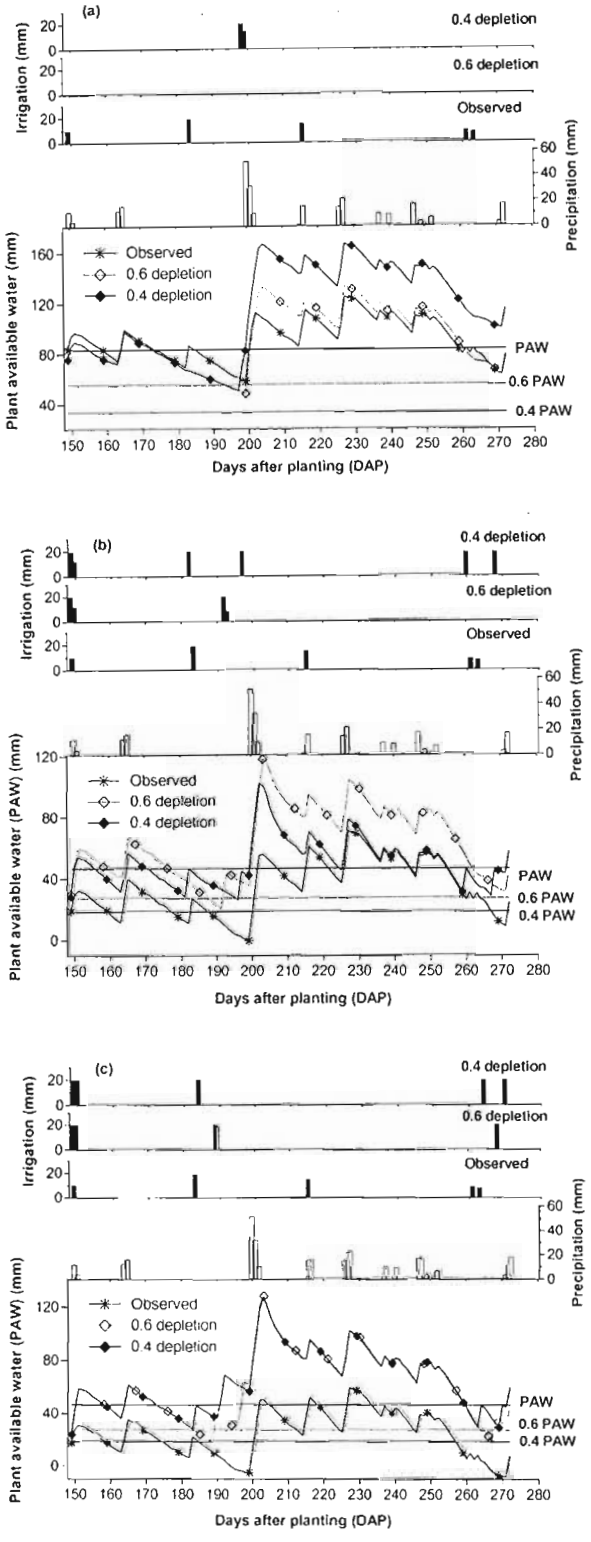

Fig. 7.4 Observed precipitation and irrigation, simulated irrigation (with 0.4 and 0.6 maximum allowable depletion) and soil water depletion for (a) oats, (b) Italian ryegrass, and (c) rye for part of the 2002 growing season at Cedara, KwaZulu-Natal, South Africa. Planting date was on April 12, 2002

Italian ryegrass and rye, because of their shallow rooting depth, required frequent irrigations with lower amount of water (Figs 7.4 (b), (c)) as compared to oats (Fig. 7.4 (a)). Accordingly the simulation using the observed irrigation application as input resulted in soil water below the critical depletion levels of the 0.4 and 0.6 depletions, several times during the growing season. For this simulation, the period of soil water deficit corresponded to the critical periods of flowering (as simulated by CropSyst). Soil water deficit at such times could have a profound effect on the crop water stress and cause a decrease in yield. The 0.6 depletion happened to schedule irrigation in Italian ryegrass just a few days before the occurrence of precipitation when the soil water was close to PAW. This resulted in plant available water that extended well above the 100% PAW line. In such instances, water may be lost as runoff and deep percolation (along with nutrients). Such excess water may interfere with the well-being of the crops through erosion of the topsoil (not simulated here), leaching of nutrients and root respiration. It may also have negative environmental effects through leaching of fertilizers, herbicides and pesticides. To lessen such damages and utilize the precipitation efficiently, irrigation scheduling should consider daily weather forecasting from meteorological stations. In addition, the soil water should be refilled to less than 100% PAW. The 0.4 depletion level in Italian ryegrass (Fig. 7.4 (b)) resulted in similar soil water depletion trend as the 0.6 depletion level but with soil water level less than that predicted using the 0.6 depletion. In case of rye, the 0.4 and 0.6 planned maximum allowable depletion irrigations resulted in a similar trend of soil water depletions during the simulation period (Fig. 7.4 (c)).

These results signify that timely irrigation scheduling with the right amount of water could be applied using the CropSyst model with reasonable accuracy. The use of the CropSyst model for timely irrigation scheduling could indicate the onset of crop water stress, and save water and nutrients from deep percolation. However, it is recognized that the automatic irrigation refill is limited to 100% PAW. For more accurate results, user specified events could be used in which the amount of irrigation to be applied is set according to the user's preferences. For example, precipitation water could be efficiently utilized if the soil water could be refilled to less than 100% PAW, leaving room for any probable precipitation that may occur later in the growing season. In addition, weather forecasts from meteorological stations could help in efficient utilization of precipitation. For more precise and accurate

irrigation scheduling, the soil water content should be updated regularly, especially following large amounts of precipitation/irrigation, for the whole soil profile.

7.4.3 Maize

Typical crop input parameters for maize and other crop species are available for use in CropSyst (Stöckle and Nelson, 2000). However, minor adjustments of these crop parameters should be made whenever field-measured data are available to account for cultivar variability. Other crop parameters were also fine-tuned within the narrow range of values as dictated by the CropSyst User's Manual (Stöckle and Nelson, 2000) for a reasonable simulation. The 1997/98 growing season was used for calibration and the growing seasons from 1998/99 to 2001/02 for validation of the model. The calibrated crop parameters are presented in Appendix E. The observed and model-simulated outputs on flowering and physiological maturity date, and grain yield are presented in Table 7.4 and Fig. 7.5. The agreement between the observed and model-simulated outputs in the length of days after planting to flowering was actually excellent. Comparison of the observed and simulated physiological maturity date seems to be good for the 1998/99 and 1999/2000 growing seasons with an over-estimation by as much as five days for the 2000/01 and 2001/02 growing seasons. A χ^2 test was conducted at 5% level of significance and resulted in no significant difference between the observed and simulated dates for both the flowering as well as maturity dates. The grain yield data points that were considered in this study were too few to allow a sound statistical analysis. However, a *RMSE*

Table 7.4 Comparison of observed and model-predicted results on growth stages and grain yield of maize at Cedara, KwaZulu-Natal, South Africa (Source data- NCT)

	Growing season	Flowering (DAP)*		Physiological maturity (DAP)		Grain yield (t ha^{-1})	
		Observed	Simulated	Observed	Simulated	Observed	Simulated
Calibration							
	1997/1998	91	91	165	165	11.13	11.13
Validation							
	1998/1999	83	83	154	154	12.10	12.26
	1999/2000	81	81	155	157	12.40	12.40
	2000/2001	85	85	163	168	12.20	11.58
	2001/2002	81	80	153	158	11.72	11.80

* DAP – days after planting

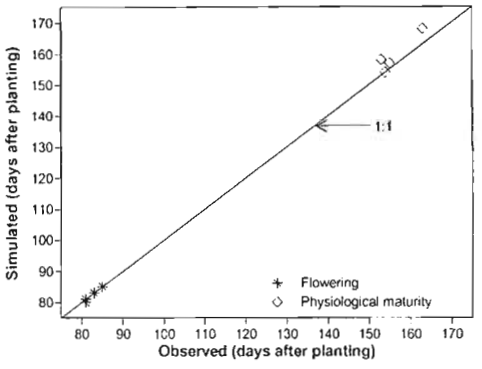

Fig. 7.5 Graphical comparison of model-simulated and field-observed phenological stages of maize over a period of four years at Cedara, KwaZulu-Natal, South Africa

(0.426 tons ha^{-1}) and relative *RMSE* (0.035) lower than previous studies conducted using the CropSyst model were achieved. From the available data points, a *d* index of 0.66 is achieved which is too low as compared to *d* index of equal or greater than 0.90 that were achieved elsewhere using the CropSyst model.

The soil water balance under maize crop was validated during the 2002/03 growing season at Cedara, KwaZulu-Natal, South Africa. The statistical results achieved from the validation of the soil water balance sub-routine of the CropSyst model under maize-planted conditions were reasonably good (Table 7.5 and Fig. 7.6). In fact, they were better than those for the fallow

Table 7.5 Statistical results of calibration of the CropSyst model soil water balance against field-measured soil water content (m^3 m^{-3}) under maize at Cedara, KwaZulu-Natal, South Africa

n = 22	Depth (mm)	Slope	Intercept	R^2	$RMSE_s$	$RMSE_u$	*RMSE*	*d*
	100	0.692	0.077	0.483	0.018	0.033	0.038	0.814
	200	0.92	0.012	0.866	0.009	0.016	0.019	0.955
	300	1.016	-0.019	0.898	0.015	0.014	0.020	0.943
	400	1.342	-0.155	0.826	0.049	0.019	0.053	0.678
	500	1.679	-0.255	0.786	0.039	0.023	0.045	0.688
	600	1.704	-0.273	0.698	0.041	0.026	0.049	0.618
	700	1.957	-0.365	0.724	0.045	0.024	0.051	0.563
	800	2.209	-0.438	0.810	0.039	0.018	0.043	0.598
	900	2.574	-0.562	0.842	0.034	0.015	0.037	0.580
	1000	2.705	-0.615	0.682	0.031	0.018	0.036	0.474

R^2 is coefficient of determination
RMSE, $RMSE_s$ and $RMSE_u$ (m^3 m^{-3}) are the total, systematic and unsystematic root mean square errors
d is Willmott's index of agreement

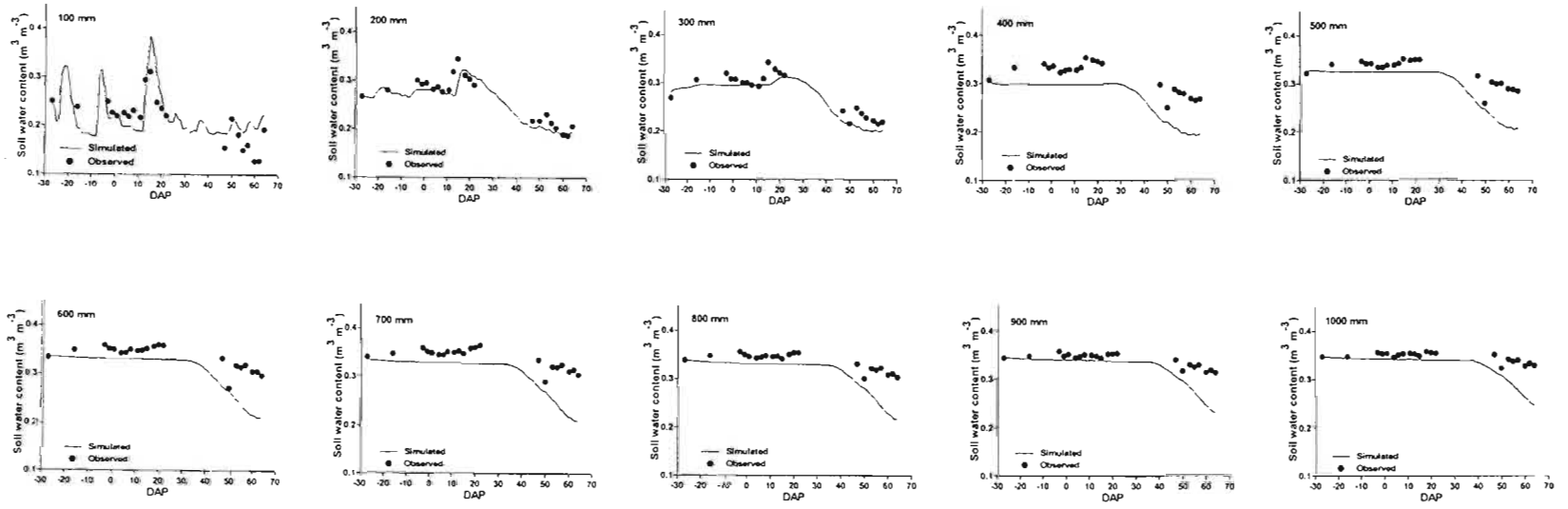

Fig. 7.6 Simulated (lines) and observed- using Diviner 2000 (points) volumetric soil water content distribution against days after planting (DAP) for the different depths under maize crop in the 2003 growing season at Cedara, KwaZulu-Natal, South Africa. Planting date was on November 21, 2002

plots (which involved the same depth but devoid of plants) (Table 7.1). In this simulation exercise, the effect of the roots in extracting water from deeper levels was apparent. Runoff was also enabled in this simulation exercise (but not in the case with oats, Italian ryegrass and rye). As a result, unlike simulation exercises with oats, Italian ryegrass and rye, the observed soil water content was higher than the simulated soil water content almost at all depths (Fig. 7.6). The trend of the soil water also seems to follow the observed soil water well during the first half of the simulation period but drifts away from the observed during the second half. The second half of the simulation corresponded to the time when only a few degree days were left to flowering (as simulated by CropSyst). At this time the model has simulated maximum growth of roots and extraction of water from deeper levels. The difference between the observed and simulated became larger and larger as the crop, as well as its roots, grew and increased in size. This discrepancy between the observed and simulated soil water could probably be due to incorrect simulation of root growth by the model.

7.5 CONCLUSIONS AND RECOMMENDATIONS

The CropSyst model was reasonably successful in simulating the soil water balance of fallow and cropped (oats, Italian ryegrass, rye and maize) plots; leaf area index (LAI) and crop evapotranspiration of rye; and crop yield and developmental stages of maize at Cedara, KwaZulu-Natal, South Africa. The soil water was under-estimated at deeper depths in fallow and maize-planted plots (runoff enabled) and over-estimated at the upper soil layers in oats, Italian ryegrass and rye-planted plots (runoff disabled) by the model. Although the agreement between the model-simulated and observed soil water was good for most applications, it would be more accurate if the modelled soil water could be updated using field observations, especially following high amount of precipitation and/or irrigation. The LAI of rye was also simulated reasonably well by the model. For precise and accurate LAI calibration and validation, PCA measurements of LAI need to be calibrated for the specific conditions in the field against direct measurements. CropSyst-simulated crop evapotranspiration using the Priestley-Taylor equation also agreed well with independent surface energy balance methods using the FAO Penman-Monteith equation. CropSyst's ability to predict phenological stages of maize was good for Cedara. CropSyst model-simulated maize grain yields also agreed well with observed grain yields.

The CropSyst model was also used to simulate timing and amount of irrigation for oats, Italian ryegrass and rye efficiently. The CropSyst model indicated the time when the crops start to experience water stress according to 0.4 and 0.6 maximum allowable depletion levels. The simulated irrigation schedules refilled the PAW to 100%. Simulated irrigation schedules just before precipitation resulted in a PAW greater than 100%. To prevent such circumstances and increase efficiency of utilizing precipitation, irrigation scheduling should consider weather forecasts from meteorological stations and/or refill the soil water to less than 100% PAW. From these it could be concluded that the CropSyst model could be used to indicate incipient water stress, prevent unnecessary loss of water and nutrients from deep percolation ensuring efficient utilization of water and increase in crop production.

8 CREATING SCENARIOS USING GENERATED WEATHER DATA

8.1 INTRODUCTION

The level of crop production is variable and hardly predictable posing certain risks and uncertainties to the agricultural community. The main constraint in assessing risk can be attributed to the lack of long-term weather data and man's inability to predict the future weather (Uehara and Tsuji, 1998). Crop simulation models could make use of long-term weather data to account for weather variability in assessing risks involved with adopting alternative management strategies at a site of interest (Uehara and Tsuji, 1998). But the length of observed weather data at most sites is insufficient for such analysis. This may prevent agricultural scientists and other potential users from running crop simulation models for assessing agricultural risks imposed by the long-term impact of weather on crop production.

Deterministic mathematical models that simulate time-series climatic variables (known as stochastic weather generators) have addressed this problem (Richardson and Wright, 1984). These models use historical observed weather data as an input and generate weather data, for as many years as required, which are similar in statistics to the historical observed weather data (Semenov and Jamieson, 1999).

The generated weather data could be used as an input to crop simulation models and offer agricultural scientists an opportunity to evaluate long-term effects of weather that were impossible with a limited observed historical dataset (Richardson, 1985). The simulation outcomes could aid in decisions that could minimize the risks by optimizing the management strategy in a single cropping season or a set of cropping sequences in multi-cropping seasons (Semenov and Jamieson, 1999). Generated weather data could also be used for tactical (real-time) management decisions in which the generated weather data are used in place of the unknown future weather, to be replaced by forecasted weather followed by real observations when they become available (Hoogenboom, 2000). Two or more management options could be used for this simulation and the resulting statistics could be used for assessing the risks involved and selection of management strategies (Hoogenboom, 2000). Also, the information obtained about crop yield and its quality before harvest can play a crucial role in decision-making. Generated weather data could also be modified by plausible projected changes of

climate means and variances to represent future climate (Smith and Hulme, 1998). The projected changes in climate could be obtained from non-model (synthetic or analogue) or model-based (global climate models) scenarios (Smith and Hulme, 1998). The modified generated weather data could serve as an input to crop simulation models and thereby assess the effects of climate changes on crop production (e.g., Donatelli *et al.*, 2000; Tubiello *et al.*, 2000). Policy makers could envisage, from the simulation results, the vulnerability of a system under possible climate changes and decide on appropriate policy responses (Smith and Hulme, 1998) through various management strategies (Uehara and Tsuji, 1998).

8.2 WEATHER DATA GENERATION USING THE ClimGen MODEL

Numerical models that generate a suite of long series synthetic weather data from observed data, to meet the inadequacy of observed weather data, have become important for analysis of agricultural, hydrological, environmental and other weather driven systems (Richardson, 1985; Annandale *et al.*, 1999; Williams *et al.*, 2001).

Richardson and Wright (1984) developed a weather generator, WGEN, that has been extensively applied in the US and the rest of the world. WGEN requires inputs of daily series of observed precipitation (Pr), minimum and maximum air temperatures (T_n and T_x), and solar radiant density (I_s) to generate long series of these weather variables. WGEN preserves the interdependence among the generated weather variables as well as the seasonal characteristics of each variable.

ClimGen (Version 4.1.05) (Stöckle and Nelson, 1999; Stöckle *et al.*, 2001) is a weather generator that has inherited some generation concepts from WGEN with inclusion of some other features that may improve model performance (Castellvi and Stöckle, 2001; Castellvi *et al.*, 2001). It has become customary to compare the performance of newly developed weather generators against WGEN. Castellvi and Stöckle (2001) pointed to some basic differences between ClimGen and WGEN: WGEN makes use of certain fixed averaged parameters that are derived from a large US database in the process of generating weather data. ClimGen, unlike WGEN, uses parameters that are calculated for each site of interest, making it applicable to any location around the world with enough information to parameterize the program. To estimate daily means and standard deviations of T_x, T_n and I_s throughout the year, ClimGen uses spline functions through the monthly parameters whereas WGEN uses a Fourier

series. The spline functions tend to match the monthly values well while the Fourier series only approximates them. WGEN also requires long-term records of daily weather data to estimate the parameters whereas ClimGen can make use of monthly summaries in the absence of daily records.

ClimGen generates daily Pr, T_x, T_n and I_s, air humidity and wind speed. It requires inputs of daily series of these weather variables to calculate parameters used in the generation process for any length of period at a location of interest. ClimGen preserves, in the generated weather data, the correlation among the weather variables as well as the seasonal characteristics in the actual weather variable at the site of interest. Precipitation occurrence (wet or dry day), determined by a first order Markov chain, is a driving variable that conditions T_x, T_n and I_s. The precipitation amount is generated using a Weibull distribution. The generation of T_x, T_n and I_s results from a serial and cross correlation 3 × 3 matrices whose coefficients are locally calibrated. In the absence of I_s, ClimGen generates daily series of T_x and T_n by reducing the generation process to 2 × 2 matrices neglecting I_s coefficients. Daily water vapour pressure is generated based on air temperature. Wind speed is also generated from a Weibull distribution, independent of other variables. ClimGen also offers an option that allows users to estimate I_s from air temperature in areas with inadequate length of weather records (Tubiello *et al.*, 2000; Castellvi and Stöckle, 2001; Castellvi *et al.*, 2001; Stöckle *et al.*, 2001).

Weather generators need to be tested and validated for locations other than for which they were developed and validated. ClimGen was tested at several locations in the world and performed reasonably well (Stöckle *et al.*, 2001). Earlier versions of ClimGen were also tested in South Africa representing a wide variety of climates (Clemence, 1997) and appeared to work satisfactorily over many of the sites tested. Clemence (1997) also used generated weather data from Cedara, one of the sites in which the model was tested, as an input to a CERES-maize crop growth model. There was reasonable agreement between simulated grain yields using observed and generated weather dataset.

8.3 CLIMATIC SCENARIOS

Agricultural crop production is significantly affected by climatic variables because PAR, heat and water are the driving forces for crop growth (Rosenzweig *et al.*, 1995; Rosenzweig and Hillel, 1998). Maximum crop production requires an optimal level of the climatic variables. It has been predicted that there will be a change in the climatic variables, especially an increase in the earth's mean surface temperature that would likely be accompanied by more intense hydrological cycle, in the coming decades due to increased greenhouse gas concentrations (Houghton *et al.*, 1992). These changes are likely to have an impact on world food security and may aggravate the already prevalent threat of providing sufficient food for the ever-increasing world population.

Although there is an increasing agreement among scientists that the increased atmospheric greenhouse gas concentrations will cause global warming, there is less agreement in estimates of how the climate will change in the future (Houghton *et al.*, 1992). At present, no method yet exists that provides confident projections of future climatic variables, hence "climatic scenarios" are used to represent the future climate in impact assessment studies (Smith and Hulme, 1998; IPCC-TGCIA, 1999). Climatic scenarios are plausible representations of the future climatic variables in a consistent manner based on the generally accepted projections of the concentrations of greenhouse gases and other pollutants in the future (Rosenzweig *et al.*, 1995; IPCC-TGCIA, 1999).

In studies of impact assessments, it is usual to use observed weather data of certain years representing recent conditions as a reference point or baseline. Such weather data is useful for characterizing and describing recent weather of the site of interest, calibrating impact models and quantifying baseline climatic impacts with which to compare future changes. The World Meteorological Organization (WMO) defined a baseline period of 30-year "normal" inclusive of 1961 to 1990. Though this period might have its own advantages, it may be superseded by 1971 to 2000 as new standard 30-year "normal" period (IPCC-TGCIA, 1999).

Smith and Hulme (1998) suggested four criteria that should be met by climate scenarios if they were to be useful for impact assessment:

(i) they should be consistent with a broad range of global warming projections based on increased concentrations of greenhouse gases;

(ii) they should not violate the basic laws of physics;

(iii) they should estimate a sufficient number of variables on a spatial and temporal scale that allows for impact assessment;

(iv) they should reflect the potential range of future regional climate change: and

(v) A fifth criterion of accessibility was added to the list by IPCC-TGCIA (1999) suggesting that they should be straight forward to obtain, interpret and apply for impact assessment.

The selection of scenarios could be controversial because all the methods used for projections carry certain flaws that violate one or more of the criterion that should be met by climate scenarios (Smith and Hulme; 1998). Smith and Hulme (1998) and IPCC-TGCIA (1999) have reviewed types of climatic scenarios that have been used in previous climatic studies and categorized them into three main classes: synthetic scenarios, analogue scenarios and scenarios from generic circulation models (GCMs) outputs.

Synthetic scenarios describe techniques in which particular climatic variables are changed by realistic but arbitrary amount, often according to a qualitative interpretation of climate model simulations for a region. Such climatic scenarios are of low cost, quick and easy to construct and require few computing resources but their arbitrary nature may prevent them from presenting a realistic set of changes that are physically plausible. However, this limitation can be overcome if the selection of synthetic scenarios is guided by information from GCMs (Smith and Hulme, 1998; IPCC-TGCIA, 1999).

Analogue scenarios are constructed by identifying recorded climate regimes from the past (temporal analogues) or from another region at the present (spatial analogue) which may resemble the future climate in a given region. These scenarios represent conditions that have actually been observed and experienced but the causes of the changes are almost certainly different from the causes underlying future, greenhouse gas induced climate changes (Smith and Hulme, 1998; IPCC-TGCIA, 1999).

GCMs are mathematical representations of the atmosphere, ocean, and land surface processes that simulate the response of the global climate system to increasing greenhouse gas concentrations based on physical laws and physically based empirical relationships. GCMs can be used in two ways to estimate the future climate: equilibrium-response and transient-response experiments. Equilibrium-response experiments have a very simple representation of the oceans and work on the assumption that the future climate will be stable. Most of the

experiments are conducted for a doubling or quadrupling of atmospheric [CO_2] or its radiative equivalent including all greenhouse gases. Transient-response experiments, in contrast, represent detailed models of the oceans linked to those of the atmosphere and examine change of climate over time due to increased greenhouse gas concentrations. GCMs, at present, are the only tools that estimate changes in climate due to increased greenhouse gas concentrations for a large number of climatic variables in a physically based consistent manner. Yet they are not good enough to fully and immaculately represent future changes in climatic variables because the resolution they use for projecting the climate change is rather coarse in relation to the scale of sites of interest for impact assessment. For better results, they should have to be complemented with synthetic climatic scenarios or made available for sub-grid scale by what is known as regionalisation or downscaling (Smith and Hulme, 1998; IPCC-TGCIA, 1999).

At present, there exist many climate change experiments that are conducted using GCMs. It is unwise to try to run one's own climate change experiment with a GCM considering the cost, time and expertise involved. It is customary to choose from the approved climate change experiments so far performed. Smith and Hulme (1998) have suggested that simulations from GCM: (i) be recent engulfing the advantages of recent developments in science and technology; (ii) represent the present-day climate most accurately, on the assumption that future climate simulation would also be represented as accurately; (iii) be representative, capturing extreme range of variables.

Future climatic scenarios can then be constructed by adjusting baseline observed or generated data using either of the synthetic, analogue or GCM scenarios or a combination thereof (Smith and Hulme, 1998; IPCC-TGCIA, 1999). Climate change in response to increasing greenhouse gas concentrations in the future can also be alternatively simulated by using simple weather models that generalise many of the processes simulated explicitly by the GCM (IPCC-TGCIA, 1999; Semenov and Jamieson, 1999).

8.4 MATERIALS AND METHODS

A 30-year dataset of daily weather record (1971-2000) on precipitation, minimum and maximum air temperatures and sunshine hours for Cedara, Department of Agriculture and Environmental Affairs, KwaZulu-Natal (29°32'S, 30°17'E, altitude 1076 m) was obtained from the Agricultural Research Council, Institute of Soil, Climate and Water, Pretoria, South

Africa. The sunshine hours were converted into solar radiant density as suggested by Reid (1986). Solar radiant density was also estimated using the D-C model (Donatelli and Bellochi, 2001) (see Chapter 6) for days with missing sunshine hours (e.g., part of the year 1998). The 30-year weather data on precipitation, minimum and maximum air temperatures and solar radiant density was used to generate another 30-year weather data series (Table 8.1) using the ClimGen model. The generated weather data series was compared with the observed weather data series for its distributions of daily rainfall and wet and dry series, monthly total rainfall and its variance, daily and monthly mean and variance of precipitation, minimum and maximum air temperatures, and solar radiant density. The distributions were compared using the χ^2 test, and the mean and variance values were compared using the t-test and F-test respectively.

In addition, daily Penman-Monteith grass reference evaporation (ET_o) values (Allen *et al.*, 1998), calculated by ClimGen for both the generated and observed weather data series, were compared using cumulative and frequency distribution functions.

The observed and generated weather data series were also used to simulate grain yields of maize at Cedara. The 30-years of observed and generated weather data series were used as inputs for the CropSyst model (Stöckle and Nelson, 2000; Stöckle *et al.*, 2003) for simulation of maize grain yields. The grain yields simulated using both weather data series were compared using a cumulative probability distribution. A Hutton, Doveton (Appendix B) type soil (MacVicar, 1977) and a PAN 6568 maize cultivar with plant row spacing of 0.75 m and plant population density of 44000 plants per hectare were assumed. Planting dates were set to day of year 309 (as practiced by farmers), and a fortnight earlier and a fortnight later. After harvest, 40% of the fraction of the straw was assumed to be left on the field to be incorporated later into the soil by tillage practices. The simulation was run for 30 continuous years in rotation along with fallow conditions. A finite difference technique was used for redistribution of water in the soil. The soil water was initialized to near field capacity following a substantial amount of precipitation at the starting day of the simulation.

In addition, the generated weather data was used as a baseline and adjusted by hypothesized environmental projections of $[CO_2]$, maximum and minimum air temperature, solar radiant density and precipitation to simulate grain yields of maize. An arbitrary doubling of equivalent $[CO_2]$ = 700 $\mu l\ l^{-1}$ was assumed. Simulations with GCMs suggest that the

Table 8.1 General statistical comparison of observed (1971 to 2000) and generated weather data series for Cedara, KwaZulu-Natal, South Africa

			Jan	Feb	Mar	Apr	May	Jun	Jul	Aug	Sep	Oct	Nov	Dec
Observed	Wet day count		542	450	449	246	124	66	69	138	275	466	513	564
	Dry day count		388	398	481	654	806	834	861	792	625	464	387	366
	Pr	mean	7.68	7.10	7.62	6.23	7.17	5.56	4.72	5.70	4.85	4.95	6.29	6.85
		std.dev.	10.36	9.33	9.65	7.42	10.41	7.18	6.21	6.54	7.02	6.33	8.25	9.26
		monthly	133.46	112.16	89.32	38.07	16.25	19.05	14.86	26.34	81.42	91.78	137.93	126.04
		std.dev.	53.82	54.41	63.39	27.68	24.96	33.06	13.12	26.10	99.20	48.45	78.95	43.51
	T_x	mean	25.28	25.50	24.50	22.75	20.89	19.31	19.08	20.90	21.93	22.43	23.45	24.74
		std.dev.	4.38	4.26	4.33	4.03	4.02	3.67	3.80	5.08	6.24	5.78	5.24	4.86
	T_n	mean	15.38	15.41	13.87	10.79	6.68	3.22	3.34	5.58	8.84	11.02	12.64	13.97
		std.dev.	2.28	2.20	2.54	2.96	3.23	2.93	2.70	3.08	3.23	2.87	2.66	2.33
	I_s	mean	19.75	19.32	17.38	15.21	13.21	12.22	12.68	14.67	16.08	17.26	19.09	20.42
		std.dev.	6.94	6.45	5.53	4.16	2.78	1.92	2.10	3.59	5.10	6.36	6.82	6.83
Generated	Wet day count		532	449	489	283	128	59	65	101	283	508	527	579
	Dry day count		398	398	441	617	802	841	865	829	617	422	373	351
	Pr	mean	7.64	7.66	7.41	5.57	5.83	5.40	6.83	5.61	6.00	5.48	6.40	7.17
		std.dev.	11.59	10.52	10.22	8.16	8.91	7.92	12.03	7.56	21.39	7.66	11.66	11.16
		monthly	119.49	110.89	80.46	33.98	19.40	11.83	13.02	32.19	74.29	91.44	111.68	130.06
		std.dev.	47.66	42.19	43.05	24.37	18.69	14.79	13.20	21.65	51.82	36.61	41.93	52.18
	T_x	mean	25.13	25.27	24.64	23.06	20.93	19.25	19.39	20.71	22.13	22.34	23.32	24.82
		std.dev.	4.58	4.30	4.19	4.00	3.97	3.58	3.95	5.08	6.17	5.89	5.38	4.73
	T_n	mean	15.25	15.23	14.05	10.74	6.67	3.22	3.51	5.70	8.88	10.84	12.58	14.16
		std.dev.	2.19	2.18	2.36	2.87	3.02	2.87	2.70	3.08	3.23	2.87	2.65	2.29
	I_s	mean	20.05	19.53	17.62	15.83	13.55	12.40	13.02	14.85	16.25	17.75	19.24	20.51
		std.dev.	7.17	6.66	5.76	4.55	3.28	2.35	2.62	3.94	5.54	6.73	7.11	7.00

Pr = precipitation (mm)
T_x = maximum air temperature (°C)
T_n = minimum air temperature (°C)
I_s =solar radiant density (MJ m^{-2})
Std.dev. = standard deviation
monthly = mean monthly total

projected increase in [CO_2] will modify the global climate by causing a widespread surface warming and enhanced global mean hydrologic cycle (Houghton *et al.*, 1992). Worldwide observations from the period of 1951 to 1990 have shown that daily mean minimum air temperature of the global landmass to have increased by about three times that of daily mean maximum air temperature, thus decreasing the daily air temperature range (Karl *et al.*, 2002). Accordingly the minimum and maximum air temperatures were modified in such a way that the increase in mean daily average air temperature should be 2 °C and 4 °C following the assumptions of IS92a emission scenario (Houghton *et al.*, 1992) for an equivalent doubling of [CO_2]. The decrease in daily temperature range is partially caused by increases in cloud cover (Karl *et al.*, 2002). Increased cloud cover would mean less solar radiant density. The increase in cloud cover accompanied by a warmer atmosphere (which can hold more water vapour) would in turn mean more intense hydrological cycle. Therefore, solar radiant density was estimated under the modified maximum and minimum air temperatures using the D-C model (Donatelli and Bellochi, 2001) (see Chapter 6), and an arbitrary increase of 10 and 20% of precipitation were assumed. Along with these hypothesized projections, the effect of planting dates on grain yield of maize were also included by considering: a locally practiced planting date (day of year 309), a fortnight earlier and a fortnight later planting dates.

Some GCM simulation outputs corresponding to a doubled [CO_2] were made for South African conditions (Schulze and Perks, 2000; Hewitson, 2001). These simulations suggest a warmer climate in the future, but are less certain with regard to precipitation. GCM simulation outputs from a regional model (PennState/NACR MM5) nested in a global model (UK Meteorological Office Unified model) suggest that there will be an increase in atmospheric humidity, although translation of this change in terms of rainfall is less clear (Hewitson, 2001). Simulation outputs from four GCMs (Hadley- including and excluding sulphates, CSM and Genesis) indicate that there will be both relative increase and decrease in precipitation for the summer rainfall areas in Southern Africa in the future (Schulze and Perks, 2000).

Most plants that are grown in elevated levels of [CO_2] have shown increased rate of photosynthesis and this manifests itself in higher biomass accumulation (Kimball, 1983). CropSyst computes daily biomass accumulation as a function of intercepted solar radiation and crop transpiration, using constant coefficients of radiation-use efficiency, e (Monteith,

1981), and biomass transpiration efficiency, K_{BT} (Tanner and Sinclair, 1983) (Section 4.3). These coefficients were modified in CropSyst as summarized by Tubiello *et al.* (2000).

8.5 RESULTS AND DISCUSSION

8.5.1 Generated weather data

The seasonal distribution of wet and dry series generated by ClimGen was compared with the observed weather data using the χ^2 statistical test at the 5% level of significance. Four out of twelve generated months were found to have a significantly different distribution (Table 8.2). These months were March, April, August and October. In all these months, with the exception of October, ClimGen generated a larger count of wet days following wet days than the observed weather data. Such incorrect distribution may obscure the effect of long dry spells on crops to be passed unnoticed especially when using crop models for growth simulation (Semenov and Jamieson, 1999). All these months will affect the well-being of plants through their effect on the soil water. For example, the month March corresponds with the grain filling stage of long season summer crops like maize and this may lead to an incorrect estimation of grain yield. The generated daily precipitation distribution was also compared with the observed weather data using χ^2 distribution at 5% level of significance. Four out of twelve generated months were found to be significantly different from the observed distribution (Table 8.2). The months that showed significant difference were the same as for the distribution of wet and dry series.

A t-test at 5% level of significance was conducted to test the equality of the monthly total precipitation, monthly means of precipitation, and minimum and maximum air temperatures and resulted in none of the generated months being significantly different from the observed (Table 8.2). All months of the ClimGen-generated mean monthly solar radiant density, but July, were not significantly different from the observed data series (Table 8.2). An F-test at 5% level of significance was also conducted to compare daily variances between the generated and observed weather data series, and showed that the variability between the two data series was not statistically significant for all the months except for precipitation in September (Table 8.2). The variance of the generated means of the monthly minimum and maximum air temperatures and monthly solar radiant density was not significantly different from the

Table 8.2 Comparison of observed (1971-2000) and generated weather data for Cedara, KwaZulu-Natal, South Africa (the numbers in the rows labeled "Rejected" indicate the number of months that gave significant results at the 5% level of significance, a large number of significant results indicate poor performance of the model)

Variable	*Pr*						T_x			T_n			I_s		
	Series	daily dist.	mon total	X	S daily	S mon	X	S daily	S mon	X	S daily	S mon	X	S daily	S mon
No. of tests	12	12	12	12	12	12	12	12	12	12	12	12	12	12	12
Rejected	4	4	0	0	1	4	0	0	0	0	0	0	1	0	1

Pr = precipitation
T_x = maximum air temperature
T_n = minimum air temperature
I_s = solar radiant density
X = monthly mean
S = variance
Series = wet and dry series
daily dist. = daily distribution
mon = monthly

observed for all months (Table 8.2). The monthly variance of precipitation, however, gave four statistically significant results out of twelve indicating that the monthly variation of precipitation was not reproduced well by ClimGen. The months for which the variance was significantly different included March, June, September and November. ClimGen consistently underestimated the monthly mean precipitation for all four months.

On the top of any application that involves generated weather data lie all the above uncertainties, and hence great care should be exercised in interpreting impact assessment responses obtained from using such weather data.

The ClimGen model also computed Penman-Monteith evaporation (ET_o) using the observed as well as the generated weather data. Cumulative probability of ET_o was calculated for both the observed and generated weather data series for 30 years (Fig. 8.1 (a)). The generated ET_o cumulative probability function followed the observed distribution well. The cumulative probability function may obscure certain phenomena where the generated weather data may have either over- or under-reproduced certain values of ET_o. For this reason, frequency distribution function (Fig. 8.1 (b)) was also performed and the generated weather data seems to follow the trend of the observed weather data series well except for ET_o values between 2 and 3 mm in which the generated weather data produced a larger proportion of its ET_o values.

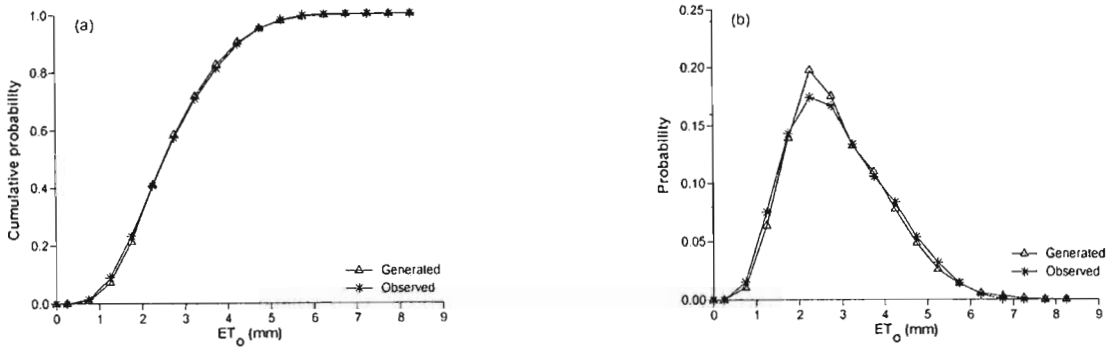

Fig. 8.1 (a) Cumulative and (b) frequency distribution functions of grass reference evaporation (ET_o) as calculated by ClimGen using the observed (1971-2000) and generated weather data series for Cedara, KwaZulu-Natal, South Africa

8.5.2 Yield simulations using observed and generated weather data

Maize grain yield was simulated by the CropSyst model using the observed and generated weather data series. Fig. 8.2 (a) a simple line graph and (b) cumulative probability function represent a comparison of the grain yields simulated from the observed and generated weather data for planting date fixed to the day of year 309. Table 8.3 also presents a basic statistical comparison of simulated grain yield from the observed and generated weather data for planting dates on the days of year 294, 309 and 323. The statistical results indicate that the mean grain yields simulated using the observed and generated weather data series are similar for the respective planting dates. A t-test conducted at 5% level of significance indicated that

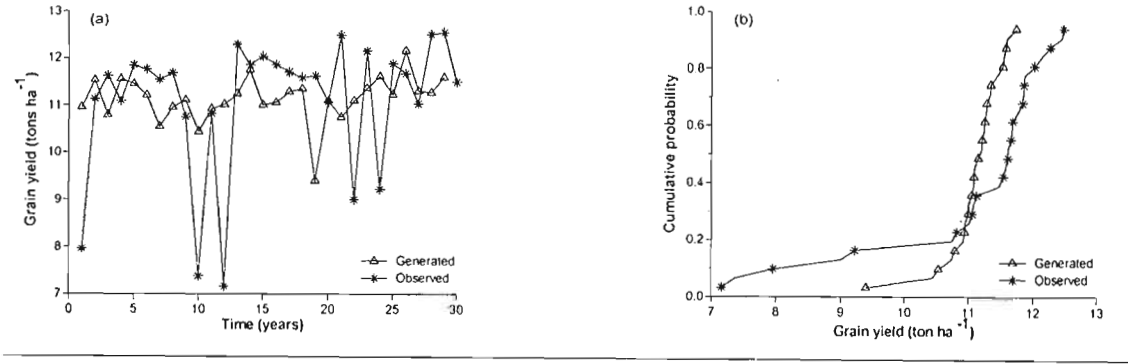

Fig. 8.2 Maize grain yield comparisons over a 30-year period as simulated by CropSyst using observed (1971-2000) and generated weather data series (a) simple line graph and (b) cumulative probability functions, for Cedara, KwaZulu-Natal, South Africa

the respective means are not statistically different from each other. But the grain yields produced from the observed data series had a wider range than the grain yields from the generated weather data series with the respective planting dates. This can be seen either from Fig. 8.2 (a) (the relative extension of yield along the ordinate) and (b) (the relative extension of the yield along the abscissa) or Table 8.3 (minimum and maximum grain yields and standard deviation from the generated weather data, somehow swallowed up within the range of the simulated grain yield values from the observed weather data). An F-test was conducted at 5% level of significance to test the equality of variances of the grain yields simulated from the observed and generated weather data series and indicated that the variance of the two simulated grain yields for the respective planting dates were not statistically similar.

The grain yields that were simulated from early planting date (day of year (doy) 294) were higher followed by the locally practiced planting date (doy 309) and late planting date (doy 323) for both the observed and generated weather data with the exception of few cases for the observed weather data (Fig. 8.3). The grain yield mainly followed the trend of the amount of precipitation received during the growing season both in the observed and generated weather data series (Fig. 8.4 (a) and (b)). In both the observed and generated weather data, the early planting, with the highest mean yield, had a larger variability than either the locally accepted or late planting dates (Table 8.3).

In few incidences, the observed weather data with the early planting date resulted in simulations of grain yields that were less than the yields simulated from the locally practiced planting date, especially for growing seasons with lower precipitation amounts. In all these incidences the amount of precipitation received by the crop during the growing season of the

Table 8.3 Maize grain yield (tons ha^{-1}) as simulated by the CropSyst model using observed (1971 to 2000) and generated weather data series of 30 years using different planting dates for Cedara, KwaZulu-Natal, South Africa

Day of planting	Weather data	Mean yield	Standard deviation	Maximum yield	Minimum yield
294 (21 October)	Observed	11.17	1.70	12.60	6.54
	Generated	11.35	0.56	12.37	10.73
309 (5 November)	Observed	11.08	1.45	12.52	7.16
	Generated	11.13	0.48	12.14	9.40
323 (19 November)	Observed	10.85	1.46	12.35	5.74
	Generated	10.88	0.41	11.73	10.12

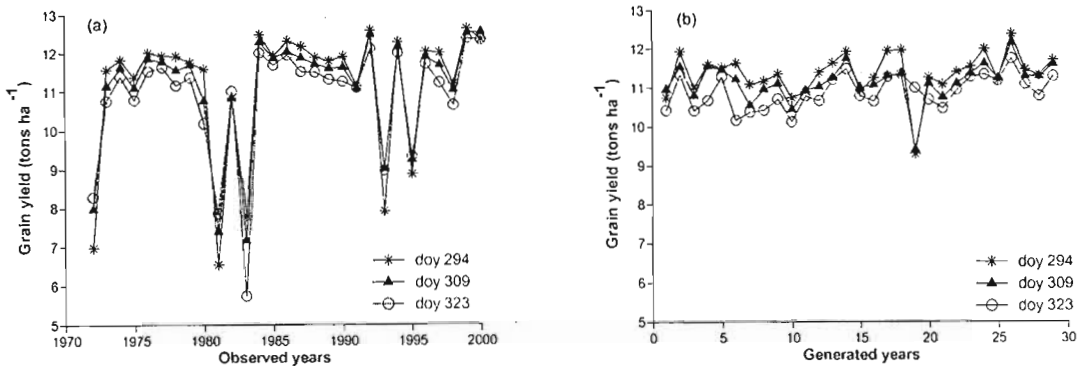

Fig. 8.3 Grain yield of maize as simulated by CropSyst model for planting days of the year 294 (October 21), 309 (November 5) and 323 (November 19) using (a) observed (1971-2000) and (b) generated weather data for Cedara, KwaZulu-Natal, South Africa

early planting date was greater or equal than with the locally practiced planting date. The reason for the lower yield could be explained by the distribution of precipitation. In the case of the early planting date for these years, most of the precipitation received during the growing season was concentrated at the early vegetative growth and in some cases also at maturity stages, with less precipitation during the sensitive flowering and grain filling stages which have a profound effect on the grain yield of the crop. A t-test that was conducted at 5% level of significance indicated that the simulated grain yield from the early planting date was not statistically greater than the locally practiced planting date using the observed weather data. All the above arguments make early planting risky for the farmer and lead to a conclusion that the locally practiced planting date for maize using the observed weather data is more suitable.

ClimGen generally produced more wet days, and also more wet days followed by wet days (eliminating the occurrence of long dry spells) during the months of October, November and December than observed in the real weather data, and produced roughly a similar distribution for the rest of the months (Table 8.1). This well-distributed precipitation could be the reason for the high grain yield that is simulated from the generated weather data in general. The early planting date that resulted in more grain yield might have the advantage of capturing early precipitation that lead to vigorous vegetative growth during the active growing stage. This could mean larger leaf area index for photosynthesis utilization. A t-test that was conducted at the 5% level of significance indicated that the mean grain yield simulated from the generated

(a)

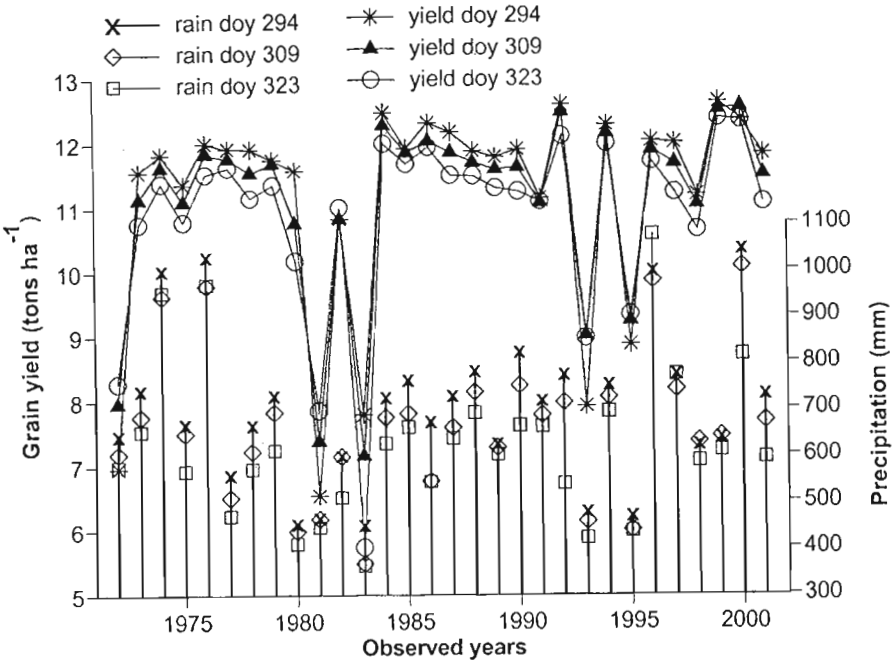

(b)

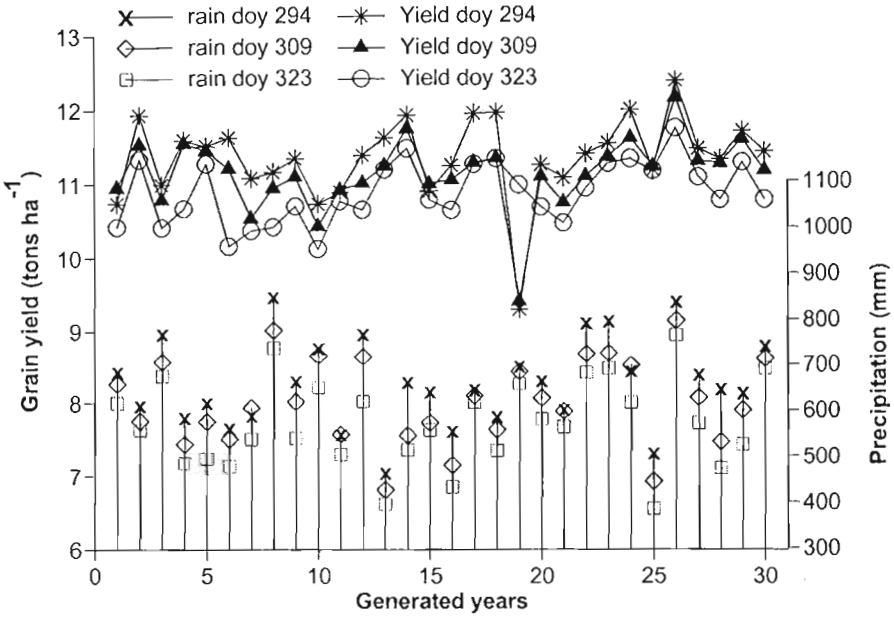

Fig. 8.4 Grain yield of maize as simulated by the CropSyst model using (a) observed (1971-2000) and (b) generated weather data series for planting days of the year 294 (October 21), 309 (November 5) and 323 (November 19) and precipitation received during the growing period at Cedara, KwaZulu-Natal, South Africa

weather data using an early planting date was significantly greater than the locally practiced and late planting dates.

The relatively low yield simulation using generated weather data along with the early and locally practiced planting dates, as depicted in Figs 8.3 (b) and 8.4 (b), is caused by a change in precipitation distribution (rather than a decrease in precipitation amount) accompanied by high air temperature (less optimum conditions) during flowering and grain filling stage. The high air temperature could result in higher evapotranspiration that increases crop water stress, further inhibiting grain yield.

8.5.3 Yield simulations under different climatic scenarios

The CropSyst model also simulated grain yield of maize for a generated baseline weather data and hypothesized scenarios created from the generated weather data. The hypothesized scenarios included (Table 8.4):

(i) $[CO_2]$ = 700 $\mu l\ l^{-1}$ (Scenario A);

(ii) $[CO_2]$ = 700 $\mu l\ l^{-1}$, 2 °C increment to the daily mean air temperature along with 10% increment to daily precipitation (Scenario B);

(iii) $[CO_2]$ = 700 $\mu l\ l^{-1}$, 2 °C increment to the daily mean air temperature along with 20% increment to daily precipitation (Scenario C);

(iv) $[CO_2]$ = 700 $\mu l\ l^{-1}$, 4 °C increment to the daily mean temperature along with 10% increment to daily precipitation (Scenario D); and

(v) $[CO_2]$ = 700 $\mu l\ l^{-1}$, 4 °C increment to the daily mean air temperature along with 20% increment to the daily precipitation (Scenario E).

The mean and standard deviation of the simulated grain yields, for the baseline and all scenarios, is presented in Table 8.4. Cumulative probability distribution of the simulated mean grain yields along with the adopted planting dates are also presented in Fig. 8.5. The 20% increment of daily precipitation did not result in any significant change in simulated grain yield as compared to the 10% increment of precipitation, hence graphs depicted for scenarios with 10% precipitation increment would suffice to represent the 20% increment as well.

Table 8.4 Simulated maize grain yields for baseline (generated weather data) and hypothesized climatic scenarios for Cedara, KwaZulu-Natal, South Africa (n = 30 years)

	Scenarios					
	Baseline	A	B	C	D	E
$[CO_2]$ µl l^{-1}	350	700	700	700	700	700
T_{av}	baseline T_{av}	baseline T_{av}	+2 °C generated from ΔT	+2 °C generated from ΔT	+4 °C generated from ΔT	+4 °C generated from ΔT
I_s	baseline I_s	baseline I_s				
Pr	baseline Pr	baseline Pr	+10%	+20%	+10%	+20%
Planting date	Grain yield (tons ha^{-1})					
Early	11.35 ± 0.56	13.12† ± 0.65	12.45† ± 0.40	12.46† ± 0.40	10.55‡ ± 0.42	10.55‡ ± 0.42
Local	11.13 ± 0.48	13.02† ± 0.49	12.21† ± 0.40	12.22† ± 0.41	10.32‡ ± 0.48	10.32‡ ± 0.48
Late	10.88 ± 0.41	12.69† ± 0.48	11.97† ± 0.38	11.98† ± 0.38	10.09‡ ± 0.47	10.09‡ ± 0.47

† simulated mean grain yield significantly greater than the mean baseline grain yield

‡ simulated mean grain yield significantly less than the mean baseline grain yield

T_{av} = average air temperature, I_s = solar radiant density, Pr = precipitation and ΔT= daily air temperature range

Equivalent doubling of $[CO_2]$ (Scenario A) (Table 8.4), unaccompanied by air temperature or water regime changes, caused an increase in simulated grain yield of maize for all planting dates by an average of 16.48% as compared to the baseline grain yield (Table 8.4 and Fig. 8.5). The increase in simulated grain yields were 15.63%, 16.94% and 16.70% for the early, local and late planting dates respectively. The amount of precipitation received during the growing season, as generated by ClimGen, was higher for the early planting date, followed by the local and late planting dates. Keeping this in mind, the local and late planting dates were relatively more efficient in utilizing the available precipitation per unit biomass accumulation under elevated $[CO_2]$ although the early-planted simulated yield was still higher. The relative response of crops to elevated $[CO_2]$ tends to be greater under water-limited growing conditions, while the actual yields may still be higher for non-stressed conditions (Chaudhuri *et al.*, 1990).

When a 2°C and 10% of precipitation were added to the mean daily air temperature and precipitation (Scenario B), the simulated grain yield was lower than the grain yield simulated with the equivalent doubling of $[CO_2]$ alone but it was still higher than the baseline simulated yield. The relative increment of the simulated grain yield was greater in case of the late planting which had less precipitation. Simulated yield increments were 9.71%, 9.71% and 10.07% for the early, local and late planting dates respectively as compared to the baseline simulated grain yield. The increase in air temperature was felt in reducing the growing season by an average of 30-days as compared to the baseline and Scenario A (which had equal

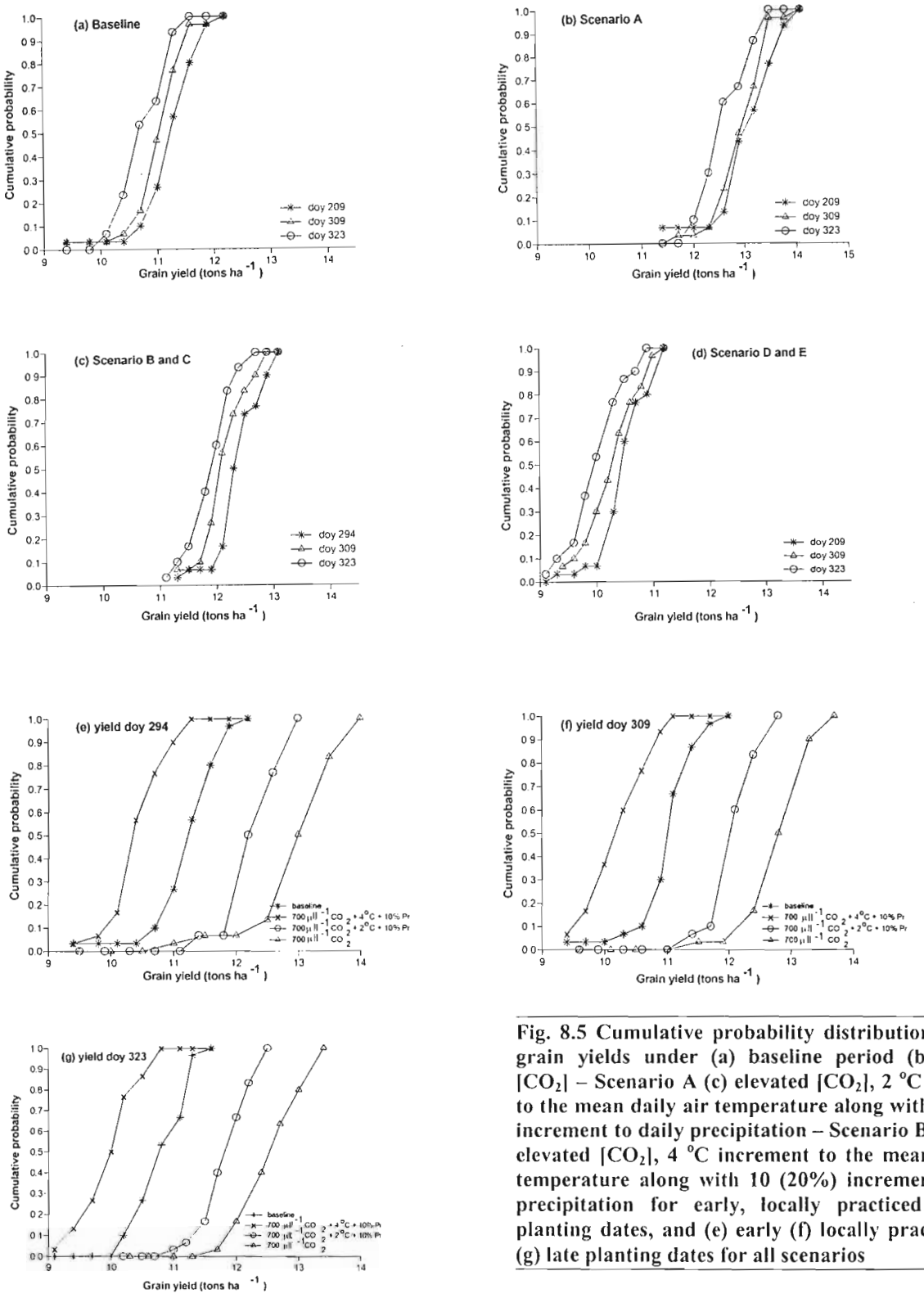

Fig. 8.5 Cumulative probability distribution of maize grain yields under (a) baseline period (b) elevated [CO_2] – Scenario A (c) elevated [CO_2], 2 °C increment to the mean daily air temperature along with 10 (20%) increment to daily precipitation – Scenario B and C (d) elevated [CO_2], 4 °C increment to the mean daily air temperature along with 10 (20%) increment to daily precipitation for early, locally practiced and late planting dates, and (e) early (f) locally practiced, and (g) late planting dates for all scenarios

growing season length) as simulated by CropSyst. This could be one cause for the reduction of simulated yield as compared to the grain yield simulated from Scenario A and yet maintaining the grain yield to a level higher than the baseline indicates that the photosynthetic rate was higher under the elevated [CO_2] than the baseline situation. The solar radiation for this simulation was also computed as a function of daily air temperature range. The 2 °C increment in daily mean air temperature is achieved by increasing the minimum air temperature by as much as three times than the maximum air temperature increment. This had a lessening effect on the daily range of air temperature observations and hence a reduced solar radiant density. One of the equations employed for calculation of biomass accumulation in CropSyst involves solar radiant density. Therefore, the reduced solar radiant density received by the crop during the growing season could also be another cause of the reduction in yield under Scenario B (Table 8.4). Adding another 10% of precipitation (Scenario C) did not result in any significant grain yield increase for the simulated years except in one or two years out of the 30-simulation years for each planting date. This can be seen from the simulated mean grain yield and standard deviations of Table 8.4.

Adding 4 °C to the mean daily air temperature and 10% to the daily precipitation under elevated [CO_2] decreased the grain yield further. The simulated grain yield was 7.06%, 7.29% and 7.21% for the early, local and late planting dates respectively below the baseline simulated grain yield. The 4 °C increment in mean daily air temperature reduced the growing season by an average of 50-days, and hence a loss of potential in accumulation of biomass. The daily air temperature range that was calculated under Scenarios D and E was so narrow that the resulting solar radiant density was greatly reduced as compared to the baseline as well as to Scenarios A, B and C. This greatly reduced solar radiant density could be a major cause for the reduction of simulated yield under both scenarios created with 4 °C increment to the mean daily air temperature (Scenarios C and E). Once again, another addition of 10% in precipitation did not result in any significant change in simulated yield for any of the simulated years.

The lack of simulated yield response to changes in precipitation from 10% to 20% signifies that the simulated water status of crops was non-limiting under both precipitation regimes. Two separate simulations were also established by applying a 10% and 20% increment to precipitation under elevated [CO_2] without a change in air temperature. The simulated grain

yield was the same as those achieved under elevated [CO_2] without air temperature and water regime changes. This indicates that the simulated grain yields, under elevated [CO2] atmosphere, are much more affected by changes in mean air temperature rather than precipitation.

Early planting, in a sense, was meant to help the crop escape the hot weather of the future environment if the currently practiced growing season were to be used. A t-test that was conducted at 5% level of significance indicated that the mean grain yield from the early planting date was significantly greater than the local and late planting dates within the respective scenarios. The effectiveness of early planting in increasing grain yield was apparent for scenarios that involved increment to the daily mean air temperature. This can be seen from the relative increment of grain yields within each scenario for the different planting dates. The early planting date had the effect of prolonging the crop's growing season in the order of two and four days as compared to the local and late planting dates within the respective scenarios. This may be the reason for the yield difference between the different planting dates within each scenario (Table 8.4).

As a complement to the above scenarios, because of the uncertain projections of precipitation in the future, the same scenarios as discussed above but with a decrease of 10% and 20% from the daily precipitation were created (results not shown). The yield simulations from a decreased daily precipitation were similar to the yield simulations with increased daily precipitation. A 10% decrease from the daily precipitation with 2 °C increment to the daily mean air temperature resulted in significantly positive simulated yield as compared to the baseline yield simulations. The individual yield simulations were similar to those resulting from 10% increment to the daily precipitation with the same air temperature change. A difference arises between the individual yield simulations when the precipitation received during the growing season was relatively low. As a result the variability in the simulated grain yield was higher for scenarios involving a decrease in daily precipitation.

A 10% decrease from the daily precipitation and 4 °C increment to the daily air temperature resulted in yield simulations that are statistically not different from the baseline yield simulations. The individual simulated yields were similar to their counterparts with a 10% increase to the daily precipitation. This indicates that the higher water use efficiency and

photosynthetic rate under elevated [CO_2] atmosphere were able to override the possible loss of yield due to the increased air temperature and decreased precipitation.

A decrease in precipitation by 20%, however, decreased the yield simulations as compared to the yield simulations using baseline scenario as well as scenarios involving 20% increment to the daily precipitation. The yield simulations from scenarios of a 2 °C increase to the mean daily air temperature were significantly greater for the 20% increase to the daily precipitation than for the 20% decrease from the daily precipitation. The yield simulations from the scenarios involving a 4 °C to the daily mean air temperature, however, did not show a significant difference in simulated yield between the 20% increase and decrease to and from the daily precipitation.

In general simulated yield resulting from scenarios involving a decrease from the daily precipitation showed a larger variability than the baseline scenarios and scenarios involving increase to the daily precipitation. The yield simulations from the early planting date were also more affected by the decrease in precipitation than the local planting date followed by the late planting dates. This suggests that under decreased precipitation scenarios the current planting date should be extended further assuming that no adaptation measures are involved.

8.6 CONCLUSIONS AND RECOMMENDATIONS

This study showed that long term weather data of precipitation, minimum and maximum air temperatures and solar radiant density could be generated from historical weather data using a stochastic weather generator, ClimGen, for yield assessment purposes. ClimGen was able to reproduce mean daily and monthly values of weather variables well at Cedara. But generated weather variables for some months of the year showed a significant difference in distributions of wet and dry series, daily precipitation, and variances of precipitation as compared to the observed weather data series. This inability to reproduce the variance was felt when the generated weather data series were used as inputs to the CropSyst model for simulation of maize grain yields. Grain yields simulated using the generated weather data had significantly smaller variance as compared to the grain yields simulated from the observed data, though the simulated mean yields were not statistically different. The response of simulated maize grain yield to early planting was not significant in the case of the observed weather data series, but significantly greater simulated grain yields were observed with generated weather data. The

cumulative probability function of grass reference evaporation (ET_o) calculated using the generated weather data series followed the observed distribution well. All the above summed up signify that great caution should be exercised in the interpretation of the responses from impact assessments when using generated weather data.

The effect of climate change on crop yields was assessed using different scenarios. Equivalent doubling of [CO_2], without air temperature or water regime change, showed increases in simulated grain yields as compared to the baseline period. Adding 2 °C to the mean daily temperature and 10% to the daily precipitation of an elevated [CO_2] reduced the grain yield but still kept it above the level of the baseline period grain yield. Adding 4 °C to the mean daily air temperature and 10% to the daily precipitation further decreased the yield. Increasing the daily precipitation by 20% instead of 10% did not result in any significant change in the simulated grain yield. This indicates that the water status of the crop was non-limiting under both precipitation regimes. The simulated grain yields were also found to be much more affected by changes in mean air temperature rather than precipitation under elevated [CO2] regimes.

Early planting dates for all scenarios also resulted in higher yields, but the relative increment in grain yield was higher for the late planting dates with scenarios that involved increment in mean air temperature.

The synthetic scenarios employed in this study do not provide information about the timing of projected climate change, hence results from transient general circulation models (GCMs) which involve time dependent projections should be employed for more realistic assessments.

9 CONCLUSIONS AND RECOMMENDATIONS

The main focus of the work was on the estimation of solar radiant density and the simulation of crop water-use and yield using soil-plant growth simulator, CropSyst. The CropSyst model was calibrated using historical weather, crop, management and soil data. The soil water balance sub-routine was validated using field trials that were established at Cedara, Department of Agriculture and Environmental Affairs, KwaZulu-Natal, South Africa, on a fallow and cropped (oats, Italian ryegrass, rye and maize) plots.

The importance of input data in crop simulation models was recognized and more emphasis was given to those inputs that are not easily measured or readily available. Most meteorological stations do not have records of solar radiant density, one of the crucial inputs in crop simulation models. In this study, observed solar radiant density was used whenever available, otherwise models/equations were used for its estimation from sunshine hours or minimum and maximum air temperatures and/or precipitation along with extraterrestrial radiant density. Location specific coefficients were developed for each model for the estimation of solar radiant density. The models were ranked according to conventional statistics and an expert system in their ability to reproduce the observed solar radiant density or that calculated from sunshine hours. In addition, the solar radiant density estimated from each model was used as input to CropSyst to simulate maize grain yields. The models were ranked according to their ability to simulate grain yields that matched to the grain yields simulated from using the solar radiant density estimated from sunshine hours. The ranking of the models according to their ability to reproduce grain yield agreed well with the expert ranking system but not with the conventional statistics. It was concluded, from this, that these models could be used with location specific coefficients to circumvent the lack of solar radiant density input in crop simulation models. The models should be evaluated and ranked according to the expert system in estimating solar radiant density for use in crop simulation models.

All the solar radiant density models/equations that have been employed in this work require quality solar radiant density data for computation of the coefficients, except one model. Future research should concentrate on developing models for estimation of solar

radiant density with reasonable accuracy over a wide range of geographical area without the need for having measured solar radiant density. Such models should also be incorporated in crop growth models so that crop simulation could be performed without the need for having measured solar radiant density. Sound and reliable evaluation and ranking of the solar radiant density models should consider multi-year data.

The CropSyst model was reasonably successful in predicting the soil water-use of fallow and cropped (oats, Italian ryegrass, rye and maize) plots; leaf area index and crop evapotranspiration of rye; and phenological stages and yield of maize. Soil water content was slightly under-estimated at deeper depths in fallow and maize planted plots and over-estimated at the upper soil layers in oats, Italian ryegrass and rye planted plots by the model, especially following large amounts of precipitation/irrigation. For more accurate soil water predictions the model-predicted soil water should be updated with field observations. High and low values of LAI were under-estimated by the model, whereas the middle values were over-estimated as compared to leaf area index measured using LAI-2000 PCA. Field measurements of leaf area index using the LAI-2000 plant canopy analyzer for model validation need to be calibrated against direct measurements of leaf area index for the specific field conditions. Model-predicted crop evapotranspiration (using the Priestley-Taylor method) slightly over-estimated lower values and under-estimated higher values of crop evapotranspiration as compared to crop evapotranspiration that was calculated using the standard surface energy balance method (FAO Penman-Monteith equation). CropSyst-simulated phenological stages of maize were in general accurate and resulted in good agreement with field observations. A χ^2 test at the 5% level of significance indicated that there was no significant difference between the observed and model-simulated phenological events. CropSyst model-simulated maize grain yields also agreed well with observed grain yields. The CropSyst model-simulated maize grain yields also resulted in *RMSE* of 0.46 tons ha^{-1} and *RRMSE* of 0.035 (better than achieved elsewhere using the CropSyst model) and a *d* index of 0.66 (lower than achieved in other studies using the CropSyst model). The CropSyst model was also used to simulate timing and amount of irrigation water for oats, Italian ryegrass and rye. It appears that the CropSyst model could simulate the soil water balance and growth and development of crops reasonably well provided that the model is calibrated for the specific conditions.

A more detailed dataset, than actually employed in this work, is required for a profound evaluation and thereby identification of crop growth model sub-routines that do not perform satisfactorily to the specific conditions at hand. Nonetheless, future research should concentrate on sharpening the accuracy of the soil water sub-routine of the CropSyst model for applications requiring absolute accuracy. Equally the instruments that are used for field data observation for validation of the model sub-routines should be of high quality, and be calibrated for the specific set of conditions when necessary. Trial and error calibration may also lead to incorrect predictions and conclusions about the model. Inclusion of iterative optimization procedures that work on the principle of minimizing certain errors for calibration of the sub-routines may obviate this problem. One aspect not pursued in this work is also the regional application by linking CropSyst with geographic information systems (GIS). This work would have many important applications including an understanding of the water-use and water-use efficiency of crops, weather and soil variability in a region.

ClimGen, a weather generator model, was also used to generate long-term weather data that is necessary for assessing risks imposed by the long term weather variability. ClimGen was able to reproduce mean daily and monthly values of weather variables well at Cedara. Few months of the year failed to reproduce distributions of wet and dry series, daily precipitation, and variances of precipitation as compared to the observed weather data series. The generated and observed weather data were used as inputs in the CropSyst model to simulate grain yields of maize. The mean simulated grain yields were not statistically different from each other; the grain yields simulated using the generated weather data had significantly smaller variance than the grain yields simulated using the observed weather data series. Grass reference evaporation (ET_o) was also computed by the ClimGen model using both data series; cumulative probability functions of ET_o calculated using the generated weather data series followed the FAO calculated distribution well.

The effect of planting date on simulated grain yields was also included in the study. In case of the generated weather data, early planting resulted in significantly greater simulated grain yields as compared to the yields simulated using the locally practiced planting date but this was hardly the case with the observed weather data series. Although ClimGen was able to reproduce the observed weather data series well, great caution should be exercised in interpreting responses from impact assessments keeping in mind that there were certain

months for which precipitation values were not reproduced well by the weather generator. Future research should concentrate on improving the algorithms and equations that are used for generation of precipitation.

The CropSyst model was also used to study the effect of potential climate change on crop productivity. The effect of planting dates (local, a fortnight earlier and a fortnight later) was also included in the study in quest of favourable growing season under the changed climate for the crop. The generated weather data was taken as a baseline period and was modified by hypothesized projections to create climatic scenarios. Constants for radiation use efficiency and biomass transpiration efficiency were modified to accommodate changes in elevated levels of [CO_2]. Equivalent doubling of [CO_2], unaccompanied by air temperature or water regime changes, showed increases in simulated grain yields as compared to the baseline period. Adding 2 °C to the mean daily temperature and 10% to the daily precipitation of a [CO_2] elevated atmosphere reduced the grain yield but still kept it above the level of the baseline period grain yield. Adding 4 °C to the mean daily temperature and 10% to the daily precipitation further decreased the yield. Increasing the daily precipitation by 20% instead of 10% did not result in any change in simulated grain yield. This indicated that the water status of the crop was non-limiting under both precipitation regimes. The simulated grain yields were also found to be much more affected by changes in mean air temperature rather than precipitation under elevated [CO2] regimes. Early planting date for all scenarios also resulted in higher yields, but the relative increment in grain yield was higher for scenarios that involved increment in mean air temperature. The synthetic scenarios of equivalent doubling of [CO_2], increased mean air temperature and precipitation employed in this study do not provide information about the timing of projected climate change. Therefore, observed or generated weather data series that are used for creating climatic scenarios should be modified from results involving transient general circulation models (GCMs) that simulate response of climate to increased greenhouse gas concentration through time.

In summary future research using the CropSyst model should focus on:

- regional application of the model by linking it with GIS;
- obtaining more detailed datasets to test more fully the crop growth model sub-routines; and improving the soil water sub-routine;

- investigate the possibility of using more accurate algorithms for generation of wet and dry series and daily precipitation distributions using the ClimGen model;
- investigate the possibility of estimating solar radiant density with reasonable accuracy over wide geographic area without the need for measured solar radiant density, and its inclusion in the CropSyst model.

References:

Acutis M, Donatelli M (2003) SOILPAR 2.00: software to estimate soil hydrological parameters and functions. Eur J Agron 18:373-377.

Addiscott TM, Wagenet RJ (1985) Concepts of solute leaching in soils: A review of modeling approaches. J Soil Sci 36:411-424.

Aggarwal PK (1995) Uncertainties in crop, soil and weather inputs used in growth models: Implications for simulated outputs and their applications. Agric Syst 48:361-384.

Allen RG, Pereira LS, Raes D, Smith M (1998) Crop evapotranspiration (guidelines for computing crop water requirements). FAO Irrig Drain Pap No.56. 300p.

Alocilja E, Ritchie JT (1990) The application of SIMOT2: Rice to evaluate profit and yield-risk in upland rice production. Agric Syst 33:315-326.

Ångström A (1924) Solar and terrestrial radiation. Quart J Roy Meteorol Soc 50:121-126.

Annandale JG, Jovanovic NZ, Benadé N, Tanner PD (1999) Modelling the long term effect of irrigation with gypsiferous water on soil and water resources. Agric Ecosys Environ 76:109-119.

Armstrong CF, Ligon JT, Mcleod MF (1987) Automated system for detailed measurement of soil water potential profiles using Watermark brand sensors. Intnl conf on measurement of soil and plant water status. Centennial of Utah State Univ, pp. 201-206.

Bellocchi G, Acutis M, Fila G, Donatelli M (2002) An indicator of solar radiation model performance based on a fuzzy expert system. Agron J 94:1222-1233.

Benadé N, Annandale JG, Van Zijl H (1996) The development of a computerized management system for irrigation schemes. Water Research Commission Report No. 513/1/95, Pretoria, South Africa.

Boote KJ, Jones JW, Pickering NB (1996) Potential use and limitations of crop models. Agron J 88:704-716.

Borg G, Grimes DW (1986) Depth development of roots with time. Trans ASAE 29:194-197.

Bristow KL, Campbell GS (1984) On the relationship between incoming solar radiation and daily minimum and maximum temperature. Agric Forest Meteorol 31:159-166.

CAMASE (1995) Newsletter of Agro-ecosystems Modelling, extra edition (Nov 1995) [online][11p.] CAMASE guidelines for modelling. Available at http://www.bib.wau.nl/camase/modguide.html (Last updated October 2001, IV). (Accessed 24/04/02).

Campbell GS (1985) Soil Physics with BASIC: Transport Models for Soil Plant Systems. Elsevier, Amsterdam, pp. 40-48.

Campbell GS (1988) Soil water potential measurements: An overview. Irrig Sci 9:265-273.

Campbell GS, Campbell MD (1982) Irrigation scheduling using soil moisture measurements: Theory and practice. Adv Irrig 1:25-42.

Campbell GS, Diaz R (1988) Simplified soil-water balance models to predict crop transpiration. In Bidinger FR and Johansen C (eds.) Drought Research Priorities for the Dryland Tropics. ICRISAT, Pantancheru, India, pp. 15-26.

Campbell GS, Stöckle CO (1993) Prediction and simulation of water use in agricultural systems. In: Intnl Crop Sci I. CSSA, Madison, Wisconsin 53711, USA, pp. 67-73.

Campbell Scientific (1996) Model 257 and 257-L (Watermark 200) soil moisture sensor. Logan, Utah, USA. 7p.

Carlson TN, Salem JE (1987) Measurement of soil moisture using gypsum blocks. Intnl Conf on Measurement of Soil and Plant Water Status. Centennial of Utah State Univ, pp. 193-200.

Cassell DK, Klute A (1986) Water potential: Tensiometry. In Methods of Soil Analysis, Part 1. Physical and Mineralogical Methods. Agron Monogr 9 (2nd ed.), ASA-SSSA 667 Madison, WI 53711, USA, pp. 563-594.

Castellvi F, Stöckle CO (2001) Comparing the performance of WGEN and ClimGen in the generation of temperature and solar radiation. Trans ASAE 44:1683-1687.

Castellvi F, Stöckle OC, Ibañez M (2001) Comparing locally calibrated versus a generalized temperature generation process. Trans ASAE 44:1143-1148.

Cengiz HS, Gregory JM, Seabaugh (1981) Solar radiation prediction from other climatic variables. Trans ASAE 24:1269-1272.

Chaudhuri UN, Kirkham MB, Kanemasu ET (1990) Root growth of winter wheat under elevated carbon dioxide and drought. Crop Sci 30:853-857.

Clemence BSE (1992) An attempt at estimating solar radiation at South African sites which measure air temperature only. S Afr J Plant Soil 9:40-42.

Clemence BSE (1997) A brief assessment of a weather data generator (CLIMGEN) at southern African sites. Water SA 23:271-274.

Cohen KJ, Cynert RM (1961) Computer models in dynamic economics. Qart J Econ 2:221-239.

Curry RB, Pearl RM, Jones JW, Boote KJ, Allen LH (1990) Simulation as a tool for analyzing crop response to climate change. Trans ASAE 33:981-998.

de Wit CT (1982) Simulation of living systems. In Penning de Vries FWT, Laar van HH (eds.) Simulation of Plant Growth and Crop Production. Wageningen, Pudoc, The Netherlands.

Delta-T Devices (2001) Users Manual for the Profile Probe. Cambridge, UK. 108p.

Donatelli M, Acutis M, Bellocchi G (2000) Two statistical indices to quantify patterns of residuals produced by model estimates. In Proc Intl Crop Sci Conf, 3rd, Hamburg Germany. 17-22 Aug. 2000. Eur Soc Agron, Hamburg, pp. 186.

Donatelli M, Bellocchi G (2001) Estimate of daily global solar radiation: new developments in the software RadEst3.00. In Proc of the 2nd Intnl Symp Modelling Cropping Systems, 16-18 july. Florence, Italy, pp. 213-214.

Donatelli M, Bellocchi G, Fontana F (2003) RadEst3.00: Software to estimate daily radiation data from commonly available meteorological variables. Eur J Agron 18: 363-367.

Donatelli M, Campbell GS (1998) A simple model to estimate global solar radiation. In Proc. Eur Soc Agron Cong, 5th, Nitra, Slovak Republic, 28 June-2 July 1998. The Slovak Agric Univ, Nitra, Slovak Republic, pp.133-134.

Donatelli M, Marletto V (1994) Estimating surface solar radiation by means of air temperature. In Proc. European Society for Agronomy Cong., 3rd, Abano-padova, Italy. 18-22 Sept., 1994. The Padova Univ, Padova, Italy, pp. 352-353.

Donatelli M, Stöckle CO (1999) The suite CropSyst to simulate cropping systems. Short course at the Univ of Ankara –Dept of Economics, Ankara, Turkey.

Donatelli M, Stöckle CO, Ceotto E, Rinaldi M (1996) CropSyst validation for cropping systems at two locations of Southern and Northern Italy. Eur J Agron 6:35-45.

Donatelli M, Tubiello F, Peruch U, Bindi M (2000) Scenarios of climate change effects on sugar beet in Northern and Central Italy. 3rd ICS-ESA Cong, Hamburg Germany.

Doorenbos J, Pruitt WO (1977) Crop water requirements. FAO Irrig Drain Pap No.24, pp. 156.

Du Plessis JG, Bruwer D deV (1999) National Cultivar Trials: Maize: Eastern Areas, 1998/99. ARC-Grain Crops Institute, Summer Grain Centre.

Du Plessis JG, Bruwer D deV (2000) National Cultivar Trials: Maize: Eastern Areas, 1999/2000. ARC-Grain Crops Institute, Summer Grain Centre.

Du Plessis JG, Bruwer D deV (2001) National Cultivar Trials: Maize: Eastern Areas, 2000/01. ARC-Grain Crops Institute, Summer Grain Centre.

Du Plessis JG, Bruwer D deV (2002) National Cultivar Trials: Maize: Eastern Areas, 2001/02. ARC-Grain Crops Institute, Summer Grain Centre.

Engel T, Hoogenboom G, Jones JW, Wilkens WP (1997) AEGIS/WIN: A computer program for the application of crop simulation models across geographic areas. Agron J 89:919-928.

Ferrer F, Stöckle CO (1996) A model for assessing crop response and water management in saline conditions. [online] [13] Available at http://www.fao.org/docrep/W4367E/w4367e0j.htm. Intnl Comm Irri Drain, FAO of the United Nations, Rome 1996. (Accessed 07/04/2002).

Fila G, Bellocchi G, Acutis M, Donatelli M (2003) IRENE: a software to evaluate model performance. Eur J Agron 18: 369-372.

Gardner WR, Hillel D, Benyamini Y (1970) Post-irrigation movement of soil water:1 redistribution. Water Resour Res 6:851-861.

Gates DM (1980) Solar radiation. In Gates DM (1980) Biophysical Ecology. Springer-Verlag, New York, pp. 97-164.

Gear RD, Dansfield AS, Campbell MD (1977) Irrigation scheduling with neutron probe. J Irrig Drain Div ASCE 103:291-298.

Geng S, Penning de Vries FWT, Supit I (1986) A simple method for generating daily rainfall data. Agric Forest Meteorol 36:363-376.

Genstat – Sixth Edition (2002) Version 6.1.0.200. Lawes Agricultural Trust.

Glover J, McCulloch JSG (1958) The empirical relationship between solar radiation and hours of sunshine. Quart J Roy Meteorol Soc 84:172-175.

Godwin DC, Jones AC (1991) Nitrogen dynamics in soil systems. In Hanks J, Ritchie JT (eds.) Modeling Plant and Soil Systems. Agron Monogr 31, ASA-CSSA-SSSA, Madison, Wisconsin, pp. 287-391.

Goodin DG, Hutchinson JMS, Vanderlip RL, Knapp MC (1999) Estimating solar irradiance for crop modeling using daily air temperature data. Agron J 91:845-851.

Gregory JM (1982) Soil cover prediction with various amount and types of crop residue. Trans ASAE 25:1333-1337.

Haise HR, Hagan RM (1967) Soil plant and evaporation measurement as criteria for scheduling irrigation. In Hagan RM, Haise HR, Edminster TW (eds.) Irrigation of Agricultural Lands. Agron Monogr 11 (30), ASA, Madison, Wisconsin, pp. 577-604.

Hargreaves GL, Hargreaves GH, Riley JP (1985) Irrigation water requirement for Senegal River Basin. J Irrig Drain Eng 111:265-275.

Hartkamp AD, White JW, Hoogenboom G (1999) Interfacing geographic information systems with agronomic modeling: A review. Agron J 91:761-772.

Hatfield JL, Fuchs M (1990) Evapotranspiration models. In Hoffman GJ, Howell TA, Solomon KH (eds.) Management of Farm Irrigation Systems. ASAE. An ASAE monograh. St Joseph, pp. 63-89.

Hewitson BC (2001) Global and regional climate modelling: Application to southern Africa. Water Research Commission Report No. 806/1/01, Pretoria, South Africa.

Hicks SK, Lascano RJ (1995) Estimation of leaf area index for cotton canopies using the LI-COR LAI-2000 Plant Canopy Analyzer. Agron J 87:458-464.

Hill RW (1991) Irrigation scheduling. In Hanks J, Ritchie JT (eds.) Modeling Plant and Soil Systems. Agron Monogr 31, ASA-CSSA-SSSA, Madison, Wisconsin, pp. 429-509.

Hillel D (1977) Computer simulation of soil water dynamics: a compendium of recent work. Ottawa, Ontario: International Development Research Centre, 214p.

Hillel D (1982) Introduction to Soil Physics. Academic Press Inc., Orlando, Florida, 364p.

Hillel D (1990) Role of irrigation in agricultural systems. In Stewart BA, Nielson DR (eds.) Irrigation of Agricultural Crops. Agron Monogr 30, ASA, Madison, Wisconsin, pp. 5-29.

Hodges T, Botner D, Sakamoto C, Hays Haug J (1987) Using the CERES-Maize model to estimate production for the U.S. Cornbelt. Agric Forest Meteorol 40:293-303.

Hoogenboom G (2000) Contribution of agrometeorology to simulation of crop production and applications. Agric Forest Meteorol 103:137-157.

Hook JE, McClendon RW (1992) Estimation of solar radiation data from long-term meteorological records. Agron J 84:739-742.

Houghton JT, Callandar BA, Varney SK (eds.) (1992) Climate change 1992. The Supplementary Report to the IPCC Scientific Assessment. Cambridge Univ Press, Cambridge, 200p.

Hunt LA, Boote KJ (1998) Data for model operation, calibration and evaluation. In Tsuji GY, Hoogenboom G, Thornton PK (eds.) Understanding Options for Crop Production. 1-7. Volume 7 of Systems Approach for Sustainable Development, edited by Penning de Vries FWT. Kluwer Academic Publishers, pp. 9-39.

Hunt LA, Kuchar L, Swanton CJ (1998) Estimation of solar radiation for use in crop modelling. Agric Forest Meteorol 91:293-300.

Hutson JL (1986) Water retentivity of some South African soils in relation to particle size criteria and bulk density. S Afr J Plant Soil 3:151-155.

IPCC-TGCIA (1999) Guidelines on the Use of Scenario Data for Climate Impact and Adaptation Assessment. Version 1. Prepared by Carter TR, Hulme M, Lal M, Intergovernmental Panel on Climate Change, Task Group on Scenarios for Climate Impact Assessment, 69p.

ISCI – Crop Science (2002) RadEst beta v 3.00. Via di Corticella, 133, 40128 Bologna, Italy. [online] Available at http://www.isci.it/ASP/RadEst.asp (accessed 07/04/2002).

ISCI (2001) IRENE beta v 1.00. Via di Corticella, 133, 40128 Bologna, Italy. [online] Available at http://www.isci.it/tools (accessed 07/04/2002).

ISCI–Crop Science (2001) SOILPAR beta v 2.00. Via di Corticella, 133, 40128 Bologna, Italy. [online] Available at http://www.isci.it (accessed 07/04/2002).

Jackson RD, Reginato RJ, and Idso SB (1977) Wheat canopy temperatures: A practical tool for evaluating water requirements. Water Resour Res. 13:651-656.

Jensen ME, Bruman RD, Allen RG (1990) Evaluation of estimating methods. In Jensen ME, Bruman RD, Allen RG (eds.) Evapotranspiration and Water Requirements. ASCE Manual of Engineering. Practical No. 70, ASAE New York, pp. 164-263.

Johnston MA (2000) Soil Science 351 and 352: Methods of analysis of soil physical properties. Univ Natal, Faculty of Science and Agriculture, Pietermaritzburg, South Africa.

Jones JW, Ritchie JT (1990) Crop growth models. In Hoffman GJ, Howell TA, Solomon KH (eds.) Management of Farm Irrigation Systems. ASAE. An ASAE monograh, St Joseph, pp. 63-89.

Jovanovic NZ, Annandale JG (1998) Measurement of radiant interception of crop canopies with the LAI-2000 plant canopy analyzer. S Afr J Plant Soil 15:6-13.

Jovanovic NZ, Annandale JG, Benadé N, Rethman NFG (1999) SWB – A mechanistic water balance-soil salinity model for irrigation with lime-treated acid mine drainage. 17th Congress of the Intl Comm Irri Drain, Special Session R.6, Granada, Spain.

Karl TR, Jones PD, Knight RW, Kukla G, Plummer N, Razuvayev V, Gallo KP, Lindseay J, Charlson RJ, Peterson TC (2002) [online] [8 p.] A new perspective on recent global warming: Asymmetric trends of daily maximum and minimum temperature. Available at h ttp://lwf.ncdc.noaa.gov/oa/climate/mxmntr/mxmntr/html NCDC (accessed 7/06/2002).

Kimball BA (1983) Carbon dioxide and agricultural yield: An assemblage and analysis of 430 prior observations. Agron J 75:779-788.

Kleijnen JPC (1994) Sensitivity analysis versus uncertainty analysis: When to use what? In Grassman J, Straten G van (eds.) Predictability and Nonlinear Modelling in Natural Sciences and Economics. Kluwer, Dordrecht, pp. 322-333.

Lal H, Hoogenboom G, Calixte JP, Jones JW, Beinorth FH (1993) Using crop simulation models and GIS for regional productivity analysis. Trans ASAE 36:175-183.

LI-COR Inc. (1990) LAI-2000 Plant Canopy Analyzer. Lincoln, Nebraska, USA.

Long IF, French BK (1967) Measurement of soil moisture in the field by neutron moderation. J Soil Sci 18:149-166.

Lukangu G, Savage MJ and Johnston MA (1999) Use of sub-hourly soil water content measured with frequency-domain reflectometery to schedule irrigation of cabbages. Irrig Sci 19:7-13.

MacRobert JF, Savage MJ (1995) The use of crop simulation model to evaluate optimal irrigation strategies for wheat in Zimbabwe. Proc S Afr Irrig Symp, pp. 167-171.

MacRobert JF, Savage MJ (1998) The use of crop simulation model for planning wheat irrigation in Zimbabwe. In Tsuji GY, Hoogenboom G, Thornton PK (eds.) Understanding Options for Crop Production. 1-7. Volume 7 of Systems Approach for Sustainable Development, edited by Penning de Vries FWT. Kluwer Academic Publishers, pp. 205-220.

MacVicar CN, de Villiers JM, Loxton RF, Vester E, Lambrechts JN, Merryweather FR, Le Roux J, van Rooyen TH, Harmse HJ von M (1997) Soil classification. A binomial system for South Africa. Sci Bull 390, Dep of Agric Tech Services, Pretoria.

Mahmood R, Hubbard KG (2002) Effect of time of temperature and estimation of daily solar radiation for the Northern Great Plains, USA. Agron J 94:723-733.

Maree PH, Bruwer D deV (1998) National Cultivar Trials: Maize: Eastern Areas, 1997/98. ARC-Grain Crops Institute, Summer Grain Centre.

Merriam JL (1960) Field method for approximating soil moisture for irrigation. Trans ASAE 3: 1-31.

Miller JB (1967) A formula for average foliage density. Aust J Bot 15:141-144.

Miracle MP (1966) Maize in Tropical Africa. The Univ of Wisconsin Press, pp. 3-19.

Monteith JL (1965) Climate and the efficiency of crop production in Britain. Phil Trans Roy Soc Lond 281:277-329.

Monteith JL (1981) Climate variations and the growth of crops. Quart J Roy Meteorol Soc 107:749-774.

Muchow RC, Sinclair TR, Bennett JM (1990) Temperature and solar radiation effect on potential maize yields across locations. Agron J 82:338-343.

Norman JM, Campbell GS (1989) Canopy structure. In Pearcy RW, Ehlringer J, Mooney HA, Rundel PW (eds.) Plant Physiological Ecology: Field Methods and Instrumentation. Chapman and Hall, London and New York, pp. 301-325.

NRC (National Research Council) (1997) Precision Agriculture in the 21st century: Geospatial and Information Technologies in Crop Management. National Academy Press, Washington, DC.

Pala M, Stöckle CO, Harris HC (1996) Simulation of Durum wheat (*Triticum turgidum* ssp. Durum) growth under different water and nitrogen regimes in a Mediterranean environment using CropSyst. Agric Sys 51: 147-163.

Passioura JB (1973) Sense and nonsense in crop simulation. J Aust Inst Agric Sci 39:181-183.

Phene CJ, Allee CP, Pierro JD (1989) Measurement soil matric potential and real-time irrigation scheduling. Agric Water Mgt 16:173-185.

Phene CJ, Hoffman GJ, Rawlins SL (1971) Measuring soil water potential *in situ* by sensing heat dissipation within a porous body: I. The theory and sensor construction. SSSA Proc 35:27-33.

Phillips J, Cane M, Rosenzweig C (2002) ENSO, seasonal rainfall patterns and Zimbabwe maize yield. [online]. [2p.] Available at http://www.giss.nasa.gov/research/intro/phillips_01/index.html (accessed 19/09/2002) NASA Goddard Institute.

Priestley CHB, Taylor RJ (1972) On the assessment of surface heat flux and evaporation using large-scale parameters. Mon Weath Rev 100:81-82.

Rabbinge R, Bastiaans L (1989) Combination models, crop growth and pests and diaseases. In Rabbinge R, Goudriaan, van Keulen H, Penning de Vries FWT, van Laar HH (eds.) Simulation and System Management in Crop Protection. Simulation Mongraphs, Pudoc, Wageningen, pp. 217-238.

Ramkrishnan BP, Ritchie JT (2000) Estimation of solar radiation in India. November 2000. [online] [1p.] Available at http://nowlin.css.msu.edu.ConfNov2000/posters/POSTEROK.pdf (accessed 20/08/2002) Nowlin Chair Crop Modeling Symposium.

Ratliff LF, Ritchie JT, Cassel DK (1983) Field-measured limits of soil water availability as related to laboratory-measured properties. Soil Sci Soc Am J 47:770-775.

Reid PCM (1986) Evaluation of the coefficients of Ångström formula for the estimation of solar radiation in South Africa. S Afr J Plant Soil 3:45-48.

Reynolds SG (1970) The gravimetric method of soil moisture determination Part I: A study of equipment and methodological problems. J Hydrol 11:258-273.

Richardson CW (1985) Weather simulation for crop management models. Trans ASAE 28:1602-1606.

Richardson CW, Wright DA (1984) WGEN: A model for generating daily weather variables. USDA, Agricultural Research Service ARS-8.

Rietveld MR (1978) A new method for estimating the regression coefficients in the formula relating solar radiation to sunshine. Agric Meteorol 19:243-252.

Ritchie JT (1972) Model for predicting evaporation from a row crop with incomplete cover. Water Resour Res 8:1204-1213.

Ritchie JT (1981) Soil water availability. Plant and Soil 58:327-338.

Ritchie JT (1985) A user-oriented model of the soil water balance in wheat. In Day W, Atkin RK (eds.) Wheat Growth and Modeling. Plenum Press, New York.

Ritchie JT (1991) Specification of the ideal model for predicting crop yields. In Muchow RC, Bellamy JA (eds.) Climatic Risk in Crop Production: Models and Management for the Semi-arid Tropics and Sub Tropics. Proc Intnl Symp, St. Lucia, Brisbane, Queensland, Australia. July 2-6, 1990. CAB International, Wallingford, UK, pp 97-122.

Ritchie JT (1998) Soil water balance and plant water stress. In Tsuji GY, Hoogenboom G, Thornton PK (eds.) Understanding Options for Crop Production. 1-7. Volume 7 of Systems Approach for Sustainable Development, edited by Penning de Vries FWT, Kluwer Academic Publishers, pp. 9-39.

Rivington K, Matthews KB, Buchan K (2002) A comparison of methods for providing solar radiation data to crop models and decision support systems. 1st biennial meeting of the International Environmental Modelling and Software Society, 24-27 June, Lugano, Switzerland, 3:193-198. [online] available at http//bamboo.mluri.sari.ac.uk/~kevinb/papers/RivingtonSRLADSS.doc (Accessed 19/09/2002).

Rosenzweig C, Allen LH, Harper LA, Hollinger SE, Jones JW (eds.) (1995) Climate Change and Agriculture: Analysis of Potential International Impacts. ASA special publication no. 59. ASA. Madison, WI.

Rosenzweig C, Hillel D (1998) Climate change: portent and challenge. In Rosenzweig C, Hillel D. Climate Change and the Global Harvest: Potential Impacts of the Greenhouse Effect on Agriculture. Oxford Univ Press, New York, pp 3-6.

Savage MJ (1993) Statistical aspects of model validation. Paper presented at Workshop on the field water balance in the modelling of cropping systems. Water Research Commission and the Univ of Pretoria, Pretoria, South Africa.

Savage MJ (2001) Computer models: Classification and structure. SPACRU, School of Applied Environmental Sci, Univ Natal, Pietermaritzburg, South Africa. Unpublished. pp. 16.

Savage MJ (2002) A spreadsheet for calculating hourly reference evaporation. SPACRU, School of Applied Environmental Sci, Univ Natal, Pietermaritzburg, South Africa.

Savage MJ, A Cass (1984) Measurement of water potential using thermocouple hygrometers. Adv Agron 37:74-126.

Savage MJ, Ritchie JT, Bland WL, Dugas WA (1996) Lower limit of soil water availability. Agron J 88:644-651.

Schmidt EJ, Schulze RE (1989) The Cedara hydrological research catchments 1974 to 1989. Agricultural Catchments Research Unit, Report no. 34.

Schulze RE (1976) A physically based method of estimating solar radiation from suncards. Agric Meteorol 16:85-101.

Schulze RE, Hutson JL, Cass A (1985) Hydrological characteristics of soils in Southern Africa 2: soil and water retention models. Water SA 11:129-136.

Schulze RE, Perks LA (2000) Assessment of the impact of climate change on hydrology and water resources in South Africa. Report to South African Country Studies for Climate Change Programme. School of Bioresources Engineering and Environmental Hydrology, Univ of Natal, Pietermaritzburg.

Seckler D, Amarasinghe U (2000) Water supply and demand, 1995 to 2025. [online] [10p.] Available at http://www.iwmi.cgiar.org/pubs/AReps/1999-2000/Scientific-WS2025.pdf IWMI, Colombo, Srilanka. (Accessed 01/04/2003).

Semenov MA, Jamieson PD (1999) [online] [25p.] Using weather generators in crop modelling. CLIMAG Geneva Workshop, Geneva, Switzerland, 28-29 Sept., 1999.http://www.start.org/projects/climag/papers/Semenov-Jamieson.pdf (accessed 20/09/2002).

Sentek Environmental Technologies (2000) Diviner 2000 Users Guide V 1.0. Australia. 69p.

Sinclair TR, Rawlins SL (1993) Inter-seasonal variation in soybean and maize yields under global environmental change. Agron J 85: 406-409.

Sinclair TR, Seligman NG (1996) Crop modeling: From infancy to maturity. Agron J 88:694-704.

Singh B, Boivin J, Kirkpatrick G, Hum B (1995) Automatic irrigation scheduling system (AISSUM): principles and applications. J Irr and Drain Eng ASCE 121:43-56.

Smith JB, Hulme M (1998) Climatic change scenarios. In Feenstra JF, Burton I, Smith JB, Tol RSJ (eds.) UNEP Handbook on Methods for Climate Change Impact Assessment and Adaptation Strategies. October 1998. [Online] [40p.] Available at http://130.37.129.100/IVM/pdf/handbook_climat.pdf (accessed 19/09/2002) UNEP.

SPE (Scientific Programming Enterprises) (1996) PlotIT for Windows 95/NT, Version 3.20b. Haslett, MI 48840.

Stegman EC (1983) Irrigation scheduling applied time criteria. Adv Irr 2:1-30.

Stöckle CO (1996) GIS and simulation technologies for assessing cropping systems management in dry environments. [online] [13p.] available at http://www.bsyse.wsu.edu.cropsyst/articles/cs_gis.htm. (Accessed 15/01/03).

Stöckle CO, Campbell GS (1985) A simulation model for predicting the effect of water stress on yield: An example using corn. Adv Irrig 3, 283-311.

Stöckle CO, Donatelli M (1996) The CropSyst model: A brief description. [online] [10p.] http://www.inea.it/isci/mdon/software/cropsyst/5PAGES.htm. (Accessed 28/03/2002).

Stöckle CO, Donatelli M, Nelson R (2003) CropSyst, a cropping systems simulation model. Eur J Agron 18:289-307.

Stöckle CO, Martin SA, Campbell GS (1994) CropSyst, a crop simulation model: Water/nitrogen budgets and crop yield. Agric Sys 46:335-59.

Stöckle CO, Nelson R (1999) ClimGen, a weather generator program. Biological Systems Engineering Dept., Washington State Univ, Pullman, Washington, USA.

Stöckle CO, Nelson R (2000) Cropping systems simulation model user's manual. Biological Systems Engineering, Washington State Univ, Pullman, Washington, USA.

Stöckle CO, Nelson R, Donatelli M, Castellvi F (2001) ClimGen: A flexible weather generation program. 2nd Intl Symp Modelling Cropping Systems, 2001, Florence, Italy.

Stroosnijder L (1982) Simulation of the soil water balance. In Penning deVries FWT, van Laar HH (eds.) Simulation of Plant Growth and Crop Prodiction. Wageningen, Pudoc, pp.175-193.

Swift LW (1976) Algorithm for solar radiation estimation on mountain slopes. Water Resour Res 12:108-112.

Tanner CB, Sinclair CR (1983) Efficient water use in crop production research or research? In Taylor HM, Jordan WR, Sinclair TR (eds.) Limitations to Efficient Water Use in Crop Production. ASA, CSSA, SSSA, Madison, WI, USA.

Taylor SA, Ashcroft GL (1972). Irrigation for maximum production. Physical Edaphology: The Physics of Irrigated and Non-irrigated Soils. Freeman, San Fransisco, California, pp. 414-473.

Thompson SJ, Armstrong CF (1987) Calibration of the Watermark model 200 soil moisture sensor. ASAE 3:186-189.

Thornton PE, Running SW (1999) An improved algorithm for estimating incident daily solar radiation from measurements of temperature, humidity and precipitation. Agric Forest Meteorol 93:211-228.

Thornton PK, Bowen WT, Ravelo AC, Wilkens PW, Farmer G, Brock J, Brink JE (1997) Estimating millet production for famine early warning: An application of crop simulation modelling using satellite and ground based data. Agric Forest Meteorol 83:95-112.

Thornton PK, MacRobert JF (1994) The value of information concerning near-optimal nitrogen fertilizer scheduling. Agric Syst 45:315-330.

Thornton PK, Wilkens PW (1998) Risk assessment and food security. In Tsuji GY, Hoogenboom G, Thornton PK (eds.) Understanding Options for Crop Production. 1-7. Volume 7 of Systems Approach for Sustainable Development, edited by Penning de Vries FWT. Kluwer Academic Publishers, pp. 329-345.

Thornton-Dobb S, Lorentz S (2001) Manual for the operation of tensiometer nests using the HOBO logger system. Univ Natal, School of Bioresources Engineering and Environmental Hydrology, Pietermaritzburg, South Africa. 14p.

Topp GC, Davis JL (1985) Time domain reflectometry (TDR) and its applications to irrigation scheduling. Adv Irrig 3:107-127.

Tubiello F, Donatelli M, Rosenzweig C, Stöckle CO (2000) Effects of climate change and elevated CO_2 on cropping systems: Model predictions at two Italian locations. Eur J Agron 13:179-189.

UC SAREP (2002a) Annual ryegrass. In UC SAREP, Cover crop database. [online] [10p.]. Available at http://www.sarep.ucdavis.edu/cgi-bin/ccrop.exe/show_crop_2 (accessed 12/10/2002). Univ California.

UC SAREP (2002b) Cereal rye. In UC SAREP, Cover crop database. [online] [16p.] Available at http://www.sarep.ucdavis.edu/cgi-bin/ccrop.EXE/show_crop_12 (accessed 12/10/2002). Univ California.

UC SAREP (2002c) Oats. In UC SAREP, Cover crop database. [online] [9p.]. Available at http://www.sarep.ucdavis.edu/cgi-bin/ccrop.EXE/show_crop_28 (accessed 12/10/2002). Univ California.

Uehara G, Tsuji GY (1998) Overview of IBSNAT. In Tsuji GY, Hoogenboom G, Thornton PK (eds.) Understanding Options for Crop Production. 1-7. Volume 7 of Systems Approach for Sustainable Development, edited by Penning de Vries FWT. Kluwer Academic Publishers, pp 1-7.

United Nations (1997) Global change and sustainable development: Critical trends. [online] [53pp] Available at http://www.rrojasdatabank.org/trends.htm#Agriculture (Accessed 01/04/2003).

United Nations (2003) Below-replacement fertility expected in 75 per cent of developing countries by year 2050 according to UN population report. [online] [6p.] Available at http://www/un.org.News/Press/docs/2003/pop850.htm Press Release, Population Division, United Nations, New York (Accessed 01/04/2003).

van Keulen H (1975) Soil submodels. In van Keulen. H Simulation of Water Use and Herbage Growth in Arid Regions. Wageningen, Netherlands: PUDOC, pp. 65-98.

van Keulen H, Penning de Vries FWT (1993) Farming under uncertainty: Terminology and techniques. In: Intnl Crop Sci I. CSSA, Madison, Wisconsin 53711, USA, pp. 139-144.

Villabos FJ, Fereres E (1989) A simulation method for irrigation scheduling under variable rainfall. ASAE 32:181-188.

Welles JM, Norman JM (1991) Instrument for indirect measurement of canopy architecture. Agron J 83:818-825.

Whisler FD, Acock B, Baker DN, Fye RE, Hodges HF, Lambert JR, Lemmon JE, McKinion JM, Reddy VR (1986) Crop simulation models and types of models. Adv Agron 40:141-208.

Williams AN, Nearing M, Habeck, Southworth J, Pfeifer R, Doering OC, Lowenberg-Deboer J, Randolph JC, Mazzocc MA (2001) [online] [7p.] Global Climate Change: Implications of Extreme Events for Soil Conservation Strategies and Crop Production in the Midwestern United States. In Stott DE, Mohtar RH and Steinhardt GC (eds.) Sustaining the Global Farm. Available at http://topsoil.nserl.purdue.edu.nserlweb/isco99.pdf.ISCOdisc/SustainingTheGlobalFarm/P191-williams.pdf (accessed 19/09/2002).

Willmott CJ (1981) On the validation of models. Phys Geog 2:184-194.

Willmott CJ (1982) Some comments on the evaluation of model performance. Bull Amer Meteorol Soc 63:1309-1313.

World Bank (2001) Food production or food aid? An African challenge. In Findings: Environment, Rural and Social Development 190, Sept., 2001. World Bank, International Bank for reconstruction and development, Washington DC. [online] [4p.] Available at http://www.worldbank.org/afr/findings/english/find190.pdf (Accessed 02/04/03).

Zhou M, Singles A, Savage MJ (2003) Physiological parameters for modelling sugar cane variety differences in canopy development. South African Sugar Technologists Meeting, Durban, South Africa, May 2003.

Appendix A: Physical and chemical soil characteristics on a layer by layer basis from an upper and lower slope during the 2002/2003 growing seasons at the experimental site, Cedara, KwaZulu-Natal, South Africa (soil texture analysis is based on United States Department of Agriculture classification system)

Location	Soil depth	Clay	Silt	Sand	Texture	Particle density	Bulk density	OC	Ca	Mg	Na	K	Fe	SAR	CEC	pH	EC
	(mm)	(%)	(%)	(%)	--	(kg m^{-3})	(kg m^{-3})	(%)	(mol m^{-3})	(mol m^{-3})	(mol m^{-3})	(mol m^{-3})	(mol m^{-3})	-	-	(KCl)	(µS cm^{-1})
Higher slope	0-100	38.00	32.35	29.65	Clay loam	2520	1294	3.1	0.83	0.60	1.01	0.07	0.14	0.85	2.51	4.49	436
	100-200	44.00	26.10	29.90	Clay	2510	1300	2.8	0.58	0.40	0.50	0.06	0.12	0.51	1.55	4.45	264
	200-300	44.00	26.80	29.20	Clay	2540	1393	2.8	0.60	0.31	0.57	0.04	0.07	0.59	1.51	4.50	258
	300-500	43.00	27.05	25.95	Clay	2580	1370	1.9	0.52	0.23	0.48	0.06	0.11	0.55	1.30	4.47	216
	500-700	43.00	24.15	32.85	Clay	2600	1315	-	0.49	0.25	0.64	0.03	0.02	0.74	1.41	4.76	235
	700-900	36.00	34.00	30.00	Clay loam	-	1290	-	-	-	-	-	-	-	-	-	-
	900-1000	38.00	31.50	30.50	Clay loam	2640	1210	-	0.38	0.36	0.86	0.03	0.01	1.00	1.63	4.65	262
Lower slope	0-100	36.00	28.40	35.60	Clay loam	2510	1433	2.3	1.49	1.09	1.48	0.19	0.03	0.92	4.26	4.93	758
	100-200	43.00	26.95	30.05	Clay	2590	1391	2.6	0.90	0.61	1.02	0.09	0.11	0.83	2.62	4.56	451
	200-300	43.00	26.10	30.90	Clay	2590	1313	1.9	0.82	0.44	0.48	0.08	0.04	0.42	1.82	4.8	338
	300-500	44.00	22.10	33.90	Clay	2500	1411	1.2	0.70	0.34	0.60	0.03	0.03	0.59	1.67	5.32	297
	500-700	44.00	24.45	31.55	Clay	2700	1369	-	0.21	0.13	0.45	0.02	0.03	0.77	0.81	5.04	124
	700-900	39.00	28.28	32.72	Clay loam	-	1380	-	-	-	-	-	-	-	-	-	-
	900-1000	39.00	28.30	32.70	Clay loam	2790	1420	-	0.10	0.13	0.67	0.03	0.03	1.41	0.93	4.40	123

Appendix B: Particle-size analysis (South Africa) for the experimental sites under National Cultivar Trials: maize, during the 1997/98 to 2001/02 growing seasons at Cedara, KwaZulu-Natal, South Africa (soil texture analysis is based on the South African classification system)

Soil depth	Clay	Fine silt	Sand and coarse silt	Texture
(mm)	(%)	(%)	(%)	--
0 to 150	40	13	47	Clay
150 to 300	39	15	46	Clay loam
300 to 450	39	15	46	Clay loam
450 to 600	38	13	49	Clay loam
600 to 750	32	15	53	Clay loam
750 to 900	32	15	53	Clay loam
900 to 1050	33	16	51	Clay loam
1050 to 1200	35	15	50	Clay loam

Appendix C: CR23X datalogger program for soil water potential sensors (tensiometers and Watermark sensors)

```
; {CR23X}
; Watermark sensors
; Wiring for each blue (UNP) or black (CSI)
wire connects to
; individual EX channel
; All reds go to their respective SE channel
; Green (UNP) or white (CSI) connect to ground
; Tensiometers
; All reds go to their respective EX channel
; All Yellow go to their respective SE channel
; Green, blue and clear go to ground
; Thermocouple
; Blue goes to high
; Red or white connect to low
; {CR23X}
;
*Table 1 Program
  01: 3600      Execution Interval (seconds)

1:  If time is (P92)
 1: 0           Minutes (Seconds --) into a
 2: 180         Interval (same units as above)
 3: 30          Then Do

2:  Batt Voltage (P10)
 1: 1           Loc [ Vbattery  ]

3:  Panel Temperature (P17)
 1: 2           Loc [ Tpanel    ]

;Six Watermark sensors
4:  AC Half Bridge (P5)
 1: 2           Reps
 2: 14          1000 mV, Fast Range
 3: 1           SE Channel
 4: 1           Excite all reps w/Exchan 1
 5: 500         mV Excitation
 6: 3           Loc [ KOhms_1   ]
 7: 1.0         Mult
 8: 0.0         Offset
5:  AC Half Bridge (P5)
 1: 2           Reps
 2: 14          1000 mV, Fast Range
 3: 3           SE Channel
 4: 2           Excite all reps w/Exchan 2
 5: 500         mV Excitation
 6: 5           Loc [ KOhms_3   ]
 7: 1.0         Mult
 8: 0.0         Offset

6:  AC Half Bridge (P5)
 1: 2           Reps
 2: 14          1000 mV, Fast Range
 3: 5           SE Channel
 4: 3           Excite all reps w/Exchan 3
 5: 500         mV Excitation
 6: 7           Loc [ KOhms_5   ]
 7: 1.0         Mult
 8: 0.0         Offset

7:  BR Transform Rf[X/(1-X)] (P59)
 1: 6           Reps
 2: 3           Loc [ KOhms_1   ]
 3: 1.0         Multiplier (Rf)

8:  Thermocouple Temp (DIFF) (P14)
 1: 1           Reps
 2: 21          10 mV, 60 Hz Reject, Slow Range
 3: 4           DIFF Channel
 4: 1           Type T (Copper-Constantan)
 5: 2           Ref Temp (Deg. C) Loc [ Tpanel
]
 6: 9           Loc [ Tsoil_1   ]
 7: 1.0         Mult
 8: 0.0         Offset.

9:  Thermocouple Temp (DIFF) (P14)
 1: 1           Reps
 2: 21          10 mV, 60 Hz Reject, Slow Range
 3: 5           DIFF Channel
 4: 1           Type T (Copper-Constantan)
 5: 2           Ref Temp (Deg. C) Loc [ Tpanel
]
 6: 11          Loc [ Tsoil_3   ]
 7: 1.0         Mult
 8: 0.0         Offset

10:  Thermocouple Temp (DIFF) (P14)
 1: 1           Reps

 2: 21          10 mV, 60 Hz Reject, Slow Range
 3: 6           DIFF Channel
 4: 1           Type T (Copper-Constantan)

 5: 2           Ref Temp (Deg. C) Loc [ Tpanel    ]
 6: 13          Loc [ Tsoil_5   ]

 7: 1.0         Mult
 8: 0.0         Offset

11:  Z=X (P31)
 1: 9           X Loc [ Tsoil_1   ]
 2: 10          Z Loc [ Tsoil_2   ]

12:  Z=X (P31)
 1: 11          X Loc [ Tsoil_3   ]
 2: 12          Z Loc [ Tsoil_4   ]

13:  Z=X (P31)
 1: 13          X Loc [ Tsoil_5   ]
 2: 14          Z Loc [ Tsoil_6   ]

14:  Beginning of Loop (P87)
 1: 0           Delay
 2: 6           Loop Count

15:  Z=X*Y (P36)
 1: 9       -- X Loc [ Tsoil_1   ]
 2: 9       -- Y Loc [ Tsoil_1   ]
 3: 15      -- Z Loc [ WP_kPa_1  ]

16:  Z=X*F (P37)
 1: 15      -- X Loc [ WP_kPa_1  ]
 2: .0106      F
 3: 15      -- Z Loc [ WP_kPa_1  ]

17:  Z=F (P30)
 1: 34.21       F
 2: 0           Exponent of 10
 3: 21      -- Z Loc [ Tscor_1   ]

18:  Z=X-Y (P35)
 1: 21      -- X Loc [ Tscor_1   ]
 2: 9       -- Y Loc [ Tsoil_1   ]
 3: 21      -- Z Loc [ Tscor_1   ]

19:  Z=X+Y (P33)
 1: 15      -- X Loc [ WP_kPa_1  ]
 2: 21      -- Y Loc [ Tscor_1   ]
 3: 15      -- Z Loc [ WP_kPa_1  ]

20:  Z=X*F (P37)
 1: 15      -- X Loc [ WP_kPa_1  ]
 2: 1.062       F
 3: 15      -- Z Loc [ WP_kPa_1  ]

21:  Z=X-Y (P35)
 1: 15      -- X Loc [ WP_kPa_1  ]
 2: 3       -- Y Loc [ KOhms_1   ]
 3: 15      -- Z Loc [ WP_kPa_1  ]

22:  Z=X*F (P37)
 1: 15      -- X Loc [ WP_kPa_1  ]
 2: .01306      F
 3: 15      -- Z Loc [ WP_kPa_1  ]

23:  Z=X/Y (P38)
 1: 3       -- X Loc [ KOhms_1   ]
 2: 15      -- Y Loc [ WP_kPa_1  ]
 3: 15      -- Z Loc [ WP_kPa_1  ]


;Make the water potentials negative

24:  Z=X*F (P37)
 1: 15      -- X Loc [ WP_kPa_1  ]
 2: -1          F
 3: 15      -- Z Loc [ WP_kPa_1  ]

25:  End (P95)

26:  Do (P86)
 1: 10          Set Output Flag High (Flag 0)

27:  Set Active Storage Area (P80)
 1: 1           Final Storage Area 1
 2: 100         Array ID
```

```
28:  Real Time (P77)
 1: 220       Day,Hour/Minute (midnight = 2400)

29:  Resolution (P78)
 1: 0         Low Resolution

30:  Sample (P70)
 1: 6         Reps
 2: 3         Loc [ KOhms_1    ]

31:  Sample (P70)
 1: 6         Reps
 2: 9         Loc [ Tsoil_1    ]

32:  Sample (P70)
 1: 6         Reps
 2: 15        Loc [ WP_kPa_1   ]

33:  End (P95)

34:  Serial Out (P96)
 1: 71        Destination Output

*Table 2 Program
  02: 3600       Execution Interval (seconds)

1:  If time is (P92)
 1: 0         Minutes (Seconds --) into a
 2: 180       Interval (same units as above)
 3: 30        Then Do

;Six tensiometers
2:  Set Port(s) (P20)
 1: 0         C8..C5 = low/low/low/low
 2: 0001      C4..C1 = low/low/low/high

3:  Delay w/Opt Excitation (P22)
 1: 1         Ex Channel
 2: 0         Delay W/Ex (units = 0.01 sec)
 3: 800       Delay After Ex (units = 0.01 sec)
 4: 0         mV Excitation

4:  Volt (SE) (P1)
 1: 1         Reps
 2: 30        Auto, 50 Hz Reject, Slow Range
(OS>1.06)
 3: 22        SE Channel
 4: 27        Loc [ SP_1       ]
 5: -.0232    Mult
 6: 8         Offset

5:  Set Port(s) (P20)
 1: 0000      C8..C5 = low/low/low/low
 2: 0000      C4..C1 = low/low/low/low

6:  Set Port(s) (P20)
 1: 0000      C8..C5 = low/low/low/low
 2: 0010      C4..C1 = low/low/high/low

7:  Delay w/Opt Excitation (P22)
 1: 1         Ex Channel
 2: 0         Delay W/Ex (units = 0.01 sec)
 3: 800       Delay After Ex (units = 0.01 sec)
 4: 0         mV Excitation

8:  Volt (SE) (P1)
 1: 1         Reps
 2: 30        Auto, 50 Hz Reject, Slow Range
(OS>1.06)
 3: 23        SE Channel
 4: 28        Loc [ SP_2       ]
 5: -.0232    Mult
 6: 8         Offset

9:  Set Port(s) (P20)
 1: 0000      C8..C5 = low/low/low/low
 2: 0000      C4..C1 = low/low/low/low

10:  Set Port(s) (P20)
 1: 0000      C8..C5 = low/low/low/low
 2: 0100      C4..C1 = low/high/low/low

11:  Delay w/Opt Excitation (P22)
 1: 1         Ex Channel
 2: 0         Delay W/Ex (units = 0.01 sec)
 3: 800       Delay After Ex (units = 0.01 sec)
 4: 0         mV Excitation

12:  Volt (SE) (P1)
 1: 1         Reps
 2: 30        Auto, 50 Hz Reject, Slow Range
(OS>1.06)
 3: 24        SE Channel
 4: 29        Loc [ SP_3       ]
 5: -.0232    Mult
 6: 8         Offset

13:  Set Port(s) (P20)
 1: 0000      C8..C5 = low/low/low/low
 2: 0000      C4..C1 = low/low/low/low

14:  Set Port(s) (P20)
 1: 0         C8..C5 = low/low/low/low
 2: 1000      C4..C1 = high/low/low/low

15:  Delay w/Opt Excitation (P22)
 1: 1         Ex Channel
 2: 0         Delay W/Ex (units = 0.01 sec)
 3: 800       Delay After Ex (units = 0.01 sec)
 4: 0         mV Excitation

16:  Volt (SE) (P1)
 1: 1         Reps
 2: 30        Auto, 50 Hz Reject, Slow Range (OS>1.06)
 3: 13        SE Channel
 4: 30        Loc [ SP_4       ]
 5: -.0232    Mult
 6: 8         Offset

17:  Set Port(s) (P20)
 1: 0000      C8..C5 = low/low/low/low
 2: 0000      C4..C1 = low/low/low/low

18:  Set Port(s) (P20)
 1: 0001      C8..C5 = low/low/low/high
 2: 0000      C4..C1 = low/low/low/low

19:  Delay w/Opt Excitation (P22)
 1: 1         Ex Channel
 2: 0         Delay W/Ex (units = 0.01 sec)
 3: 800       Delay After Ex (units = 0.01 sec)
 4: 0         mV Excitation

20:  Volt (SE) (P1)
 1: 1         Reps
 2: 30        Auto, 50 Hz Reject, Slow Range (OS>1.06)
 3: 14        SE Channel
 4: 31        Loc [ SP_5       ]
 5: -.0232    Mult
 6: 8         Offset

21:  Set Port(s) (P20)
 1: 0000      C8..C5 = low/low/low/low
 2: 0000      C4..C1 = low/low/low/low

22:  Set Port(s) (P20)
 1: 0010      C8..C5 = low/low/high/low
 2: 0000      C4..C1 = low/low/low/low

23:  Delay w/Opt Excitation (P22)
 1: 1         Ex Channel
 2: 0         Delay W/Ex (units = 0.01 sec)
 3: 800       Delay After Ex (units = 0.01 sec)
 4: 0         mV Excitation

24:  Volt (SE) (P1)
 1: 1         Reps
 2: 30        Auto, 50 Hz Reject, Slow Range (OS>1.06)
 3: 15        SE Channel
 4: 32        Loc [ SP_6       ]
 5: -.0232    Mult
 6: 8         Offset

25:  Set Port(s) (P20)
 1: 0000      C8..C5 = low/low/low/low
 2: 0000      C4..C1 = low/low/low/low

26:  Do (P86)
 1: 10        Set Output Flag High (Flag 0)

27:  Set Active Storage Area (P80)
 1: 2         Final Storage Area 2
 2: 200       Array ID

28:  Real Time (P77)
 1: 220       Day,Hour/Minute (midnight = 2400)

29:  Minimum (P74)
 1: 1         Reps
 2: 1         Value with Seconds
 3: 1         Loc [ Vbattery   ]

30:  Sample (P70)
 1: 6         Reps
 2: 27        Loc [ SP_1       ]

31:  End (P95)

32:  Serial Out (P96)
```

```
 1: 71       Destination Output

*Table 3 Subroutines

End Program

-Input Locations-
1 Vbattery  5 1 1
2 Tpanel    1 3 1
3 KOhms_1   5 4 2
4 KOhms_2   25 2 2
5 KOhms_3   13 2 2
6 KOhms_4   25 2 2
7 KOhms_5   13 2 2
8 KOhms_6   17 2 2
9 Tsoil_1   5 5 1
10 Tsoil_2   1 1 1
11 Tsoil_3   5 2 1
12 Tsoil_4   1 1 1
13 Tsoil_5   5 2 1
14 Tsoil_6   1 1 1
15 WP_kPa_1  1 8 8
16 WP_kPa_2  1 1 0
17 WP_kPa_3  1 1 0
18 WP_kPa_4  1 1 0
19 WP_kPa_5  1 1 0
20 WP_kPa_6  1 1 0
21 Tscor_1   1 2 2
22 Tscor_2   1 0 0
23 Tscor_3   1 0 0
24 Tscor_4   1 0 0
25 Tscor_5   1 0 0
26 Tscor_6   1 0 0
27 SP_1      1 1 1
28 SP_2      1 1 1
29 SP_3      1 1 1
30 SP_4      1 1 1
31 SP_5      1 1 1
32 SP_6      1 1 1
-Program Security-
0000
0000
0000
-Mode 4-
-Final Storage Area 2-
5000
-CR10X ID-
0
-CR10X Power Up-
3
-CR10X Compile Setting-
3
-CR10X RS-232 Setting-
-1
Final Storage Label File for:  WMTEPP_J.CSI
Date:  10/11/2002
Time:  16:42:15

100 Output_Table 3600.00 Sec
1 100 L
2 Day_RTM  L
3 Hour_Minute_RTM  L
4 KOhms_1  L
5 KOhms_2  L
6 KOhms_3  L
7 KOhms_4  L
8 KOhms_5  L
9 KOhms_6  L
10 Tsoil_1  L
11 Tsoil_2  L
12 Tsoil_3  L
13 Tsoil_4  L
14 Tsoil_5  L
15 Tsoil_6  L
16 WP_kPa_1  L
17 WP_kPa_2  L
18 WP_kPa_3  L
19 WP_kPa_4  L
20 WP_kPa_5  L
21 WP_kPa_6  L

200 Output_Table 3600.00 Sec
1 200 L
2 Day_RTM  L
3 Hour_Minute_RTM  L
4 Vbattery_MIN  L
5 Vbattery_Sec_MIN  L
6 SP_1  L
7 SP_2  L
8 SP_3  L
9 SP_4  L
10 SP_5  L
11 SP_6  L


Estimated Total Final Storage Locations used per day
768.0

Program Trace Information File for:  WMTEPP_J.CSI
Date: 10/11/2002
Time: 16:42:15

T = Program Table Number
N = Sequential Program Instruction Location Number
Instruction = Instruction Number and Name

Inst ExTm = Individual Instruction Execution Time
Block ExTm = Cumulative Execution Time for program block,
             i.e., subroutine
Prog ExTm = Cumulative Total Program Execution Time
```

			Output Flag High					
			Inst ExTm	Block ExTm	Prog ExTm	Inst ExTm	Block ExTm	Prog ExTm
T	N	Instruction	(msec)	(msec)	(msec)	(msec)	(msec)	(msec)
1	1	92 If time is	0.4	0.4	0.4	0.4	0.4	0.4
1	2	10 Batt Voltage	2.5	2.9	2.9	2.5	2.9	2.9
1	3	17 Panel Temperature	2.8	5.7	5.7	2.8	5.7	5.7
1	4	5 AC Half Bridge	8.8	14.5	14.5	8.8	14.5	14.5
1	5	5 AC Half Bridge	8.8	23.3	23.3	8.8	23.3	23.3
1	6	5 AC Half Bridge	8.8	32.1	32.1	8.8	32.1	32.1
1	7	59 BR Transform Rf[X/(1-X)]	8.5	40.6	40.6	8.5	40.6	40.6
1	8	14 Thermocouple Temp (DIFF)	39.5	80.1	80.1	39.5	80.1	80.1
1	9	14 Thermocouple Temp (DIFF)	39.5	119.6	119.6	39.5	119.6	119.6
1	10	14 Thermocouple Temp (DIFF)	39.5	159.1	159.1	39.5	159.1	159.1
1	11	31 Z=X	0.4	159.5	159.5	0.4	159.5	159.5
1	12	31 Z=X	0.4	159.9	159.9	0.4	159.9	159.9
1	13	31 Z=X	0.4	160.3	160.3	0.4	160.3	160.3
1	14	87 Beginning of Loop	0.2	160.5	160.5	0.2	160.5	160.5
Execution times in the loop are calculated for one pass only.								
1	15	36 Z=X*Y	0.7	161.2	161.2	0.7	161.2	161.2
1	16	37 Z=X*F	0.7	161.9	161.9	0.7	161.9	161.9
1	17	30 Z=F	0.5	162.4	162.4	0.5	162.4	162.4
1	18	35 Z=X-Y	0.7	163.1	163.1	0.7	163.1	163.1
1	19	33 Z=X+Y	0.7	163.8	163.8	0.7	163.8	163.8
1	20	37 Z=X*F	0.7	164.5	164.5	0.7	164.5	164.5
1	21	35 Z=X-Y	0.7	165.2	165.2	0.7	165.2	165.2
1	22	37 Z=X*F	0.7	165.9	165.9	0.7	165.9	165.9
1	23	38 Z=X/Y	1.5	167.4	167.4	1.5	167.4	167.4
1	24	37 Z=X*F	0.7	168.1	168.1	0.7	168.1	168.1
1	25	95 End	0.2	168.3	168.3	0.2	168.3	168.3
1	26	86 Do	0.2	168.5	168.5	0.2	168.5	168.5

```
 Output Flag Set @ 126 for Array 100
1|27|80 Set Active Storage Area      0.2  168.7  168.7      0.2  168.7  168.7
1|28|77 Real Time                    0.1  168.8  168.8      2.2  170.9  170.9
 Output Data 2 Values
1|29|78 Resolution                   0.4  169.2  169.2      0.4  171.3  171.3
1|30|70 Sample                       0.1  169.3  169.3      1.7  173.0  173.0
 Output Data 6 Values
1|31|70 Sample                       0.1  169.4  169.4      1.7  174.7  174.7
 Output Data 6 Values
1|32|70 Sample                       0.1  169.5  169.5      1.7  176.4  176.4
 Output Data 6 Values
1|33|95 End                          0.2  169.7  169.7      0.2  176.6  176.6
1|34|96 Serial Out                     *  169.7  169.7        *  176.6  176.6

Program Table 1 Execution Interval 3600.000 Seconds

Table 1 Estimated Total Program Execution Time in msec  169.7 w/Output  176.6

Table 1 Estimated Total Final Storage Locations used per day  504.0


--------------- Table 2 ---------------
2|1|92 If time is                     0.4    0.4    0.4      0.4    0.4    0.4
2|2|20 Set Port(s)                    6.6    7.0    7.0      6.6    7.0    7.0
2|3|22 Delay w/Opt Excitation     8000.5 8007.5 8007.5   8000.5 8007.5 8007.5
2|4|1 Volt (SE)                   131.7 8139.2 8139.2    131.7 8139.2 8139.2
2|5|20 Set Port(s)                   6.6 8145.8 8145.8      6.6 8145.8 8145.8
2|6|20 Set Port(s)                   6.6 8152.4 8152.4      6.6 8152.4 8152.4
2|7|22 Delay w/Opt Excitation     8000.5 16152.9 16152.9   8000.5 16152.9 16152.9
2|8|1 Volt (SE)                   131.7 16284.6 16284.6    131.7 16284.6 16284.6
2|9|20 Set Port(s)                   6.6 16291.2 16291.2      6.6 16291.2 16291.2
2|10|20 Set Port(s)                  6.6 16297.8 16297.8      6.6 16297.8 16297.8
2|11|22 Delay w/Opt Excitation    8000.5 24298.3 24298.3   8000.5 24298.3 24298.3
2|12|1 Volt (SE)                  131.7 24430.0 24430.0    131.7 24430.0 24430.0
2|13|20 Set Port(s)                  6.6 24436.6 24436.6      6.6 24436.6 24436.6
2|14|20 Set Port(s)                  6.6 24443.2 24443.2      6.6 24443.2 24443.2
2|15|22 Delay w/Opt Excitation    8000.5 32443.7 32443.7   8000.5 32443.7 32443.7
2|16|1 Volt (SE)                  131.7 32575.4 32575.4    131.7 32575.4 32575.4
2|17|20 Set Port(s)                  6.6 32582.0 32582.0      6.6 32582.0 32582.0
2|18|20 Set Port(s)                  6.6 32588.6 32588.6      6.6 32588.6 32588.6
2|19|22 Delay w/Opt Excitation    8000.5 40589.1 40589.1   8000.5 40589.1 40589.1
2|20|1 Volt (SE)                  131.7 40720.8 40720.8    131.7 40720.8 40720.8
2|21|20 Set Port(s)                  6.6 40727.4 40727.4      6.6 40727.4 40727.4
2|22|20 Set Port(s)                  6.6 40734.0 40734.0      6.6 40734.0 40734.0
2|23|22 Delay w/Opt Excitation    8000.5 48734.5 48734.5   8000.5 48734.5 48734.5
2|24|1 Volt (SE)                  131.7 48866.2 48866.2    131.7 48866.2 48866.2
2|25|20 Set Port(s)                  6.6 48872.8 48872.8      6.6 48872.8 48872.8
2|26|86 Do                           0.2 48873.0 48873.0      0.2 48873.0 48873.0
 Output Flag Set @ 226 for Array 200
2|27|80 Set Active Storage Area      0.2 48873.2 48873.2      0.2 48873.2 48873.2
2|28|77 Real Time                    0.1 48873.3 48873.3      2.2 48875.4 48875.4
 Output Data 2 Values
2|29|74 Minimum                      1.1 48874.4 48874.4      4.4 48879.8 48879.8
 Output Data 2 Values
2|30|70 Sample                       0.1 48874.5 48874.5      1.7 48881.5 48881.5
 Output Data 6 Values
2|31|95 End                          0.2 48874.7 48874.7      0.2 48881.7 48881.7
2|32|96 Serial Out                     * 48874.7 48874.7        * 48881.7 48881.7

Program Table 2 Execution Interval 3600.000 Seconds

Table 2 Estimated Total Program Execution Time in msec 48874.7 w/Output 48881.7

Table 2 Estimated Total Final Storage Locations used per day  264.0


Estimated Total Final Storage Locations used per day  768.0

*Execution time is unknown.
```

Appendix D: CR10X datalogger Program for PR1 profile probe sensor and rainguage to measure soil water content and rainfall/irrigation

```
; {CR10X}
; Record of wetting front and normal water
content
; monitoring using the PR1 profile probe
; Select to have table 1 or table 2 on
; Table 1: 10 s interval for monitoring
wetting front
; Switch off table 1 by pressing *1 A 0 A *0
;
; Table 2: 3600 s interval for normal
monitoring
; Switch off table 2 by pressing *2 A 0 A *0

; PR1 profile probe
; Yellow 1H, Green 1L
; Black 2H, Green 2L
; Brown 3H, Green 3L
; White 4H, Green 4L
; Turquoise 5H, Green 5L
; Pink 6H, Green 5L
; Red goes to Switched 12 V
; Blue goes to G (power 0 V)
; Connect a wire between Switched 12 V Control
and C8

*Table 1 Program
  01: 10          Execution Interval (seconds)

1:  Batt Voltage (P10)
 1: 1           Loc [ Vbattery  ]

2:  If time is (P92)
 1: 0           Minutes (Seconds --) into a
 2: 2           Interval (same units as above)
 3: 30          Then Do

3:  Set Port(s) (P20)
 1: 1000        C8..C5 = high/low/low/low
 2: 0000        C4,C3,C2,C1 Options

4:  Ex-Del-Diff (P8)
 1: 6           Reps
 2: 15          2500 mV Fast Range
 3: 1           DIFF Channel
 4: 1           Excite all reps w/Exchan 1
 5: 200         Delay (units 0.01 sec)
 6: 0000        mV Excitation
 7: 2           Loc [ Voltage_1 ]
 8: 0.001       Mult
 9: 0.0         Offset

5:  Polynomial (P55)
 1: 6           Reps
 2: 2           X Loc [ Voltage_1 ]
 3: 8           F(X) Loc [ WC_1       ]
 4: -.084       C0
 5: 1.77        C1
 6: -3.88       C2
 7: 9.42        C3
 8: 0.0         C4
 9: 0.0         C5

6:  Set Port(s) (P20)
 1: 0000        C8..C5 = low/low/low/low
 2: 0000        C4,C3,C2,C1 Options

7:  Pulse (P3)
 1: 1           Reps
 2: 1           Pulse Channel 1
 3: 2           Switch Closure, All Counts
 4: 14          Loc [ Irrig     ]
 5: 1.0         Mult
 6: 0.0         Offset

8:  Do (P86)
 1: 10          Set Output Flag High (Flag 0)

9:  Set Active Storage Area (P80)
 1: 1           Final Storage Area 1
 2: 100         Array ID

10:  Real Time (P77)
 1: 1220        Year,Day,Hour/Minute (midnight =
2400)

11:  Minimum (P74)
 1: 1           Reps
 2: 00          Time Option
 3: 1           Loc [ Vbattery  ]

12:  Sample (P70)
 1: 12          Reps
 2: 2           Loc [ Voltage_1 ]

13:  Totalize (P72)
 1: 1           Reps
 2: 14          Loc [ Irrig     ]

14:  End (P95)

*Table 2 Program
  02: 3600      Execution Interval (seconds)

1:  Batt Voltage (P10)
 1: 1           Loc [ Vbattery  ]

2:  If time is (P92)
 1: 0           Minutes (Seconds --) into a
 2: 180         Interval (same units as above)
 3: 30          Then Do

3:  Set Port(s) (P20)
 1: 1000        C8..C5 = high/low/low/low
 2: 0000        C4,C3,C2,C1 Options

4:  Ex-Del-Diff (P8)
 1: 6           Reps
 2: 15          2500 mV Fast Range
 3: 1           DIFF Channel
 4: 1           Excite all reps w/Exchan 1
 5: 200         Delay (units 0.01 sec)
 6: 0000        mV Excitation
 7: 2           Loc [ Voltage_1 ]
 8: 0.001       Mult
 9: 0.0         Offset

5:  Polynomial (P55)
 1: 6           Reps
 2: 2           X Loc [ Voltage_1 ]
 3: 8           F(X) Loc [ WC_1       ]
 4: -.084       C0
 5: 1.77        C1
 6: -3.88       C2
 7: 9.42        C3
 8: 0.0         C4
 9: 0.0         C5

6:  Set Port(s) (P20)
 1: 0000        C8..C5 = low/low/low/low
 2: 0000        C4,C3,C2,C1 Options

7:  Pulse (P3)
 1: 1           Reps
 2: 1           Pulse Channel 1
 3: 2           Switch Closure, All Counts
 4: 14          Loc [ Irrig     ]
 5: 1.0         Mult
 6: 0.0         Offset

8:  Do (P86)
 1: 10          Set Output Flag High (Flag 0)

9:  Set Active Storage Area (P80)
 1: 1           Final Storage Area 1
 2: 200         Array ID

10:  Real Time (P77)
 1: 1220        Year,Day,Hour/Minute (midnight = 2400)

11:  Minimum (P74)
 1: 1           Reps
 2: 00          Time Option
 3: 1           Loc [ Vbattery  ]

12:  Sample (P70)
 1: 12          Reps
 2: 2           Loc [ Voltage_1 ]

13:  Totalize (P72)
 1: 1           Reps
 2: 14          Loc [ Irrig     ]

14:  End (P95)

*Table 3 Subroutines

End Program

-Input Locations-
1 Vbattery  1 2 2
```

```
2 Voltage_1 5 4 2
3 Voltage_2 9 4 2
4 Voltage_3 9 4 2
5 Voltage_4 9 4 2
6 Voltage_5 9 4 2
7 Voltage_6 17 4 2
8 WC_1      5 2 2
9 WC_2      9 2 2
10 WC_3     9 2 2
11 WC_4     9 2 2
12 WC_5     9 2 2
13 WC_6     17 2 2
14 Irrig    1 2 2

-Program Security-
0000
-Mode 4-
-Final Storage Area 2-0
-CR10X ID-0
-CR10X Power Up-3

Final Storage Label File for:  CR10X.CSI
Date:  3/3/2003
Time:  09:21:01

100 Output_Table  10.00 Sec
1 100 L
2 Year_RTM  L
3 Day_RTM  L
4 Hour_Minute_RTM  L
5 Vbattery_MIN  L
6 Voltage_1  L
7 Voltage_2  L
8 Voltage_3  L
9 Voltage_4  L
10 Voltage_5  L
11 Voltage_6  L
12 WC_1  L
13 WC_2  L
14 WC_3  L
15 WC_4  L
16 WC_5  L
17 WC_6  L
18 Irrig_TOT  L

200 Output_Table 3600.00 Sec
1 200 L
2 Year_RTM  L
3 Day_RTM  L
4 Hour_Minute_RTM  L
5 Vbattery_MIN  L
6 Voltage_1  L
7 Voltage_2  L
8 Voltage_3  L
9 Voltage_4  L
10 Voltage_5  L
11 Voltage_6  L
12 WC_1  L
13 WC_2  L
14 WC_3  L
15 WC_4  L
16 WC_5  L
17 WC_6  L
18 Irrig_TOT  L


Estimated Total Final Storage Locations used
per day 155952.0
```

```
Program Trace Information File for:  CR10X.CSI
Date: 3/3/2003
Time: 09:21:01

T = Program Table Number
N = Sequential Program Instruction Location Number
Instruction = Instruction Number and Name

Inst ExTm = Individual Instruction Execution Time
Block ExTm = Cumulative Execution Time for program block,
             i.e., subroutine
Prog ExTm = Cumulative Total Program Execution Time
```

T|N|Instruction	Inst ExTm (msec)	Block ExTm (msec)	Prog ExTm (msec)	Output Flag High Inst ExTm (msec)	Block ExTm (msec)	Prog ExTm (msec)
1|1|10 Batt Voltage	8.3	8.3	8.3	8.3	8.3	8.3
1|2|92 If time is	0.7	9.0	9.0	0.7	9.0	9.0
1|3|20 Set Port(s)	11.3	20.3	20.3	11.3	20.3	20.3
1|4|8 Ex-Del-Diff	24034.5	24054.8	24054.8	24034.5	24054.8	24054.8
1|5|55 Polynomial	20.4	24075.2	24075.2	20.4	24075.2	24075.2
1|6|20 Set Port(s)	11.3	24086.5	24086.5	11.3	24086.5	24086.5
1|7|3 Pulse	2.2	24088.7	24088.7	2.2	24088.7	24088.7
1|8|86 Do	0.3	24089.0	24089.0	0.3	24089.0	24089.0
Output Flag Set @ 18 for Array 100						
1|9|80 Set Active Storage Area	0.3	24089.3	24089.3	0.3	24089.3	24089.3
1|10|77 Real Time	0.2	24089.5	24089.5	3.8	24093.1	24093.1
Output Data 3 Values						
1|11|74 Minimum	2.0	24091.5	24091.5	8.0	24101.1	24101.1
Output Data 1 Values						
1|12|70 Sample	0.2	24091.7	24091.7	5.3	24106.4	24106.4
Output Data 12 Values						
1|13|72 Totalize	1.6	24093.3	24093.3	2.7	24109.1	24109.1
Output Data 1 Values						
1|14|95 End	0.2	24093.5	24093.5	0.2	24109.3	24109.3

```
Program Table 1 Execution Interval   10.000 Seconds

Table 1 Estimated Total Program Execution Time in msec 24093.5 w/Output 24109.3

Table 1 Estimated Total Final Storage Locations used per day 155520.0
```

---------- Table 2 ----------						
2|1|10 Batt Voltage	8.3	8.3	8.3	8.3	8.3	8.3
2|2|92 If time is	0.7	9.0	9.0	0.7	9.0	9.0
2|3|20 Set Port(s)	11.3	20.3	20.3	11.3	20.3	20.3
2|4|8 Ex-Del-Diff	24034.5	24054.8	24054.8	24034.5	24054.8	24054.8
2|5|55 Polynomial	20.4	24075.2	24075.2	20.4	24075.2	24075.2
2|6|20 Set Port(s)	11.3	24086.5	24086.5	11.3	24086.5	24086.5
2|7|3 Pulse	2.2	24088.7	24088.7	2.2	24088.7	24088.7
2|8|86 Do	0.3	24089.0	24089.0	0.3	24089.0	24089.0
Output Flag Set @ 28 for Array 200						
2|9|80 Set Active Storage Area	0.3	24089.3	24089.3	0.3	24089.3	24089.3
2|10|77 Real Time	0.2	24089.5	24089.5	3.8	24093.1	24093.1
Output Data 3 Values						
2|11|74 Minimum	2.0	24091.5	24091.5	8.0	24101.1	24101.1
Output Data 1 Values						
2|12|70 Sample	0.2	24091.7	24091.7	5.3	24106.4	24106.4
Output Data 12 Values						
2|13|72 Totalize	1.6	24093.3	24093.3	2.7	24109.1	24109.1
Output Data 1 Values						
2|14|95 End	0.2	24093.5	24093.5	0.2	24109.3	24109.3

```
Program Table 2 Execution Interval 3600.000 Seconds

Table 2 Estimated Total Program Execution Time in msec 24093.5 w/Output 24109.3

Table 2 Estimated Total Final Storage Locations used per day  432.0


Estimated Total Final Storage Locations used per day 155952.0
```

Appendix E: Crop parameters for oats, Italian ryegrass, rye and maize

Crop parameters	Oats[$]	Ryegrass	Rye	Maize[£], $[CO_2]$=700 $\mu l l^{-1}$
Growth parameters				
Biomass-transpiration coefficient (kPa kg m^{-3})	4.50	4.00	4.00	10.00 [13.30]
Light to above ground biomass conversion (g MJ^{-1})	1.90	1.34	1.50	4.00 [4.00]
At/Pt ratio that limits leaf area growth	0.80	0.80	0.10	0.90* [0.90]
At/Pt ratio that limits root growth	0.20	0.20	0.10	0.50 [0.50]
Optimum mean daily temperature (°C)	15.00	15.00	15.00	25.00 [25.00]
Maximum water uptake (mm day^{-1})	9.00	9.00	9.00	14.00 [14.00]
Leaf water potential at onset of stomatal closure (kPa)	-1500	-1500	-1500	-1200 [-1200]
Wilting leaf water potential (kPa)	-2000	-2000	-2000	-1800 [-1800]
Crop morphology				
Maximum rooting depth (m)	0.70	0.40	0.40	1.50 [1.50]
Initial green leaf area index (m^2 m^{-2})	0.011	0.011	0.011	0.011 [0.011]
Maximum expected leaf area index (LAI) (m^2 m^{-2})	5.00	5.00	5.00	5.00 [5.00]
Fraction of maximum LAI at physiological maturity	0.40*	0.40*	0.40*	0.95* [0.95]
Specific leaf area (m^2 kg^{-1})	21.00*	20.00*	21.00*	22.00 [22.00]
Stem/leaf partition coefficient	1.80	0.80	2.00	2.80 [2.80]
Leaf duration (degree-days)	900*	900*	1200*	876* [876]
Extinction coefficient for solar radiation	0.54	0.53	0.54	0.50 [0.50]
Leaf duration sensitivity to water stress	0.95	0.95	0.95	1.00 [1.00]
ET crop coefficient at full canopy	1.15	1.00	1.15†	1.20† [1.20]
Crop phenology				
Growing degree days (GDD) emergence (°C days)	50	50	50	61‡ [61]
GDD flowering (°C days)	-	-	1000*	785‡ [785]
GDD grain filling (°C days) (°C days)	-	-	-	860‡ [860]
GDD physiological maturity (°C days)	2000	2000	1800	1530‡ [1530]
GDD peak LAI (°C days)	950	950	1040	765* [765]
Base temperature (°C)	4.00	4.00	4.00	10.00* [10.00]
Cutoff temperature (°C)	25.00	25.00	25.00	30.00 [30.00]
Phenologic sensitivity to water stress	1.00	1.00	1.00	1.00 [1.00]
Harvest				
Unstressed harvest index	0.45	0.45	0.45	0.45* [0.45]
Sensitivity to water stress during flowering	0.00	0.00	0.00	0.1 [0.1]
Sensitivity to water stress during grain filling	0.00	0.00	0.00	0.1 [0.1]
Translocation to grain factor	0.20	0.2	0.2	0.4* [0.4]

[$] Crop parameters for oats, ryegrass and rye are obtained from Jovanovic *et al.* (1999) unless indicated otherwise.
[£] Crop parameters for maize are obtained from default values in CropSyst model (Stöckle and Nelson, 2000) unless indicated otherwise. Values in brackets indicate crop parameters under elevated $[CO_2]$.
* determined by calibration
† taken from Allen *et al.* (1998)
‡ determined from field trial data